University of Kentucky
UKnowledge

University of Kentucky Doctoral Dissertations | Graduate School

2011

MOLECULAR AND GENOMIC APPROACHES TO UNDERSTANDING HOST-VIRUS INTERACTIONS IN SHAPING THE OUTCOME OF EQUINE ARTERITIS VIRUS INFECTION

Yun Young Go
University of Kentucky, imsirenita@gmail.com

Right click to open a feedback form in a new tab to let us know how this document benefits you.

Recommended Citation
Go, Yun Young, "MOLECULAR AND GENOMIC APPROACHES TO UNDERSTANDING HOST-VIRUS INTERACTIONS IN SHAPING THE OUTCOME OF EQUINE ARTERITIS VIRUS INFECTION" (2011). *University of Kentucky Doctoral Dissertations*. 840.
https://uknowledge.uky.edu/gradschool_diss/840

This Dissertation is brought to you for free and open access by the Graduate School at UKnowledge. It has been accepted for inclusion in University of Kentucky Doctoral Dissertations by an authorized administrator of UKnowledge. For more information, please contact UKnowledge@lsv.uky.edu.

STUDENT AGREEMENT:

I represent that my thesis or dissertation and abstract are my original work. Proper attribution has been given to all outside sources. I understand that I am solely responsible for obtaining any needed copyright permissions. I have obtained and attached hereto needed written permission statements(s) from the owner(s) of each third-party copyrighted matter to be included in my work, allowing electronic distribution (if such use is not permitted by the fair use doctrine).

I hereby grant to The University of Kentucky and its agents the non-exclusive license to archive and make accessible my work in whole or in part in all forms of media, now or hereafter known. I agree that the document mentioned above may be made available immediately for worldwide access unless a preapproved embargo applies.

I retain all other ownership rights to the copyright of my work. I also retain the right to use in future works (such as articles or books) all or part of my work. I understand that I am free to register the copyright to my work.

REVIEW, APPROVAL AND ACCEPTANCE

The document mentioned above has been reviewed and accepted by the student's advisor, on behalf of the advisory committee, and by the Director of Graduate Studies (DGS), on behalf of the program; we verify that this is the final, approved version of the student's dissertation including all changes required by the advisory committee. The undersigned agree to abide by the statements above.

Yun Young Go, Student

Dr. Peter J. Timoney, Major Professor

Daniel Howe, Ph.D., Director of Graduate Studies

MOLECULAR AND GENOMIC APPROACHES TO UNDERSTANDING HOST-VIRUS INTERACTIONS IN SHAPING THE OUTCOME OF EQUINE ARTERITIS VIRUS INFECTION

DISSERTATION

A dissertation submitted in partial fulfillment of the
requirements for the degree of Doctor of Philosophy in the
College of Agriculture
at the University of Kentucky

By

Yun Young Go

Lexington, Kentucky

Co-Directors: Dr. Peter J. Timoney, Professor of Veterinary Science and

Dr. Udeni B.R. Balasuriya, Professor of Virology

Lexington, Kentucky

2011

Copyright © Yun Young Go 2011

ABSTRACT OF DISSERTATION

MOLECULAR AND GENOMIC APPROACHES TO UNDERSTANDING HOST-VIRUS INTERACTIONS IN SHAPING THE OUTCOME OF EQUINE ARTERITIS VIRUS INFECTION

Equine arteritis virus (EAV) is the causal agent of equine viral arteritis, a disease of equids. During natural outbreaks of the disease, EAV can cause abortion in pregnant mares and persistent infection in stallions. Understanding how host cellular proteins interact with viral RNA and viral proteins, as well as their role in viral infection, will enable better characterization of the pathogenesis of EAV and establishment of persistent infection in stallions. Accordingly, we hypothesized that both viral factors and host genetically related factors could influence the outcome of EAV infection in horses. To test this hypothesis, we first combined contemporary molecular biology techniques with dual color flow cytometric analysis to characterize the interactions of viral structural proteins and the equine peripheral blood mononuclear cells *in vitro*. Results from this study demonstrated that interactions between GP2, GP3, GP4, GP5 and M envelope proteins of EAV play a major role in determining the $CD14^+$ monocyte tropism while the tropism of $CD3^+$ T lymphocytes is determined by GP2, GP4, GP5 and M envelope proteins but not the GP3 protein. Secondly, a genome wide association study using SNP genotyping identified a common haplotype associated with the *in vitro* $CD3^+$ T lymphocyte/resistance to EAV infection among four breeds of horses. Subsequently, these studies were extended to establish a possible correlation between the *in vitro* susceptibility of $CD3^+$ T lymphocytes to EAV and establishment of persistent infection in stallions. Interestingly, carrier stallions with susceptible $CD3^+$ T lymphocyte phenotype to EAV may represent those at higher risk of becoming persistently infected. Finally, the precise effect of EAV on the immune system of horses, innate and humoral immunity, was studied. Horses were shown to mount a strong humoral antibody response to nonstructural proteins (nsps) 2, 4, 5 and 12 of EAV, whereas nsps 1, 2 and 11 suppressed the type I interferon production. The data presented in this dissertation suggest new directions for future EAV research using genomic and proteomic approaches to study host cell factors involved in EAV attachment and entry and establishment of persistent infection in the stallions.

KEYWORDS: Equine arteritis virus, Equine viral arteritis, Susceptibility/resistance, Humoral immunity, Innate immunity

Yun Young Go

December 10, 2011

MOLECULAR AND GENOMIC APPROACHES TO UNDERSTANDING HOST-VIRUS INTERACTIONS IN SHAPING THE OUTCOME OF EQUINE ARTERITIS VIRUS INFECTION

By

Yun Young Go

Peter J. Timoney
Co-Director of Dissertation

Udeni B.R. Balasuriya
Co-Director of Dissertation

Daniel Howe
Director of Graduate Studies

December 10, 2011

To my parents for their unconditional love and support

ACKNOWLEDGMENTS

The completion of my doctorate would not have been possible without the support, patience and guidance of many people that I have met and worked with during my graduate studies. It is a pleasure to convey my gratitude to everyone in my humble acknowledgment.

I am heartily thankful to Dr. Peter J. Timoney for his advice, supervision, and generous support throughout my studies. He opened the doors for me to join the program and has since provided support and care for me the entire time. His encouragement inspired and enriched my growth as a student, a researcher and a scientist. I truly appreciate the years that I have spent under his guidance.

I owe my deepest gratitude to Dr. Udeni B.R. Balasuriya for his advice and supervision, as well as giving me an extraordinary experience throughout my studies. I was fortunate to have such an excellent mentor. The true joy and passion he has for science was motivational and served as the driving force to keep up with my research even during difficult times in the Ph.D. pursuit. I am indebted for all his contributions of time, ideas and help to make my graduate experience productive and stimulating. I sincerely appreciate his friendship and the care he provided, sometimes like a brother and a father, in my personal life as well; I am indebted to him more than he knows.

I would like to express my sincere gratitude to my Ph.D. dissertation committee members: Drs. David Horohov, Neil Williams, Donald Cohen and the outside examiner, Dr. Darrell Jennings, for their time, interest, helpful comments and insightful questions during the doctoral examination.

The genome-wide association study discussed in this dissertation would not have been possible without the help of Dr. Ernest Bailey. I would like to thank him for kindly sparing his time to answer my naïve questions about genetics at any time.

I thank Dr. Eric Snijder at Leiden University Medical Center, The Netherlands, for inviting us to collaborate on the study identifying a new open reading frame of EAV and for fruitful discussions. It is always an honor and pleasure working with him and his graduate/postdoctoral fellows.

I would like to show my gratitude to Dr. Susan Wong at Wadsworth Center, New York State Department of Health, whose collaborative work on developing a fluorescent microsphere immunoassay was enjoyed very much and resulted in my very first publication. It was a favorable learning experience to realize what a good collaboration is.

I gratefully thank Dr. Ying Fang and her graduate student, Yanhua Li, at South Dakota State University for performing luciferase expression assays for the EAV innate immune response study. I would also like to thank Dr. Dongwan Yoo, College of Veterinary Medicine, University of Illinois at Urbana-Champaign, for inspirational discussions regarding these experiments. I thank Dr. Kuey-Chu Chen, Department of Molecular and Biomedical Pharmacology, University of Kentucky, for introducing me to the world of pathway analysis and allowing me to use the Ingenuity Pathway Analysis software for our genetic study.

I have benefited from advice and fruitful ideas offered by Dr. Frank Cook who helped me in shaping up the research and writing. I would especially like to thank Dr. Daniel Howe for his support in the role of Director of Graduate Studies. I extend my appreciation to the faculty and staff in the deparment, particularly to the laboratories of Drs. Bailey, Chambers, Cook, Horohov, Howe, MacLeod and Lear for allowing me use their equipment and showing me how to operate them.

I would also like to thank both past and present fellow graduate students, in particular, Debbie Cook for performing the SNP data analysis and Stephen Coleman for sharing the equine gene annotation data with us.

I would like to express my special thanks to people in the EAV labs who supported me in many respects during the completion of my project. I am particularly indebted to Jianqiang Zhang, a master of cloning, who taught me how to make complicated recombinant viruses. I thank him for his contribution to various projects, being a good companion for long nights of experiments and most importantly his friendship. I would also like to thank Zhengchun Lu as a good friend who was always willing to help and give her best suggestions. I am grateful to Kathy Shuck who patiently corrected my writing and proofed manuscripts for improvements. Many thanks to Pam Henney, Gong Seoul, Bora Nam, Fabien Miszczak, Juliana Campos, Yanqiu Li, Kathryn

Smith, Jessica Hennig and other people in the laboratory for their help and friendship; it would have been a lonely lab without them.

I would also like to thank all of the administrative staff of the Department of Veterinary Science, especially Diane Furry, Patsy Garrett, Roy Leach, Debbie Mollet, and Gail Watkins who were always ready to help and with their assistance made being a graduate student in the department pleasant.

I gratefully acknowledge the funding sources, Grayson Jockey Club, Morris Animal Foundation and Frederick Van Lennep Chair Endowment funds that made my Ph.D. work possible. The Geoffrey C. Hughes Foundation Fellowship program is greatly acknowledged for providing my personal financial stipend.

My time in Lexington was made enjoyable mainly due to many friends, especially Eunsil Park, Sanghee Lee, and Yoonie Choi who became a part of my life. I am grateful for time spent with friends and memories we share. It is a pleasure to express my gratitude wholeheartedly to Dr. Timoney's family for their kind hospitality and Tina Bryant's family, my host family, who always made sure I felt at home during my stay in Lexington.

Lastly, I would like to thank my family for their unconditional love, trust and, encouragement, especially my dad, Chang Ock Go, who supported me in all my pursuits and my mom, Ga Hyang Kim, who truly raised me with care and love. My brother, Myong Hyun Go, deserves special thanks for showing me the joy of intellectual pursuit and caring. I love you!

TABLE OF CONTENTS

Acknowledgments iii
List of Tables x
List of Figures xi
Chapter One - Literature review 1
1.1. Introduction 2
1.2. Order *Nidovirales* 4
1.3. Family *Arteriviridae* 7
1.4. Equine arteritis virus 9
1.4.1. Genome properties and organization 10
1.5. Equine arteritis virus life cycle 11
1.5.1. Genome replication and transcription 13
1.5.2. EAV replication/transcription complex 16
1.6. Nonstructural proteins of EAV 16
1.6.1. Nsp1 18
1.6.2. Nsp2 19
1.6.3. Nsp3 19
1.6.4. Nsp4 20
1.6.5. Nsp5, nsp6, nsp7α/β and nsp8 21
1.6.6. Nsp9 22
1.6.7. Nsp10 22
1.6.8. Nsp11 23
1.6.9. Nsp12 23
1.7. Structural proteins of EAV 23
1.7.1. Minor envelope proteins 25
1.7.2. Major envelope proteins 31
1.8. Genetic variation and molecular epidemiology of EAV 34
1.9. Equine viral arteritis 35
1.9.1. Seroprevalence, distribution and modes of transmission 35
1.9.2. Clinical signs 36
1.9.3. Persistent infection 37

1.9.4. Pathogenesis 39
1.10. Immune response to EAV infection 41
1.10.1. Innate immune response 41
1.10.2. Humoral immune response 43
1.10.3. Cell mediated immune response 46
1.11. Diagnosis of equine viral arteritis 47
1.11.1. Virus isolation 47
1.11.2. Molecular diagnostics 47
1.11.3. Serological diagnosis 48
1.12. Prevention and treatment of equine viral arteritis 50
1.12.1. Vaccine 50
1.12.2. Antivirals 51
1.13. Recent advances in EAV research and future directions 52
1.13.1. Reverse genetics 52
1.14. Host-virus interaction and genomic studies 53
1.15. Scope and outline of dissertation 55

Chapter Two - Complex interactions between the major and minor envelope proteins of equine arteritis virus determine its tropism for equine $CD3^+$ T lymphocytes and $CD14^+$ monocytes 59
2.1. Summary 59
2.2. Introduction 60
2.3. Materials and Methods 63
2.4. Results 70
2.5. Discussion 84

Chapter Three - Genome-wide association study identifies a common haplotype in horses associated with $CD3^+$ T cell susceptibility to equine arteritis virus infection 89
3.1. Summary 89
3.2. Introduction 91

3.3. Materials and Methods 92
3.4. Results 96
3.5. Discussion 106

Chapter Four - Assessment of correlation between in vitro $CD3^+$ T cell susceptibility to EAV infection and clinical outcome following experimental infection ..115
4.1. Summary 115
4.2. Introduction 116
4.3. Materials and Methods 117
4.4. Results 125
4.5. Discussion 133

Chapter Five - *In vitro* susceptibility of $CD3^+$ T lymphocytes to EAV infection reflects genetic trait of stallions at risk of becoming carriers 138
5.1. Summary 138
5.2. Results and Discussion 139

Chapter Six - EAV does not induce type I interferon α/β production in equine endothelial cells: Identification of nsp1 as a main interferon antagonist 145
6.1. Summary 145
6.2. Introduction 146
6.3. Materials and Methods 147
6.4. Results 151
6.5. Discussion 160

Chapter Seven - A newly discovered ORF5a protein is critical for EAV production 163
7.1. Introduction 163
7.2. Materials and Methods 164
7.3. Results 166
7.4. Discussion 168

Chapter Eight - Development of a fluorescent-microsphere immunoassay for detection of antibodies specific to EAV and comparison with the virus neutralization test 171
8.1. Summary 171
8.2. Introduction 172
8.3. Materials and Methods 174
8.4. Results 182
8.5. Discussion 192

Chapter Nine - Characterization of equine humoral antibody response to the nsps of EAV 198
9.1. Summary 198
9.2. Introduction 199
9.3. Materials and Methods 200
9.4. Results 210
9.5. Discussion 217

Summar of Dissertation 222
Appendices
Appendix 1. List of abbreviations 227
Appendix 2. Experimental methods 230
References 289
Vita 320

LIST OF TABLES

Table 1.1. Order *Nidovirales* 3
Table 1.2. Nonstructural proteins of EAV 18
Table 1.3. Structural proteins of EAV 25
Table 2.1. Comparative amino acid analysis of rVBS, HK116, and rMLV envelope proteins 62
Table 3.1. ECA11 SNPs selected for the MassARRAY® system.....95
Table 3.2. Results from GWAS using the Illumina Equine SNP50 Beadchip 100
Table 3.3. P-values of case and control groups for combined set and for individual breed of horses 102
Table 3.4. List of genes located in the vicinity of the highest associated haplotype block.....113
Table 4.1. Horses used in the study 118
Table 4.2. PCR primers and TaqMan® MGB probes for equine cytokines.....124
Table 5.1. Haplotype of carrier and non-carrier stallions for selected SNPs in ECA11: 49572804-49643932 143
Table 8.1. Primer pairs used for PCR amplification of full-length and partial-length segments of ORFs 5, 6, and 7 176
Table 8.2. Sensitivities and specificities of MIAs using individual recombinant EAV structural proteins.....188
Table 8.3. Sensitivity and specificity of VNT and $GP5_{55-98}$ MIA for determination of antibodies to EAV.....189
Table 8.4. Distribution of numbers of samples giving false-negative results in the $GP5_{55-98}$ MIA.....195
Table 9.1. Serologic responses of horses to EAV nsps following experimental infection, vaccination and in cases of persistent virus infection.....202
Table 9.2. Primers used for PCR amplification of individual nsps for cloning into pCAGGS vector 204
Table 9.3. Primers used for PCR amplification of individual nsps for cloning into pQE-TriSystem His-Strep 2 vector 206

LIST OF FIGURES

Figure 1.1. Schematic diagram of order *Nidovirales* 5
Figure 1.2. Comparison of genome organization of representative nidoviruses 6
Figure 1.3. Genome organization and polycistronic nature of EAV genome.....11
Figure 1.4. Schematic overview of EAV life cycle 12
Figure 1.5. Illustration of two transcription models in nidoviruses: "leader-primed transcription" and "discontinuous extension of minus-strand RNA" models 15
Figure 1.6. Schematic representation of EAV replicase polyproteins 17
Figure 1.7. Proteolytic processing of EAV replicase polyprotein pp1a through the major and minor pathways 21
Figure 1.8. Predicted membrane topology of minor envelope proteins: E, GP2, GP3 and GP4 proteins 27
Figure 1.9. Two predicted models of GP2-GP3-GP3 heterotrimer 29
Figure 1.10. Amino acid sequences of ORF5a protein of five representative arterivirus sequences 30
Figure 1.11. Predicted membrane topology of ORF5a protein.....30
Figure 1.12. Predicted structure of GP5 and M heterodimer 32
Figure 2.1. Differences in susceptibility of $CD3^+$ T lymphocytes to infection with the VB and MLV strains of EAV 71
Figure 2.2. Susceptibility differences between $CD4^+$ and $CD8^+$ T lymphocytes and $CD21^+$ B lymphocytes to infection with the VB and MLV strains of EAV.....73
Figure 2.3. Infection of monocytes with the VB and MLV strains of EAV.....74
Figure 2.4. Detection of EAV N protein expression in T lymphocytes infected with the VB strain 76
Figure 2.5. Replication of the VB and MLV strains of EAV in blood-derived monocytes of group A horses 78
Figure 2.6. Infection of lymphocytes and monocytes with recombinant EAV.....81
Figure 2.7. Predicted membrane topology of minor (GP2, GP3, and GP4) and major

(GP5 and M) EAV envelope proteins 83
Figure 3.1. Schematic representation of the study design 94
Figure 3.2. Effect of breeds on prevalence of T cell susceptible/resistant phenotype .98
Figure 3.3. Manhattan plot.....99
Figure 3.4. Linkage disequilibrium (LD) plots 103
Figure 3.5. Frequency of the GGGGAGGT haplotype with selected SNPs in ECA11: 49572804-49643932 104
Figure 3.6. Pathway analysis 106
Figure 3.7. Subcellular location of candidate genes and EAV life cycle 112
Figure 4.1. Schematic representation of study design and timeline for experimental EAV inoculation and sample collections 120
Figure 4.2. Phenotypic analysis of horses used to identify two experimental groups in the study 126
Figure 4.3. The body temperatures, peripheral blood lymphocyte counts, and virus titers in nasal secretions and blood 128
Figure 4.4. Representative examples of clinical signs following experimental inoculation with EAV rVBS 129
Figure 4.5. Serum neutralizing antibody responses in both groups of horses inoculated with EAV rVBS 130
Figure 4.6. Relative quantification (RQ) of proinflammatory and immunomodulatory cytokine mRNA expression in Group A and Group B horses 132
Figure 5.1. Dual-color immunofluorescence flow cytometric analysis of carrier and non-carrier stallions 141
Figure 6.1. Inhibition of type I IFN production after EAV infection 152
Figure 6.2. EAV nsps involved in suppression of IFN-promoter activation 154
Figure 6.3. EAV nsp1 inhibits both IRF-3 and NF-κB pathways but not AP-1 155
Figure 6.4. EAV nsp1 inhibits the IRF-3 signaling pathway.....157
Figure 6.5. EAV nsp1 inhibits the NF-κB signaling pathway 158
Figure 6.6. Effect of EAV nsp1 in IRF-3 and NF-κB nuclear translocation 160
Figure 7.1. Schematic representation of ORF5a expression in EAV 167

Figure 7.2. Comparison of plaque morphology of wild-type EAV and ORF5a knockout mutants 168
Figure 8.1. Recombinant EAV structural proteins expressed in *E. coli* 183
Figure 8.2. Comparison of antibody responses to EAV as determined by $GP5_{55-98}$ MIA and VNT using sequential serum samples from experimentally infected horses 185
Figure 8.3. $GP5_{55-98}$ and N_{1-110} MIA analyses of serially diluted serum samples.....186
Figure 8.4. ROC curves depicting the sensitivities and specificities of the $GP5_{55-98}$ and N_{1-110} MIAs compared to the VNT 190
Figure 8.5. Analysis of the correlation between the $GP5_{55-98}$ MIA and the VNT for detection of anti-EAV antibodies in equine sera 191
Figure 8.6. Aligned deduced amino acid sequences of $GP5_{55-98}$ proteins from laboratory (rVBS and 030H) and field (KY84, CA95G, WA97, and IL93) strains of EAV.....196
Figure 9.1. Expression of EAV nonstructural proteins in mammalian cells 210
Figure 9.2. Western blot analyses of recombinant nsp4, nsp7, nsp8, nsp9, nsp10, and nsp12 of EAV expressed in *E. coli* 212
Figure 9.3. Immunoprecipitation analyses of nsp2 and nsp5 using sera from experimentally infected, vaccinated and persistently infected horses.....214
Figure 9.4. Immunoprecipitation analysis of nsp12 with sera from experimentally infected, vaccinated and persistently infected horses 215
Figure 9.5. Immunoprecipitation analyses of nsp4 and nsp12 using sera from experimentally infected, vaccinated and persistently infected horses 216

CHAPTER ONE

Literature Review

1.1. INTRODUCTION

Positive-stranded RNA viruses constitute the largest virus group and comprise a wide variety of pathogens of plants and animals. Positive-stranded RNA viruses that consist of linear, single-stranded genomes of mRNA polarity can initiate viral gene expression immediately after genome uncoating in infected cells. These viruses replicate in the cytoplasm of infected cells. RNA viruses have evolved having extremely diverse genomes and replicative mechanisms due to presumably low fidelity of their RNA synthesis [1,2]. Among RNA viruses, nidoviruses are considered the most genetically complex group with relatively large genomes. The complex feature of nidoviral RNA replication and transcription involving numerous virus-encoded proteins with enzymatic activities is a unique feature of the members of the order *Nidovirales* [3,4,5,6]. In particular, generation of a nested set of subgenomic (sg) mRNAs is the hallmark of their genome expression from which the name *Nidovirales* (the Latin word *nidus* means "nest") is derived. Nidovirus infections are often associated with severe diseases such as human severe acute respiratory syndrome (SARS), feline infectious peritonitis, infectious bronchitis of chickens, porcine reproductive and respiratory syndrome (PRRS) and yellow head disease of prawns. Recently, efforts to understand nidovirus replication and transcription have been facilitated by development of reverse genetic systems for many coronaviruses and arteriviruses. Another important goal is to understand the mechanisms of virus entry, assembly and egress from infected cells which involves studies concentrated on interactions between viral and host cellular proteins. Most recently, the host-virus interaction has become one of the most focused areas of nidovirus research. The host's innate immune response is critical in controlling infections and effectively inhibiting spread of the virus in the early phase of infection. Thus, viruses have evolved mechanisms to counteract the innate immune response in order to survive in the host.

Nidoviruses have also developed mechanisms to suppress type I interferon induction and signaling, the details of which are still to be determined. Unraveling such mechanisms will enable development of antiviral drugs and therapeutics to combat devastating diseases caused by some nidoviruses.

Table 1.1. Order *Nidovirales*

Order	***Family***	***Subfamily***	***Genus***	***Species***
Nidovirales	*Arteriviridae*		*Arterivirus*	***Equine arteritis virus***
				Lactate dehydrogenase-elevating virus
				Porcine reproductive and respiratory syndrome virus
				Simian hemorrhagic fever virus
	Coronaviridae	*Coronavirinae*	*Alphacoronavirus*	***Alphacoronavirus 1***
				Human coronavirus 229E
				Human coronavirus NL63
				Miniopterus bat coronavirus 1
				Miniopterus bat coronavirus HKU8
				Porcine epidemic diarrhea virus
				Rhinolophus bat coronavirus HKU2
				Scotophilus bat coronavirus 512
			Betacoronavirus	*Betacoronavirus 1*
				Human coronavirus HKU1
				Murine coronavirus
				Pipistrellus bat coronavirus HKU5
				Rousettus bat coronavirus HKU9
				Severe acute respiratory syndrome-related coronavirus
				Tylonycteris bat coronavirus HKU4
			Gammacoronavirus	***Avian coronavirus***
				Beluga whale coronavirus SW1
		Torovirinae	*Bafinivirus*	***White bream virus***
			Torovirus	*Bovine torovirus*
				Equine torovirus
				Human torovirus
				Porcine torovirus
	Roniviridae		*Okavirus*	***Gill-associated virus***

1.2. ORDER *NIDOVIRALES*

The order *Nidovirales* is comprised of the families *Coronaviridae*, *Arteriviridae*, and *Roniviridae* [7,8,9] (Table 1.1). The family *Arteriviridae* is comprised of the single genus *Arterivirus*. Recently, the family *Coronaviridae* has been reorganized and now consists of two subfamilies, *Coronavirinae and Torovirinae*. The subfamily *Coronavirinae* is subdivided into three genera, *Alphacoronavirus, Betacoronavirus* and *Gammacoronavirus*; and *Torovirinae* is subdivided into two genera, *Bafinivirus* and *Torovirus*. The family *Roniviridae* has a single genus *Okavirus*. Although nidoviruses are significantly different in virion morphology, genome length and host specificity, they belong to the same order based on similarities in their genome organization, gene expression mechanisms, and in sharing common ancestry of the key replicase gene [10,11,12,13].

Nidoviruses infect a wide range of hosts, including invertebrates, avian, human and many other mammalian species [14]. Porcine reproductive and respiratory syndrome virus (PRRSV), a member of the *Arteriviridae* family, is associated with significant economic losses in the swine industry [15]. Coronaviruses (CoV) are well-known agents of respiratory, enteric, and neurologic disease in humans and domestic animals (alphacoronaviruses and betacoronaviruses: mammals; gammacoronaviruses: avian species) and are the only nidovirus group that has been reported to cause disease in humans (http://www.ictvonline.org/virusTaxonomy.asp?version=2009). In 2003, SARS emerged from China as a potentially fatal and untreatable human respiratory disease which was caused by a previously unknown CoV strain [16,17,18,19]. Discovery of SARS-CoV triggered a search for the reservoir species. After extensive investigative studies over a number of years certain species of bats were inflicted as reservoir hosts of the virus. This finding led to the discovery of many novel bat coronaviruses [20]. In 2008, a highly divergent coronavirus was identified from a deceased captive beluga whale and grouped as a gammacoronavirus [21]. The ronivirus yellow head virus (YHV) infects black tiger shrimp causing high mortality and resulting in severe economic losses for shrimp farms [22]. Except for SARS-CoV, which infects a broad range of mammals, the majority of nidoviruses have restricted host specificity, infecting one or a narrow range of closely related species. In 2011, the first insect-associated nidovirus, tentatively

named Cavally virus (CAVV), was reported in association with the tropical rainforest. It shares genetic features in common with members of the order *Nidovirales* [23]. These findings indicate that the virus has evolved and resultant genomic changes have likely facilitated cross-species transmission.

Nidoviruses are enveloped, positive-sense, single-stranded RNA viruses and include mammalian, avian and invertebrate viruses [14]. Arterivirus particles are spherical with smaller envelope projections. In contrast, virions of coronaviruses and toroviruses are spherical and disk-shaped, respectively, that contain tubular helical nucleocapsids with large surface projections on the envelope formed by membrane-spanning viral proteins. Bafinivirus and ronivirus particles are rod-shaped and contain tubular nucleocapsids with helical symmetry (Figure 1.1) [14].

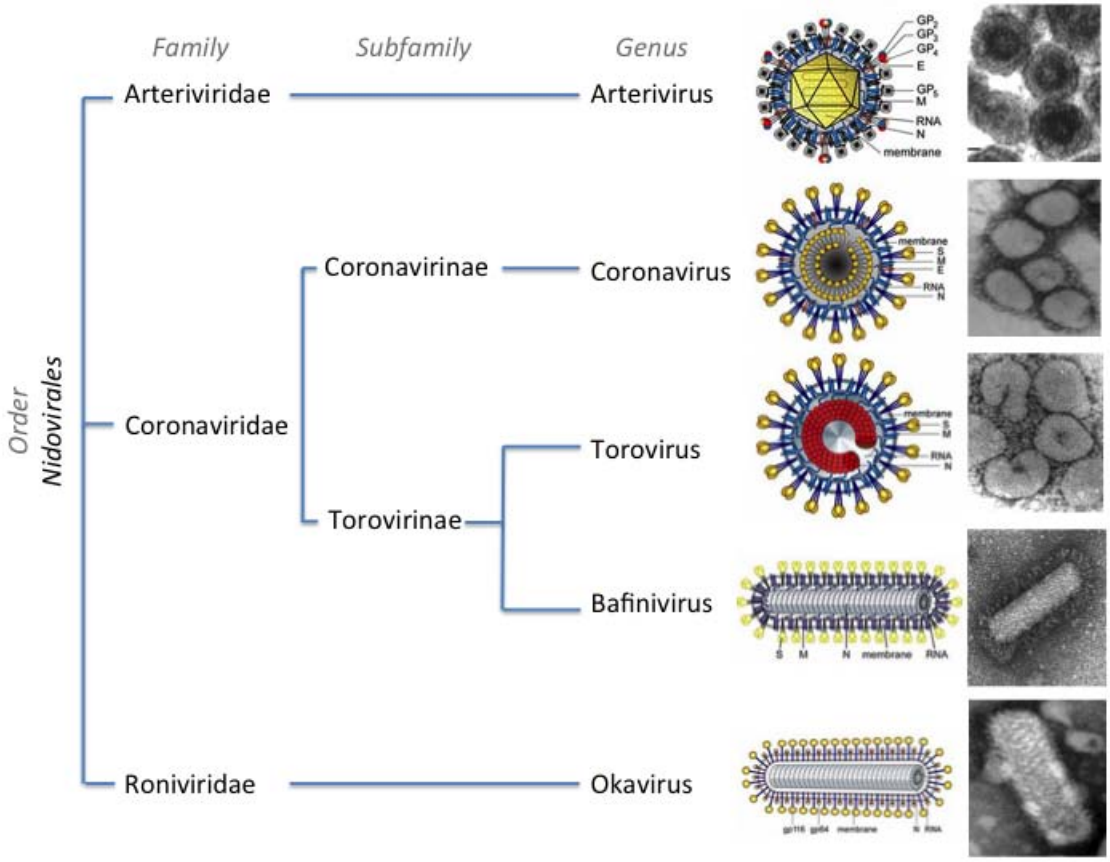

Figure 1.1. Schematic diagram of order *Nidovirales*. The tree represents known members of order *Nidovirales* based on the virion architecture representative of five main nidovirus genera: arterivirus, coronavirus, torovirus, bafinivirus and okavirus. Schematic

representations and electron micrograph pictures were adapted from Enjuanes *et al.* [24] and Snijder *et al.* [14] with permission.

The size and the number of genes encoded in the genome vary considerably among families of the order *Nidovirales.* Members of the *Arteriviridae* family have smaller genomes (12.7-15.7 kb) compared to other nidoviruses. In contrast, the *Coronaviridae* and *Roniviridae* families possess the largest RNA genomes (26.2-31.3 kb) [8]. Despite the wide genome size differences, sequence analysis has shown that all nidoviruses share a similar genomic organization (Figure 1.2.).

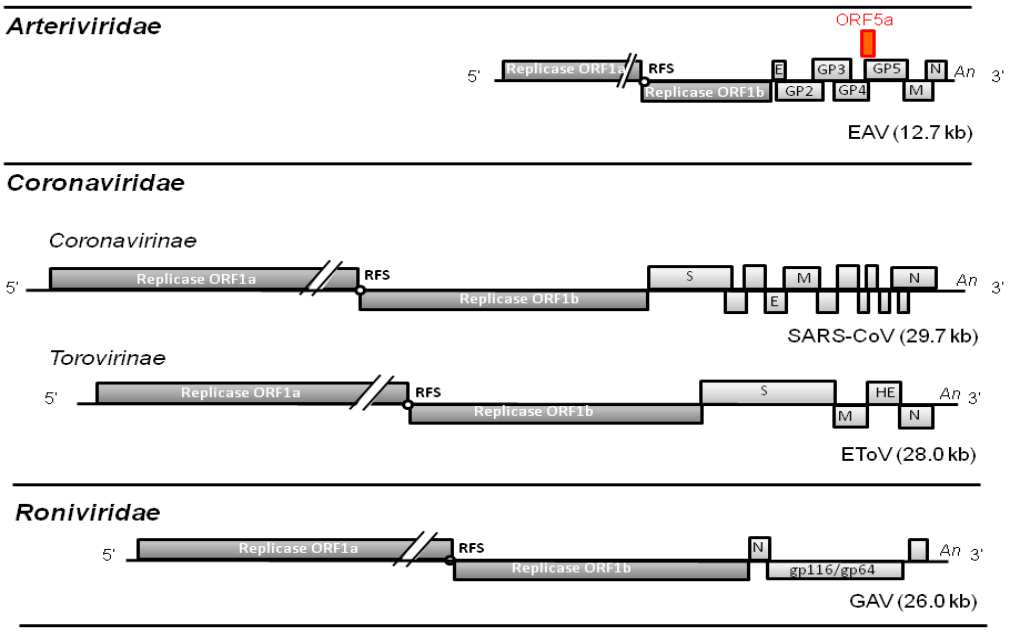

Figure 1.2. Comparison of genome organization of representative nidoviruses. The genomic RNA of representative viruses of the families *Arteriviridae, Coronaviridae* and *Roniviridae* are shown to the same scale. The open reading frames (ORFs) encoding replicase proteins and viral structural proteins are depicted. The ribosomal frame shift (RFS) of the ORF1a/1b and the 3' poly A tail (A_n) are indicated. The newly identified ORF5a in arteriviruses is depicted with a red box. EAV, equine arteritis virus; SARS-CoV, severe acute respiratory syndrome coronavirus; EToV, equine torovirus; GAV, gill-associated virus. Modified figure from *Nidoviruses* book chapter [5] with permission.

Arteriviruses have 9 to 12 open reading frames (ORFs), coronaviruses encode 9 to 14 ORFs, toroviruses have six ORFs and roniviruses have only four ORFs. The genome carries a 5'-capped structure and a 3'-polyadenylated (poly A) tail. It also contains untranslated regions (UTR) at the 5'- and 3'-ends of the genome. At the 5'-proximal two-thirds to three-quarters of the genome, the nonstructural proteins (nsps) are encoded by the two largest ORFs, ORF1a and ORF1b connected by a -1 ribosomal frameshift site (RFS) [25]. The translation of genomic RNA starts at the start codon of ORF1a resulting in the production of a polyprotein, pp1a. In some cases, specific RNA signals promote ribosomal frameshifting at a -1 RFS or "slippery" sequence between ORF1a and ORF1b which results in the C-terminal extension of pp1a with the ORF1b-encoded polypeptide, pp1ab. The pp1a and pp1ab are co- and post-translationally processed by two to four virus-encoded proteases to produce 13-16 nsps [26]. These products of the large replicase protein, possibly with other viral and cellular proteins, assemble into a replication/transcription complex (RTC) bound to modified intracellular membranes. The different groups of nidoviruses encode different sets of structural proteins that result in distinctive virion morphology for each group. The genes encoding viral structural proteins and, in the case of coronaviruses, "accessory or niche-specific" proteins are located at the remaining 3'-proximal thirds of the genome downstream of the replicase gene. The structural and accessory proteins are expressed from a 3' co-terminal nested set of sg mRNAs [27,28,29,30].

1.3. FAMILY *ARTERIVIRIDAE*

EAV was first isolated in 1953, LDV in 1960 and SHFV in 1968; the porcine arterivirus, PRRSV, was not isolated until the late 1980s [15]. Initially, equine arteritis virus (EAV) was classified as a non-arthropod-borne togavirus along with pestiviruses and rubiviruses, lactate dehydrogenase-elevating virus (LDV), simian hemorrhagic fever virus (SHFV), and cell fusion virus [31]. Although structural proteins of LDV and EAV differed from those of togaviruses, EAV, LDV and SHFV were assigned to a new genus *Arterivirus* within the family *Togaviridae* [32] in 1984. Subsequently, molecular characterization studies have shown that genomic organization and replication strategy of EAV resemble those of corona- and toroviruses suggesting that it is evolutionally related

to the coronavirus-like superfamily [10,33]. In 1996, the family *Arteriviridae* was established comprising four viruses: EAV, PRRSV, SHFV and LDV of mice [7,34]. Arterivirus particles are spherical with a diameter of 40 to 60 nm. The buoyant density of arteriviruses is 1.13 to 1.17 g/cm^3 in sucrose, and their sedimentation coefficient ranges from 214S to 230S [35,36,37,38]. The icosahedral core, 25 to 35 nm in diameter, is surrounded by a relatively smooth envelope that lacks large projections.

The natural host range of arteriviruses is highly restricted. Arterivirus infection can vary from acute symptomatic or asymptomatic infection, abortion or lethal hemorrhagic fever and persistent infection. Interestingly, all four arteriviruses have the ability to give rise to long-term persistent infection in their respective hosts. The severity of disease can vary greatly and seems to be influenced by the strain of the virus, the condition and age of the infected animal and various environmental factors. Macrophages appear to be the primary target cell for all arteriviruses [15].

PRRSV was first recognized in the United States in 1987 and independently in Germany in 1990,; it was identified as the cause of a “mystery swine disease” [39,40]. At present, PRRSV is globally disseminated. The early PRRSV isolates from North America and Europe, PRRSV-NA and PRRSV-EU, were genetically distinct from each other with the genotypes sharing only ~63% nucleotide homology [41,42]. Since its initial discovery, the virus has continued to evolve. A new strain of PRRSV has been identified in the US [43,44], and a highly virulent strain has appeared in China [45,46,47] which subsequently spread to neighboring countries [48,49]. PRRSV is transmitted primarily via the respiratory route; however, venereal transmission is an important secondary route of spread of PRRSV, as well as for EAV, due to constant shedding of virus in semen of infected males.

The natural host of LDV is the house mouse, *Mus musculus domesticus* [50]. LDV is characterized by an increased level of lactate dehydrogenase in the blood of infected mice, hence the derivation for the name of the virus [51]. The virus infects a renewable subpopulation of macrophages and is able to escape immune surveillance [15]. Although most cases of persistent infection caused by LDV are asymptomatic, neurovirulent LDV variants can cause fatal age-dependent poliomyelitis in certain inbred mouse strains [52].

SHFV was isolated after devastating outbreaks of hemorrhagic fever in colonies of captive macaque monkeys [53,54]. The virus causes an asymptomatic persistent infection among several different species of African monkeys and remains endemic in affected populations. Different strains of SHFV vary considerably in their cellular tropism, virulence and immunogenicity based on infection studies in African monkeys. Transmission of SHFV from African to Asian monkeys results in hemorrhagic fever with a high case-fatality rate. Vascular damage and disseminated intravascular coagulation are principal to the pathogenesis of simian hemorrhagic fever (SHF) [55].

The size of the arterivirus replicase gene, in particular ORF1a, varies widely among arteriviruses, encoding between 1,727 amino acids (aa) in EAV and 2,500 aa in PRRSV, while the ORF1b region is more conserved. Seven to ten small genes encoding structural proteins are located downstream of the replicase gene and most of them have both 5'- and 3'- terminal sequence regions overlapping with neighboring genes. With the exception of SHFV, the organization of structural proteins is generally well conserved in the arterivirus genome except for. Downstream of the SHFV replicase gene are three additional ORFs, comprising about 1.6 kb, which may have arisen from the duplication of ORFs 2 to 4.

1.4. EQUINE ARTERITIS VIRUS

EAV, the causative agent of equine viral arteritis (EVA), is the prototype virus of the family *Arteriviridae*. The virion of EAV is spherical with a diameter of 40 to 60 nm. The isometric core particle (25 to 35 nm in diameter) is surrounded by a relatively smooth envelope that lacks large projections. EAV genome is encapsidated by the nucleocapsid (N) protein (14 kDa) encoded by ORF7 which forms an icosahedral core structure (Figure 1.1) [10,34,56]. The lipid bilayer that surrounds the nucleocapsid contains six envelope proteins (E, GP2, GP3, GP4, GP5 and M) encoded by ORFs 2a, 2b, 3-6, respectively, that are located at the 3' proximal quarter of the genome [34,56,57,58,59].

EAV is stable at -70°C for years without significant loss of infectivity. Virus infectivity is lost within six months at room temperature, and after a month at 37°C [60].

It has been reported that tissue culture fluid containing the experimentally derived virulent Bucyrus strain (VBS) of EAV survived ≥75 days at 4°C, 2~3 days at 37°C, and 20~30 min at 56°C [61]. Lyophilized virus is highly stable at -20°C and moderately stable at 4°C [62].

1.4.1. Genome properties and organization

EAV genome length varies between 12,704 to 12,731 bp among different strains [7,34,63]. The EAV genome includes a 5' leader sequence and at least nine ORFs [10,64] (Figure 1.3). The two most 5'-proximal ORFs (1a and 1b) occupy approximately three-quarters of the genome and encode two replicase polyproteins (pp1a and pp1ab). The two precursor proteins are extensively processed after translation into at least 13 nsps (nsp1-12, including nsp7 α/β) by three viral proteases (nsp1, nsp2 and nsp4) [34,65,66]. The structural proteins of EAV are expressed from a 3'-coterminal nested set of sg mRNAs and not from the genomic RNA. Three of the minor envelope proteins (GP2, GP3 and GP4) form a heterotrimer in the EAV particle. The two major envelope proteins (M and GP5) form a disulfide-linked heterodimer in the EAV virion [59,67,68]. The GP5 protein expresses the known major neutralization determinants of EAV [69,70,71,72,73,74,75]. Although there is considerable variation in the sequence of the GP5 protein of field strains of the virus, there is only one known major serotype of EAV and all strains evaluated thus far are neutralized by polyclonal equine antiserum raised against the Bucyrus strain of EAV [76,77]. However, field strains differ both in their neutralization and virulence phenotypes and not all strains are neutralized to the same degree [63,74,78,79,80].

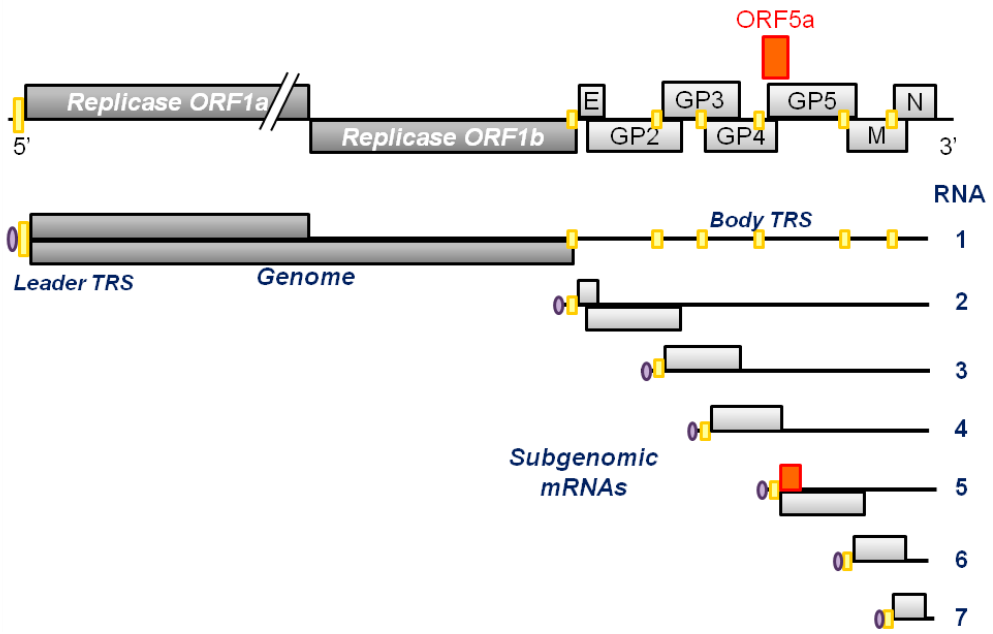

Figure 1.3. The genome organization and polycistronic nature of EAV genome. The leader sequence and leader TRS (transcription regulating sequence) located at the 5'-end of genome are indicated as a purple circle and a yellow box, respectively. Translation of E and GP2 genes occurs by leaky scanning of the 5'-proximal end of sg mRNA2 [58]. The red square indicates the newly identified open reading frame, ORF5a and the protein is likely to be expressed from the same sg mRNA [81]; see chapter 7.

1.5. EQUINE ARTERITIS VIRUS LIFE CYCLE

Enveloped viruses typically have surface molecules that bind to cell surface receptors which mediate the process of cell attachment and membrane fusion with the host cell membrane. While receptors for EAV have not yet been identified, it has been suggested that EAV is taken up via clathrin-dependent endocytosis and is delivered to acidic endosomal compartments [82]. Following entry and release into the cytosol, the plus-stranded RNA genome is uncoated and translated into two replicase polyproteins (pp1a and pp1ab) from which at least 13 nsps are released by autoproteolytic processing mediated by the virus proteases [66,83]. The nsps assemble into a membrane-bound RTC [84,85,86,87]. The RTC generates minus-stranded RNA genomes that are used as templates for genome replication and subgenomic mRNA transcription. The

subgenomic mRNAs are translated into the viral structural proteins. The newly synthesized genome is encapsidated into the N proteins forming the nucleocapsid (NC), which becomes enveloped by budding through the ER-Golgi intermediate compartment (ERGIC) that contains membranes with viral envelope proteins. Newly formed virions mature in the golgi complex during their exocytic pathway and are ultimately released from infected cells (Figure 1.4).

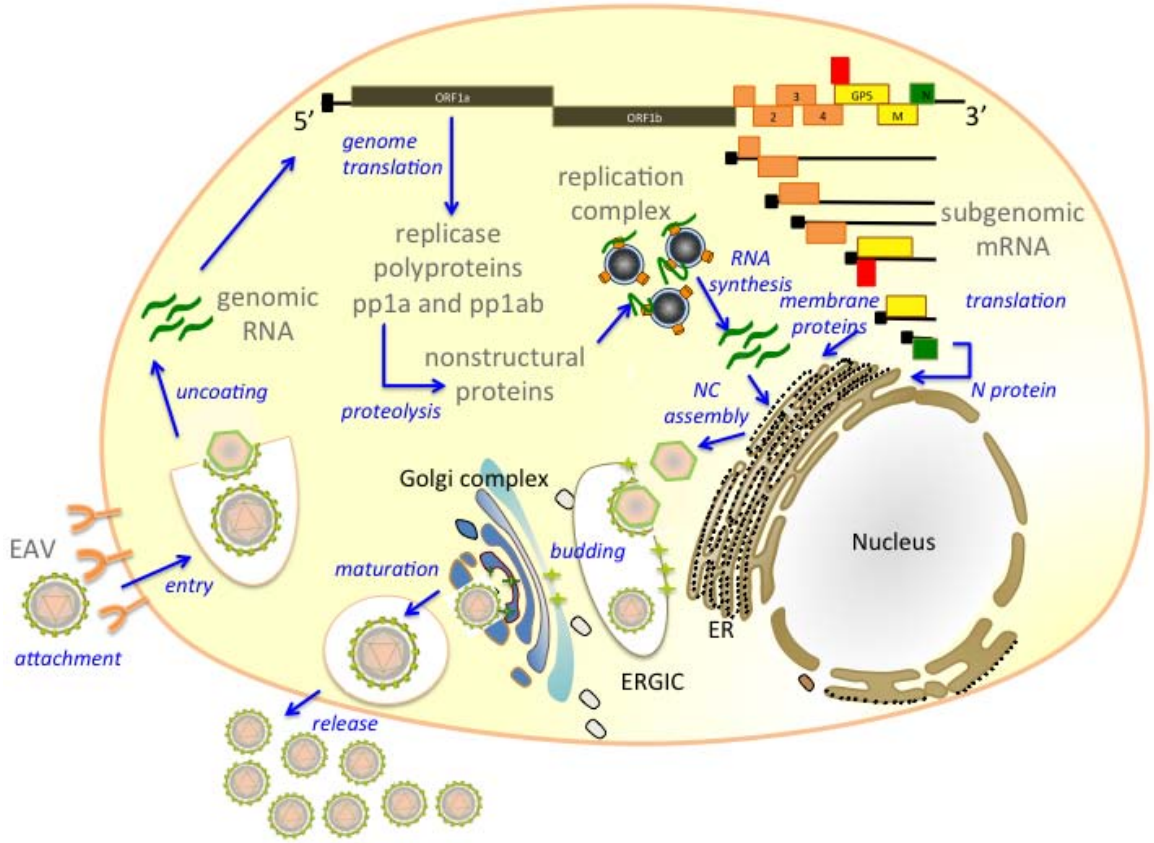

Figure 1.4. Schematic overview of EAV life cycle. ER: endoplasmic reticulum; ERGIC: ER-Golgi intermediate compartment; NC: nucleocapsid. Red square represents newly identified ORF5a protein.

1.5.1. Genome replication and transcription

The EAV genome is an RNA polycistronic molecule with a 5' cap and 3' poly A structure [34]. The 5' UTR (leader), comprising approximately 208 nucleotides (nt), functions as a template for the host translation machinery and as a protective element against degradation by exonucleases [88]. Among nidoviruses, replication and transcription are processed through different minus-strand intermediates: a full-length minus-strand template is used for replication, while subgenome-sized minus strands produced during a process of discontinuous RNA synthesis are used to synthesize sg mRNAs [89,90,91,92]. The initiation of full-length minus-strand RNA (or anti-genome) synthesis, which is also used as template for new genome RNA replication, occurs after recognition of RNA signals near the 3' end of the viral genome by the RNA-dependent RNA polymerase (RdRp) complex [93]. For production of new genomic RNA, recognition of signals present close to the 3' end of the anti-genome must be used [4,94]. During viral RNA synthesis, more plus strands are produced than minus-strand RNAs [95]. There are two widely considered but conflicting models of arterivirus transcription: leader-primed transcription and discontinuous extension of minus-strand RNA synthesis (Figure 1.5). In both models, the TRS elements play a critical role. The TRSs are short and conserved sequence elements (5'-UCAAC-3') that determine a base-pairing interaction between positive and nascent minus-strand RNA and are essential for leader-to-body joining [92,96,97]. In the "leader-primed transcription model", transcription is initiated from the 3' end of the minus-strand genome to produce a leader primer from which the 3'-terminal leader TRS base pairs with the anti-TRS in the minus-strand genome. The leader transcript is extended to complete the sg mRNA. This model proposes that the discontinuous step occurs during the plus-strand synthesis and the body TRS complementary to the minus-strand genome acts as promoter for transcription [27,29,30]. On the other hand, according to the nidovirus transcription model proposed by Sawicki and Sawicki [90] which is the widely accepted model, sg mRNAs are produced by a discontinuous transcription mechanism controlled by the transcription regulation sequence (TRS). The EAV sg mRNAs contain a common 5' sequence of 208 nt, called "leader", identical to the 5' end of viral genomic RNA [34]. The leader TRS is located in a hairpin loop structure at the 3' end of the leader [98] and the body TRSs are

present upstream of every structural protein gene [28,99]. The EAV genome contains multiple UCAAC sequences that could be transcriptionally silent. For example, the RNA3 uses three alternative leader-body junction sites, TRSs 3.1, 3.2, and 3.3 among which TRSs 3.1 and 3.3 are noncanonical junction sites. There are two UCAAC boxes upstream of ORF4, -5 and -7 whereas three UCAAC sequences are found upstream of ORF2 and -2b [100]. However, only a single TRS has been identified as an active site for each of these sg mRNAs. Moreover, a number of 5' UCAAC 3' sequences were also identified in the replicase gene [99]. The TRSs are thought to regulate transcription of the genome template and to serve as signals for either attenuation or termination of minus-strand RNA synthesis in all nidoviruses, thus producing subgenome-sized minus strands that are utilized later as templates for sg mRNA synthesis [95]. Minus-strand RNA synthesis, initiated at the 3'-end of the viral genome, is attenuated at one of the body TRS regions [89,91]. Subsequently, the nascent minus strand carrying the body TRS complement at its 3' end is translocated to the 5' end of the genomic template. In EAV, the genomic leader TRS serves as a base-pairing target for the 3' end of the nascent minus strand that is facilitated by its presence in the loop of an RNA hairpin. When minus-strand synthesis resumes, nascent strands are extended with the complement of the genomic leader sequence, yielding a nested set of subgenome-length minus-strand templates that are used for the subsequent synthesis of the various sg mRNAs. If attenuation does not occur, minus-strand RNA synthesis proceeds to yield a full-length complement of the genome, the intermediate required for its replication. During the discontinuous transcription mechanism, the TRS at the 3' end of the leader transcript base pairs with the complement of the body TRS in the negative-stranded template allowing extension of the complement of the genomic leader sequence in the nascent negative strand [90]. The resulting sg negative-stranded RNA serves as template for the synthesis of the corresponding sg mRNA. With the exception of the last one, each sg mRNA, is structurally polycistronic, although they are functionally monocistronic. With some exceptions, only the 5'-proximal ORF is translated from each sg mRNA; therefore, the number of sg mRNA produced is proportional to the number of ORFs located downstream of ORF1b.

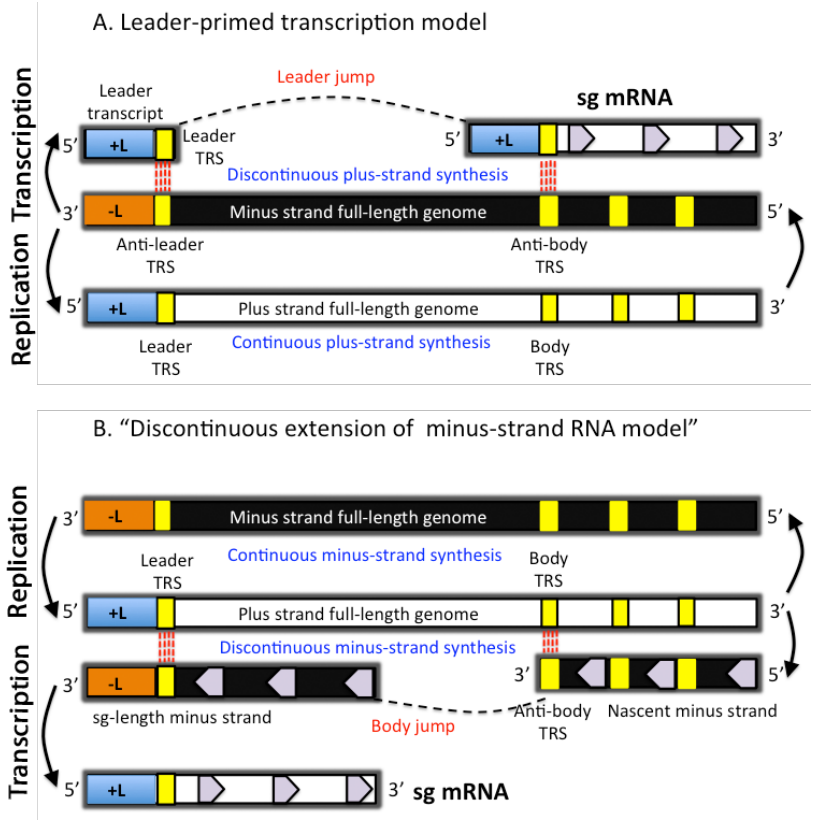

Figure 1.5. Illustration of two transcription models in nidoviruses: "leader-primed transcription" [27,29,30] and "discontinuous extension of minus-strand RNA" [90] models. (A) The "leader-primed transcription" proposes that the discontinuous step of viral sg mRNA synthesis occurs during the plus-strand synthesis. After transcription of a leader primer (+L) from the 3' end of minus-strand full-length genome, the leader TRS in this primer joins to the anti-body TRS in the minus-strand genome and is extended to generate sg mRNA. (B) The alternative model, "discontinuous extension of minus-strand RNA model" proposes that sg-length negative strand is produced that functions as a template for generation of sg mRNA. The anti-body TRS may serve as a "jump" signal of the nascent minus strand to leader TRS located at the 5'-end of the plus-strand full-length genome. After the anti-leader (-L) is added to the nascent minus strand, the sg-length minus strand functions as template for transcription. The later model has gained stronger experimental support from biochemical and genetic studies. Modified from Pasternak *et al.* (2006) [89] with permission.

1.5.2. EAV replication/transcription complex

Formation of paired membranes and double-membrane vesicles (DMVs) at 3-6 h post-infection is a typical feature of arterivirus replication [101,102,103,104,105]. Frequently, RTCs of positive-strand RNA viruses are found to be associated with modified intracellular membranes. The transmembrane nsps are incorporated into cellular organelles, particularly the ER, where early viral RNA synthesis occurs and results in increased expression of replicase proteins. Interaction of accumulated nsps with membranes results in membrane pairing and vesiculation [84]. It is supposed that formation of DMVs is based on interactions between luminal domains of transmembrane proteins of either virus and/or cellular origin to bring opposite membranes together. In nidovirus-infected cells, newly synthesized viral RNA and many replicase subunits were found in the perinuclear region together with a large number of DMVs [84,106,107]. Immunoelectron microscopy revealed that viral nsps that are part of RTC and nascent viral RNA are associated with DMVs [84,107,108,109]. Therefore, DMVs are presumed to carry the enzyme complex responsible for virus replication and sg mRNA synthesis. Expression of EAV nsp2-3 is critical in inducing formation of DMVs [84,85]. Among the EAV replicase subunits, the nsp2, nsp3, and nsp5 encode a considerably large portion of hydrophobic regions that are presumed to have a structural function by inducing DMV formation [85] and anchoring the RTC to the membrane [86,110,111]. More recently, isolated RTC contained replicase subunits that were involved in DMV formation (nsp2 and nsp3) or viral replication (nsp9 and nsp10) and were cosedimented with newly synthesized viral RNA in a heavy membrane fraction [112] which confirmed their association with DMV and their essential role in RTC function.

1.6. NONSTRUCTURAL PROTEINS OF EAV

The replicase gene, ORF1a and ORF1b, occupies 75% of the 5’ end of the EAV genome,. Translation of genomic RNA results in two large polyproteins, 187-kDa pp1a (1728 aa) and 345-kDa pp1ab (3175 aa). Expression of pp1ab occurs through a -1 ribosomal frameshift mechanism in the overlapping region of ORF1a and ORF1b [10]. The polyproteins undergo an extensive proteolytic processing by three virus-encoded proteases (nsp1, nsp2, and nsp4) resulting in 13 nsps [66,113] (Figure 1.6; Table 1.2).

The mature nsps are involved in the formation of a membrane-anchored RTC that directs viral genome replication and synthesis of a nested set of sg mRNAs [89,91]. The structural proteins are expressed from sg mRNAs whose genes are located downstream of the replicase gene. The ORF1a encodes two papain-like cysteine protease domains ("accessory proteases" located in nsp1 and nsp2) and a chymotrypsin-like serine protease ("main protease") in nsp4. The ORF1a protein is cleaved at seven sites resulting in eight cleaved end products, nsp1 to nsp8, plus a number of processing intermediates [110,111,114]. The ORF1b is processed into four major end products by nsp4 protease, including RNA-dependent RNA polymerase and NTPase/RNA Hel domains essential for viral RNA replication and mRNA transcription [10,11]. Immunofluorescence studies have shown that the ORF1b-encoded replicase subunits are localized in the perinuclear region of the EAV-infected cells suggesting that they may be associated with intracellular membranous compartments [87], most likely the ER.

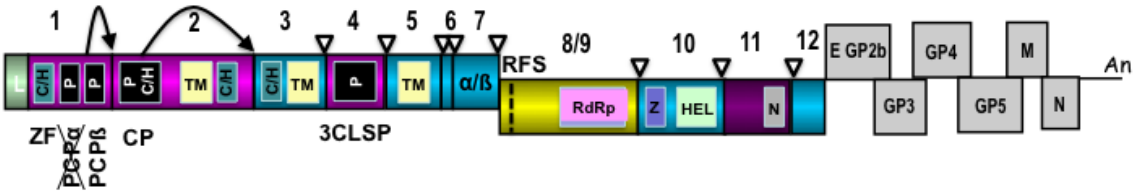

Figure 1.6. Schematic representation of EAV replicase polyproteins. The numbers of nsps are indicated above corresponding nsps. The predicted PCPβ and CP cleavage sites are indicated by black arrows. The 3CLSP cleavage sites are indicated by open arrowheads. The genes encoding structural proteins are depicted in grey. PCP, papain-like cysteine protease; CP, cysteine protease; 3CLSP, 3chymotrypsin-like serine protease; ZF, predicted zinc finger; C/H, cysteine/histidine-rich clusters; TM, predicted transmembrane domains; P, protease domain; Z, zinc-binding domain; N, NendoU. Figure modified from *Nidoviruses* book chapter [26] with permission.

Table 1.2. Nonstructural proteins of EAV.

ORF	Nucleotide position (bp)[a]	Protein	Protein length (aa)	Predicted M.W. (kDa)
ORF1a	225-5399 (5175)	1a polyprotein	1728	190
ORF1b	5405-9751 (4347)	-	-	-
ORF1ab	225-9751 (9527)	1ab polyprotein	3176	349.3
Nonstructural proteins	225-1004 (780)	nsp1	260	28.6
	1005-2717 (1713)	nsp2	571	61.4
	2718-3416 (699)	nsp3	233	25
	3417-4028 (612)	nsp4	204	21
	4029-4514 (486)	nsp5	162	18.1
	4515-4580 (66)	nsp6	22	2.3
	4581-5255 (675)	nsp7	225	25.2
	5256-5405 (150)	nsp8	50	5.5
	5256-7333 (2078)	nsp9	693	76.8
	7334-8734 (1401)	nsp10	467	50.5
	8735-9391 (657)	nsp11	219	24.2
	9392-9748 (357)	nsp12	119	12.5

[a] The nucleotide positions are based on the sequence of the experimentally derived EAV VBS strain (GenBank accession number: DQ846750).

1.6.1. Nsp1

The 29-kDa nsp1 (260 aa) is the first viral protein expressed and is the most N-terminal replicase cleavage product produced. It contains an "accessory protease" which is not involved directly in proteolytic processing of RdRp and helicase. Three domains have been identified in the nsp1 region: predicted zinc finger (ZF) domain, papain-like cysteine protease (PCP) α and PCPβ. The predicted ZF domain present near the N terminus of nsp1 contains four Cys and His residues [26]. ZFs found in many cellular transcription factors are involved in protein-nucleic acid and protein-protein interactions [115]. The nsp1 is released from the replicase polyprotein by the autocatalytic activity of PCPβ, which is responsible for cleavage of nsp1/2, located in its C-terminal domain [110,116]. The cleavage and release of nsp1 from the replicase polyprotein was found to be essential for viral RNA synthesis [117]. In EAV, the PCPα is functionally inactive due to its loss of an active Cys site during virus evolution [118]. However, PCPα may

possess RNA-binding and/or protein-binding activities (along with PCPβ), serving as a platform for the ZF during transcription. Therefore, the structural integrity of nsp1 is essential since all three domains are required for trans-activation of sg RNA synthesis [119]. It has been reported that nsp1 is essential for sg RNA transcription but dispensable for genome replication [119]. The nsp1 not only plays a crucial role in processing of replicase polyprotein and production of sg mRNA but it is also important for virion biogenesis [119] [117]. Nsp1 is the only EAV replicase subunit that localizes both in the nucleus and cytoplasm where it associates with modified cytoplasmic membranes of the replication complex [84,120]. During the early stages of infection, nsp1 is primarily located in the nucleus while its cytoplasmic localization, especially in the perinuclear region, becomes evident later in infection [120].

1.6.2. Nsp2

The 61-kDa nsp2 serves as a cofactor in the processing of the downstream part of the polyprotein directed by the nsp4 protease [85]. The nsp2 contains two hydrophobic regions around aa 450 and 490 and a main hydrophobic region between aa 520 and 640, large enough to span the lipid bilayer several times. However, the exact topology of this protein needs further characterization [85]. The N-terminal domain of nsp2 contains cysteine protease activity responsible for cleavage of the nsp2/3 site [121]. Therefore, nsp2 is released from the polyprotein by internal cysteine autoprotease activity [110]. In the major processing pathway, the mature nsp2 acts as cofactor for the processing of the nsp4/5 site by the nsp4 serine protease (SP). The nsp2 interacts strongly with nsp3 or nsp3- containing precursors (e.g. nsp3-8), a property that may be required for processing the nsp4/5 site by the nsp4 SP (Figure 1.7). When there is no interaction between nsp2 and nsp3-8, its internal site nsp4/5 cannot be cleaved and further processing of the replicase subunits occurs via the minor processing pathway (Figure 1.7).

1.6.3. Nsp3

The 22-kDa nsp3 is highly hydrophobic and is presumed to be a tetra-spanning transmembrane molecule [122]. It contains four conserved cysteine residues in the predicted first luminal domain (aa 853 to 902) that are likely to be involved in membrane

pairing and DMV formation [122]. Due to the multiple spanning nature of the protein, nsp3 is considered to play a key role in the interaction between the EAV RTC and host cell membranes. Site-directed mutagenesis studies have shown that mutation of nsp3 impairs the interaction of the protein with the ER, disrupts the formation of DMVs, affects replicase polyprotein processing and inhibits viral RNA synthesis [85,122]. It is possible that the N-terminal domain (aa 833 to 993) of nsp3 could function as a signal sequence for membrane insertion of nsp2/3 polyprotein before its cleavage by nsp2 [122]. However, the mechanism of interaction between nsp3 and the membranes or with other replicase subunits involved in DMV formation remains poorly understood.

1.6.4. Nsp4

The 33-kDa nsp4 contains chymotrypsin-like SP activity at the N-terminal domain. As the protease name indicates, the main catalytic residue of this C-like protease in arteriviruses is Ser. Nsp4 is the "main protease" which controls the production of the viral RNA-dependent RNA polymerase and RNA helicase [66,123]. It is responsible for processing the polypeptides (nsp3-8 and nsp3-12) that remain after nsp1 and nsp2 have been autocatalytically released from pp1a and pp1ab [65,110,111,114,116,121]. The nsp4 SP cleaves at five sites in the ORF1a protein [114] and three sites in the ORF1b protein [111]. The nsp4 SP processes the C-terminal half of the ORF1a (nsp3-8) protein via two alternative pathways (Figure 1.7). In the major processing pathway, nsp2 associates with nsp3-8 (96 kDa) as a cofactor which triggers nsp4 SP to cleave the majority of nsp3-8 precursors at the nsp4/5 site resulting in nsp3-4 (50 kDa) and nsp5-8 (44 kDa) intermediates. Subsequently, the nsp5-8 is cleaved at the nsp7/8 site while the nsp5/6 and nsp6/7 are inaccessible to the protease [111]. In the minor processing pathway, the nsp4/5 site remains intact while the nsp5/6 and nsp6/7 sites are cleaved (Figure 1.7) [111].

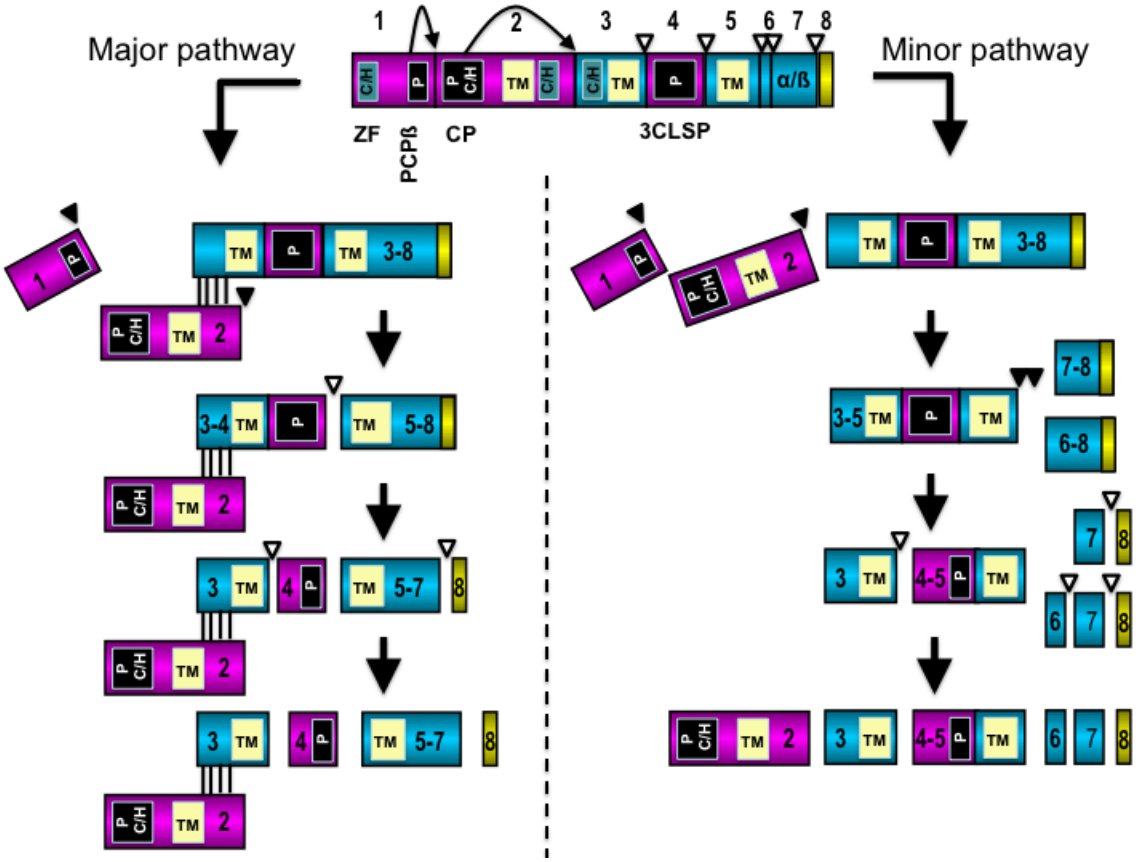

Figure 1.7. Proteolytic processing of EAV replicase polyprotein pp1a through the major and minor pathways. The proteases involved in processing are depicted in a black box with "P". The PCPβ and CP cleavage sites are indicated with black arrowheads. The 3CLSP nsp4 cleavage site is indicated by open arrowheads. PCP, papain-like cysteine protease; CP, cysteine protease; 3CLSP, 3chymotrypsin-like serine protease; TM, predicted transmembrane domains. Figure modified from *Nidoviruses* book chapter [26] with permission.

1.6.5. Nsp5, nsp6, nsp7α/β and nsp8

The processing intermediate nsp5/6/7/8 is a result of cleavage of the nsp4/5 junction upon association of nsp2 as a cofactor with nsp3-8. In the major pathway, nsp3/4 and nsp7/8 junctions are cleaved, but not the nsp5/6 and nsp6/7; therefore, cleaved nsp6 and 7 are not generated. In the minor pathway, nsp4/5 is not cleaved; instead, nsp4 cleaves the nsp3/4, nsp5/6, nsp6/7, and nsp7/8 junctions of the nsp3-8 intermediate

producing cleaved nsp6 and nsp7 [111]. Fully processed nsp5, nsp6, nsp7, and nsp8 are approximately 41, 3, 25, and 5.5 kDa, respectively [110].

The nsp5 contains a significant portion of the highly hydrophobic domain suggesting a role in the membrane association of the EAV replication complex [86,110]. Moreover, the presence of hydrophobic nsp5 in the N-terminus of processing intermediates, like nsp5-8, nsp5-7 and even larger intermediates such as nsp5-12, supports its probably association with the intracellular membrane [86].

Little is known about the nsp6 and nsp8 proteins [110]. Currently, there are no references to either protein in the literature.

An internal cleavage site (nsp7α/β) has been identified in mature nsp7 which is cleaved by nsp4 protease and produces nsp7α (123 aa; ~13.5 kDa) and nsp7β fragments corresponding to the N- and C-terminal regions of nsp7, respectively [113]. Most recently, the solution structure of nsp7α, the most conserved region of nsp7, has been determined by Nuclear Magnetic Resonance (NMR) [124]. The nsp7α contains four hydrophobic regions needed for correct folding of the proteins; it has a unique conformation consisting of three α-helices packed against a mixed β-sheet [124]. Although this study did not reach a definite conclusion about the function of nsp7, it confirmed that nsp7α is critical for arterivirus RNA synthesis [124].

1.6.6. Nsp9

The 80-kDa EAV nsp9 (aa 1678 to 2370 of pp1ab) contains the RdRp domain which functions as the catalytic subunit of the viral RTC and directs viral RNA synthesis in conjunction with other viral proteins and host cellular proteins. The EAV nsp9/RdRp initiates RNA synthesis by a *de novo* mechanism involving homopolymeric templates in a template-specific manner. Increased intracellular concentration of Zn^{2+} can block the initial step of viral RNA replication carried out by nsp9/RdRp [125].

1.6.7. Nsp10

The 51-kDa EAV nsp10 contains a predicted zinc-binding domain (ZBD) in its N-terminus and the nucleoside triphosphate-binding/helicase (Hel) motif in its C-terminal domain [10,11,126]. The nsp10 is the most conserved replicase subunit of the viral RNA

synthesis machinery [127,128,129]. The nsp10 has ATPase and nucleic acid duplex-unwinding activities that require the presence of 5' single-stranded regions indicating 5'-3' polarity of the reaction [130]. The ZBD region, especially the 13 conserved Cys and His residues that are most likely to be associated with zinc binding, is critical for ATPase and duplex-unwinding activities of the C-proximal helicase domain [10,11,126,131]. Reverse genetic studies have shown that mutation of conserved Cys/His residues in ZBD disrupted interactions between the ZF and enzymatic domains, thus completely blocking viral RNA synthesis and virion biogenesis [126,131]. Taken together, the nsp10-associated ZF domain has multiple functions specifically involved in viral RNA replication, sg mRNA transcription and virion biogenesis [126].

1.6.8. Nsp11

The 26-kDa nsp11 is considered as a multifunctional protein with a crucial role in viral RNA synthesis. The nsp11 contains a highly conserved endoribonuclease (NendoU; *n*idoviral-*endo*nuclease specific for *U*) domain which is not present in other RNA viruses and is therefore considered a unique genetic marker of the order *Nidovirales* [132,133]. The NendoU possesses pyrimidine (uridylates in particular)-specific endoribonuclease activity independent of divalent cations (e.g. Mn^{2+}) *in vitro* [134]. Studies using reverse genetics have shown the importance of NendoU activity for viral RNA synthesis [132,134]. However, identification of substrate and molecular characterization of NendoU still remain unclear.

1.6.9. Nsp12

Little is known about the 12-kDa nsp12 of arteriviruses. There are no current references available in the literature.

1.7. STRUCTURAL PROTEINS OF EAV

The ORFs encoding the structural proteins of EAV are located downstream of ORF1a and 1b that encode viral replicase proteins. The ORF2a, 2b and 3 through 7 are expressed from a 3' co-terminal nested set of subgenomic mRNAs. The viral RNA genome is packaged by the N protein, encoded by ORF7, into an icosahedral core

surrounded by a lipid-containing envelope with small surface projections [135,136]. Six viral proteins, encoded by ORF2 to 6, have been identified in the EAV envelope (Table 1.3.) [57,58,137]. The envelope (E) protein is the third most abundant protein in the viral membrane and is encoded by ORF2a. The GP2b, GP3, and GP4 proteins, encoded by ORF2b, -3 and -4 respectively, are minor envelope glycoproteins that exist in equimolar amounts in virus particles [57,137]. The minor envelope proteins are covalently associated and form a heterotrimeric complex on the surface of the virion. The nonglycosylated membrane protein M and glycosylated GP5 protein are the major envelope proteins and are the most abundant envelope proteins. These major envelope proteins are presented as disulfide-linked heterodimers in virus particles [67]. Wieringa *et al.* [59] has shown that the major envelope proteins (GP5 and M) and the N protein are essential for EAV particle formation. In contrast, neither E protein nor the minor envelope proteins are required for production of viral particles since absence of either of these proteins did not inhibit incorporation of viral genomic RNA or change buoyant density or microscopic appearance of the virus [59]. In contrast, all major and minor structural proteins are required for production of infectious progeny virus as has been shown by individually knocking out the expression of each structural protein separately [59].

Table 1.3. Structural proteins of EAV.

ORF	Nucleotide position (bp)*	Protein	Protein length (aa)	Predicted M.W. (kDa)
ORF2a	9751-9954 (204)	E	67	7.4
ORF2b	9824-10507 (684)	GP2	227	25.0
ORF3	10306-10797 (492)	GP3	163	17.9
ORF4	10700-11158 (459)	GP4	142	15.6
ORF5a	11112-11291 (180)	ORF5a	59	6.5
ORF5	11146-11913 (768)	GP5	255	28.0
ORF6	11901-12389 (489)	M	162	17.8
ORF7	12313-12645 (333)	N	110	12.1

* The nucleotide positions are based on the sequence of experimentally derived EAV VBS strain (GenBank accession number: DQ846750).

1.7.1. Minor envelope proteins

E protein

The EAV E protein is a small 8 kDa (67 aa) protein encoded by ORF2a [58]. ORF2a and ORF2b are both expressed from a bicistronic mRNA2. The E protein lacks N-linked oligosaccharide side chains and its single cysteine residue does not form intermolecular disulfide bonds. E protein is stable, highly hydrophobic and is predicted to be an integral membrane protein with an uncleaved signal-anchor sequence in the central part of the molecule (Figure 1.8). The E protein could be either a type III integral membrane protein or it may span the lipid bilayer twice with both termini located in the cytoplcasmic face of the membrane [58]. It contains a conserved site for myristoylation in the N-terminal domain followed by a phosphorylation site for casein kinase II [138]. The E protein is found in intermediate amounts in infected cells [58]. E protein along with GP2 protein is essential for production of infectious progeny virus [58]. Data suggest that the E protein is noncovalently associated with the GP2, GP3 and GP4 trimeric complex. In the absence of the minor envelope protein complex, the amount of

E protein in viral particles is diminished by 60 to 80 %. Similarly, the absence of E protein completely blocks the incorporation of the minor envelope proteins (GP2, GP3 and GP4) into viral particles [59].

GP2

The GP2 protein is a 25 kDa minor envelope protein encoded by ORF2b (Figure 1.8). GP2 is a type I membrane glycoprotein with a single N-glycosylation site at position 155 (Asn-155) [139]. It has three amino-terminal (extracellular) cysteine residues likely to be important for dimerization and protein function and one in its transmembrane anchor domain [139]. The Cys-102 is responsible for the cystine bridge with the GP4 protein while Cys-48 and Cys-137 form an intramolecular disulfide bond [140]. The GP2 protein occurs in several distinct conformations, as four monomers as a result of different disulfide-bonded structures and as a disulfide-linked dimer [139]. However, only the dimeric form of GP2, which is associated with GP3 and GP4 proteins as a heterotrimeric complex, is assembled into viral particles and the GP2 monomers are retained in the endoplasmic reticulum of infected cells [139]. GP2 is abundant in EAV-infected cells, but is expressed in low amounts in viral particles. It has been shown that GP2 protein is not essential for viral RNA replication and transcription [58,141]. Sequence comparison analysis indicated that the GP2 protein is highly conserved between EAV isolates [142].

GP3

The GP3 is encoded by ORF3 and is a membrane-associated protein of 36 to 42 kDa with six potential N-glycosylation sites, Asn-28, Asn-29, Asn-49, Asn-96, Asn-106 and Asn-118 [137,143]. The membrane topology of GP3 proteins has still not been clearly demonstrated. The protein could be either a class II protein, anchored into the lipid bilayer by its uncleaved amino-terminal signal sequence, or a class IV protein, possibly embedded by both sides of the hydrophobic terminal domains (Figure 1.8) [137,143]. While the GP3 protein has two putative N-myristoylation sites and three casein kinase II phosphorylation motifs, it is unclear whether there are active sites. Little is known about the function of this protein; however, inactivation of ORF3 expression

inhibited the production of infectious virus particles indicating that GP3 protein has an essential role in the viral replication cycle.

GP4

The GP4 protein, encoded by ORF4, is a typical class I integral membrane glycoprotein with amino-terminal signal sequence and its predicted carboxy-terminal hydrophobic membrane anchor (Figure 1.8) [137]. Three of the four predicted N-glycosylation sites (Asn-33, Asn-55, Asn-65 and Asn-90) are functional and produce a fully glycosylated protein with a molecular mass of 28 kDa [137]. However, Wieringa *et al.* [137] reported that N-glycosylation of the GP4 protein is an inefficient process and only a few portions of the protein acquire N-linked glycans in EAV-infected cells. Moreover, only the fully glycosylated form of GP4 is found in virus particles, which indicates that a small fraction of the ORF4 products produced in EAV-infected cells are incorporated into virus particles [137]. The function of GP4, as well as the GP3 protein, is not well characterized, but both are essential in the viral replication cycle.

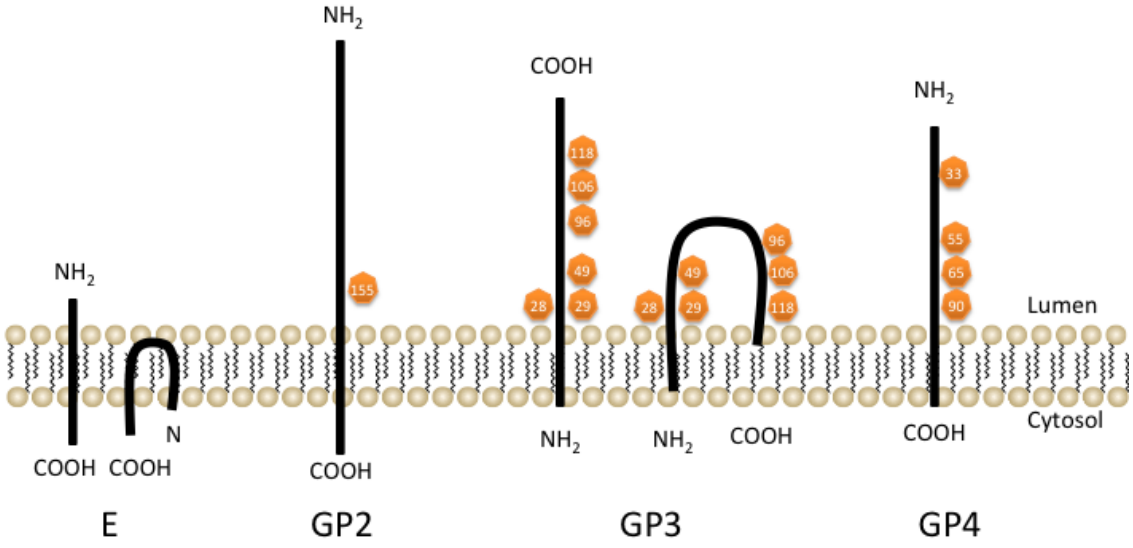

Figure 1.8. Predicted membrane topology of minor envelope proteins: E, GP2, GP3 and GP4 proteins. Two alternative predictions of E protein and GP3 membrane topology are shown. Putative N-glycosylation sites are indicated in yellow with corresponding amino acid positions.

GP2/GP3/GP4 heterotrimeric complex

The GP2, GP3 and GP4 proteins are incorporated into virions as a covalently associated heterotrimeric complex and lack of one of the components blocks the successful incorporation of the other minor envelope proteins [59]. After the release of virus particles from infected cells, GP3 becomes disulfide-linked to the GP2/GP4 heterodimers which results in a 66-kDa complex consisting of covalently bound GP2, GP3 and GP4 [144]. Due to this post-assembly modification, both GP2/GP4 heterodimers and GP2/GP3/GP4 heterotrimers are detected in EAV particles [144]. The cystine bridges play essential roles in the formation and stabilization of the trimeric complex. The cysteine residues at positions 48 and 137 (Cys-48 and Cys-137, respectively) of GP2 are linked by an intrachain disulfide bond while the cysteine residue at position 102 (Cys-102) of GP2 forms an intermolecular cystine bridge with one of the cysteines of the GP4 protein [140]. The covalent association of GP3 with the GP2/GP4 heterodimer likely occurs through the GP4 protein; however, the precise cysteine residue forming the intermolecular disulfide bond between GP4 and GP3 has not yet been determined (Figure 1.9). Similarly, the cysteine residue of GP4 that interacts with Cys-102 of GP2 has not been identified. The GP2/GP3/GP4/E heterotrimeric complex is most likely involved in the virus entry process into the cell based on the observation that it is not required for EAV virus particle formation, but is essential for production of infectious progeny virus.

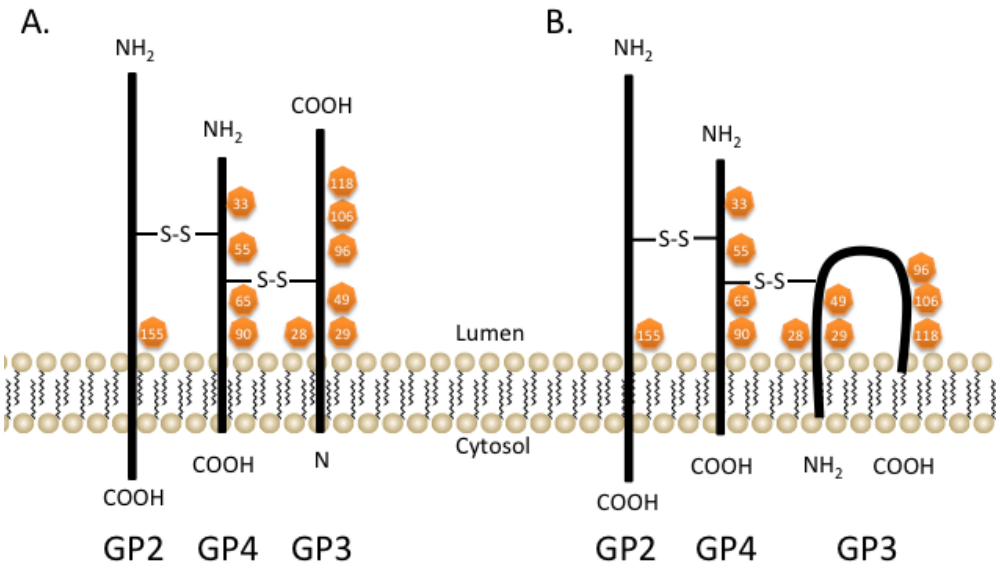

Figure 1.9. Two predicted models of GP2-GP3-GP4 heterotrimer. The two alternative models differ in membrane topology of GP3 that is currently not determined. The GP3 protein may be either a class II membrane protein (A) or a class IV membrane protein (B). The intermolecular cystine bridges are depicted arbitrarily with disulfide bonds (S-S) since the Cys positions have not yet been determined. N-glycosylation sites are indicated in orange with corresponding amino acid positions. Modified from Wieringa *et al.* [144] with permission.

A novel structural protein GP5a

A detailed computational analysis revealed an additional ORF which overlaps the 5' end of ORF5, named ORF5a, that is conserved in all arterivirus species [81]. The ORF5a protein is 59 aa long and is likely to be expressed from the same subgenomic mRNA (sg mRNA5) as the GP5 protein, possibly involving leaky ribosomal scanning. The ORF5a protein is predicted to be a type III membrane protein with a short (5-12 aa) amino terminal domain into the lumen, a central signal-transmembrane sequence and a carboxy-terminal domain into the cytosol (Figures 1.10 and 1.11) [81]. The function of this protein is yet to be characterized, but studies using reverse genetics suggested that this novel protein may be the eighth structural protein of arteriviruses and is important for arterivirus infection [81].

Putative Type III Membrane Protein

```
EAV       MFFYDWYVGLNDVIYDCIAILALGCAITCLLLILHRSALHRLHLVYADGSRRYCQFAAI    aa 59
PRRSV-NA  MFKYVGEMLDRGLLLAIAFFVVYRAVLFCCARQRQQQQQLPSTADLQLDVM aa 46-51
PRRSV-EU  MFSQIGAFLDSALLLLVAFFAVYRLVLVLCRWQRRQLDIPIHI aa 46
LDV       MFEEIGQWLDTITVIAILFYFVFSLYRKCLRRRQQLNQEFDLQLNLV aa 47
SHFV      MFREIGDSVDRFVPHLIYIYLMVLCAFLCLYYIQQHRRIREQHRYDLDQHIKVSVIAAESDHKP aa 64
```

Luminal NH2-terminal domain (aa 5-12) | Signal-anchor/TM domain (19-22 aa) | Cytoplasmic carboxy-terminal domain (13-31 aa)

Figure 1.10. Amino acid sequences of ORF5a protein of five representative arterivirus sequences. The ORF5a is predicted to be a type III membrane protein and the predicted transmembrane domain is indicated in yellow. The lengths, variable among species, of amino-, caryboxy-terminal and signal-anchor/transmembrane domains are indicated. Figure adapted from Firth *et al.* (2011) with permission [81].

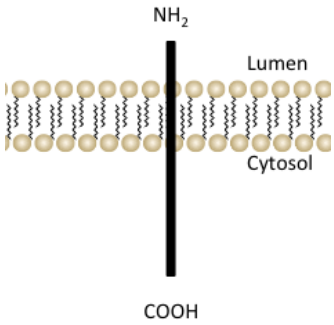

ORF5a

Figure 1.11. Predicted membrane topology of ORF5a protein. The ORF5a protein is predicted to be a class III membrane protein with the carboxy-terminal domain in the cytosol and the amino-terminal domain in the lumen.

1.7.2. Major envelope proteins

GP5

The 30- to 42-kDa GP5 protein is encoded by ORF5 and contains one or two potential N-glycosylation sites (Asn-56 and Asn-81). It is known that most of the laboratory adapted EAV strains contain only the N-linked sugar moiety at position Asn-56 [74,145,146]. A third potential N-glycosylation site at aa 73 (Asn-73) was observed in five EAV isolates from clinical specimens obtained from the 2006-2007 EVA occurrence in the USA [63]. GP5 is one of the most abundant proteins in the EAV particle. The GP5 protein is a type IV integral membrane protein with triple-membrane spanning domains from aa 116 to 181 (Figure 1.12) [57]. The ectodomain of GP5 is 95 aa long and contains an N-terminal signal sequence that is cleaved [68]. The smear appearance of the GP5 protein after analysis by denaturing SDS-PAGE, is due to the addition of poly-N-acetyllactosamine during its transport through the secretory pathway [57,67]. However, the function of poly-N-acetyllactosamine modification of the GP5 protein is unclear. The GP5/M forms a disulfide-linked heterodimer in the virus particle [67]. Proper posttranslational modification and folding of the GP5 protein occurs only in the presence of the M protein suggesting that the latter may act as its essential scaffold protein [73]. Studies using EAV chimeras have shown that replacement of the GP5 ectodomain with that of different arterivirus species did not alter the cell tropism of EAV, indicating that GP5 is not involved in receptor binding [147].

Equine neutralizing antibodies and monoclonal antibodies against EAV bind to the N-terminal hydrophilic ectodomain (aa 19 to 115) of GP5 [74,145,148,149,150]. Four distinct neutralization determinants of the virus have been identified: aa 49 (site A), 61 (site B), 67 to 90 (site C) and 99 to 106 (site D) [74,145,148,149,151,152]. Except for site A located in the C_1 region, these sites are located in the V_1 variable region (aa 61-121) within the second half of the N-terminal ectodomain of GP5. Site D expresses several overlapping linear epitopes [145,151] in the protein that may possibly interact with three other sites to form conformational epitopes [74].

The membrane (M) protein

The 16-kDa M protein is encoded by ORF6. The M protein is the most highly conserved envelope protein of arteriviruses [57]. The M protein has three internal membrane-spanning segments and a short amino terminus exposed at the viral surface (10 to 18 aa long) and its carboxy terminus (approximately 72 aa long) is buried within the virus interior (Figure 1.12) [34,57]. It lacks N-glycosylation sites and contains five methionines and one cysteine. The M protein forms a disulfide-linked heterodimer with the GP5 protein in the virus particle [67]. The M protein also forms covalently linked homodimers, but only the GP5/M heterodimers are incorporated into virus particles. It is possibly involved in virus budding.

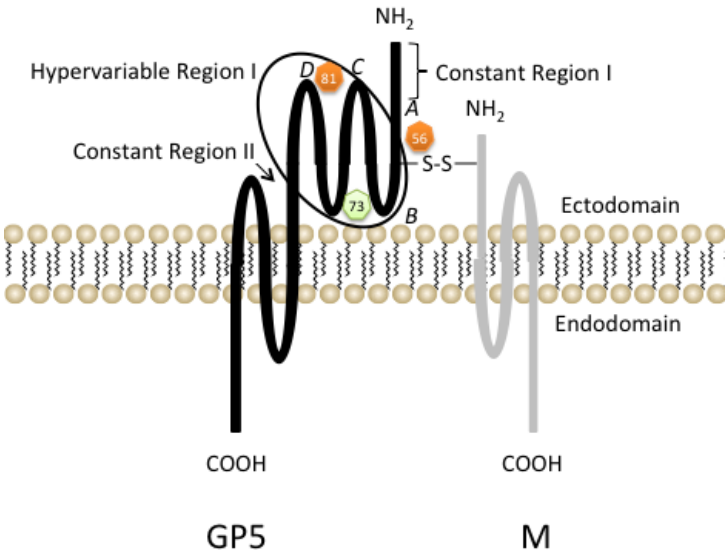

Figure 1.12. Predicted structure of GP5 and M heterodimer. The neutralization sites A (aa 49), B (aa 61), C (aa 67-90) and D (aa 99-106) are shown. The predicted N-glycosylation sites (Asn-56 and Asn-81) are depicted with orange circle. The green circle represents the N-glycosylation site (Asn-73) found in isolates of a recent EVA outbreak. The GP5 and M proteins are covalently linked by a disulfide bond (S-S) formed between Cys-34 in the GP5 protein and Cys-8 in the M protein. Modified from Balasuriya *et al.* [76] with permission.

GP5/M heterodimeric complex

The GP5 and M proteins form a disulfide-linked heterodimer and occur in equimolar amounts in the virion (Figure 1.12). These proteins associate with each other with different kinetics and efficiencies in infected cells. Newly synthesized GP5 proteins rapidly interact with M protein, while newly produced M proteins are incorporated slowly into the heterodimer. Presence of a high concentration of M protein in the ER is a prerequisite for efficient recruitment of GP5 protein into the GP5/M heterodimeric complex [67]. The interaction between the two major envelope proteins is determined by the formation of the disulfide bridge between the cysteine residue at position 8 (Cys-8) of M and Cys-34 of GP5 since abolition of either cysteine residue completely inhibited heterodimerization of the two proteins [68].

The GP5/M heterodimeric complex is essential for EAV assembly where the interaction between nucleocapsid and viral envelope is most likely to be mediated by the disulfide-bonded GP5/M heterodimers since the minor envelope proteins are not required for generation of virus particles. Covalent association of the GP5 and M proteins is indispensable for the production of infectious arteriviruses [68,153]. In addition, expression of both GP5 and M proteins as a heterodimer is required for induction of neutralizing antibodies [154]. Nonetheless, peptides derived from just the GP5 ectodomain were also able to induce neutralizing antibodies to EAV in horses [148,155].

The nucleocapsid (N) protein

The 14-kDa (110 aa) N protein, encoded by ORF7, is the most abundant viral protein in EAV-infected cells. The N protein is synthesized in the cytoplasm of EAV-infected cells and possibly binds to envelope protein domains exposed to the cytoplasm during the budding process. Most of the N protein localizes in the cytoplasm of infected cells, while a small fraction resides in the nucleus where it seems to accumulate in nucleoli. This suggests a possible post-translational modification of some molecules of N protein, such as phosphorylation. An important function of the N protein is the packaging of the viral genome into a putative icosahedral core. The N-terminal domain (aa 1-47) of the N protein, the least conserved region, is thought to interact with the viral genomic RNA during nucleocapsid assembly [120]. The C-terminal (aa 49-110) of the

EAV N protein forms a dimer consisting of a β-sheet that is capped and flanked by α-helices. In the crystal structure, the N protein forms a dimer-dimer, in other words a tetramer, organized via a quasi-twofold axis [156]. The N protein comprises more than 30% of the protein molecules in an EAV particle.

1.8. GENETIC VARIATION AND MOLECULAR EPIDEMIOLOGY OF EAV

Although only one major serotype of EAV has been recognized to date [157], there is considerable antigenic variation among EAV field strains. Genomic variation among field strains of EAV has been demonstrated [142,158,159,160,161,162] by comparative sequence analysis of ORFs 2 to 7. ORF5 was found to be a main target due to the variable regions within ORF5; it is valuable for tracing the origin of EAV strains [80,142,146,158,159,163,164,165,166,167,168]. Phylogenetic analyses based on M and N protein genes confirmed EAV strain variation [159]. Distinct geographic groups of EAV isolates from Europe and the USA were separated based on sequence analysis of the M protein gene [161]. Comprehensive phylogenetic analyses have identified two phylogenetic groups: Group I consists of viruses isolated mainly in North America and Group II consists mainly of viruses isolated in Europe [146,158,164,166,169]. In addition, several subgroups have been identified within each group. However, American lineage viruses were isolated in Europe and vice versa indicating interchange of viruses between the two continents, which is thought to have resulted mainly as an outcome of the movement of carrier stallions and/or shipment of virus-infective semen. The nucleotide identity between North American and European isolates of EAV is about 85% [158,164]. However, a genetically very diverse strain of EAV has been isolated from the semen of a donkey in South Africa which has been reported to have nucleotide identity of only 60-70% compared to sequences of EAV strains isolated from North American and European horses and donkeys [170].

1.9. EQUINE VIRAL ARTERITIS

1.9.1. Seroprevalence, world distribution and modes of transmission

EAV, the causative agent of EVA is distributed throughout the world [171,172,173,174,175,176], but the seroprevalence of EAV infection varies between countries and horses of various breeds and ages. There is a marked difference in seroprevalence of EAV infection between Standardbred and Thoroughbred horses in countries in which this has been studied. EAV is endemic among adult Standardbred horses in the United States, (seroprevalence of 78 to 84%), whereas only 0 to 5% of Thoroughbred horses are seropositive [177]. Antibodies against EAV have been found in horses, donkeys and mules in South Africa [176,178,179,180] but not in free-ranging or captive zebra species in southern Africa [181,182]. EAV-specific neutralizing antibodies were detected in 51 zebras (24%) of the Burchell's zebra population in the Serengeti National Park [183]. There is only one report of the detection of EAV nucleic acid from aborted alpaca fetal tissue by reverse-transcription polymerase chain reaction (RT-PCR) and neutralization antibodies were found in a high percentage of its cohorts [184].

Transmission of EAV between horses occurs primarily via either the respiratory or venereal route [77,185,186,187,188,189]. Respiratory transmission of EAV occurs by dispersal of infectious respiratory tract secretions from acutely infected horses. This is the most important and primary route of dissemination of EAV during outbreaks [187]. High titers of EAV are present in respiratory secretions for some 7 to 14 days during the acute phase of infection [177,187]. Similarly, the virus may be detected in the buffy coat for up to 28 days after exposure with some strains of EAV [177,190]. The second most important mode of transmission of EAV is venereal, from acutely or chronically infected stallions. Venereal transmission of EAV occurs during natural breeding or by artificial insemination with infective semen from persistently infected stallions [188,189]. Persistently infected stallions shed virus solely by the venereal route and up to 85 to 100% of seronegative mares bred to long-term carrier stallions seroconvert within 28 days after breeding. Persistence of virus in semen of carrier stallions does not appear to cause any short- or long-term virus-related fertility problems [177,188]. Persistently infected stallions are the primary natural reservoir of EAV; they disseminate and perpetuate the

virus in equine populations. Recent study by Broaddus *et al.* (2011) demonstrated that there could also be a risk of EAV transmission resulting from *in vivo* embryo transfer from a donor mare inseminated with EAV infective semen [191]. Dissemination of EAV by indirect contact through contaminated fomites (e.g. personnel, vehicles, twitches, apparel and shanks) is believed to play a minor role; however, its significance varies between outbreaks [77,192,193]. Other sources of EAV can be an infected teaser stallion or nurse mare [77]. It has recently been reported that exposure of pregnant mares to EAV very late in gestation can result in transplacental transmission of the virus and congenital infection of the fetus [194].

1.9.2. Clinical signs

Equine viral arteritis is a contagious infectious disease of equids caused by EAV. The virus was first isolated during an outbreak of abortion and respiratory illness on a Standardbred breeding farm near Bucyrus, Ohio in 1953 [185,195]. The disease was named after the distinctive vascular lesions present in acutely infected horses [196]. Many years earlier, EVA was commonly referred to as “epizootic cellulitis-pinkeye” or as “equine influenza” [197,198]. EAV is present in equine populations in many countries throughout the world [77,177,199,200]. The outcome of EAV infection in horses ranges from subclinical infection to an influenza-like illness in adult horses, abortion in pregnant mares, and interstitial pneumonia or pneumoenteritis in young foals [77,194,201,202,203]. Development of clinical signs depend on a variety of factors including strain of virus, challenge dose, route of infection, age and physical condition of the horse(s) and environmental conditions [77,204]. The incubation period can range from 3 to 14 days (usually 6 to 8 days following venereal exposure) followed by development of pyrexia of up to 41°C (39-41°C) which may persist for 2 to 9 days. In addition to pyrexia, typical cases of the disease may exhibit all or any combination of the following signs: depression, anorexia, nasal and/or ocular discharge, conjunctivitis, rhinitis, leukopenia, periorbital or supraorbital edema, edema of the limbs, edema involving the scrotum and prepuce of the stallion and mammary glands of the mare, urticaria around the head, sides of neck and/or body, and abortion of pregnant mares [77,192,195,204,205,206]. The most consistent clinical features of EVA are pyrexia and leukopenia. Regardless of clinical severity,

most naturally infected horses recover spontaneously from EVA. However, the virus can cause a rapidly progressive pneumoenteric syndrome and severe fulminating interstitial pneumonia in neonatal foals [194,207] and foals up to a few months of age [208]. Abortion in pregnant mares may occur late in the acute phase or early in the convalescent phase of EAV infection [77,195,209,210]. Abortions have been documented anywhere from 3 to over 10 months of gestation following natural or experimental infection [77,210,211]. It has been shown that it is safe to vaccinate healthy pregnant mares up to 3 months before foaling and during the immediate postpartum period with a commercial modified live virus vaccine (MLV, ARVAC®, Pfizer Animal Health) but not during the last 2 months of gestation due to an increased risk of abortion [212]. In natural outbreaks of EVA, abortion rates have varied from less than 10% to between 50 to 60% [77]. Although mortality is very low in natural outbreaks of EVA, experimental inoculation with the experimentally derived EAV VBS strain can cause up to 60% case-fatality in adult horses [77,213].

1.9.3. Persistent infection

Persistence of virus in the semen of infected stallions is a unique feature of EAV infection. Frequency of the carrier state can vary from less than 25% to 65% in stallions exposed to EAV via the respiratory route [188,190,214,215]. The virus appears to be restricted to the male reproductive tract and is localized mainly in the ampulla of the vas deferens [77]. Not withstanding high neutralizing antibody titers in serum, carrier stallions continuously shed infectious virus in their semen. The virus is associated with the sperm-rich and not the pre-ejaculatory fluid fraction of semen. Duration of virus persistence can vary; carrier stallions can stop shedding virus in their semen weeks to years after infection with no evidence of reversion to a shedding status later. However, the mechanism of spontaneous viral clearance in persistently infected stallions has not yet been identified [77]. Many outbreaks are initiated following venereal transmission of infection to a susceptible mare by a carrier stallion. Subsequent spread of virus to seronegative cohorts occurs via the respiratory transmission route [78,79]. The carrier stallion is mainly responsible for maintenance and dissemination of EAV in the equine

population; thus, they are clearly central to the epidemiology of EAV infection [78,79,216].

Although the detailed mechanism of establishment of the carrier state in stallions is still unidentified, Little *et al.* [217] have reported that shedding of EAV in the semen of persistently infected stallions is testosterone-dependent [217,218]. Surgical castration of carrier stallions resulted in either viral clearance or significant reduction of virus shedding in their semen [218] has been convincing. The effects of testosterone on reproductive tissues, such as immunosuppressive activities or maintenance of susceptible host cell population, that could maintain EAV persistence have also been considered [219,220]. Other studies have related persistence to the interaction between the host immune response and EAV in the reproductive tract [190,221,222]. It was suggested that high levels of circulating testosterone is essential for long-term persistence but not for viral replication or persistence of intermediate duration [223]. Experimental infection of prepubertal and peripubertal colts with EAV have shown that the virus can replicate in the male reproductive tract for a variable period of time (intermediate duration) even in the absence of circulating concentration of testosterone similar to those of sexually mature stallions after clinical recovery [223]. However, none of the prepubertal colts maintained long-term virus persistence comparable to that of experimentally or naturally infected stallions [223]. Therefore, long-term persistent EAV infection does not occur either in colts exposed to the virus before the onset of puberty or mares, geldings or fetuses [177,189,218].

It is assumed that virus persists by continuously re-infecting susceptible tissues in the reproductive tract together with constant evolution of antigenic variants of the virus [79,80,164]. In contrast to the relative genetic stability of EAV during infection associated with respiratory transmission, significant evolution and genetic heterogeneity of EAV quasispecies occur during persistent infection of individual carrier stallions [78,79,80]. Sequence analyses of EAV isolated from semen of carrier stallions have demonstrated that there is a significant evolution of EAV quasispecies during long-term persistence that results in emergence of novel variants with divergent phenotypes responsible for major EVA outbreaks [79,80,224]. High rates of nonsynonymous changes occur in regions of GP3 and GP5 proteins [80,164] indicating that these viral

proteins are under strong selective pressure during establishment and maintenance of persistent EAV infection [74,80]. Particularly, amino acid changes in the GP5 protein that occur during persistent infection of stallions are found to be restricted to the critical V1 neutralization region [74,224]. It has also been observed that development of clinical signs of EVA was more common in susceptible mares bred to certain carrier stallions than others [189]. Thus, genetic variation of EAV during persistent infection results in both altered neutralization phenotype and emergence of variants of variable virulence phenotypes [80,164].

Persistent infection of cell cultures has been reported previously for numerous viruses including certain nidoviruses [101,225,226,227,228,229,230,231,232,233,234,235]. Since there is no information available about host and viral factors, other than testosterone, involved in establishment and maintenance of persistent EAV infection, Zhang *et al.* [236] developed an *in vitro* model system in an attempt to elucidate the mechanism of EAV persistence. This study showed that viral determinants are also critical in mediating persistent infection of EAV *in vitro*. Reverse genetic studies using an EAV infectious cDNA clone clearly demonstrated that amino acid changes in the structural proteins were responsible for the persistence in HeLa cells, indicating a multigenic effect on EAV persistence [236]. This *in vitro* model system could serve as a suitable method to determine viral and/or host factors involved in EAV persistence as well as possibly help to define the mechanisms of EAV persistence *in vivo*.

1.9.4. Pathogenesis

Most of the information on the pathology and pathogenesis of EVA is derived from experimental studies in horses inoculated with the experimentally derived Bucyrus strain of EAV [187,195,210,213,237,238,239]. The most frequently observed gross necropsy findings in horses inoculated with the Bucyrus strain of EAV are edema, congestion, and hemorrhage in subcutaneous tissues, lymph nodes, and viscera of the thoracic and abdominal cavities [195,206,213,239]. There is considerable variation in the quantitative distribution of EAV between experimental studies, which may reflect differences in the route of infection, virus dose, strain of virus, and quality of the

specimens and cell culture systems used for virus isolation. Apart from its incidental recovery from buffy coat cells [240,241], and with the possible exception of the reproductive tract of stallions and colts, EAV is not generally isolated after 28 days following infection.

The exact mechanism of EVA pathogenesis remains to be determined. The vascular lesions are likely caused by the direct effect of viral replication on vascular endothelium. EAV replicates in pulmonary macrophages and endothelial cells following respiratory infection and rapidly spreads first to the draining lymph nodes and then systematically by a cell-associated viremia [51,187,213,242]. Although endothelial cells and macrophages are the principal sites of virus replication, selected epithelia, mesothelium, and smooth muscle cells of the tunica media of smaller arteries, venules, and the myometrium may also be infected [76,242]. Increased vascular permeability and leukocyte infiltration resulting from generation of chemotactic factors leads to hemorrhage and edema around affected vessels [238]. The clinical manifestations of EVA likely reflect endothelial cell injury and increased vascular permeability; however, the relative roles and importance of direct virus-mediated endothelial cell injury and virus-induced vasoactive and inflammatory cytokines in the pathogenesis of EAV-induced vascular injury have not yet been clearly defined [76].

The pathogenesis of EAV-induced abortion is still controversial. Fetuses aborted after natural or experimental infection with EAV frequently do not show any gross or histopathological lesions [195,206,210,243,244]. Fetuses are usually partially autolyzed at the time of expulsion and may have increased peritoneal and pleural fluid, and petechial hemorrhages in the mucosal linings of the respiratory and digestive tracts and on the serosal lining of peritoneal and pleural cavities [195,206,210]. The placenta typically is grossly unremarkable and expelled with the fetus. Doll *et al.*[210] concluded that fetal expulsion is the result of a lethal fetal infection and not maternal factors such as fever, toxemia, or debilitation. However, Jones *et al.*[245] suggested that abortions result from an impaired uterine and placental blood supply due to systemic vascular necrosis in the mare. Coignoul and Cheville [243] also suggested that abortion may result from myometritis of the mare rather than fetal infection with the virus, based upon light and electron microscopic studies of tissues from the genital tracts, placentae and fetuses of

mares experimentally infected with experimentally derived Bucyrus strain of EAV. In contrast, MacLachlan *et al.*, [213] suggested that abortion likely results from direct infection of the fetus by EAV. Fetal stress and subsequent activation of the fetal hypothalamic-pituitary axis due to viral infection of the developing fetus likely contribute significantly to the pathogenesis of EAV-induced abortion.

1.10. IMMUNE RESPONSE TO EAV INFECTION

The immune response to viruses can be considered under two categories. The innate immune response, the first line of defense, plays an important role in the detection of invading pathogens and in limiting their spread. The second category is the adaptive immune response, the second line of defense, is responsible for total clearance of pathogens. While the innate immunity is activated immediately, the adaptive immunity takes longer to develop. While antibodies are clearly important in preventing reinfection with viruses, removal of virus-infected cells during acute infection typically is mediated by the cellular arm of the immune system.

1.10.1. Innate immune response

Natural EAV infection of horses primarily occurs via either the respiratory tract following exposure to infective secretions/excretions or the reproductive tract following venereal exposure [77,246]. Thus, it is the innate immune response of the mucosal lining of the respiratory and genital tracts that constitutes the first line of defense that EAV encounters in cases of natural exposure. There are few detailed studies that describe the innate immune response of horses to EAV or other viruses, thus information pertaining to innate antiviral immunity is largely derived from the study of other viruses of order *Nidovirales*.

The innate immune response is the first line of the host's defense against a virus infection; it also plays an important role in activation of the adaptive immune response. Type I IFNs (IFN-α and IFN-β) are major players in the innate immune response and are expressed in response to most intracellular infectious agents, especially viruses [247]. They induce expression of genes encoding antiviral proteins and also function as an important link between innate and adaptive immune responses. There is mounting

evidence that PRRSV circumvents the host innate response, resulting from inadequate induction of type I IFNs [248,249,250]. As a consequence, there is a delayed production of IFN-γ, cellular immunity and neutralizing antibodies [76,251], and in consequence, delayed viral clearance [250,252,253]. Additionally, it has been shown that PRRSV infection of alveolar macrophages fails to elicit any significant expression of genes encoding proinflammatory cytokines, including TNF-α [254,255]. Furthermore, the sensitivity and induction of IFN-α in porcine alveolar macrophages (PAMs) differ significantly among different strains of PRRSV [256]. Some of the North American PRRSV strains strongly down regulate the induction of IFN-α in PAMs [256].

Viral components are recognized by specific host pathogen recognition receptors (PRRs) that trigger the activation of IRF3, NF-kB and AP-1, three regulators of IFN-β expression. IFN-β is responsible for the induction of interferon stimulated genes (ISGs) that encode antiviral effectors important in limiting viral spread and in establishing an antiviral state in the infected cells as well in the neighboring non-infected cells.

In previous studies, it has been shown that EAV infects alveolar macrophages (AMΦ) after respiratory infection of horses, but recent *in vitro* studies using cultured equine AMΦ confirmed that although these cells were susceptible to infection, they were refractory to productive replication of EAV [257]. In contrast, productive replication occurred following EAV infection of cultured blood-derived equine macrophages (BMΦ) [257]. EAV infection of both equine AMΦ and BMΦ resulted in increased transcription of genes encoding proinflammatory mediators, including IL-1β, IL-6, IL-8 and TNF-α, with the release of substantial quantities of TNF-α into the culture medium [257]. Furthermore, virulent and avirulent strains of EAV induced different quantities of TNF-α and other proinflammatory cytokines (IL-1β, IL-6, IL-8), and the magnitude of the cytokine response of equine AMΦ and BMΦ to EAV infection reflected the virulence of the infecting virus strain [257]. These studies clearly show that cytokine mediators are produced by EAV infected equine cells and, presumably, these play an important role in determining the nature and severity of the outcome of infection. However, a more specific and detailed investigation into innate and adaptive immune responses to EAV has not been carried out.

1.10.2. Humoral immune response

The humoral immune response to EAV is characterized by the development of both complement-fixing (CF) and virus-specific neutralizing (VN) antibodies [157,258]. The CF antibodies appear between 1-2 weeks and peak 2-3 weeks after EAV infection in adult horses and ponies [157]. Interestingly, avirulent strains of EAV (e.g. MLV) stimulate a stronger CF antibody response than that elicited by virulent strains, such as the VBS of EAV [157]. The mechanism of EAV neutralization by specific antisera is not clear. Several *in vitro* studies indicate that neutralization of EAV is complement-dependent [259,260,261,262]. These studies have shown that EAV neutralizing activity of horse, hamster, guinea pig and rabbit antisera was decreased following heat inactivation, and restored by addition of fresh complement. Homologous complement appeared to be more efficient in neutralizing the sensitized virus than heterologous complement [157,263]. Complement dependent EAV neutralizing antibody activity is associated with the IgG fraction of late antiserum, but not with early antisera or their IgM and IgG fractions [261]. The requirement of complement for efficient virus neutralization is also dependent on the virus strain [176,263].

EAV infection in horses induces long-lasting immunity that protects against reinfection with all strains of the virus [76,196,264,265,266]. Appearance of neutralizing antibodies (7-14 days post infection) coincides with the disappearance of virus from the circulation of infected horses [240,267]. However, virus does persist in the reproductive tract of the carrier stallion for a variable period despite the presence of high titers of VN antibodies in serum [77]. The humoral immune response to structural EAV proteins in naturally or experimentally infected horses varies widely with the infecting EAV strain, the interval after infection, and the individual horse [150,221,268]. The variation in the antibody response to EAV structural proteins was also observed in horses immunized with the modified live EAV vaccine [221,268]. Vaccination of horses with either live attenuated virus strains or inactivated virus vaccines also induce long-term VN antibodies in horses [266,269,270]. In addition, horses immunized with recombinant GP5 protein (residues 55 to 98) or synthetic oligopeptides (residues 75 to 97) also developed neutralizing antibodies to EAV [148]. Foals acquire EAV-specific antibodies from the colostrum of seropositive (immune) dams and these antibody levels decrease with time.

Furthermore, passively acquired antibodies protect young foals that received colostrum from EAV seropositive mares against EAV infection confirming the importance of antibodies in protection against the disease [271,272]. However, VN antibodies are not detected in sera from foals prior to nursing suggesting that the passive immunity does not occur through the placenta *in utero* [271]. The maternally acquired antibody titer is high at 1 week of age and declines until no longer detectable after 2-6 months. The mean biological half-life of maternal antibodies in serum from foals was 32 days [272]. Foals that received colostrum should be vaccinated after maternal antibodies disappear since these antibodies in their serum are able to neutralize the vaccine virus [271]. The time to implement vaccination of foals is dependent on the duration of passively acquired immunity to EAV [272].

The humoral immune response to EAV is mainly directed to the major envelope proteins, GP5, M and N proteins [148,221,268,273,274,275,276]. Early studies on characterization of antigenicity and function of viral proteins using monoclonal antibodies (MAbs) have identified that neutralization determinants of EAV are located in the GP5 protein [149,151,152]. Different neutralization abilities of MAbs suggested that while they recognize different epitopes, they all recognized the GP5 protein. To induce neutralizing antibodies in mice, co-expression of GP5 and M in eukaryotic cells is required [73]. In contrast, non-neutralizing MAbs were directed to either the GP5 or N protein [74,145,149,151,152,273,277,278]. Initially, Balasuriya *et al.* [151] identified a critical neutralizing epitope present between residues 99 to 104 using MAbs, neutralization-resistant mutants and recombinant proteins of individual viral proteins. Amino acid mutations within this region were found in neutralization-resistant mutants [151,152]. Similarly, Chirnside *et al.* identified a linear epitope between residues 55 and 98 of the GP5 protein using the expression vector pGEX system [148]. Additionally, Glaser *et al.* [145] recognized that resistance to VN is associated with mutations around positions 99 and 100 based on testing different EAV isolates. Taken together, the dominant neutralizing domain was recognized as between aa residues 75 and 104 within the GP5 protein [145]. The study conducted by Balasuriya *et al.* [74] further characterized at least four potential neutralization sites on the N-terminal hydrophilic ectodomain of the GP5 protein, including aa 49 (site A), 61 (site B), 67-90 (site C), and

99-106 (site D). Most of the neutralization epitopes, except for aa 49, are located in the variable region V1 (aa 61-121) of the GP5 protein [74]. Studies using MAbs and reverse genetics have shown that aa changes at aa 61 (site B) and 67-90 (site C) of the GP5 protein influence the expression of conformational neutralizing epitopes and similar changes could also be responsible for antigenic variation among EAV field strains [69,74]. Therefore, it is likely that aa changes in the GP5 N-terminal ectodomain, especially if they occur during persistent infection in carrier stallions, contribute to the emergence of EAV strains with different neutralization phenotypes [69]. Besides neutralizing antibodies recognizing GP5 protein, horses also produce non-neutralizing anti-GP5 antibodies in response to EAV infection or immunization with an inactivated whole-virus vaccine [274,279].

Non-neutralizing antibodies which recognized N and M proteins [221,268,279] were detected as early as 14 days post-infection (dpi) and lasted at least 145 days in sequential sera from horses experimentally infected with EAV [276]. The M protein is the most consistently recognized among the EAV structural proteins by convalescent sera from EAV-infected horses [221,268] while response to the N and GP5 proteins was variable. The GP2 protein was poorly recognized by equine antisera [268]. The C-terminal domain of the M protein (aa 88-162) contains linear epitopes and is recognized by all EAV-specific horse antisera [280]. The ORF7 encoding the N protein is highly conserved among strains [159]. The portion between aa 1-69 of the N protein has been identified as the most immunoreactive region. Sera from persistently infected stallions consistently recognized GP5, N and M proteins [268]. In contrast, most convalescent sera from mares, geldings and stallions that did not become carriers after exposure to EAV recognized the carboxy-terminal region of the M protein [268].

Until now, characterization of the humoral immune response to EAV has been mainly focused on the structural proteins of EAV. The nonstructural proteins of EAV are the first viral proteins synthesized in cells infected with EAV and are essential to the viral replication cycle. Based on their expression levels and immunogenicity, it is reasonable to think that antibodies to nsps are generated during early infection. However, little is known about the equine humoral immune response to the nonstructural proteins. In response to this need, chapter 9 of the dissertation is focused on determining the humoral

immune response of EAV-infected horses to each of the nsps encoded by the ORF1a and ORF1b region of the viral genome.

1.10.3. Cell mediated immune response

Both innate and adaptive immunological responses are mediated by leukocytes, and among these cells, lymphocytes are the pivotal population [281]. Castillo-Olivares *et al.* [282] described EAV-specific cytotoxic T-lymphocyte (CTL) responses using peripheral blood mononuclear cells (PBMCs) from convalescent EAV-infected (experimental) ponies. The data showed that cytotoxicity induced by EAV-stimulated PBMCs was virus-specific, genetically-restricted, and mediated by $CD8^+$ T cells, and that EAV-specific CTL precursors persist for at least 1 year after infection in ponies [282]. Other than this study, there are no comprehensive studies that describe either the innate or cell-mediated immune (CMI) response to the MLV vaccine or to any other strains of EAV in horses.

In contrast to EAV, CMI responses to two other arteriviruses (PRRSV and LDV) have been characterized in detail [15,76,250,283,284]. PRRSV-specific T cell responses (both $CD4^+$ and $CD8^+$) in infected pigs occur between 4 and 12 weeks after infection and it is suggested that the unglycosylated M envelope protein may be an important target of the CMI response [283,284].

The murine arterivirus LDV causes lifelong persistent infection in mice and evades both humoral and cell mediated immune responses. The virus escapes the neutralizing antibodies by generating neutralizing-escape variants. Furthermore, during the acute phase of LDV infection, mice mount a strong CTL immune response that disappears within 30 days [285]. It has been suggested that this may be due to the clonal deletion (exhaustion) of LDV-specific $CD8^+$ T cells in the thymus as well as inhibition of IL-4 with suppression of helper T cells [15].

In summary, it has been clearly shown that PRRSV and LDV have their own mechanisms to evade the host immune response, but nothing is known about immune evasion by EAV in horses.

1.11. DIAGNOSIS OF EQUINE VIRAL ARTERITIS

1.11.1. Virus isolation

EAV infects a wide variety of cell types. The virus can be propagated in a number of continuous cell lines such as baby hamster kidney (BHK-21), African green monkey kidney (Vero and BSC-1), rhesus monkey kidney (LLC-MK2), rabbit kidney (RK-13 and LLC-RK1), equine ovary cells (EO), hamster lung (HmLu), and canine hepatitis virus-transformed hamster tumor cells (HS and HT-7) [60,103,145,261,265,286,287,288,289]. The cytopathic effect (CPE) and virus titer can vary significantly among cell lines. The CPE in EAV infected cells is usually characterized by rounding, vacuolation, increased optical density, refraction and detachment from culture vessels [60,61,290,291].

The presence of EAV in body fluid, tissue samples, blood, semen and placenta can usually detected by virus isolation in cell culture. The most appropriate specimens for virus isolation from live animals are nasopharyngeal swabs, conjuctival swabs and citrated or EDTA blood samples for separation of buffy coat cells. Isolation of EAV is currently performed using a high passage RK-13 cell line. Virus isolation (VI) is the current gold standard test, approved by World Organization for Animal Health (OIE), for the detection of EAV in semen from stallions and is the prescribed test for international trade [292].

1.11.2. Molecular diagnostics

Rapid and highly specific diagnostic systems for detection and characterization of EAV in diagnostic specimens are critical to ensure proper management of infected animals and to provide effective control measures of the disease. The modern nucleic acid-based tests are widely available to test clinical specimens for many infectious disease agents. The molecular diagnostic tests are often more sensitive, faster and less expensive. A number of sensitive standard RT-PCR, RT-nested PCR and real-time RT-PCR based assays have been developed for the detection of EAV nucleic acid in tissue culture fluid, nasal secretions and semen [293,294,295,296,297,298,299,300]. Initially, published primer sets were specific to the 3’ end of ORF1b of the viral polymerase gene [293,294,297,298]. However, more conserved regions of the viral genome were also

used as targets. Comparative nucleotide and amino acid sequence analysis of ORF7 (encoding N protein) deduced the aa sequences of ORF7 which are highly conserved and less likely to be the subject of antigenic variation. Therefore, both TaqMan®-based [299,300] and TaqMan® minor-groove-binding (MGB) group-based [301] real-time RT-PCR have been developed targeting ORF7 of the EAV genome. These assays have been compared and validated using a large number of equine semen and tissue culture fluid (TCF) samples. Lu *et al.* [302] compared specificity and sensitivity of two TaqMan®-based RT-PCR assays, described by Balasuriya *et al.* (T1) [299] and Westcott *et al.* (T2) [300]. Both T1 and T2 assays showed high sensitivities, 100% and 95.2%, respectively, for detecting EAV RNA in TCF. However, these assay were less sensitive, 93.4% and 42.6%, respectively, than the OIE-prescribed VI test (gold standard) for detection of EAV RNA in semen. In an attempt to increase the diagnostic sensitivities of the T1 and T2 assays for testing semen samples, Miszczak *et al.* [303] used three different one-step real-time RT-PCR reagents in combination with two different magnetic bead-based RNA extraction methods to test 409 semen samples. The study determined that under strictly defined conditions with respect to the nucleic acid extraction method and testing reagents, the T1 assay provides sensitivity equal to or slightly higher than virus isolation for the detection of EAV in semen. Taken altogether, the real-time RT-PCR can reliably detect EAV nucleic acid when the reagents for nucleic acid extraction and amplification methods are optimized. Therefore, this assay has the potential to provide a faster, convenient and more economical test for detection of EAV nucleic acid in TCF and equine semen and be an alternative to VI.

1.11.3. Serological diagnosis

The virus neutralization test (VNT) is considered the “gold standard” for detection and determination of antibodies to EAV [292]. Currently, the VNT is the only validated test accepted for international trade. Although, the VNT is highly sensitive and accurate, it has several disadvantages: it is expensive, labor-intensive and time-consuming to perform. In addition, results can vary among laboratories when adequate attention is not paid to standardization of both test reagents and procedure. Moreover, serum cytotoxicity caused by anti-cellular antibodies directed against RK-13 cells can to

the inexperienced, be mistaken for viral CPE and can give rise to difficulties in test interpretation at lower serum dilutions. Also, the VNT cannot differentiate the antibody response of vaccinated from naturally infected horses. To overcome these disadvantages, several enzyme-linked immunoassays (ELISA) have been described using whole virions, recombinant GP5, M and/or N proteins expressed from bacterial- or baculovirus systems with ovalbumin-conjugated synthetic oligopeptides of GP5 protein as antigen [150,221,254,274,275,304,305,306]. Given the importance of the GP5 protein to virus neutralization, it was the logical target as an antigenic protein for development of serological diagnostic assays. An ELISA using a recombinant fusion protein expressing GP5 55-98 had a sensitivity and specificity of 99.6% and 90.1%, respectively [274]. An ELISA based on a cocktail of recombinant GP5, M and N proteins expressed in baculoviruses had 100% specificity and 92.3% sensitivity when tested with sera from naturally or experimentally infected horses. However, the test was not reliable in detecting antibodies in sera of vaccinated horses [221]. A blocking ELISA using partially purified EAV and MAb against the GP5 protein with 99.4% sensitivity and 97.7% specificity was developed [254]. Another ELISA based on GP5 protein, the ovalbumin-conjugated synthetic peptide containing amino acids 81-106 of GP5 (G_L-OVA) had a sensitivity and specificity of 96.7% and 95.6%, respectively [150]. Due to the conserved nature of the nucleotide sequence of M and N proteins among different EAV strains and isolates, they are considered appropriate candidates for diagnostic purposes as well [159]. Jeronimo and Archambault (2002) demonstrated that the carboxy terminus of the M protein (aa 88-162) is consistently recognized by EAV-specific horse sera, thus suggesting this region be used as the antigen for serology tests such as ELISA [280]. However, none of the above mentioned assays were sensitive and specific enough to replace the current VNT. Currently, there is a commercially available ELISA, Ingezim Arteritis ELISA (Ingenasa, Madrid, Spain); however, sensitivity and specificity of the assay was considerably lower compared to VNT making this commercially available ELISA unsuitable for screening of samples [307]. As discussed in chapter 8, a new immunological assay to detect antibodies to EAV in horses was developed using the microsphere assay system. This particle array using microspheres (microbeads) incorporates three well-developed technologies: bioassays, solution-phase microspheres

and flow cytometry. The microsphere immunoassay (MIA) has several advantages over traditional ELISAs: accuracy, high sensitivity and specificity, reproducibility, high-throughput sample analysis and multiplex capability. In our study, the assay was based on recombinant structural proteins with putative antigenic regions. Among tested recombinant structural proteins, either full-length or partial, $GP5_{55-98}$ MIA showed the highest sensitivity and specificity of 92.6% and 92.9%, respectively. Currently, we are in the process of maximizing the sensitivity of this assay by incorporating a cocktail of recombinant EAV proteins including structural and nonstructural proteins. Hopefully, the new strategy will improve the sensitivity and specificity of the assay and it can be used as a reliable serological diagnostic test to detect antibodies to EAV.

1.12. PREVENTION AND TREATMENT OF EQUINE VIRAL ARTERITIS

1.12.1. Vaccine

The development of a safe and effective vaccine against an infectious disease is always of paramount importance in preventing a disease outbreak and minimizing economic losses. The modified live virus (MLV) vaccine against EVA was developed many years ago following serial passage (P266) of the experimentally derived Bucyrus strain of EAV in horse kidney (HK), rabbit kidney (RK) and equine dermal (ED) cells [62,308]. This attenuated strain of virus did not show any reversion to virulence after five consecutive passages in horses [264,267]. Experimental vaccination studies have been performed to ensure the safety of the vaccine for use in stallions [309,310]. However, vaccination of pregnant mares is not recommended especially in the last trimester of pregnancy. The commercial modified live virus vaccine, ARVAC® (passage history HK-131, RK-111 and ED-24), and the strains of earlier passage history were shown to be effective for protection against disease [264,266,267,309]. Vaccination studies using the MLV showed that a single dose of vaccine stimulates only low, transient levels of VN antibodies; however, additional doses boost antibody levels with titers maintained for at least 9-12 months [193,310,311]. Similarly, formalin-inactivated virus vaccine without adjuvant was shown to induce high titers of VN antibodies after repeated doses [269,270,312,313]. The modified live virus vaccine, ARVAC® is

currently in use in North America, while the adjuvanted killed virus vaccine, ARTERVAC®, is approved for use in several European countries.

Current serological tests cannot discriminate between naturally infected and vaccinated horses. Therefore, an effort was undertaken to develop vaccines that might make such discrimination possible e.g. sub-unit vaccine.

DNA vaccination using GP5 and N proteins of EAV has been tested using mice [314]. The highest VN antibodies were induced when animals were vaccinated with plasmid DNA encoding ORF5 [314]. Later, a DNA vaccine expressing ORFs 2, 5, and 7 in combination with equine interleukin-2 was tested in horses [315]. After the initial immunization, three boosters were administered at two-week intervals. All vaccinated horses developed high VN antibody titers regardless of age and VN antibodies were still detectable over a year later [315]. The N-terminal ectodomain (aa 18-122) of GP5 expressed in bacterial cells induced higher neutralizing antibody titers compared to other GP5 polypeptides in ponies [155].

Balasuriya *et al.* [154] explored the possibility of using alphavirus replicon particles (VRP) co-expressing GP5/M as a vaccine and of inducing protective immunity in horses. Previously, they established that VRP expressing GP5/M heterodimer can induce neutralizing antibodies in mice. This study showed that the VRP system could be used as a strategy for developing a vaccine against EAV and other viral pathogens.

1.12.2. Antivirals

Antiviral potentials of phosphorodiamidate morpholino oligomers (PMOs) directed against EAV have been studied [316,317]. PMOs are single-stranded DNA analogues [318], usually 20-25 bases in length, water-soluble and nuclease-resistant [319]. PMOs can base pair with a complementary RNA target sequence and form a steric blockade to interfere with gene expression, particularly with translation of the genome [319,320]. Peptide-conjugation to the PMO (P-PMO) greatly improves delivery of PMO into cells [321]. The 5' UTR of the EAV genome was found to contain the most sensitive targets for inhibition with P-PMOs [317]. Treatment with an antisense P-PMO targeting the EAV 5'-terminus at a concentration of 5-10 µM eliminated the virus from persistently infected HeLa cells [316]. However, the efficacy of P-PMO against EAV *in vivo* remains

to be evaluated. Moreover, several carbohydrate-binding agents such as plant and non-plant lectins have been shown to have antiviral activities against nidoviruses [322]. It has also been reported that EAV could not be propagated in 100 U/ml recombinant equine IFN-γ when 100 $TCID_{50}$ of infectious virus was inoculated into horse cells [323]. Furthermore, horse cells transfected with small interfering RNA (siRNAs) targeting the ORF1ab prior to infection with EAV drastically reduced virus titers in cell culture [324]. Although the antiviral effects shown *in vitro* are promising, *in vivo* application of the above mentioned antiviral agents may be limited due to the large body weight of horses and the costs involved.

1.13. RECENT ADVANCES IN EAV RESEARCH AND FUTURE DIRECTIONS

1.13.1. Reverse genetics

The naked genome of a positive-strand RNA virus is infectious: it serves as an mRNA for translation of viral replicase, thus, infection starts by a simple transfection of the genome into the host cell. Construction of full-length cDNA clones has greatly enhanced our understanding of RNA virus replication and gene expression by manipulating the genetic information. They can serve as potential tools for fundamental studies of virus replication and pathogenesis.

To date, the first two cDNA clones of the original Bucyrus strain were derived from a highly cell culture adapted strain [325,326] and one of these clones, pEAV030 (GenBank accession number: Y07862) was found to be attenuated in horses [327]. The third clone was derived from a horse adapted, experimentally derived VBS strain of EAV [328]. The recombinant virus generated from this infectious cDNA clone (rVBS) causes severe disease in experimentally infected horses [328]. Recently, a full-length cDNA clone of MLV has been constructed [329]. Infectious RNAs can be produced *in vitro* from full-length EAV cDNA clones using T7 RNA polymerase.

Availabililty of EAV cDNA clones have greatly increased our knowledge of molecular characterization of genetic expression and replication of EAV using reverse genetics technology. Balasuriya *et al.* (2004) employed an infectious cDNA clone and reverse genetics technology to generate a panel of chimeric and mutant viruses by means

of site-directed mutagenesis and to characterize neutralization determinants of EAV [69]. However, manipulation of the genome of arteriviruses is complicated due to the compact and overlapping gene arrangement. de Vries *et al.* (2000) investigated the importance of the overlapping gene organization in the virus life-cycle by constructing a series of mutant full-length cDNA clones in which EAV ORFs 4/5 or ORFs 5/6 or ORFs 4/5/6 were separated [325]. RNA transcribed from each of these plasmids was infectious, indicating that the overlapping gene arrangement is not crucial for viability of the virus. The fact that small changes in the spacing between ORFs 4/5 and ORFs 5/6 mutant viruses have only a limited effect on virus yields, was a big advantage for generation of recombinant chimeric viruses between virulent and attenuated strains of EAV. Genes encoding structural and nonstructural proteins are often interchanged between strains of EAV of differing virulence and are used to study virulence determinants, mechanisms of pathogenesis and persistent infection [236,330,331]. Assessment of viral proteins involved in T lymphocyte tropism is described in this dissertation (chapter 2).

EAV cDNA clones have also been used as a vector for heterologous gene expression, such as enhanced green fluorescence protein (eGFP) [332]. The infectious recombinant EAV expressing GFP (EAV-GFP2) from its replicase had similar growth characteristics to those of the wild-type virus. The recombinant virus EAV-GFP2 is a convenient tool for basic and applied research. The same approach, namely insertion of a foreign gene in the arterivirus replicase gene for intracellular expression, could be used for vaccine development.

It is clear that infectious clones and reverse genetics are valuable and powerful tools that can increase our understanding of many aspects of the viral infection process and life cycle, as well as virulence. Specifically, it offers possibilities for exploring vaccine production as well as vector development.

1.14. HOST-VIRUS INTERACTION AND GENOMIC STUDIES

Viruses constantly adapt to and modulate the host environment to their advantage during replication and propagation. Therefore, virus interaction with host target cells is complex and it is possible that almost every step of the virus infection cycle may rely on

the recruitment of cellular proteins and basic machineries by viral proteins. Moreover, as a virus that induces persistent infection, EAV could have developed strategies to overcome the antiviral activity of the host factors, possibly through its own set of viral proteins by modulating the cellular environment. Therefore, dissecting the molecular interaction between the host and EAV is key to understanding the pathogenesis of EAV and to develop strategies to control EAV replication.

For initial host cell attachment and entry, the virus uses attachment factors and cellular receptors as yet to be identified for EAV. Subsequently, EAV penetrates into the cell by a clathrin-dependent endocytosis and low pH is required in the endocytic compartments [82]. Similarly, PRRSV also utilizes a low pH-dependent endocytic pathway to enter cells, most likely clathrin-dependent endocytosis [333]. It is not clear whether there are other means of entry for EAV; however, the clathrin-mediated pathway is the only mechanism of EAV entry that has been reported so far. Still remaining to be identified are the factors required for fusion of endosomal membrane and viral envelope and the subsequent uncoating step that are both essential steps for releasing the viral genome into the cytoplasm. Following uncoating, the genome is translated and following proteolytic processing of the replicase polyprotein, viral RNAs are synthesized and are used as templates for genome replication. In addition, transcription of subgenomic mRNAs that encode the structural proteins occurs. Arteriviruses acquire their envelope by budding preformed nucleocapsids into the smooth endoplasmic reticulum and/or the Golgi complex [101,102,136]. After budding, virions accumulate in intracellular vesicles which are transported to the plasma membrane for release of progeny virus. However, our knowledge about viral proteins that interact with the cytoplasmic molecules during this process is very limited.

In addition to regulating cellular factors to support efficient replication of the virus itself, viruses have also evolved with a view to counteracting the host innate and adaptive immune responses. In the last several years, it has been increasingly clear that viruses have evolved multiple strategies to escape the IFN system, which is the first line of defense to virus infection. They either inhibit IFN synthesis, bind and inactivate secreted IFN molecules, block IFN-activated signaling, or disturb the action of IFN-induced antiviral proteins.

With the advent of genomic tools, it became possible to study virus-host interactions at the molecular level. Many new methodologies have been developed in genomic and proteomic fields of research to identify host molecules that closely interact during the virus life cycle. Thus, the "genomics revolution" offers high-throughput tools to study the complex virus-host interaction. Microarray technology has been extended *inter alia* to genotyping of the host (SNP analysis). Therefore, genetic and genomic technologies offer ample opportunities to discover the mechanisms of virus infections and virus interaction with the host, which will have great implications for vaccine development and drug design.

Over the past few years, autoimmune disease and human infectious diseases have been investigated extensively in genome-wide association studies (GWAS). Researchers have used a variety of approaches to investigate how the genes identified in GWAS relate to disease pathogenesis. Studies revealed links between disease developments to regions of the host genome that are involved in host-virus interactions. The field of interaction between EAV with host factors is discussed in chapter 3. We believe that some of host factors found during the study directly or indirectly interact with EAV to influence its replication.

1.15. SCOPE AND OUTLINE OF DISSERTATION

A virus is a small infectious agent that can replicate only inside of living cells of organisms; in other words, it depends solely on the host/cellular machinery to make new products. Therefore, successful infection depends on the interaction between the host and virus that are complex and multifactorial. At the molecular level, interactions that occur between cellular and viral gene products determine host susceptibility to infection. The series of events that occur during viral infection in a host may result in a disease that is the outcome of the effects of virus replication in the host and the host defense system. Thus, elucidating the genetic and functional roles that viral proteins play during productive viral infection as well as studying the host immune response to combat the viral infection are critical to preventing and treating viral diseases.

The objective of this study was to characterize the virus-host interactions in EAV infection by combining contemporary molecular biology techniques and host genomic analysis using GWAS. The interaction between the virus and the host is important for viral replication, virulence and pathogenesis. The availability of full-length infectious cDNA clones and reverse genetic systems greatly facilitates the functional analysis of viral proteins in relation to cellular tropism and the immune response. The interactions of viral structural proteins that determine the host cell tropism is discussed first, and possible genetic and host cell factors that determine susceptibility/resistance of equine PBMCs to EAV infection are then addressed. The recent availability of the equine genome sequence and development of genome-wide screening technologies offer unparalleled opportunities to identify variants associated with increased susceptibility/resistance to infectious disease agents such as EAV. Understanding how cellular proteins interact with viral RNA or viral proteins, as well as their role in viral infection, will allow for better characterization of the mechanisms of EAV pathogenesis and persistent infection in stallions. Furthermore, the findings from this study should allow the design of novel antiviral agents based on these interactions and appropriate preventive measures.

Chapter 1, literature review, provides a broad perspective on the molecular biology of EAV and EVA in horses.

Chapter 2 investigates the altered tropism of EAV VBS during extensive cell culture passage that resulted in the modified live virus vaccine strain for equine $CD3^+$ T lymphocytes and $CD14^+$ monocytes. Evaluation of chimeric viruses demonstrates that cellular tropism in PBMCs is determined by the amino acid sequence of viral envelope proteins. Combined interactions of both major (GP5 and M) and minor (GP2, GP3 and GP4) envelope proteins of the EAV VBS are needed for efficient infection of $CD3^+$ T lymphocytes (predominantly $CD4^+$ T lymphocytes) and $CD14^+$ monocytes.

Chapter 3 describes the identification of a distinct phenotypic trait that can be used as a marker to divide equine populations, regardless of breed, into susceptible and resistant groups based on dual color flow cytometric analysis of $CD3^+$ T cells infected with EAV. The GWAS demonstrates the putative candidate genes associated with susceptibility/resistance of $CD3^+$ T lymphocytes to EAV are located on horse

chromosome 11. Biological pathways analysis reveals several cellular genes within this region encoding proteins associated with virus attachment and entry, cytoskeletal organization and NFκB pathways that may be associated with the trait responsible for the *in vitro* susceptibility/resistance of $CD3^+$ T lymphocytes to EAV infection. The data presented in this study demonstrate a strong association of certain genetic markers with *de facto* proof that the trait is under genetic control.

Chapter 4 addresses whether the differences in the susceptibility or resistance of $CD3^+$ T cells *in vitro* correlate with development and severity of clinical signs *in vivo*. Horses were divided into two groups based on their *in vitro* $CD3^+$ T cell susceptible or resistant phenotype and challenged with the recombinant EAV VBS. The data show that there was a significant difference between the two groups of horses in terms of cytokine mRNA expression and increased clinical signs in horses possessing the *in vitro* $CD3^+$ T cell resistant phenotype. Thus, there was an inverse correlation between the *in vitro* susceptibility or resistance phenotype of $CD3^+$ T lymphocytes and the variable clinical/cytokine expression responses observed in horses following infection with EAV. This study provides further insight into the variation in clinical signs seen among horses after infection with virulent strains of EAV.

Chapter 5 establishes a correlation between susceptibility of $CD3^+$ T lymphocytes to EAV infection and establishment of persistent infection in stallions. The data suggest that carrier stallions that have the phenotype of susceptible $CD3^+$ T lymphocytes to EAV infection may represent those at higher risk of becoming persistently infected compared to stallions that do not possess this phenotype. The *in vitro* assay described is currently the most precise method for determining the phenotype. Findings from this study will allow us to develop diagnostic tools to predict possible carrier stallions of EAV and prevent further spread of the virus.

Chapter 6 investigates the effect of EAV on type I IFN production and signaling. IFN-β mRNA level in equine endothelial cells (EECs) infected with EAV VBS strain was not increased compared to that in mock-infected cells; whereas Sendai virus infection strongly induced production of IFN-β mRNA. Protein levels determined by IFN bioassay provided additional confirmation of this finding. Among 12 nonstructural proteins, nsp1 exhibited the strongest inhibitory effect, namely the ability to inhibit both IFN synthesis

and signaling. Based on these findings, we propose that failure to induce type I IFN in infected cells may allow the virus to subvert the equine innate immune response, and nsp1 may play a critical role in inducing this effect.

Chapter 7 addresses discovery of a novel short coding sequence in the 3'-proximal end of the EAV genome, named ORF5a. Its biological significance in the EAV life cycle was investigated using EAV reverse genetics systems. The effect of ORF5a knockout mutant was independently confirmed using two molecular clones, the pEAV515 and pEAVrVBS of the EAV VBS. This study suggest that the ORF5a protein may be the eighth structural protein of EAV, although further studies are needed to obtain more detailed information into its yet unknown function.

Chapter 8 describes development and validation of an MIA to detect equine antibodies to the major structural proteins of EAV. Of the eight recombinant proteins, the partial $GP5_{55-98}$ protein showed the highest concordance with the VNT. The sensitivity and specificity of the MIA were 92.6% and 92.9%, respectively. The $GP5_{55-98}$ MIA and VNT test outcomes correlated significantly (r =0.84; p-value <0.0001). Although the $GP5_{55-98}$ MIA is less sensitive than the standard VNT, it has the potential to provide a rapid, convenient and more economical test for screening equine sera for the presence of antibodies to EAV with the VNT used as a confirmatory assay.

Chapter 9 describes evaluation of the humoral immune response of horses to each of the nonstructural proteins (nsps) of EAV by ORFs 1a and 1b of the viral genome. To characterize the humoral immune response to EAV nsps, serum samples from horses that were seropositive to EAV were reacted with recombinant proteins in immunoprecipitation assays. The data showed that nsp2, nsp5 and nsp12 were the most immunogenic proteins of the nsps. Information from this study will be used in ongoing efforts to develop improved methods for the serologic diagnosis of EAV infection in horses.

Copyright © Yun Young Go 2011

CHAPTER TWO

Complex Interactions Between the Major and Minor Envelope Proteins of Equine Arteritis Virus Determine its Tropism for Equine $CD3^+$ T Lymphocytes and $CD14^+$ Monocytes

J. Virol. 2010, 84(10): 4898-911

Reprinted with permission

2.1. SUMMARY

Extensive cell culture passage of the virulent Bucyrus (VB) strain of equine arteritis virus (EAV) to produce the modified live virus (MLV) vaccine strain has altered its tropism for equine $CD3^+$ T lymphocytes and $CD14^+$ monocytes. The VB strain primarily infects $CD14^+$ monocytes and a small subpopulation of $CD3^+$ T lymphocytes (predominantly $CD4^+$ T) as determined by dual-color flow cytometry. In contrast, the MLV vaccine strain has significantly reduced ability to infect $CD14^+$ monocytes and has lost its capability to infect $CD3^+$ T lymphocytes. Using a panel of five recombinant chimeric viruses, we demonstrated that interactions between GP2, GP3, GP4, GP5 and M envelope proteins play a major role in determining the $CD14^+$ monocyte tropism while the tropism of $CD3^+$ T lymphocytes is determined by GP2, GP4, GP5 and M envelope proteins but not the GP3 protein. The data clearly suggest that there are intricate interactions among these envelope proteins that affect binding of EAV to different cell receptors on $CD3^+$ T lymphocytes and $CD14^+$ monocytes. This study shows for the first time that $CD3^+$ T lymphocytes may play an important role in the pathogenesis of equine viral arteritis when horses are infected with the virulent strains of EAV.

2.2. INTRODUCTION

Equine arteritis virus (EAV) is a small enveloped virus with a positive-sense, single-stranded RNA genome of 12.7 kb that belongs to the family *Arteriviridae* (genus *Arterivirus*, order *Nidovirales*), which also includes porcine reproductive and respiratory syndrome virus, simian hemorrhagic fever virus, and lactate dehydrogenase-elevating virus of mice [7,34]. The EAV genome includes nine known functional open reading frames [58]. Open reading frames (ORFs) 1a and 1b encode two replicase polyproteins (pp1a and pp1ab) that are post-translationally processed by three ORF1a-encoded proteinases (nsp1, 2, and 4) to yield at least 13 nonstructural proteins (nsp1-12, including nsp 7α and 7β [34,66,113], and the remaining seven ORFs (2a, 2b and 3-7) encode structural proteins of the virus. These include four minor envelope proteins (E, GP2, GP3, and GP4 encoded by ORFs 2a, 2b, 3 and 4, respectively), two major envelope proteins (GP5 and M encoded by ORFs 5 and 6) and the highly conserved nucleocapsid protein (N encoded by ORF7) [93]. The two major envelope proteins GP5 and M form a disulfide-linked heterodimer [67,68] and the three minor envelope proteins GP2, GP3 and GP4 form a covalently associated heterotrimeric complex in the virion [140,144]. By independently knocking out the expression of each structural protein, it was shown that all major and minor structural proteins are required for the production of infectious progeny virus [141].

EAV is the causative agent of equine viral arteritis (EVA) [185,195]. Geographically and temporally different strains of EAV vary in the severity of the clinical disease they induce and in their abortigenic potential [77,78,216,224]. While most EAV infections are asymptomatic, some infected horses can exhibit clinical manifestations such as an influenza-like illness, abortion in pregnant mares, and pneumonia or pneumoenteritis in neonatal foals [77,194,202,203,208,244,334,335]. Following experimental infection of horses by the respiratory route, the virus initially replicates in both macrophages and endothelial cells in the lung [187,237]. EAV is then transported to the draining lymph nodes, where it replicates and is released into the blood and lymphatic system for transportation throughout the body. The virus infects the smaller blood vessels, especially the arterioles, causing a panvasculitis [187,213,242]. A number of studies have demonstrated that different strains of EAV vary significantly in

their pathogenicity, with very different clinical outcomes upon experimental inoculation of horses [154,240,327,328,334]. The horse-adapted Bucyrus (VB) strain of EAV is highly velogenic and causes severe clinical disease with a case-fatality rate of 50-60% under experimental conditions [213,239]. Horses inoculated with virulent strains of EAV (e.g. VB and recombinant VB [rVBS] strains, and KY84) develop severe lymphopenia with a high titered viremia ($6x10^3$-$1x10^5$ pfu/ml) [154,213,244,328]. In contrast, horses inoculated with the attenuated modified live virus (MLV) vaccine strain, or other avirulent strains of EAV (e.g. 030H and CA95G) [224,327] develop a mild, transient lymphopenia with only a very low-titer viremia ($\leq 1x10^1$ pfu/ml) [61,62,264,265,267,336].

The modified live virus (MLV) vaccine (ARVAC®, Fort Dodge Animal Health) that is in current use in the United States and Canada [61,264,265,267,336], was developed by serial passage of the VB strain of EAV in primary horse kidney cells (HK131 passages), primary rabbit kidney cells (RK111 passages) and equine dermis cells (ED24 passages) which resulted in attenuation of the virus [62]. Previously, it has been shown that the VB strain was fully attenuated for horses by 116th passages in primary horse kidney cells (EAV HK116) [265,267,291]. Subsequently, EAV HK116 virus was further passaged in HK cells for additional 15 times (HK131) and in two other cell lines (RK111 and ED24) to obtain the MLV vaccine virus (HK131, RK111, ED24) used in this study. There are 23 additional amino acid substitutions that accumulated in GP2, GP3, GP4, GP5 and M envelope proteins during cell culture passage of the HK116 virus to generate the current MLV strain (ARVAC®; Table 2.1) which may have contributed to further attenuation of the vaccine strain of EAV and increased the safety of the vaccine for horses. Recently, using reverse genetics we showed that a chimeric virus containing the nonstructural proteins of VB virus and the structural proteins of HK116 (rVBS/HK116 S) [331] strain has an attenuated phenotype in horses. The data showed that critical amino acid substitutions in structural protein genes of HK116 virus were responsible for attenuation of the VB strain.

Table 2.1. Comparative amino acid analysis of rVBS, HK116 and rMLV envelope proteins

ORF	Protein (aa length)	Amino acid difference			
		Position	rVBS	HK116	rMLV
ORF2a (9751-9954)	E (67)	-	-	-	-
ORF2b (9824-10507)	GP2 (227)	62	Tyr	Tyr	His
		92	Ile	Thr	Thr
		158	Gly	Gly	Glu
		223	Arg	Pro	Pro
ORF3 (10306-10797)	GP3	80	Leu	Leu	Val
	(rVBS and HK116: 163;	123	Leu	Leu	Ser
	rMLV 168)	160	Cys	Cys	Tyr
		164	Stop	Stop	Gln
		165			Phe
		166			Tyr
		167			Leu
		168			His
		169			Stop
ORF4 (10700-11158)	GP4 (152)	4	Tyr	Tyr	Ser
ORF5 (11146-11913)	GP5 (255)	69	Leu	Leu	Pro
		72	Gln	Gln	Lys
		81	Asn	Asp	Asp
		100	Ser	Gly	Gly
		104	Asn	Gly	Gly
		106	Met	Met	Val
		170	Ala	Ala	Ser
		214	Gly	Gly	Glu
ORF6 (11901-12389)	M (162)	38	Leu	Leu	Ser
		49	Phe	Phe	Leu
		71	Val	Val	Ala
		81	Met	Thr	Thr
		122	Ile	Val	Val
		150	Phe	Phe	Cys
		154	Ala	Thr	Met

Note: Amino acid substitutions located in predicted ectodomain on each protein are indicated in bold. All potential N-glycosylation sites are conserved in GP2 (aa 155), GP3 (aa. 28, 29, 49,96, 106, 118) and GP4 (aa. 33, 55, 90).

To enhance fundamental understanding of the pathobiology of EAV infections it is important to identify those peripheral blood mononuclear cells (PBMCs) that are most closely associated with the virus during vascular transport and how genetic changes associated with an attenuated phenotype alter the dynamics of virus/host-cell relationships in

blood. Thus, we hypothesized that VB and MLV strains differ in their ability to infect PBMCs and that the altered tropism of the attenuated MLV strain of EAV in PBMCs is associated with amino acid changes in the viral proteins. To test this hypothesis we used three previously described recombinant viruses (rVBS [328], rVBS/HK116 S [331] and rMLV [329]), as well as four newly generated chimeric viruses (rVBS/MLV S, rMLV/VBS S, rMLV/VBS 234 and rMLV/VBS 56) and infected *ex* vivo preparations of PBMCs collected from horses. The data suggested that the difference in cellular tropism and virulence phenotype of VB and MLV strains is associated with the collective interactions of both major (GP5 and M) and minor (GP2, GP3 and GP4) envelope proteins of EAV. Furthermore, this study also demonstrated that $CD3^+$ T lymphocyte tropism is primarily determined by amino acid substitutions in the GP2, GP4, GP5 and M envelope proteins but not the GP3 minor envelope protein. However, the macrophage tropism is mainly determined by intricate interactions among GP2, GP3, GP4, GP5 and M envelope proteins of the virus.

2.3. MATERIALS AND METHODS

Cell lines

Equine pulmonary artery endothelial cells (EECs) were maintained in Dulbecco's modified essential medium (Mediatech, Herndon, VA) with sodium pyruvate, 10% fetal bovine serum (Hyclone Laboratories, Inc., Logan, UT), 100U/ml of penicillin/streptomycin and 200mM L-glutamine [154,213,328]. The rabbit kidney cells (RK-13, ATCC CCL-37; American Type Culture Collection, Manassas, VA) were grown in Eagle's minimum essential medium with 10% ferritin supplemented bovine calf serum (Hyclone Laboratories, Inc., Logan, UT) and 100U/ml of penicillin/streptomycin (Gibco, Carlsbad, CA).

Horses

A total of 10 horses of different breeds (Thoroughbreds, n=4; Standardbreds, n=2; mixed breeds, n=4) were used in this study. The horses were maintained on pasture at the Department of Veterinary Science's Maine Chance Farm, Lexington, KY. All horses were confirmed seronegative for EAV neutralizing antibodies using previously described

protocols [337]. The horses were clinically evaluated prior to collection of blood samples for isolation of peripheral blood mononuclear cells. Furthermore, complete blood counts and differential counts were performed to establish that all animals had normal blood cell values. Blood samples were collected according to a protocol approved by Institutional Animal Care and Use Committee at University of Kentucky, Lexington, KY.

Antibodies

To determine the phenotype of EAV infected mononuclear cells, the following monoclonal antibodies (MAbs) directed against different cell-type-specific surface molecules were used in this study: anti-equine $CD3^+$ T lymphocytes (UC F6G; kindly provided by Dr. Jeff Stott, University of California at Davis; [338], anti-equine $CD4^+$ T lymphocytes and anti-equine $CD8^+$ T lymphocytes (CVS4 and CVS8, respectively; Serotec, Raleigh, NC; [339,340]. A MAb specific for human CD14 (Alexis Biochemicals, Lausen, Switzerland) that cross-reacts with equine CD14 [341] was used to identify equine monocytes and R-phycoerythrin (R-PE) conjugated anti-human CD21 (B-ly4; BD Pharmingen, San Jose, CA) previously shown to cross-react with equine B cells was used [342]. R-phycoerythrin (R-PE)-conjugated $F(ab')_2$ fragment of goat anti-mouse IgG_1 (Southern Biotech, Birmingham, AL) was used as a secondary antibody.

To detect EAV antigens in infected cells, MAbs against EAV nonstructural protein-1 (nsp1; MAb 12A4) and nucleocapsid protein (N; Mab 3E2) were used [213,306]. Mouse ascitic fluid containing MAbs 12A4 and 3E2 were purified using a Melon™ Gel IgG Spin Purification Kit (Pierce, Rockford, IL). Purified IgG was directly conjugated to Alexa Fluor® 488 (Invitrogen, Carlsbad, CA) following manufacturer's instructions. Briefly, purified IgG from MAbs 12A4 and 3E2 were diluted with PBS to a concentration of 2 mg/ml and 1 M sodium bicarbonate (pH 8.3) was added. Subsequently, diluted IgG solution was incubated with Alexa Fluor® 488 reactive dye for 1 h at room temperature in the dark with slow stirring. The reaction mixture was loaded onto a fine size exclusion purification resin column for separation of labeled antibodies from unincorporated dye. Fractions of Alexa Fluor® 488 labeled antibodies were collected and stored at 4°C. To detect nonspecific binding, mouse IgG_1 (MOPC; Sigma,

St. Louis, MO) and Alexa Fluor® 488 conjugated mouse IgG_1 isotype controls (Invitrogen, Carlsbad, CA) were used.

Viruses

Two strains of EAV, the virulent Bucyrus (VB) strain (ATCC VR-796; [185,195] and the modified live virus (MLV) vaccine strain (ARVAC®, Fort Dodge Laboratories, Fort Dodge, IA, [62,309], were used for *in vitro* study of identifying the EAV target cell population in PBMCs. Each virus was propagated once in EECs to prepare high titered working stocks as previously described [343,344]. Briefly, EECs infected with each virus were frozen at -80°C when 90-100% cytopathic effect (CPE) was observed. Cell lysates were clarified by centrifugation (500 ×*g*) at 4°C for 15 min, followed by ultracentrifugation (Beckman Coulter, Miami, FL) at 121,600 ×*g* through a 20% sucrose cushion in NET buffer (150 mM NaCl, 5 mM EDTA, and 50 mM Tris-HCl, pH 7.5) at 4°C for 4 h to pellet the virus. Purified preparations of each strain of EAV were resuspended in phosphate buffered saline (PBS; pH 7.4) and frozen at -80°C. Virus stocks were titrated by standard plaque assay in RK-13 cells and titers were expressed as PFU/ml [291].

Construction of chimeric cDNA clones of EAV and recovery of recombinant viruses

Infectious cDNA clones of the virulent VB strain of EAV and modified live virus (MLV) vaccine strain of EAV (pEAVrVBS and pEAVrMLV, respectively) were recently constructed in our laboratory [328,329]. The *in vitro* and *in vivo* characterization of these viruses showed that they are phenotypically indistinguishable to that of their respective wild-type parental viruses. Five chimeric infectious cDNA clones, pEAVrVBS/HK116 S, pEAVrVBS/MLV S, pEAVrMLV/VBS S, pEAVrMLV/VBS 234 and pEAVrMLV/VBS 56 were constructed by using standard molecular biological techniques [236,328,331]. The recombinant chimeric infectious cDNA clone pEAVrVBS/HK116 S was generated by substituting the genes (ORFs 2a to 7) encoding the structural proteins of pEAVrVBS by the corresponding genes from the HK116 virus [331]. The recombinant chimeric infectious cDNA clone pEAVrVBS/MLV S was constructed by replacing the structural protein genes (ORFs 2a to 7) of the infectious cDNA clone pEAVrVBS [328], which was

derived from the VB strain of EAV, with the corresponding genes of pEAVrMLV clone [329]. A similar approach was used to construct the recombinant infectious cDNA clones pEAVrMLV/VBS S where the structural protein genes (ORFs 2a to 7) of the infectious cDNA clone pEAVrMLV were substituted with the corresponding genes of the pEAVrVBS clone; the pEAVrMLV/VBS 234 clone in which the minor envelope protein genes (ORFs 2a to 4) of the rMLV were replaced with the corresponding genes of pEAVrVBS; and the rMLV/VBS 56 clone in which the major envelope protein genes (ORFs 5 and 6) of the pEAVrMLV were replaced with the corresponding genes of pEAVrVBS.

The recombinant viruses, rVBS, rMLV, rVBS/HK116 S, rVBS/MLV S, rMLV/VBS S, rMLV/VBS 234 and rMLV/VBS 56, were generated by *in vitro* transcription of infectious viral RNAs from *XhoI*-linearized full-length infectious cDNA clones and electroporated into EECs following previously described protocols [328]. Virus particles were harvested from cell culture supernatant at 48 to 72 h after electroporation when cytopathic effect (CPE) was evident, clarified of cell debris by centrifugation, and stored at -80°C in single-use aliquots (passage 0 [P0]). Recombinant viruses (P0) harvested from transfected EECs were used to prepare high titered working stocks by passing one more time in EECs (P1) as described above and purified viruses were used for *in vitro* infection studies.

Comparative amino acid sequence analysis and membrane topology prediction of EAV envelope proteins

The published sequences of rVBS, rMLV, HK116 were downloaded from the GenBank database (http://www.ncbi.nlm.nih.gov/ Genbank/index.html; accession numbers DQ846751 [328], EU586275 [329], and EU586274 [331], respectively). ORFs 2a, 2b, 3, 4, 5 and 6 were translated into amino acid sequences and aligned with the Vector NTI Advance™ 11 software (Invitrogen, Carlsbad, CA). Prediction of membrane topology for viral envelope proteins was performed using four most commonly used topology prediction methods available on the Internet: PSIPRED (http://www.psipred.net/psiform.html) [345,346], TMHMM (http://www.cbs.dtu.dk/services/TMHMM/) [347], TMPred

(http://www.ch.embnet.org/software/TMPRED_form.html), TOPPRED (http://www.bioweb.pasteur.fr/seqanal/interfaces/toppred.html) [348]. All user-adjustable parameters were left at their default values.

Preparation of peripheral blood mononuclear cell (PBMC) cultures

Blood (150-200ml) was collected aseptically from each of 10 horses using vacutainer tubes containing 15% EDTA solution (Kendall Healthcare, Mansfield, MA). Peripheral blood mononuclear cells (PBMC) were isolated from the buffy coat fraction by centrifugation through Ficoll-Paque Plus™ (Amersham Biosciences, Piscataway, NJ) at 500 ×*g* for 30 min at 25°C. The PBMC layer was collected, washed twice with PBS (pH 7.4) by centrifuging at 100 ×*g* for 10 min to eliminate the platelets. The cells were resuspended in complete RPMI (c-RPMI) 1640 medium (Gibco, Carlsbad, CA) supplemented with 10% heat-inactivated fetal bovine serum (Hyclone Laboratories, Logan, UT), 2 mM glutamine, 100U/ml penicillin/streptomycin and 55 µM 2-mercaptoethanol and counted using a Vicell Counter-XR (Beckman Coulter, Miami, FL). The adherent and non-adherent cell populations were separated by plating out the PBMCs in 100 mm tissue culture dishes (Corning, Corning, NY). Briefly, the cells were incubated at 37°C for 4 h to allow adherent cells to attach, and after incubation, the unattached cells were removed, centrifuged and resuspended to be counted and plated out as a non-adherent cell population in 100 mm tissue culture dishes containing 5ml of c-RPMI medium. The adherent cells were washed twice with PBS to remove remaining non-adherent cells and replaced with 5 ml of fresh c-RPMI medium. Both adherent and non-adherent cells were incubated at 37°C until infected with EAV.

Sorting of lymphocytes and monocytes

Positive selection of five different cell populations ($CD3^+$, $CD4^+$, $CD8^+$, $CD21^+$ and $CD14^+$ cells) was performed using aseptically obtained horse blood and a MoFlo Cell Sorter (Dako Cytomation, Glostrup, Denmark). Briefly, 5×10^7 PBMCs were incubated with specific MAbs against equine CD3, CD4 or CD8 for T lymphocytes and human CD14 that cross-react with equine monocytes. Equine B lymphocytes were sorted by two-way sorting using R-PE conjugated anti-human CD21 antibody that cross react with

equine B lymphocytes on cells already incubated with anti-equine CD8 MAb. All antibodies were incubated on ice in sorting buffer (1% FBS in Hanks' Balanced Salt Solution, pH 7.4; Gibco, Carlsbad, CA) for 20 min. After incubation with primary antibody, cells were washed and stained with goat anti-mouse IgG_1-R-PE (Southern Biotechnology Inc., Birmingham, AL) or goat anti-mouse IgG-FITC (Caltag Laboratories, Burlingame, CA) on ice for 20 min.

In vitro infection of lymphocytes and monocytes

Cultures of lymphocytes and monocytes were infected with either wild-type (VBS and MLV) or recombinant viruses (rVBS, rMLV, rVBS/HK116 S, rVBS/MLV S, rMLV/VBS S, rMLV/VBS 234 and rMLV/VBS 56) of EAV at an m.o.i. of 2. As negative controls, mock infected lymphocytes and monocytes were cultured under identical conditions.

Dual-color immunofluorescence staining and flow cytometry

For two color immunofluorescence staining of wild-type or recombinant virus infected cells, lymphocytes (1×10^6 cells) were incubated on ice for 30 min with MAbs specific for equine $CD3^+$, $CD4^+$ or $CD8^+$ T cells and R-PE conjugated anti-human CD21 antibody for B cells. Blood-derived monocytes (1×10^6 cells) were stained with anti-human CD14 monoclonal antibody. After washing, cells were incubated with secondary R-PE-conjugated goat anti-mouse IgG_1 (Southern Biotech, Birmingham, AL) for 30 min on ice. After washing to remove unbound secondary antibody, cells were fixed with 4% paraformaldehyde and then washed once in PBS-saponin buffer (PBS [pH 7.4] supplemented with 1% FBS, 0.1% saponin and 0.1% sodium azide). Intracellular staining for EAV antigen was performed using an Alexa Fluor® 488 conjugated anti-EAV nsp1 MAb 12A4 or anti-EAV N MAb 3E2 in PBS-saponin buffer and incubated on ice for 30 min. After incubation, washed cells were resuspended in PBS containing 0.5% paraformaldehyde for two-color cytometric acquisition using a FACSCalibur (Becton Dickinson, San Jose, CA). Lymphocytes and monocytes were gated and selected based on forward and side-scatter parameters of analysis. Cells were evaluated by a two-color plot of anti-EAV antigen (FL-1) vs. cell surface antigen (FL-2), and the percentage of

$CD3^+$, $CD4^+$, $CD8^+$, $CD21^+$ or $CD14^+$ and EAV antigen positive cells was determined by CellQuest™ quadrant statistics. Results were expressed as the percentage of lymphocytes or monocytes infected with EAV, after subtraction of the non-specific staining of mock-infected cells.

Virus growth curve and quantitative EAV real-time TaqMan® RT-PCR assay

Sorted $CD3^+$, $CD4^+$, $CD8^+$ T lymphocytes, $CD21^+$ B lymphocytes and $CD14^+$ monocytes were infected with VB or MLV strains of EAV at an m.o.i. of 2. Tissue culture supernatants were collected at 0, 1, 6, 12, 18, 24, 36, 48, 60 and 72 hpi for one-step growth curve and quantitative EAV real-time TaqMan® RT-PCR assays. For one-step growth curve analysis, virus titers in tissue culture supernatants were determined according to the method of Reed and Muench [349], and expressed as 50% tissue culture infective dose ($TCID_{50}$)/50 µl. To detect EAV nucleic acids, a one-tube real-time TaqMan® RT-PCR assay was performed using the TaqMan® One-Step RT-PCR Master Mix (Applied Biosystems, Foster City, CA) in an Applied Biosystems 7500 Fast Real-Time PCR System according to a previously published protocol [299,302]. The copy numbers of EAV molecules were determined by absolute quantification with an IVT ORF7 RNA standard curve as described previously [299,302].

Statistical analysis

The student's t-test was used to establish significant difference among infected lymphocyte subpopulations and monocytes between group A and B horses. Statistical analysis was performed using Sigma Plot 11 (Systat Inc., Richmond, CA).

Nucleotide sequence accession numbers

The nucleotide sequences of the rVBS/HK116 S, rVBS/MLV S, rMLV/VBS S, rMLV/VBS 56 and rMLV/VBS 234 were deposited in GenBank under the accession numbers GU732202, GU732201, GU732200, GU732199 and GU732198, respectively.

2.4. RESULTS

Differences in susceptibility of equine peripheral blood mononuclear cells (PBMCs) to infection with virulent and attenuated strains of EAV

To investigate the susceptibility of equine PBMCs to virulent and attenuated strains of EAV, PBMCs collected from ten randomly selected horses were infected either with the VB or MLV strains of the virus. Dual fluorescent antibody staining of PBMC cultures was performed using a panel of leukocyte differentiation antigen-specific monoclonal antibodies (MAbs) specific for pan $CD3^+$ T lymphocytes, $CD4^+$ helper T lymphocytes, $CD8^+$ cytotoxic T lymphocytes and $CD21^+$ B lymphocytes, as well as a MAb specific for the EAV nsp1. Dual immunofluorescence labeling with CD3 specific MAb and antibody against EAV nsp1 indicated that $CD3^+$ T lymphocytes recovered from six of the ten tested horses could be infected with the VB strain of EAV (Figure 2.1 A). At 12 hpi, the mean percentage of $CD3^+$ T lymphocytes double-labeled with cell surface antibody and MAb to EAV nsp1 antigen was 0.5% (± 0.02). The mean percentage of double-labeled $CD3^+$ T lymphocytes increased to 5.5% (± 1.0) by 24 hpi. The EAV nsp1 antigen expression peaked with a mean percentage of 6.6% (± 0.8) of double-labeled $CD3^+$ T cells at 36 hpi and decreased to 4% (± 0.4) at 48 hpi. Interestingly, none of the $CD3^+$ T lymphocytes from the remaining four horses were infected with the VB strain of EAV (Figure 2.1 B). Based on the phenotype of $CD3^+$ T lymphocyte subpopulations to *in vitro* infection with VB strain of EAV, the ten horses could be divided into susceptible (Group A; 6/10) and resistant (Group B; 4/10) groups. Contrary to infection with the VB strain, T lymphocytes from none of the 10 donor horses were susceptible to infection with the MLV vaccine strain of EAV (Figures 2.1 A and B).

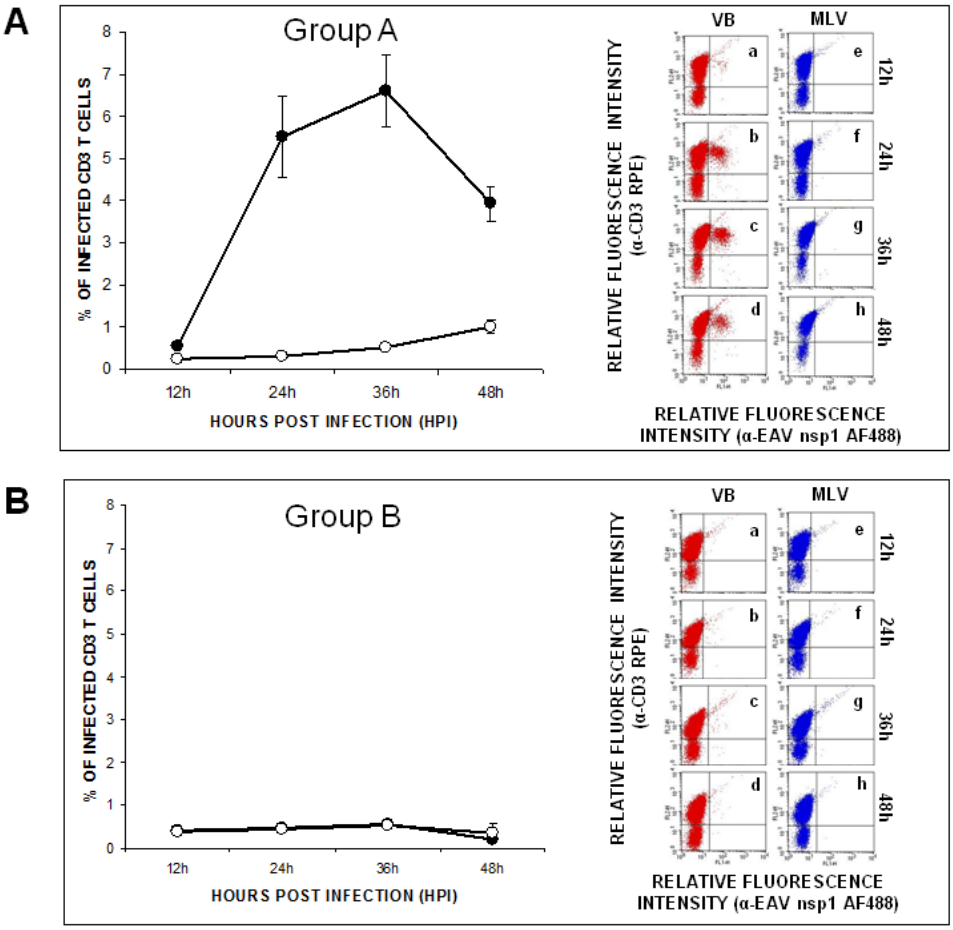

Figure 2.1. Differences in susceptibility of CD3$^+$ T lymphocytes to infection with VB and MLV strains of EAV. Dual color immunofluorescence flow cytometric analysis was performed at various hours post-infection (hpi). (A) Values represent the mean percentage of infected CD3$^+$ T cells (± S.E.M) with VB (black circles) and MLV (white circles) for 6 horses with T lymphocytes susceptible to EAV VB infection (Group A). Percentages of infected cells at the indicated times (data points on the curve) were determined by using dot plots derived from dual fluorescence flow cytometric analyses of cells (representative dot plots of VB infection, insets *a* through *d*; MLV infection, insets *e* through *h*). (B) Values represent the mean percentage of infected CD3$^+$ T cells (± S.E.M) with VB (black circles) and MLV (white circles) for 4 horses with T lymphocytes resistant to EAV VB infection (Group B) as determined by using dot plots derived from dual fluorescence flow cytometric analyses of cells (representative dot plots of VB infection, insets *a* through *d*; MLV infection, insets *e* through *h*).

In an attempt to define the T lymphocyte subpopulation susceptible to VB infection, lymphocytes from Group A horses were infected with the VB strain and were stained with either CD4 or CD8 specific MAb and antibody to EAV nsp1. Similar to $CD3^+$ T lymphocytes, the mean percentage of double-labeled $CD4^+$ T cells increased to 4.4% (± 0.8) by 24 hpi. The EAV nsp1 antigen expression peaked at 36 h after inoculation with a mean percentage of 5% (± 0.7) of double-labeled $CD4^+$ T cells which decreased subsequently to 2.8% (± 0.3) at 48 hpi (Figure 2.2 A). The mean percentage of double-labeled $CD8^+$ T cells ranged from 0.03 to 1.1% ([± 0.03 to 0.2]; Figure 2.2 B) through to the completion of the experiment. These findings indicated that the majority of $CD3^+$ T lymphocytes infected with the VB strain were $CD4^+$ T lymphocytes rather than $CD8^+$ T lymphocytes. Not surprisingly, in a similar experiment neither $CD4^+$ nor $CD8^+$ T lymphocytes from the four horses in group B could be infected with the VB strain of EAV (data not shown). EAV nsp1 antigen expression was not detected in the $CD21^+$ B lymphocyte cultures from either group A or B horses inoculated with either the VB or MLV vaccine strains (Figure 2.2 C) indicating that B lymphocytes are not susceptible to EAV infection. In summary, viral antigen could be detected primarily in $CD4^+$ T lymphocyte subpopulations from Group A horses infected with VB strain of EAV. These data showed that only $CD4^+$ T lymphocytes from some horses are susceptible to infection with the VB strain but none of them are susceptible to infection with MLV strain indicating that attenuation of the VB strain has altered its cellular tropism.

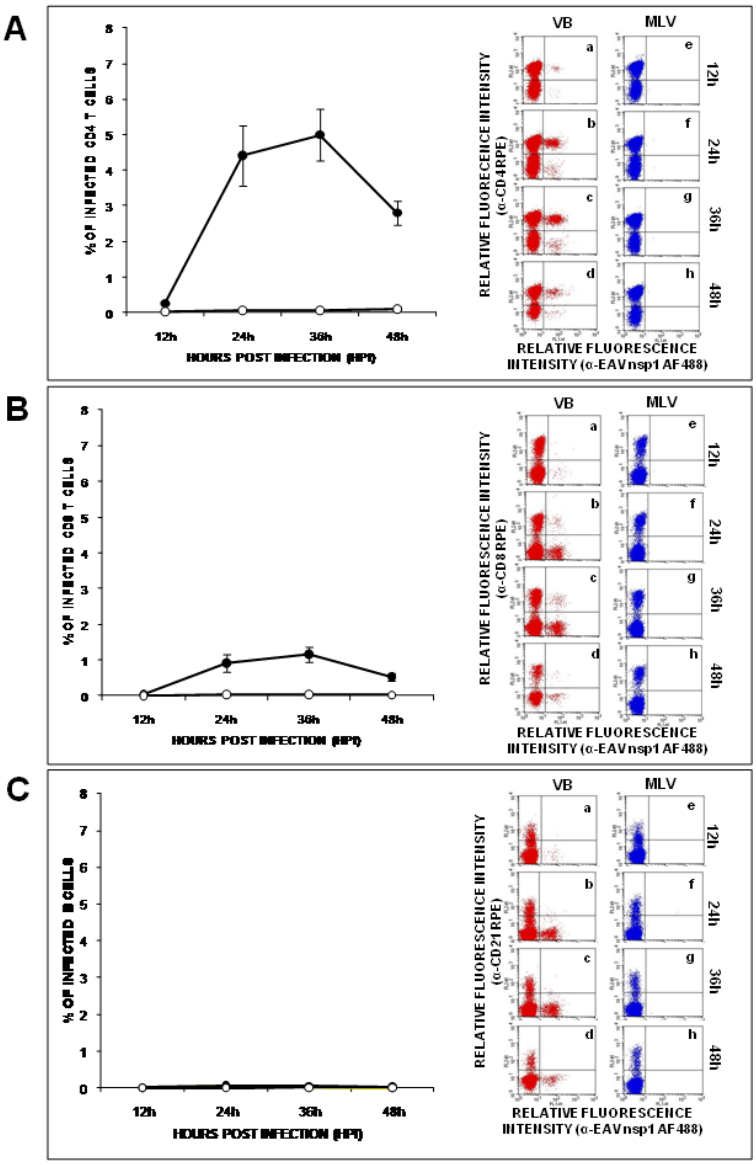

Figure 2.2. Susceptibility differences between CD4$^+$ and CD8$^+$ T lymphocytes and CD21$^+$ B lymphocytes to infection with VB and MLV strains of EAV. Dual color immunofluorescence flow cytometric analysis was performed at various time p.i. Values represent the mean percentage of (A) infected CD4$^+$ T cells, (B) infected CD8$^+$ T cells and (C) infected CD21$^+$ B cells (± S.E.M) with VB (black circles) and MLV (white circles) strains of EAV. Percentages of infected cells at the indicated times (data points on the curve) were determined by using dot plots derived from dual fluorescence flow cytometric analyses of cells (representative dot plots of VB infection, insets *a* through *d*; MLV infection, insets *e* through *h*).

To investigate whether monocytes are equally susceptible to infection with VB and MLV strains of EAV, dual immunofluorescence staining was performed using MAbs specific for $CD14^+$ monocytes and MAb specific for the EAV nsp1. Using the adherent cells obtained from PBMCs derived from two of each group of horses, the percentage of $CD14^+$ monocytes ranged from 60 to 75% depending on the preparation. Double-labeled flow cytometric analysis showed that monocytes from all of the tested horses could be infected with VB and MLV strains of EAV (Figure 2.3).

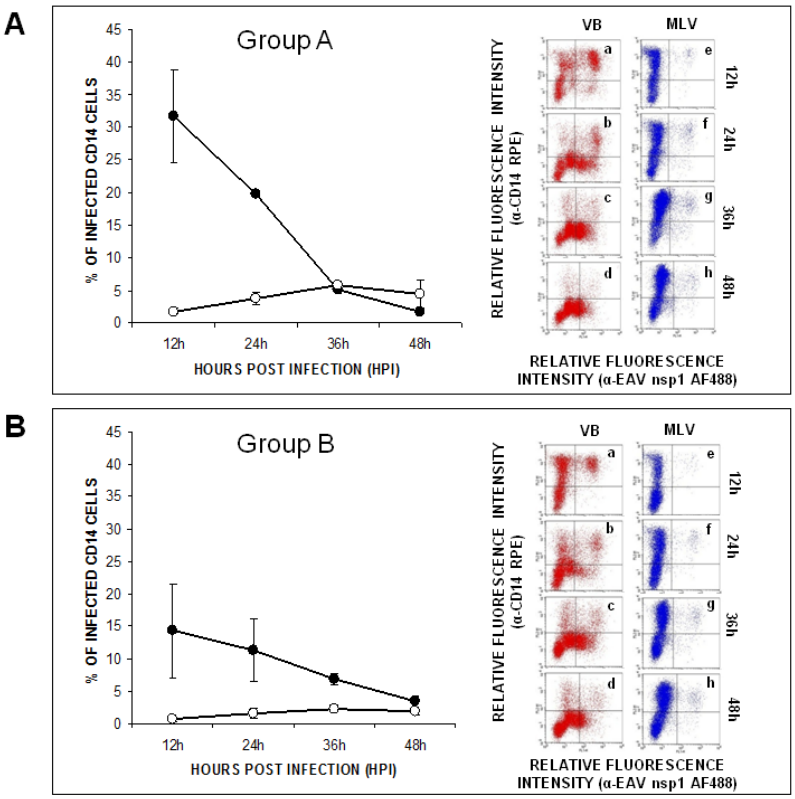

Figure 2.3. Infection of monocytes with the VB and MLV strains of EAV. (A and B) Dual color immunofluorescence flow cytometric analysis was performed at various time p.i. Values represent the mean percentage of infected monocytes (± S.E.M) with VB (black circles) and MLV (white circles) for (A) 2 horses with T lymphocytes susceptible to EAV VB infection (Group A) and (B) 2 horses with T lymphocytes resistant to EAV VB infection (Group B). Percentages of infected cells at the indicated times (data points on the curve) were determined by using dot plots derived from dual fluorescence flow cytometric analyses of cells (representative dot plots of VB infection, insets *a* through *d*; MLV infection, insets *e* through *h*).

However, the mean percentage of MLV infected cells was significantly lower and remained near the lower limit of detection throughout the experimental time course compared to those detected in VB infected monocytes (Figures 2.3 A and B) from both group of horses. In the case of cultures infected with the VB strain, the maximum mean percentage of cells expressing EAV nsp1 antigen in monocytes from Group A horses (n=2) was approximately 31.8% (± 7.2) at 12 hpi, after which it had declined sharply by (1.8 ± 0.2%) 48 hpi (Figure 3A; Group A). Similar patterns were noted for monocytes purified from the Group B horses (n=2; Figure 2.3 B; Group B). However, the overall mean percentage of cells expressing EAV antigen was significantly lower in monocytes from the Group B horses (14.3% ± 7.3 at 12 hpi and 11.3% ± 4.7 at 24 hpi) compared to monocytes from the susceptible horses (Group A) at 12 and 24 hpi (Figures 2.3 A and B). The mean percentage of infected monocytes in MLV inoculated cultures was minimal at 12 hpi after which it gradually increased. Although similar patterns of infection were shown for cells derived from horses in groups A and B, the mean percentage of infected cells in the case of the former was significantly higher than in the case of the latter (Figures 2.3 A and B). Furthermore, these findings confirm that not only T lymphocytes but also monocytes differ in their susceptibility to infection with VB and MLV strains of EAV.

Expression of the structural proteins of EAV in PBMCs infected with virulent and attenuated strains of EAV

One of the key findings of this study is the susceptibility of $CD3^+$ T (predominantly $CD4^+$ T) lymphocytes of Group A horses to VB infection as determined by the expression of the nsp1 protein. To investigate whether viral structural protein genes are also expressed in infected cultures, two-color flow cytometric analysis was performed using MAbs specific for cell surface markers and MAb specific for the EAV nucleocapsid (N) protein. When T lymphocytes isolated from horses in Group A were infected with the VB strain, both nsp1 and N protein expression were detected in $CD3^+$, $CD4^+$ and $CD8^+$ T lymphocytes (Figure 2.4, panels *a* through *c* [nsp1] and panels *d* through *f* [N]).

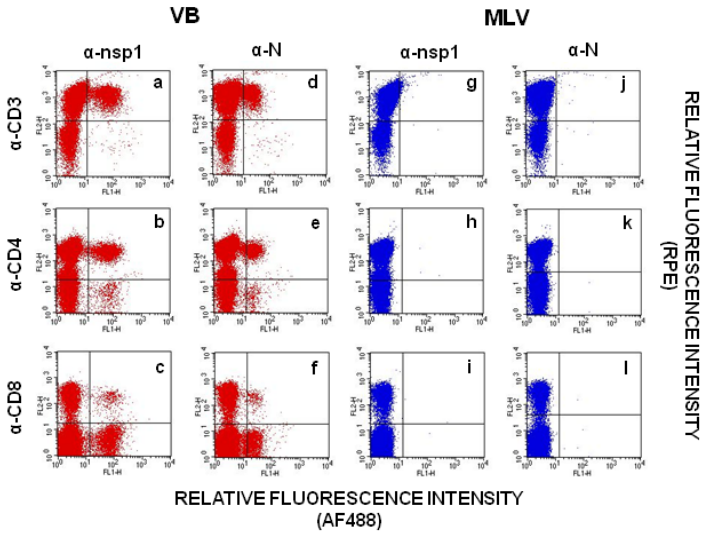

Figure 2.4. Detection of EAV nucleocapsid (N) protein expression in T lymphocytes infected with the VB strain. The $CD3^+$, $CD4^+$ and $CD8^+$ T lymphocytes from Group A horses infected with VB and MLV strains of EAV were examined by dual-color immunofluorescence flow cytometric analysis using MAbs against EAV nsp1 (MAb 12A4) and N (MAb 3E2) proteins and MAbs for cell specific cell surface antigens at 24 hpi. (Panels *a* through *c*) Lymphocytes infected with VB strain were stained with anti-EAV nsp1 AF488 MAb and one of the specific antibodies for T lymphocytes including MAbs to CD3, CD4, and CD8, respectively. (Panels *d* through *f*) Dot plots derived from same cultures stained with anti-EAV N AF488 MAb and specific antibodies for $CD3^+$, $CD4^+$ and $CD8^+$ T lymphocytes, respectively. (Panels *g* through *i*) Lymphocytes infected with MLV strain were stained with anti-EAV nsp1 MAb and specific antibodies for T lymphocytes including MAbs to CD3, CD4, and CD8, respectively. (Panels *j* through *l*) Dot plots derived from same cultures stained with anti-EAV N AF488 MAb and specific antibodies for $CD3^+$, $CD4^+$ and $CD8^+$ T lymphocytes, respectively.

In contrast, $CD3^+$, $CD4^+$ and $CD8^+$ T lymphocytes were completely refractory to infection with the MLV strain since neither nsp1 nor N protein expression could be

observed in inoculated cultures (Figure 2.4, panels *g* through *i* [nsp1] and panels *j* through *l* [N]). The data indicated that a virus replication cycle, at least up to expression of structural proteins, occurred in VB infected T lymphocytes but not in MLV infected T lymphocytes of Group A horses. However, release of progeny virus particles could not be detected in VB inoculated cultures of sorted $CD3^+$, $CD4^+$ and $CD8^+$ T lymphocytes from any of tested horses based on virus one step growth curve and quantitative real-time RT-PCR (qrRT-PCR) results (data not shown). Furthermore, we also investigated the expression of N protein in monocytes infected with the VB and MLV strains of EAV (Figure 2.5.A.). In contrast to T lymphocytes, expression of both nsp1 and N protein were detected in monocytes infected with VB and MLV strains. Not surprisingly, the percentage of monocytes expressing nsp1 and N proteins was significantly greater in VB infected cultures (24.8% ± 4.4 and 18.3% ± 1.8, respectively [panels *a* and *b*]) compared to the corresponding percentage of cultures infected with the MLV strain (5.5% ± 1.9 and 3.7% ± 1.8, respectively; Figure 2.5 A [panels *c* and *d*]). Additionally, viral titers and viral nucleic acid copy numbers from sorted $CD14^+$ monocytes inoculated with VB and MLV strains of EAV confirmed the findings from double-staining flow cytometric analysis (Figures 2.5.B and 2.5.C, respectively). In monocyte cultures inoculated with the VB strain, viral titers increased gradually by 18 hpi reaching a maximum titer of approximately 10^5 $TCID_{50}$/50 µl at 36 hpi. After reaching this peak level, titers gradually declined to 10^4 $TCID_{50}$/50 µl by the final sample collection time at 72 hpi. Although, productive viral replication also occurred in MLV inoculated monocytes, viral titers were lower than those detected in VB inoculated cells (Figure 2.5.B). Interestingly, while MLV titers remained low until 48 hpi, they showed a significant increase by 72 hpi. The trends in the viral growth curves were similar to those observed in nucleic acid copy numbers quantified by qrRT-PCR (Figure 2.5.C). Monocytes infected with the VB strain had increased viral nucleic acid copy numbers from 18 hpi reaching a maximum after 48 hpi in both groups of horses. In contrast to VB infected monocytes, viral nucleic acid copy numbers in monocytes infected with the MLV strain remained low throughout the time course of the experiment, though they had started to increase at 72 hpi which was consistent with the viral growth curve results (Figure 2.5.C). These data confirmed that

the MLV strain replicates slower and to lower titers in monocytes compared to the VB strain of EAV in Group A horses.

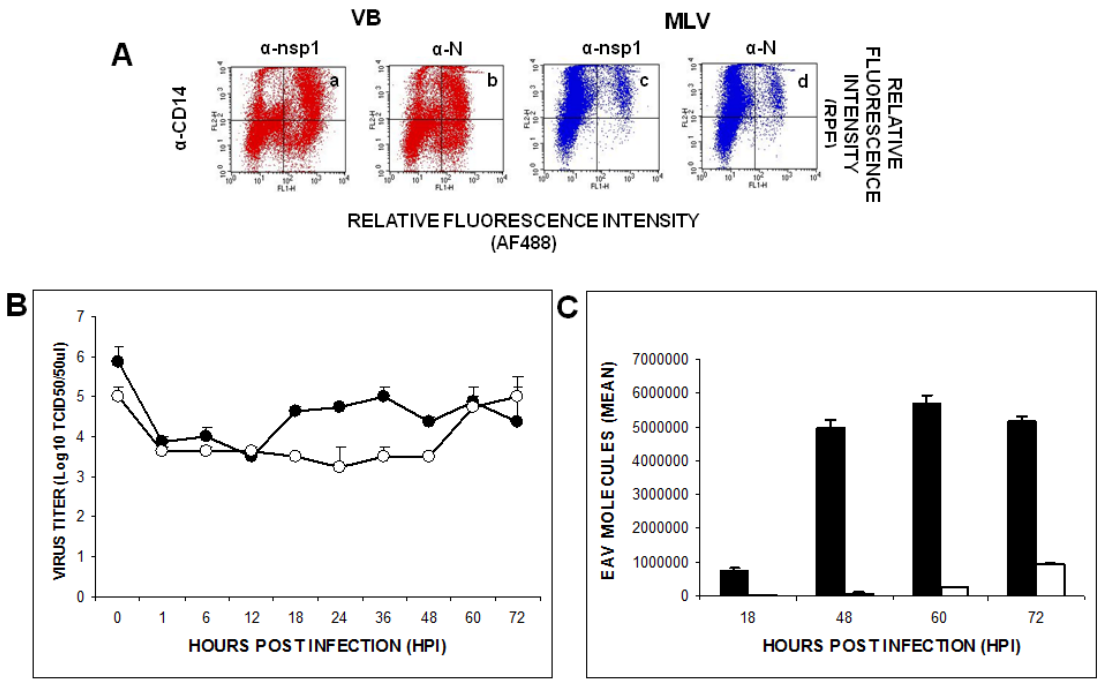

Figure 2.5. Replication of VB and MLV strains of EAV in blood-derived monocytes of Group A horses. (A) The $CD14^+$ monocytes infected with VB and MLV strains of EAV were examined by dual-color immunofluorescence flow cytometric analysis using MAbs against EAV nsp1 (12A4) and N (3E2) proteins and MAbs for cell specific cell surface antigens at 24 hpi. (Panels *a*, *b*) Monocytes infected with VB strain were stained with anti-EAV nsp1 MAb (panel *a*) or N MAb (panel *b*) and a specific antibody to cell surface antigen, CD14 MAb. (Panels *c*, *d*) Monocytes infected with MLV strain were stained with anti-EAV nsp1 MAb (panel *c*) or N MAb (panel *d*) and a specific antibody to cell surface antigen, CD14. (B) Replication of VB (black circles) and MLV (white circles) strains in purified monocytes. Tissue culture fluids were collected at indicated times and viral titers were determined as $\log_{10}$ 50% tissue culture infective dose ($TCID_{50}$)/50µl. Values shown are the mean viral titers ± S.E.M. (C) Quantification of viral RNA copy number in cell culture fluid from purified monocytes infected with VB (black bars) and MLV (white bars) strains using qrRT-PCR. Results are expressed as mean (± S.E.M) values.

Infection of CD3$^+$ T lymphocytes and CD14$^+$ monocytes with EAV recombinant chimeric viruses

A marked disparity in the ability of VB and MLV strains to infect subpopulations of susceptible CD3$^+$ T lymphocytes and monocytes (Group A horses) suggested that there is a clear difference in cellular tropism between the two strains. In our preliminary studies, the recombinant viruses, rVBS and rMLV, had similar growth kinetics in equine endothelial cells (EECs; data not shown) and an equivalent capacity for lymphocyte infectivity as confirmed by flow cytometry analysis (Figure 2.6; panels *a* through *d* [rVBS] and *i* through *l* [rMLV]) when compared to their respective wild-type parental viruses, VB and MLV. To identify the viral proteins responsible for the differential cellular tropism between VB and MLV, we attempted to assess the impact of amino acid changes accumulated during cell culture passage of HK116 strain, which is fully attenuated for horses as compared to the VB strain. Therefore, we used the previously described rVBS/HK116 S chimeric virus [331] containing the structural proteins of EAV HK116 virus in backbone of rVBS genome to infect PBMCs from Group A horses. When susceptible T lymphocytes were inoculated with chimeric rVBS/HK116 S, the number of T lymphocytes expressing EAV nsp1 antigen decreased significantly compared to rVBS (2.3% to 0.2%; Figure 2.6; panels *e* through *g*). In contrast, the percentage of infected monocytes was comparable to that using the rVBS virus indicating that the tropism of the HK116 strain had changed for lymphocytes but not for monocytes following 116 passages in primary horse kidney cells (Figure 2.6; panel *h*). In summary, these data showed that amino acid substitutions in the structural protein genes of HK116 strain changed CD3$^+$ T lymphocyte tropism of the virus without any significant effect on its CD14$^+$ monocyte tropism.

In an attempt to further identify the specific viral proteins responsible for the differential tropism among VB, HK116 and MLV strains in equine PBMCs, we generated a new panel of four recombinant chimeric viruses using the infectious cDNA clones of the VB and MLV strains (rVBS and rMLV, respectively). The panel consisted of reciprocal chimeric viruses containing interchanged structural and nonstructural protein genes of the VB and MLV strains (Figure 2.6). When susceptible lymphocytes and monocytes were infected with rVBS/MLV S and rMLV/VBS S viruses, rVBS/MLV S

did not infect any $CD3^+$ T lymphocytes and only replicated in $CD14^+$ monocytes at a very low level which was identical to that observed in rMLV infection (Figure 2.6; panels *m* through *p*). In contrast, the rMLV/VBS S infected and replicated in both $CD3^+$ T lymphocytes and $CD14^+$ monocytes similar to rVBS but there was a reduction in viral protein expression in lymphocytes compared with that observed in cells infected with rVBS virus (Figure 2.6; panels *q* through *t*). These results suggest that the structural proteins of the VB strain are responsible for determining its tropism for lymphocytes and monocytes. Furthermore, comparison of dual-color flow cytometric data of PBMCs infected with rVBS/HK116 S and rVBS/MLV S showed significant differences in $CD14^+$ monocyte infectivity, indicating that amino acid substitutions that occurred during further cell culture passage of HK116 may have contributed to the change in monocyte tropism. Taken together, the data suggest that viral tropism for $CD3^+$ T lymphocyte and $CD14^+$ monocyte was altered by amino acid changes in structural proteins of EAV.

To further investigate the role of minor and major envelope proteins of EAV in cellular tropism, additional recombinant viruses, rMLV/VBS 234 and rMLV/VBS 56, were generated with the MLV infectious cDNA clone as the viral backbone and used for *in vitro* infection of susceptible lymphocytes and monocytes. Recombinant rMLV/VBS 234 virus contained the genome sequence identical to that of the rMLV virus except for ORFs 2a, 2b, 3 and 4 (encoding for E, GP2, GP3 and GP4 minor envelope proteins) that were replaced by the corresponding regions of the rVBS virus. In the case of rMLV/VBS 56 virus, whose ORFs 5 and 6 (encoding for GP5 and M major envelope proteins) were replaced with the corresponding genes of rVBS in the rMLV backbone (Figure 2.6). In contrast to expectations, neither rMLV/VBS 234 nor rMLV/VBS 56 chimeras were able to infect T lymphocytes (Figure 2.6; panels *u* through *w* [rMLV/VBS 234] and panels *y* through *z'* [rMLV/VBS 56]). However, comparisons in monocytes showed that while the percentage of cells infected with rMLV/VBS 56 virus was similar to that of rMLV and rVBS/MLV S viruses, infection rates for rMLV/VBS 234 virus were significantly lower (Figure 2.6; panels *z''* and *x*, respectively). Therefore, the higher relative fluorescence intensity values observed in monocytes with rMLV/VBS 56 (Figure 2.6; panel *z''*) compared to rMLV/VBS 234 (Figure 2.6; panel *x*) suggest GP5 and M amino acid sequences may play a more critical role than those of E, GP2, GP3 and GP4 in facilitating

monocyte infections. Taken together, these data demonstrate the minor envelope glycoproteins as well as the two major envelope proteins play a critical role in determining monocyte tropism.

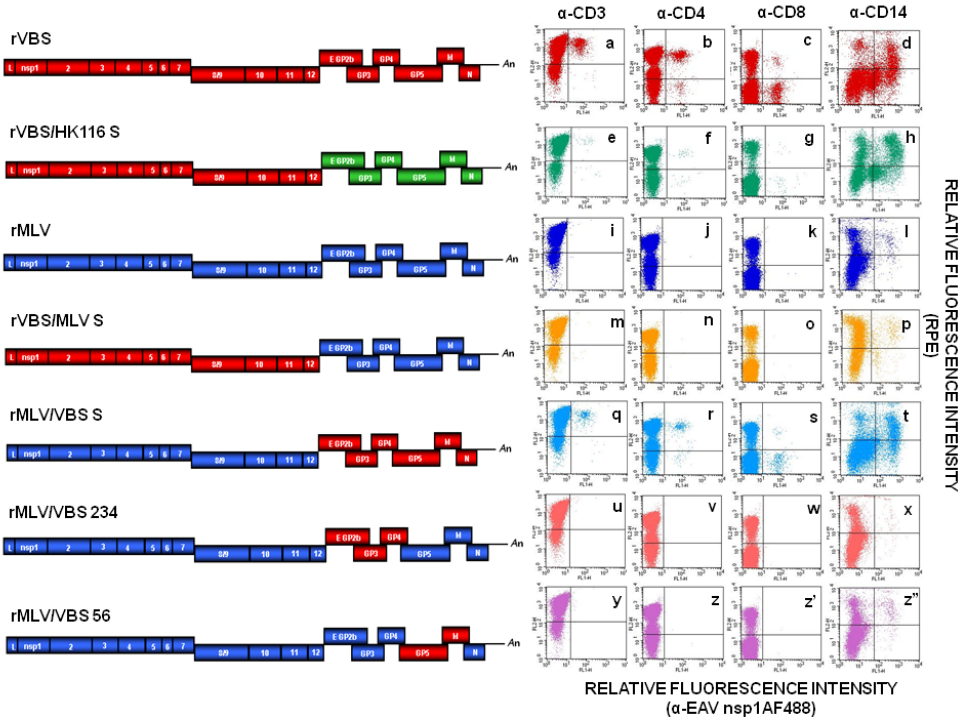

Figure 2.6. Infection of lymphocytes and monocytes with recombinant EAV. The genome of the infectious full-length cDNA clone of rVBS (red boxes) and the genome of rMLV clone (blue boxes) are depicted. The genes encoding structural proteins of EAV HK116 virus are shown in green. The four chimeric viruses containing nonstructural and structural protein genes of either rVBS, or rMLV virus are also depicted. L, leader; *A*n, poly A. The $CD3^+$, $CD4^+$ and $CD8^+$ T lymphocytes and $CD14^+$ monocytes infected with recombinant viruses rVBS (panels *a* through *d*), rVBS/HK116 S (panels *e* through *h*), rMLV (panels *i* through *l*), rVBS/MLV S (panels *m* through *p*), rMLV/VBS S (panels *q* through *t*), rMLV/VBS 234 (panels *u* through *x*) and rMLV/VBS 56 (panels *y* through *z''*) were examined by dual-color immunofluorescence flow cytometric analysis using MAbs against EAV nsp1 (12A4) and MAbs for cell specific cell surface antigens at 24 hpi.

Comparative amino acid sequence analysis of GP2, GP3, GP4, GP5 and M proteins of rVBS, HK116 and rMLV viruses

The reverse genetic studies using recombinant chimeric viruses clearly indicated that collective interactions among all EAV envelope proteins are required for efficient infection of susceptible subpopulations of $CD3^+$ T lymphocytes and $CD14^+$ monocytes, and these interactions were disabled or altered by the amino acid changes which had occurred during extensive serial passage of the VB strain resulting in the HK116 and MLV vaccine strains of EAV. Accordingly, the nucleotide sequences of ORFs 2 to 6 from VB, HK116 and MLV strains have been translated, aligned and analyzed in the context of the predicted topography of each viral structural protein. The E minor envelope protein encoded by ORF2a was conserved (100% identity) among VB, HK116 and MLV strains and therefore it is almost certainly not responsible for the differences in tropism among the three EAV strains (Table 2.1). When compared to the VB strain, the GP2, GP4, GP5 and M envelope proteins of HK116 strain had several amino acid substitutions (2, 1, 3 and 3 substitutions respectively; Table 2.1). With the exception of amino acid substitutions in the M protein and one amino acid substitution in the GP2 protein (223R>P) of HK116 virus, all the amino acid changes were located in the ectodomain of these proteins (Table 2.1 and Figure 2.7). Interestingly, in contrast to GP2, GP4, GP5 and M envelope proteins, the amino acids of the GP3 protein of HK116 strain were identical to the parental VB strain. The data indicated that loss of $CD3^+$ T lymphocyte tropism of HK116 virus is primarily due to substitutions involving the GP2, GP4, GP5 and M envelope proteins rather than the GP3 minor envelope protein. However, further cell culture passage of this HK116 strain resulted in numerous other non-synonymous amino acid substitutions in ORFs 2b, 3-6 (Table 2.1, Figure 2.7). All of these substitutions appear to be non-conservative and therefore are likely to affect secondary and tertiary structure, which may change the interactions between these envelope proteins (Figure 2.7). Analysis of ORF3 demonstrated a U→C substitution at position 10,795 in rMLV resulting in the removal of the normal stop codon present in rVBS and HK116 and permitting the addition of five amino acids to the carboxyl-terminus of GP3.

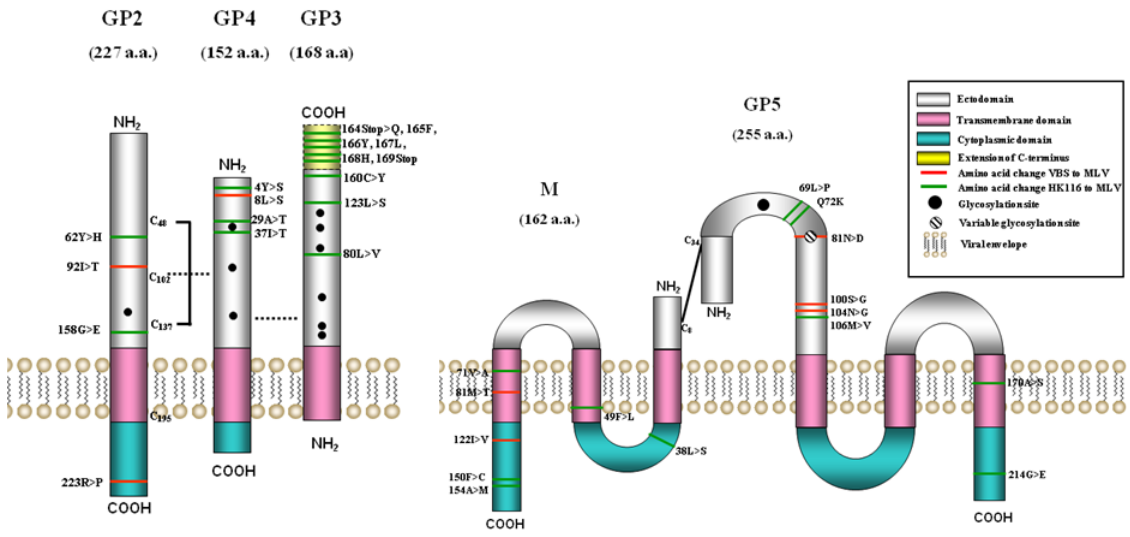

Figure 2.7. Predicted membrane topology of minor (GP2, GP3 and GP4) and major (GP5 and M) EAV envelope proteins. Amino acid substitutions occurred during extensive cell culture passage of the VB strain of EAV resulting in the HK116 and MLV strain of the virus are indicated. A predicted model for the disulfide-bonded structure of covalently linked minor envelope proteins GP2, GP3 and GP4 proteins is depicted based on previous experimental studies [137,139,140,143,144]. The major envelope GP5 and M proteins are covalently linked by a disulfide bond (S-S) formed between Cys-8 in the M protein and the Cys-34 in the GP5 protein [68].

Furthermore, there are three other non-synonymous nucleotide substitutions between rMLV and rVBS (as well as the intermediate HK116 strain) in ORF3 of which leucine to serine at amino acid position 123 and cysteine to tyrosine at position 160 appear to be non-conservative (Table 2.1, Figure 2.7). In common with ORF3, all four non-synonymous nucleotide substitutions in ORF4 are predicted to occur in the ectodomain of GP4, a trend also observed in ORF5 where six of the eight non-synonymous substitutions occur within the same predicted domain for GP5 (Table 2.1, Figure 2.7). Therefore, it appears as if most of the variation in amino acid content between the structural proteins of rVBS and rMLV occurs in those regions that could interact directly with host-cell receptor molecules. An exception to this is in ORF6

where all seven non-synonymous nucleotide substitutions between rMLV and rVBS are predicted to occur in the endodomain or transmembrane-spanning domain of the M protein. During extensive cell culture passage, the second putative N-linked glycosylation site at amino acid position 81 (81N>D) in GP5 was lost leaving the GP5 of MLV with only the conserved putative N-linked glycosylation site at amino acid position 56. Taken together, these data clearly demonstrate that the failure of MLV to infect $CD3^+$ T lymphocytes was determined by the amino acid changes in the GP2, GP4, GP5 and M proteins but not the GP3 protein. In contrast, the reduced monocyte tropism of the MLV strain appears to be due to the amino acid changes in the GP3 protein. However, additional amino acid substitutions in GP2, GP4, GP5 and M protein may also have contributed to the altered monocyte tropism. Since the nucleocapsid protein (N) encoded by ORF7 is not exposed on the virus surface, it is unlikely that this protein has contributed to the change in cellular tropism of EAV. Therefore, it is more likely that tropism of $CD3^+$ T lymphocytes and $CD14^+$ monocytes was altered due to the changes in major and minor envelope proteins of EAV.

2.5. DISCUSSION

In contrast to attenuated strains of EAV, highly pathogenic strains are highly cell-associated with PBMCs and cause high titered viremia [154,213,328]. However, until now the interaction between EAV and PBMCs has not been fully characterized and the specific cell types infected with EAV were not identified. Therefore, the primary objective of this study was to unequivocally establish which components of the PBMC population were susceptible to EAV infection and then identify the viral proteins responsible for infection of these cells. Based on dual-color flow cytometric analysis and conventional viral titration assay along with qrRT-PCR on infected cell culture fluids, we demonstrated that the predominant host cell type susceptible to virulent VB strain of EAV are $CD14^+$ cells of the monocyte/macrophage lineage. Furthermore, under *ex-vivo* culture conditions these cells were permissive for complete productive replication of the VB strain. Although this is an important finding, it is perhaps not surprising in view of the fact EAV antigens have been found in alveolar macrophages in infected horses [76,257] and that all other members of the *Arteriviridae* family are

monocyte/macrophage tropic [51]. However, the finding that the VB strain can infect $CD3^+$ T lymphocytes (predominantly $CD4^+$ T cells) of some but not all horses is the first report of a member of this virus family being associated with T lymphocytes. Surprisingly, there was a clear difference in the horse population based on the susceptibility of their $CD3^+$ T lymphocytes and $CD14^+$ monocytes with *in vitro* VB infection. As a result, horses were categorized as Group A in which almost one third of monocytes along with $CD3^+$ T lymphocyte (mainly $CD4^+$ T cells) subpopulations were susceptible to infection with the virulent EAV strain or as Group B in which monocyte susceptibility was only half of that observed in Group A horses and all $CD3^+$ T lymphocyte subpopulations were resistant to EAV infection. Based on this finding, we assumed that horse's genetic background may play a significant role in determining the clinical outcome of primary infection with EAV as reported in other species [350,351]. Efforts are underway in our laboratory to investigate if there is a genetic basis for the differences between horses in the susceptibility of their monocytes and $CD3^+$ T lymphocytes to VB infection by analyzing possible associations with single nucleotide polymorphisms (SNP). Furthermore, an *in vivo* study is planned in which Group A and B horses are infected with rVBS to establish the relationship between PBMCs susceptibility and the severity of clinical illness or EVA, respectively.

Expression of nsp1 and N proteins in $CD3^+$ T lymphocytes demonstrated the VB strain undergoes initial replication steps such as binding/entry, uncoating and translation of nonstructural and structural proteins. However, production of progeny virus was not evident in sorted $CD3^+$, $CD4^+$ and $CD8^+$ T lymphocytes from any of the tested horses based on the virus one-step growth curve results or qrRT-PCR results despite synthesis of the full complement of viral proteins. This indicates that the number of progeny virions generated is either below the limit of detection, a possible reflection of the relatively small numbers of T lymphocytes infected (about 5%), or there is a blockage at a later stage in viral assembly and/or release. It remains to be determined if these cells represent "dead-end" hosts or if they are fully permissive. In contrast to the VB strain, expression of MLV nsp1 or N could not be detected in $CD3^+$ T lymphocytes from any tested horses demonstrating that the amino acid substitutions that occurred during the attenuation process of the VB strain prevented entry and replication of MLV strain in these cells. In addition,

the number of $CD14^+$ monocytes expressing viral nsp1 or N proteins following infection with the attenuated MLV strain was significantly less than observed with VB virus.

Data derived from this study suggested that the amino acid substitutions in major and minor envelope proteins that occurred during cell culture passage of the VB strain contributed to the altered tropism of MLV virus for $CD3^+$ T lymphocytes and $CD14^+$ monocytes. In an attempt to identify the viral proteins associated with infection of T lymphocytes and greater numbers of monocytes, we generated a panel of recombinant chimeric viruses in which the structural and nonstructural protein genes of the parental rVBS were replaced with corresponding genes of the rMLV strain. *In vitro* evaluation of rMLV/VBS S chimeric virus demonstrated conclusively that cell tropism was determined by envelope proteins of the virus. The role of the viral envelope proteins in $CD3^+$ T lymphocyte and macrophage tropism was further defined by using recombinant chimeric viruses in which sequences encoding the minor envelope glycoproteins (GP2, GP3 and GP4) or major envelope proteins (GP5 and M) of the MLV strain were replaced with the corresponding genes of rVBS in an rMLV backbone (designated rMLV/VBS 234 and rMLV/VBS 56, respectively). Recombinant chimeric viruses derived from these infectious cDNA clones were unable to infect T lymphocytes and numbers of monocytes expressing nsp1 were either lower (rMLV/VBS 234) or equivalent (rMLV/VBS 56) to those observed when these cells were infected with parental rMLV. For the first time evidence is presented suggesting that infection of T lymphocytes along with the ability to infect relatively large numbers of monocytes is dependent on cooperative interactions between five out of the six envelope proteins of EAV (GP2, GP3, GP4, GP5 and M). This, in turn, suggests that the infection process of these cell types is complex, possibly involving multiple receptor and/or receptor accessory molecules. Furthermore, the data also indicated that during extensive sequential cell culture passage, viral envelope protein genes have coevolved resulting in a synergistic effect on cellular tropism. Interestingly, based on findings with the rVBS/HK116 S chimeric virus, the GP3 protein is not associated with altered tropism for $CD3^+$ T lymphocytes. Substitutions in the other two minor envelope glycoproteins (GP2 and GP4) and the two major envelope proteins (GP5 and M), however, play a critical role in changing the tropism for these cells. The dual-color flow cytometry data clearly demonstrated that the HK116 strain was significantly

different from both VB and MLV strains. By 116th passages of the VB strain in primary HK cells, the virus lost its permissiveness for CD3^{+} T lymphocytes but its ability to infect CD14^{+} monocytes remained similar to the parental VB strain. Further cell culture passage of HK116 virus in different cell lines (HK15, RK111 and ED24) to obtain the MLV strain, resulted in significant reduction in its ability to infect macrophages (27% to 5%; Fig. 6; panels *h* and *l*, respectively). However, it is important to note that the attenuated phenotype of EAV HK116 for horses correlates with the loss of permissiveness for T lymphocytes while the ability to infect monocytes remains similar to that of the parental VB strain. This suggests that either directly or indirectly tropism for T lymphocytes has a significant role in the pathogenesis of VB infections *in vivo*. Therefore, the susceptibility of CD3^{+} T lymphocytes to virulent and avirulent field strains of EAV and their role in the pathogenesis of EVA warrants further in-depth investigation.

Interestingly, based on comparative amino acid sequence and predicted membrane topology of the envelope proteins, the majority of the amino acid variations between VB and MLV viruses, as well as HK116, are located within the predicted ectodomain of each envelope protein, except for the M protein, in which the changes are in the transmembrane and cytoplasmic domains (Figure 2.7). It is known that GP5 and M exist in the virion as a heterodimer while the minor envelope proteins (GP2, GP3 and GP4) occur in particles as heterotrimeric complexes constituting a virion-exposed structure that is predicted to mediate binding of the virion to the primary receptor [144]. Formation of the heterotrimeric minor envelope complex is dependent on intramolecular cysteine bonding with GP2 and GP3 being linked via interactions with GP4 [140]. The existence of these complexes coupled with the fact that most of the amino acid substitutions appear to be non-conservative, suggest that the cell tropism of MLV and VB strains is determined by conformational differences in structural envelope proteins that are manifested at the tertiary and quaternary levels. Therefore, the amino acid substitutions located within the various ectodomains may have direct and indirect effects on interactions with host cells as well as associations between the viral structural proteins. Consistent with our findings, a recent published study on porcine reproductive and respiratory syndrome virus has shown that inter-glycoprotein interactions are critical for mediating interactions with the receptor responsible for virus entry into host cells [352].

Specifically, it has been demonstrated strong interaction between GP4 and GP5, as well as weak interactions among other minor envelope proteins resulting in the formation of multiprotein complex. Furthermore, in a previous study we have also demonstrated that change in cellular tropism and establishment of persistent infection in HeLa cells by VB strain of EAV was associated with amino acid substitutions in the envelope proteins [236]. Reverse genetic studies further confirmed that substitutions in the minor envelope proteins E and GP2 or GP3 and GP4 alone were unable to change cellular tropism and establishment of persistent infection in HeLa cells but recombinant viruses with combined substitutions in the E, GP2, GP3 and GP4 as well as a single amino acid substitution in the GP5 were able to alter cellular tropism of VB strain of EAV and favor establishment of persistent infection in HeLa cells. Nevertheless, the situation is further complicated by the fact so little is known about the EAV receptor and whether this is restricted to a single molecule or if the virus can use multiple alternatives but potentially cell-type specific molecules.

In summary, for the first time we demonstrate that extensive cell culture passage of the VB strain of EAV to produce the MLV vaccine strain has altered its cellular tropism for equine PBMCs. Evaluation of chimeric viruses demonstrated that cellular tropism in PBMCs is determined by the amino acid sequence of viral envelope proteins. Specifically the data suggest that the GP2, GP4, GP5 and M envelope proteins play a critical role in $CD3^+$ T lymphocyte tropism while three minor envelope proteins (GP2, GP3 and GP4) as well as the GP5 and M major envelope proteins determine the $CD14^+$ monocyte tropism of EAV.

CHAPTER THREE

Genome-Wide Association Study Identifies a Common Haplotype in Horses Associated with CD3$^+$ T Cell Susceptibility to Equine Arteritis Virus Infection

J. Virol. 2011, 85 (24):13174-84

Reprinted with permission

3.1. SUMMARY

Equine viral arteritis (EVA) is a reproductive and respiratory disease of horses caused by equine arteritis virus (EAV), the prototype virus of the family *Arteriviridae*. Recently, we have shown that horses could be divided into susceptible and resistant groups based on an *in vitro* assay using dual color flow cytometric analysis of CD3$^+$ T cells infected with EAV. We hypothesized that the differences in *in vitro* susceptibility of CD3$^+$ T lymphocytes to EAV infection may have a genetic basis. To investigate the possible hereditary basis for this trait, we conducted a genome-wide association study (GWAS) using the Illumina Equine SNP50 chip to compare susceptible and resistant phenotypes. Initial testing with Thoroughbred horses (n= 37) implicated an association between a region of equine chromosome 11 (ECA11) and the CD3$^+$ T cell susceptibility/resistant trait. The results were extended and confirmed by retesting 267 horses (Thoroughbred [n=94], American Saddlebred [n=60], Quarter Horse [n=53] and Standardbred [n=60]) for additional SNPs in this region, leading to the identification of a common, genetically dominant haplotype associated with the susceptible phenotype in the region ECA11: 49572804-49643932. The presence of a common haplotype indicates that the trait occurred in a common ancestor for all four breeds suggesting that it may be segregating among other modern horse breeds. Biological pathways analysis revealed several cellular genes within this region encoding proteins associated with virus attachment and entry, cytoskeletal organization and NFκB pathways that may be associated with the trait responsible for the *in vitro* susceptibility/resistance of CD3$^+$ T lymphocytes to EAV infection. The data presented in this study demonstrated a strong association of genetic markers with *de facto* proof that the trait is under genetic control.

To our knowledge, this is the first GWAS of an equine infectious disease and the first GWAS of EVA.

3.2. INTRODUCTION

Equine arteritis virus (EAV) is a small enveloped virus with a positive-sense, single-stranded RNA genome of 12.7 kb that belongs to the family *Arteriviridae* (genus *Arterivirus*, order *Nidovirales*) [7,34]. EAV is the causal agent of equine viral arteritis (EVA), a disease of equids. The vast majority of EAV infections are inapparent or subclinical [77,353]. However, some acutely infected horses may develop any combination of the following clinical signs: pyrexia, depression, anorexia, dependent edema (scrotum, ventral trunk, and limbs), conjunctivitis, lacrimation and swelling around the eyes (periorbital or supraorbital edema), respiratory distress, urticaria, and leukopenia [77,353]. During natural outbreaks of the disease, the virus can cause abortion in pregnant mares with abortion rates varying from 10 to 71%, depending on the virus strain [77,353]. Following EAV infection, a variable proportion of stallions (30-70%) can become persistently infected and continuously shed the virus in their semen [77,190]. The mechanism of persistence of EAV in the male reproductive tract is not clear. However, studies have established that persistence of EAV in stallions is testosterone-dependent [217,218]. Moreover, the prevalence of EAV infection differs markedly among different breeds of horses, strengthening the assumption of genetic influence on susceptibility to infection [77]. The seroprevalence of EAV infection of horses varies between countries and among horses of different breeds and ages, with marked disparity between the prevalence of infection among Standardbred (STB) and Thoroughbred (TB) horses [175]. EAV infection is considered endemic in STB horses but not in TBs in the U.S, with 77.5% to 84.3% of all STBs but only up to 5.4% of TBs being seropositive to the virus [175,354,355,356]. Furthermore, the seroprevalence of EAV infection among Warmblood stallions is also very high in a number of European countries, as about 55 to 93% of Austrian Warmblood stallions are positive for antibodies to EAV [357]. Although many of these differences are likely attributable to circulating virus strains and environmental or management conditions, inherent genetic differences may also play a significant role in determining clinical outcome and influence severity of disease following exposure to EAV.

In a recent study using dual color flow cytometry, we demonstrated that the EAV VBS can infect a small population of $CD3^+$ T lymphocytes *in vitro* from some but not all

horses [330]. The data suggested that the $CD3^+$ T lymphocyte subpopulation of individual horses varied in their susceptibility to *in vitro* EAV VBS infection and they could be divided into susceptible and resistant groups [330]. The $CD3^+$ T lymphocyte susceptible/resistant phenotypes were not associated with age, prior exposure to EAV or presence of antibodies to EAV but appeared to show an association with breed in preliminary studies. Therefore, we hypothesized that susceptibility/resistance of equine $CD3^+$ T lymphocytes to EAV reflects genetic differences between horses in their response to infection with the virus. The primary objective of this study was to identify chromosomal regions and candidate genes associated with susceptibility/resistance of $CD3^+$ T lymphocytes to EAV infection in horses by using a genome-wide association study (GWAS). Genetic factors contribute to host susceptibility and progression of disease, but the genes responsible for disease development are largely unknown. Until now, there was no evidence to indicate what role genetic factors play in determining the susceptibility to and outcome of EAV infection in horses. Availability of the equine genome sequence and development of genome wide screening technologies offer unparalleled opportunities to identify variants associated with increased susceptibility/resistance to infectious disease agents such as EAV [358]. In this study, we describe the identification of a distinct phenotypic trait that can be used as a marker to divide equine populations, regardless of breed, into susceptible and resistant groups based on an *in vitro* assay system. Using GWAS in combination with biological pathways analysis, we have identified for the first time several cellular genes that may be associated with the trait responsible for *in vitro* $CD3^+$ T lymphocyte susceptibility/resistance to EAV infection.

3.3. MATERIALS AND METHODS

Virus and antibodies

The virulent Bucyrus strain of EAV (EAV VBS; ATCC VR-796, American Type Culture Collection, Manassas, VA) was used for *in vitro* infection of equine PBMCs as previously described [330]. The monoclonal antibody (MAb) to equine CD3 surface molecule, UC F6G, was kindly provided by Jeff Stott, University of California, Davis. The R-PE conjugated $F(ab')_2$ fragment of goat anti-mouse IgG1 (Southern Biotech,

Birmingham, AL) was used as the secondary antibody. To detect EAV antigen in infected cells, Alexa Fluor 488-labeled MAb against nonstructural protein 1 (nsp1; MAb 12A4) was used [306,330].

Horses

A total of 310 horses of different breeds, ASB (n=60), STB (n=60), TB (n=137), and QH (n=53) were used in the study.

Phenotypic trait

The susceptible or resistant phenotype of each animal was defined by dual color flow cytometric analysis of *in vitro* EAV infected $CD3^+$ T lymphocytes as described previously [330]. The horses were classified into susceptible or resistant groups based on their $CD3^+$ T lymphocyte susceptible/resistant phenotype to *in vitro* EAV infection.

DNA extraction

Genomic DNA (gDNA) was obtained from PBMCs of each animal using Puregene whole blood extraction kit (Qiagen, Valencia, CA) following the manufacturer's instructions. DNA quality and concentration was assessed using Nanodrop® (Thermo Scientific, Wilmington, DE) at absorbance ratio $OD_{260nm/280nm}$.

Genotyping and quality control

Samples were genotyped using EquineSNP50 Genotyping BeadChip (Illumina, San Diego, CA) at the core facility for the Mayo Clinic in Rochester, MN. This array contains 59,355 SNPs derived from the EquCab2.0 SNP database of the horse genome (http://www.broadinstitute.org/mammals/horse) with an average probe spacing of 43.2 kb between adjacent variants. For the initial GWAS analysis (N=37), DNA samples from 16 TB horses known to be susceptible and 21 TB horses known to be resistant for the *in vitro* EAV infectivity trait were used for the EquineSNP50 Genotyping BeadChip (Illumina Inc, San Diego, CA; Figure 3.1).

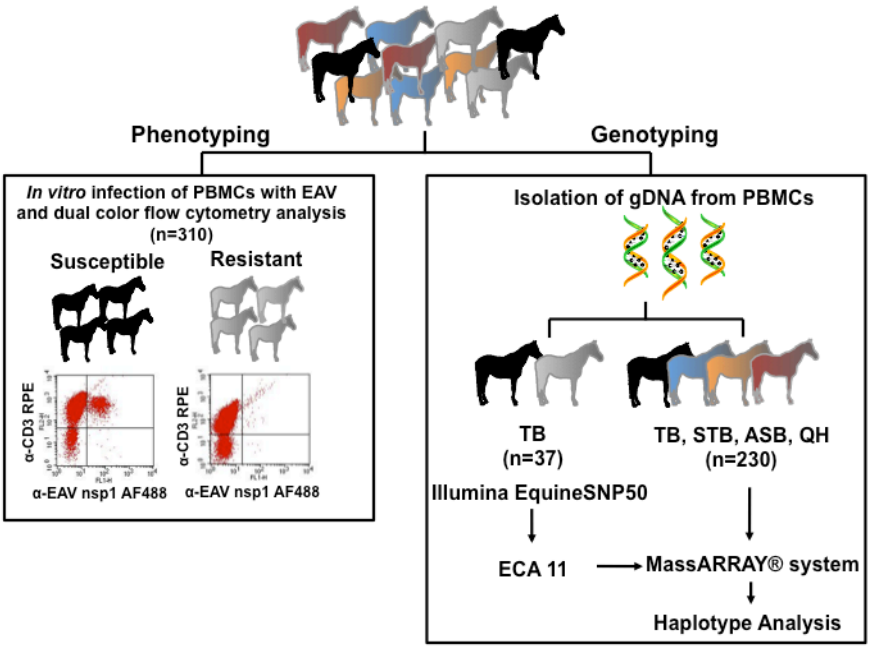

Figure 3.1. Schematic representation of the study design. Horses were phenotyped first and grouped into susceptible or resistant phenotype based on their $CD3^+$ T cell infectivity to EAV. To identify the region associated with EAV susceptible/resistant phenotype, gDNA from 37 TB horses was isolated and analyzed using Illumina EquineSNP50. Results from the initial study were confirmed by genotyping 267 additional horses, including TBs tested with Illumina Equine SNP50, with MassARRAY® system technologies. TB, Thoroughbreds; STB, Standardbreds; ASB, American Saddlebreds; QH, Quarter horses.

Subsequently, additional SNPs from the region (Table 3.1) were selected using the Broad Institute Equine SNP database (http://www.broadinstitute.org/ftp/distribution/horse_snp_release/v2/) for further testing along with some of the original SNPs. The second SNP assay was conducted at Geneseek, Inc (Lincoln, NE) using the Sequenom MassARRAY® system (Sequenom Inc., San Diego, CA; http://www.sequenom.com). Horses tested in this second assay included a second population of TB horses (n=57) as well as horses of several different breeds (60 ASB horses, 60 STB horses, 53 QH) plus the 37 TB horses tested in the original Illumina assay.

Table 3.1. ECA11 SNPs selected for the MassARRAY® system

SNP	Position on ECA11 (bp)	SNP	Position on ECA11 (bp)
BIEC2-157847	49389493	BIEC2-166028[b]	49649380
BIEC2-157867[a]	**49424839**	BIEC2-166029	49660962
BIEC2-157892	49446386	**BIEC2-157989**	**49663560**
BIEC2-157899[b]	49459247	BIEC2-166033	49665617
BIEC2-165951[b]	49473877	BIEC2-166034	49676359
BIEC2-165967[b]	49475165	BIEC2-166036	49682023
BIEC2-157944	49509504	BIEC2-166040	49684089
BIEC2-157945	49514091	**BIEC2-157998**	**49684299**
BIEC2-165988	49529433	BIEC2-166042[b]	49688617
BIEC2-157947	**49529680**	**BIEC2-158000**	**49691181**
BIEC2-165991	49533085	BIEC2-166044	49693957
BIEC2-165992	49537432	BIEC2-166047	49696679
BIEC2-157953[b]	49541824	BIEC2-166049	49700501
BIEC2-165997	49545584	BIEC2-166050	49707607
BIEC2-165998	49549767	BIEC2-166052[b]	49711761
BIEC2-165999	49558533	BIEC2-166056	49716340
BIEC2-166001	49564266	BIEC2-166060	49724419
BIEC2-166003	49569444	BIEC2-166065	49729958
BIEC2-166005	49572804	BIEC2-166066	49747467
BIEC2-166006	49580531	BIEC2-158024[b]	49757978
BIEC2-166009	49584513	BIEC2-166449	50863263
BIEC2-166011	49589952	**BIEC2-158587**	**51188148**
BIEC2-166013[b]	49594275	**BIEC2-159231**	**52379156**
BIEC2-166014[b]	49604594		
BIEC2-166015	49613954		
BIEC2-166016	49621050		
BIEC2-166018	49627471		
BIEC2-166020	49634340		
BIEC2-166021	49637772		
BIEC2-166027	49643932		

Data analyses

Data from both assays were analyzed using the Golden Helix SNP & Variation Suite 7 (Bozeman, MT). Of the 59,355 SNPs, 53,747 had call rates above 95%. The rest were excluded from the analyses. Filtering for minor allele frequencies (removing SNPs with minor allele frequencies below 55%) and genotyping (excluding SNPs with

genotypes involving less than 90% of the horses) 42,506 SNPs were evaluated. Data from both studies were evaluated using the association (chi-square) in the additive model and linkage disequilibrium.

Gene ontology clustering and pathway analysis

Unsupervised analysis was performed using Ingenuity Pathways Analysis (IPA) tool (Ingenuity Systems Inc., Redwood City, CA) to investigate biological and molecular networks associated with genes identified within the selected region. The IPA builds networks relevant to queried genes based on their functional annotation and known molecular interaction which data are supported by peer-reviewed scientific publications and stored in Ingenuity Pathways Knowledge Base (IPKB). A list of interactions between genes identified in the GWAS ('focus genes') and all other genes stored in the IPKB was obtained with a maximum network size of 35 genes. Networks of direct or indirect interactions among genes are displayed graphically. In addition, IPA computes a score for each network, the –log (p-value), which indicates the likelihood of the 'focus genes' in a network from IPKB being found together due to random chance. To investigate the molecular and biological functions, genes identified within the region were categorized using the PANTHER classification system (www.pantherdb.org). In addition to above mentioned database analyses, functional information was also obtained from a literature search.

3.4. RESULTS

Phenotype analysis based on *in vitro* susceptibility of $CD3^+$ T lymphocytes to EAV infection

Horses from four different breeds TB, American Saddlebred (ASB), STB and Quarter Horse (QH), a total of 310 horses, were randomly selected from farms in central Kentucky for this study. In an attempt to define the $CD3^+$ T lymphocyte susceptible or resistant phenotype, blood was collected from each horse and peripheral blood mononuclear cells (PBMCs) were isolated. PBMCs were infected with EAV VBS and subsequently subjected to dual-color flow cytometric analysis to identify horses with the $CD3^+$ T lymphocyte-susceptible or -resistant phenotype to EAV infection. Cells from

horses with a $CD3^+$ T lymphocyte susceptible phenotype were stained with antibodies to both $CD3^+$ T lymphocyte surface molecule and intracellular EAV antigen (nonstructural protein 1 [nsp1]). In contrast, cells from horses with a $CD3^+$ T lymphocyte resistant phenotype were stained with antibody to $CD3^+$ T lymphocyte surface molecule but not to intracellular EAV antigen. Consistent with previously reported results, horses were divided into two distinct groups, $CD3^+$ T cell susceptible or resistant. Of the 310 horses, 167 horses had the $CD3^+$ T lymphocyte susceptible phenotype and 143 horses had the $CD3^+$ T lymphocyte resistant phenotype. Subsequently, data were analyzed by individual horse breed. In the susceptible phenotype group, there was no significant difference in the percentage of the EAV infected $CD3^+$ T lymphocyte subpopulation, regardless of breed. The percentage of the $CD3^+$ T cell subpopulation susceptible to EAV was 4.0% ± 0.95 in TB, 5.4% ± 0.4 in STB, 7.2% ± 0.6 in ASB and 3.9% ± 0.4 in QH (Figure 3.2.A).

The results confirm that determination of the EAV susceptible/resistant $CD3^+$ T cell phenotype is consistent in horses, regardless of breed. Interestingly, there was a clear difference in prevalence of the susceptibility/resistance phenotype among breeds. Ninety-five percent of STBs tested in this study were of the susceptible phenotype (57 out of 60). Similarly, 53 out of 60 ASBs had the $CD3^+$ T lymphocyte susceptible phenotype (~90%). The lowest prevalence of the susceptible phenotype was in TB, 32 out of 137 (23%), and QHs had both phenotypes evenly distributed with approximately 50% prevalence of each phenotype (Figure 3.2.B).

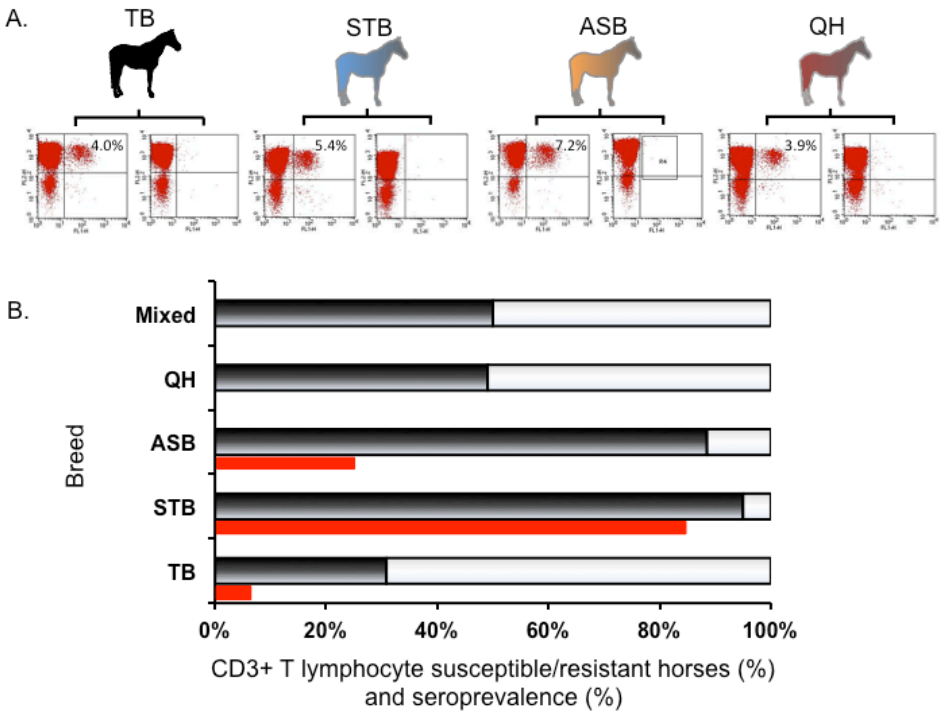

Figure 3.2. Effect of breeds on prevalence of T cell susceptible/resistant phenotype. (A) Representative dot plots from flow cytometry analysis for each breed are shown. The mean percentage of $CD3^+$ T cells with intracellular EAV nsp1 antigen is indicated in the right upper quadrant for susceptible phenotype. (B) The percentage of susceptible (black) and resistant (white) phenotype for each breed is indicated in a bar graph. Seroprevalence of each breed (red) is indicated below the bar representing phenotypic prevalence where available. TB, Thoroughbreds (n=137); STB, Standardbreds (n=60); ASB, American saddlebreds (n=60); QH, Quarter horses (n=53).

Genome-wide association study (GWAS)

To investigate the possibility of genetic influence on susceptibility/resistance of $CD3^+$ T lymphocyte to *in vitro* infection to EAV, we applied the GWAS to identify the genetic element(s) associated with this phenotypic trait. In order to simplify the process of defining any genetic differences between positive and negative groups, we initially focused on TB horses since they have less diversity for genetic markers than most other breeds of horses. A group of 80 TB yearlings, serologically negative for EAV were

tested for the phenotype described above. Only 16 out of 80 TB yearlings had the $CD3^+$ T lymphocyte susceptible phenotype. Thus, 37 horses were selected for the GWAS including 16 with the susceptible phenotype and 21 with the resistant phenotype. DNA from these horses (Illumina TBs) was genotyped for single nucleotide polymorphisms (SNPs) using the EquineSNP50 BeadChip (Illumina Inc., San Diego, CA). Using the option for association studies, the distribution of SNPs was compared between the susceptible horses and the resistant horses. The results from this study are represented graphically in a Manhattan plot (Figure 3.3) showing the P-values when comparing the distribution of markers for susceptible and resistant horses for each SNP. The values from a region of ECA11 showed a distinctive peak.

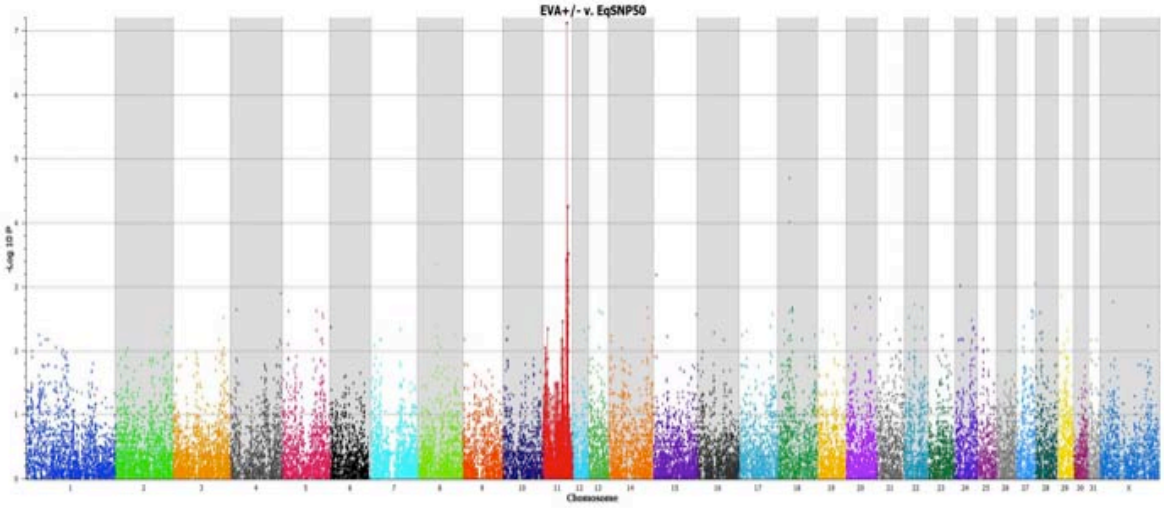

Figure 3.3. Manhattan plot. The distribution of probability values ($-\log_{10}$ transformed) for the 42,506 SNPs investigated using the 37 Thoroughbred horses (16 susceptibles and 21 resistants) is depicted. Genomic positions are indicated by chromosome with different colors.

The 10 highest associations that were found included 7 SNPs in one region on ECA11 (Table 3.2). The single highest association was found for SNP marker BIEC2-157867 from ECA11 which had a statistical significance of $P=7.42 \times 10^{-8}$ (uncorrected) and P=0.003 using the Bonferroni correction for the number of assays. None of the other

markers achieved statistical significance when factoring the correction to the probability value.

Table 3.2. Results from the GWAS using the Illumina Equine SNP50 Beadchip

SNP#	Chromosome	Position	Uncorrected P-Value
BIEC2_157867	11	49424839	7.42×10^{-8}
BIEC2_409206	18	24674961	2.00×10^{-5}
BIEC2_158932	11	51677777	5.42×10^{-5}
BIEC2_409219	18	24736336	9.69×10^{-5}
BIEC2_159231	11	52379156	2.90×10^{-4}
BIEC2_158587	11	51188148	3.06×10^{-4}
BIEC2_158588	11	51188190	3.06×10^{-4}
BIEC2_157160	11	48595739	3.63×10^{-4}
BIEC2_157720	11	49039853	3.98×10^{-4}
BIEC2_1046042	8	40043641	4.47×10^{-4}

Representation of 10 highest associations found using the Ilumina Equine SNP50 BeadChip based on 37 Thoroughbreds exhibiting the *in vitro* infection phenotype (N=16 susceptible) and the *in vitro* resistance phenotype (N=21 resistant)

Study validation and haplotype analysis

To confirm and extend the results from this initial study, additional SNPs were selected from the EquCab2.0 SNP database (Table 3.2) along with some of the original SNPs for the region on ECA11 and tested using the Sequenom MassARRAY® system (Sequenom Inc., San Diego, CA). The Illumina TB horses served as controls, being tested in both SNP assays, and had identical results for the 12 SNPs in common in the two assays. Table 3.3 provides the results from comparing the distribution of SNPs among susceptible and resistant horses for all horses (combined), TB horses alone, QH alone, ASB horses alone and STB horses alone. The SNP showing the strongest association in the Illumina study, BIEC2-157867 had a significant and slightly higher P-

value of 5.84×10^{-5} for this new set of TB horses. The most significant value was found for BIEC2-166050 with the combined set of horses ($P=1.77 \times 10^{-22}$). For the group of TB horses, the most significant P-value was for BIEC2-166057 ($P=4.96 \times 10^{-7}$). All breeds except STB showed statistically significant associations for the trait with SNPs in this region.

Next, linkage disequilibrium (LD) among the SNPs in this region was investigated and compared to the distribution of cases and controls in the different populations. A haplotype defined by 8 SNPs, BIEC2- 166005, 166006, 166009, 166011, 166015, 166018, 166021 and 166027, spanning 71 kb from ECA11: 49572804-49643932 had the highest association across all breeds. The SNP BIEC2-166016 did not contribute to definition of the haplotype and was therefore not included in the haplotype definition. The haplotype associated with the susceptibility phenotype was defined by the presence of nucleotides GGGGAGGT at those 8 SNP sites. Figure 3.4 shows a schematic representation of LD for the haplotype among all groups of horses tested. The schematic representations are similar for all groups except the STB, in which this haplotype is almost completely fixed in the breed.

Figure 3.5 provides the frequencies for this haplotype among susceptible and resistant horses as well as the statistical significance for the differences in each group. In each breed, including STB, this haplotype was associated with susceptible horses. The haplotype was also present among the resistant horses but at a much lower frequency. Among the 13 TB cases, all but one horse were heterozygous for the haplotype, possessing one copy of the haplotype; the remaining susceptible TBs did not possess the haplotype (data not shown). Among the 44 resistant TB horses, 8 horses possessed one copy of the haplotype while two horses were homozygotes (data not shown). Similar results were found for the distribution of the haplotype in other breeds.

Table 3.3. P-values of case and control groups for the combined set and for the individual breed of horses

BIEC2-SNP#	Position	P-Combined	P-TB	P- QH	P-ASB	P-STB
166050	49707607	1.73×10^{-22}	6.11×10^{-4}	3.00×10^{-3}	6.18×10^{-11}	n/a
166027	49643932	1.49×10^{-21}	4.96×10^{-7}	1.62×10^{-3}	1.24×10^{-5}	0.61
166011	49589952	1.17×10^{-19}	1.46×10^{-4}	1.07×10^{-3}	1.74×10^{-6}	n/a
165991	49533085	1.70×10^{-19}	7.64×10^{-5}	6.26×10^{-4}	2.00×10^{-4}	0.72
166065	49729958	3.44×10^{-19}	7.02×10^{-5}	9.40×10^{-4}	9.48×10^{-5}	n/a
166015	49613954	4.99×10^{-19}	2.74×10^{-4}	9.40×10^{-4}	4.11×10^{-5}	n/a
166021	49637772	5.97×10^{-19}	1.87×10^{-4}	9.40×10^{-4}	4.11×10^{-5}	n/a
166009	49584513	6.30×10^{-19}	1.87×10^{-4}	9.40×10^{-4}	3.24×10^{-5}	n/a
166047	49696679	3.23×10^{-18}	7.02×10^{-5}	9.40×10^{-4}	9.48×10^{-5}	0.61
166018	49627471	6.03×10^{-18}	3.72×10^{-4}	1.64×10^{-3}	4.11×10^{-5}	n/a
157944	49509504	5.75×10^{-17}	5.78×10^{-4}	3.02×10^{-3}	2.00×10^{-4}	0.56
166001	49564266	3.10×10^{-13}	2.69×10^{-3}	0.01	3.89×10^{-4}	0.44
157867[a]	49424839	1.12×10^{-9}	5.84×10^{-5}	0.50	1.66×10^{-5}	0.48
157847	49389493	3.60×10^{-9}	0.01	0.17	2.97×10^{-6}	0.93
165999	49558533	5.45×10^{-9}	0.10	0.18	0.10	0.34
165997	49545584	2.28×10^{-5}	0.26	0.23	0.69	0.80
166056	49716340	6.52×10^{-5}	3.93×10^{-3}	0.07	0.02	0.46

[a] The most highly associated SNP in the initial assay.
n/a represents no variation observed between resistant and susceptible.

NOTE: The table shows SNPs in ECA 11 with the lowest 17 P-values of combined set of horses (N=267) and the individual groups of Thoroughbred (TB, N=57), Quarter Horse (QH, N=53), American Saddlebred (ASB, N=60) and Standardbred (STB, N=60).

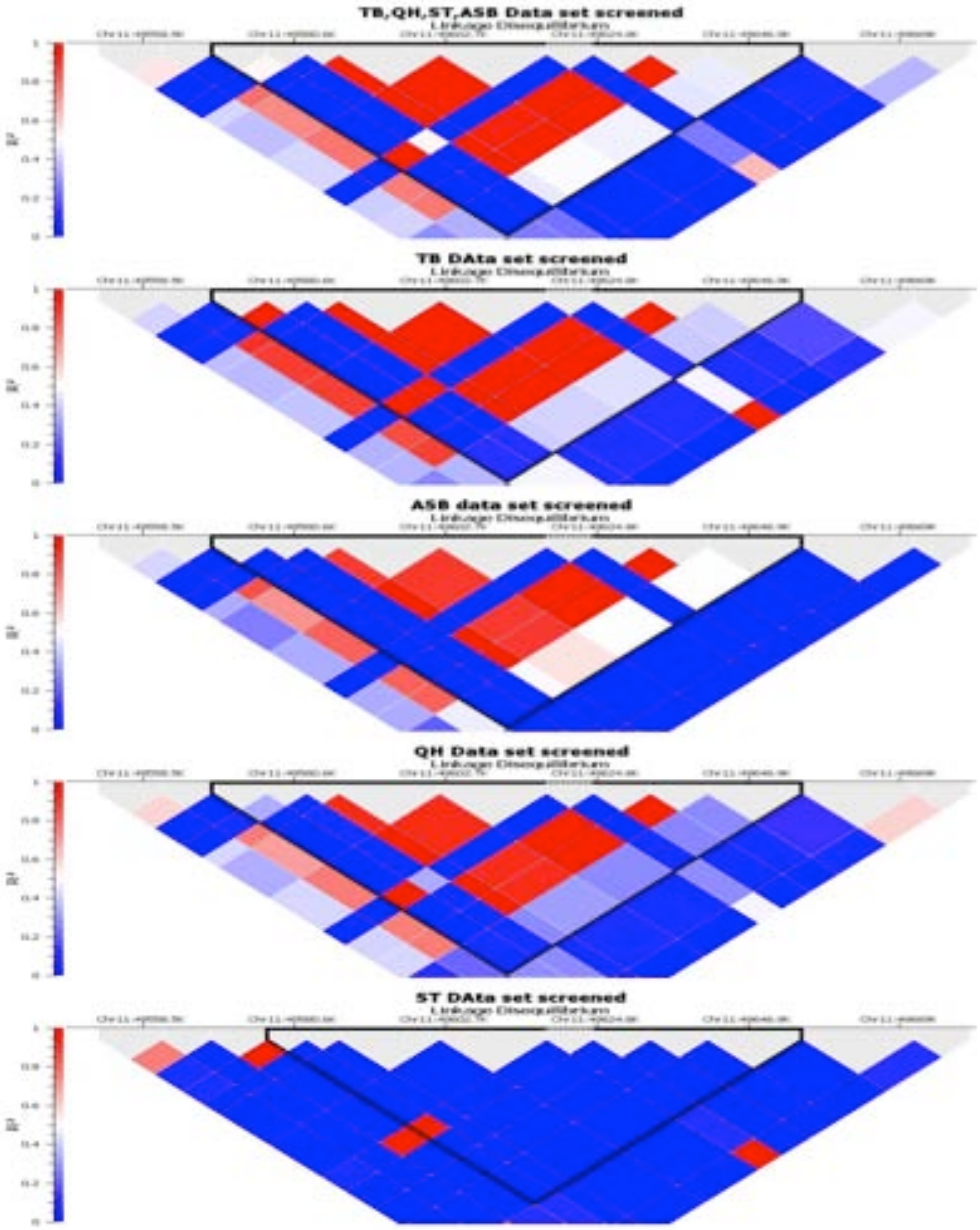

Figure 3.4. Linkage disequilibrium (LD) plots. The shown region represents the strongest association with the EVA susceptibility haplotype from ECA11:49572804-49643932**.** The haplotype block is highlighted with black line.

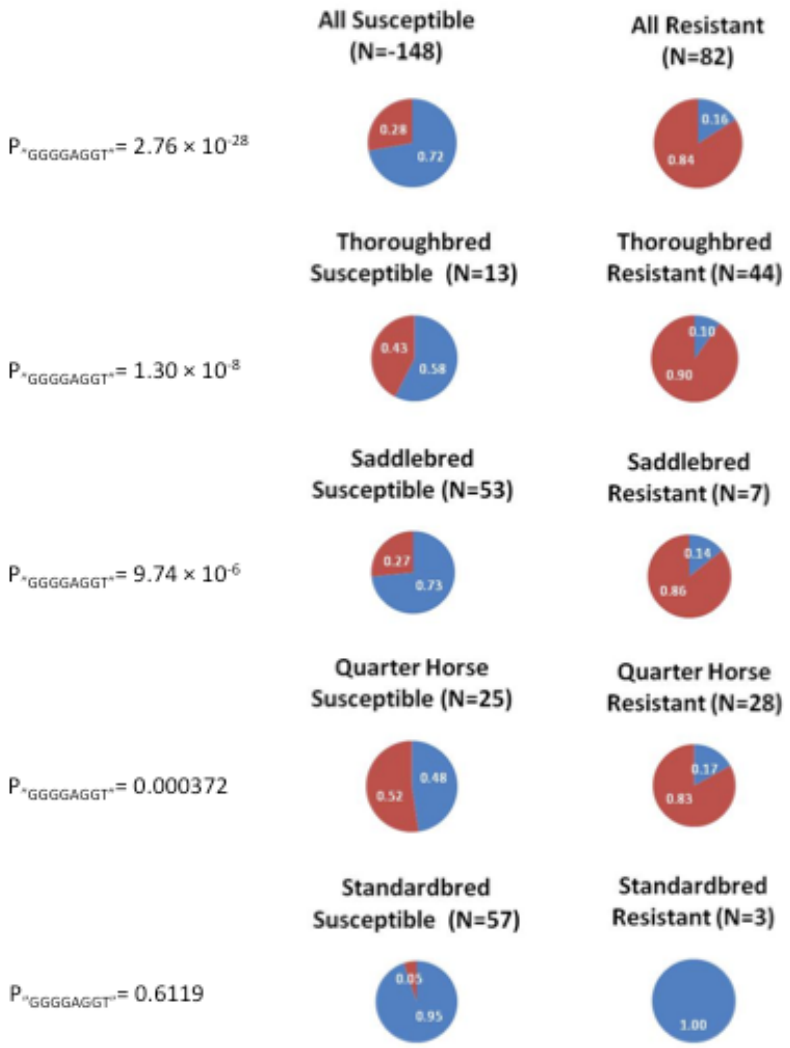

Figure 3.5. Frequency of the GGGGAGGT haplotype found for selected SNPs in ECA11: 49572804-49643932. The frequency represented by each section of the pie chart is shown on the pie chart in white. Data are represented for all horses together (All) and for the individual breeds (Thoroughbred, American Saddlebred, Quarterhorse and Standardbred). The statistical significance for the frequency differences of the GGGGAGGT haplotype between susceptible and resistant horses is shown to the left of each set of pie charts ($P_{"GGGGAGGT"}$).

Gene network analysis

The EAV-associated haplotype is located in a block with strong LD expanding ~71 kb. This LD block includes five genes: SPAG7, ENO3, PFN1, CHRNE and MINK1. For the purpose of analyzing possible functional relationship among genes using the Ingenuity Pathway Analysis (IPA, Ingenuity Systems) and the PANTHER classification system, we have included those genes in high LD and genes located outside of this particular LD block (500 kb upstream and downstream of the most significantly associated gene, KIF1C). Unsupervised IPA analysis retrieved three top networks that were merged into a single interaction network (Figure 3.6.A). The network contained 22 genes showing significant correlation with networks implicated in cell morphology and cellular movement. Similarly, genes categorized by biological functions were mostly involved in cellular movement ($P=1.2 \times 10^{-5}$), cell death ($P=1.45 \times 10^{-3}$), cell morphology ($P=1.45 \times 10^{-3}$), cellular assembly and organization ($P=1.45 \times 10^{-3}$) and cellular function and maintenance ($P= 1.45 \times 10^{-3}$). We also classified the genes from the region by their molecular function and biological process categories using the PANTHER classification database. The enriched molecular function categories included binding, catalytic activities and receptors suggesting these genes might mediate viral-cellular interaction and facilitate viral entry (Figure 3.6.B). Furthermore, there was a predominance of genes regulating metabolic and cellular processes as well as cell communication and immune responses (Figure 3.6.C; Table 3.4).

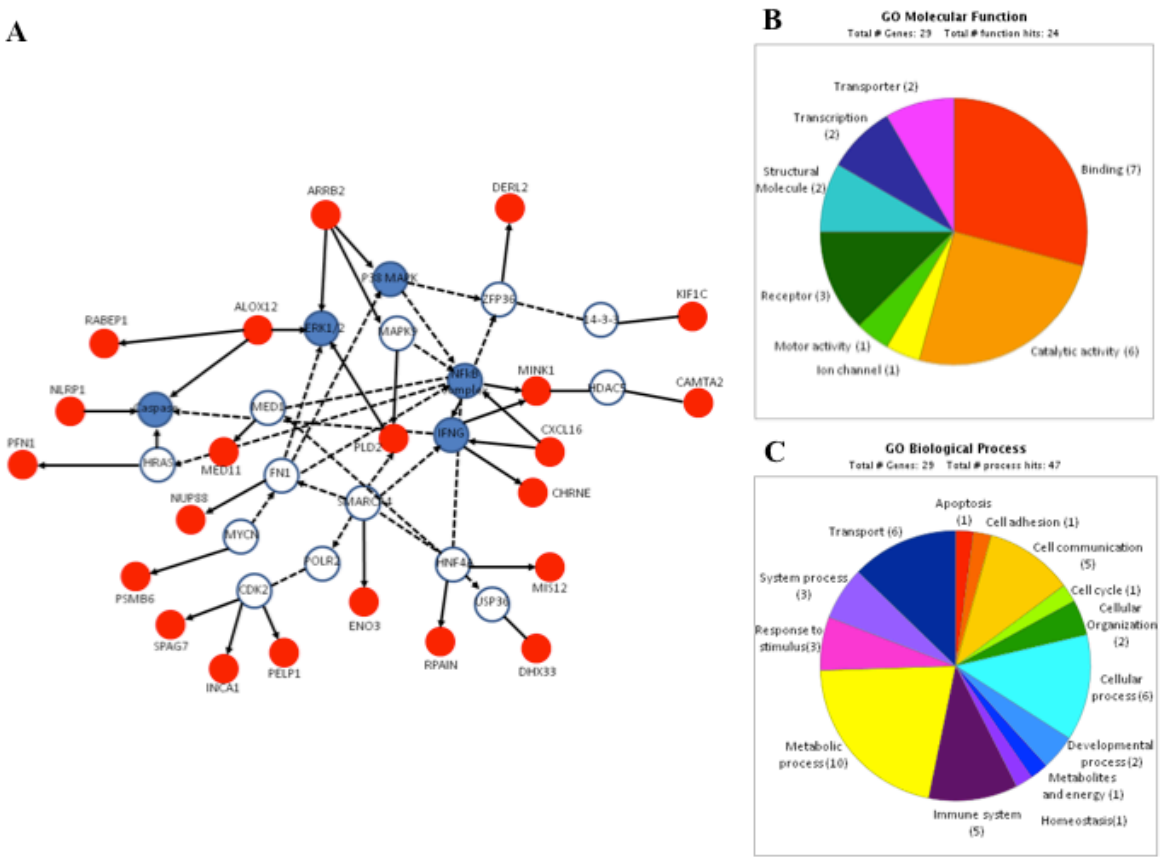

Figure 3.6. Pathway analysis. (A) Three top networks retrieved using unsupervised IPA analysis were merged into a single interaction network. Red nodes represent molecules encoded by genes found in the region of ECA11; white nodes are genes identified by IPA with direct or indirect interactions with genes of ECA11. The blue nodes represent molecules/complexes identified by IPA involved in canonical pathways. Classification of candidate molecules based on their (B) molecular functions and (C) biological processes.

3.5. DISCUSSION

The data presented in this study demonstrate a very strong association of genetic markers with the susceptible phenotype described for *in vitro* infection of $CD3^+$ T lymphocytes with EAV. Association of genetic markers with a trait is *de facto* proof that the trait is under genetic control. To our knowledge, this is the first GWAS of an equine infectious disease and the first GWAS of EVA. We have developed an easy and reliable

in vitro assay based on dual color flow cytometry to phenotype an equine population. The data presented in this study clearly demonstrated that there was a genetic difference within and among the horse populations based on the susceptibility of their $CD3^+$ T lymphocytes to *in vitro* infection with the EAV VBS of EAV. The *in vitro* assay described is currently the most precise method for determining the phenotype. However, it is expensive, time consuming and cumbersome to run on a routine or large-scale basis. The association of the ECA11 haplotype with the phenotype will allow us to use the molecular test in large-scale studies to determine the impact of this phenotype on the consequences of infection.

Interestingly, distinct phenotypic prevalence of each breed found in this study was similar to EAV seroprevalence that has been reported previously (Figure 3.2.B) [175,356]. Similar distribution in both seroprevalence and $CD3^+$ T lymphocyte susceptible trait strengthened our hypothesis that genetic factors might play a role in determining the $CD3^+$ T lymphocyte susceptibility/resistance of horses to EAV infection. The haplotype associated with the trait was distributed among horses in a manner characteristic for that harboring a gene with a dominant mode of action. However, the association of the trait with the genetic markers was imperfect since several susceptible horses were found without the implicated genetic markers implicated for susceptibility and, conversely, some resistant horses were found with susceptibility markers. However, this is not surprising since the 53 SNPs under study represented a very small proportion from the three million bp long region and the chances of having selected the SNP defining the actual mutation defy expectations. Although additional work is needed to investigate candidate genes and re-sequencing of candidate regions, it is clear that a gene or genes within the region of ECA11: 49572804-49643932 plays a major role in determining the $CD3^+$ T lymphocyte susceptibility phenotype. In a parallel study, we have experimentally inoculated both groups of horses and assessed the severity of clinical disease, virus shedding, and production of proinflammatory/immunomodulatory cytokines in PBMCs using real-time quantitative RT-PCR (Go *et al.*, in revision). The data showed that there was a significant difference between the two groups of horses in terms of cytokine mRNA expression and increased clinical signs in horses possessing the *in vitro* $CD3^+$ T cell resistant phenotype. Thus, there was a clear correlation between the

in vitro susceptibility or resistance phenotype of $CD3^+$ T lymphocytes and the different clinical/cytokine expression responses observed in horses following infection with EAV. Therefore, further studies on genes located in ECA11 will enhance our understanding of the pathogenesis of EAV infection, variation in susceptibility to establishment of the carrier state in stallions, and hopefully, lead to identification of putative EAV cell receptor(s).

The association of the haplotype with $CD3^+$ T lymphocyte susceptibility in all four breeds is remarkable. This implies that the trait first appeared in a common ancestor of these breeds. Although these horses are products of four different breed registries, they are known to have common ancestors within the last 100 years [359]. The use of the four breeds together also produced the strongest associations for the trait using both the haplotype and individual SNPs (Table 3.3). This was a product of the wide differences among the selected horse breeds for the susceptibility/resistance trait. The choice of TB horses for the initial stage of the study was fortuitous since the susceptibility/resistance trait is highly polymorphic among TB horses. Had the initial study been conducted among STBs, the association would not have been uncovered because almost all STBs have the susceptibility phenotype. Indeed, STBs appear almost fixed for the genes and the trait. Therefore, the results of this study suggest that preliminary studies of such traits might best be conducted using pools of different horse breeds when that trait is manifested across breed lines.

Furthermore, we have identified for first time a significant number of candidate genes that might be associated with $CD3^+$ T lymphocyte susceptibility to EAV infection and these genes may also play a major role in pathogenesis and persistent infection in the stallion. We used IPA in an unsupervised manner, allowing identification of gene-gene relationships without *a priori* assumptions. This analysis linked 22 of 28 genes to other nodes in a highly significant network (Figure 3.6.A). These genes might be functionally interrelated and may play a direct or indirect role in susceptibility to EAV infection and pathogenesis of EVA. In relation to virus life cycle and host response to virus infections, these genes can be broadly classified into several categories based on molecular functions and biological processes (Figure 3.6.B and 3.6.C; Table 3.4). The proteins encoded by these genes are involved in virus attachment and entry pathway (putative cellular

receptors for viral entry, molecules associated with cytoskeleton and endocytosis), various transcription factors, cell-signaling molecules and molecules associated with inflammatory response, innate and adaptive immunity. Interestingly, some of these proteins that are already identified, have been associated with other virus infections (Table 3.4), may contribute to the pathogenesis of EVA as well.

We found several proteins, such as CHRNE, CXCL16, RABEP1, ARRB2, and PELP1 that may be involved in EAV attachment and entry into the cell. Although, the cellular receptor for EAV is not yet known, it is plausible that some of these molecules (e.g. CHRNE, CXCL16 and PELP1) may act as putative EAV receptor(s) or if not directly, serve as essential component(s) in viral attachment and entry process. The CXCL16 belongs to the macrophage scavenger receptor family which is the receptor family in which the porcine reproductive and respiratory syndrome virus receptor and human hepatitis C virus, CD168 and SR-BI, respectively, belong [360]. Recently, it has been demonstrated that EAV is taken up via clathrin-dependent endocytosis and is delivered to acidic endosomal compartments during entry into the cell [82]. Thus, proteins involved in the endocytic pathway may also play a critical role in the resistance or susceptibility of cells to EAV. ARRB2 encodes β-arrestin-2, a multifunctional adaptor protein, which is involved in desensitization and endocytosis of cell surface receptors in clathrin-coated pits [361,362,363]. Similarly, RABEP1 is indirectly involved in receptor internalization and endosome fusion, besides its function of interacting with proteins involved in endoplasmic reticulum (ER) to Golgi transport [364]. Interestingly, both ASGPR1 and ASGPR2, well-studied endocytic recycling receptor molecules, are located in the same chromosome approximately 800 kb downstream of RABEP1, making them attractive receptor candidates in line with clathrin-dependent endocytosis [82].

In relation to the viral life cycle, intracellular trafficking of molecules, cell movements, cell-to-cell communication as well as cell-substrate adhesion pattern and cell polarization are critical in virus infection in cells and spreading processes. All these processes can be modified by viral infections, contributing to the pathogenesis and disease progression. It has become apparent that numerous viruses interact with cytoskeletal components at various stages of their life cycle disrupting or remodeling cytoskeletal networks to their own advantage. Some viruses can directly or indirectly

hijack cytoskeletal cell component organization to their own advantage often altering cell behavior and cell fate. In EAV infected cells, cytopathic effect (CPE) is characterized by rounding, vacuolation, increased optical density, refraction and detachment from the supporting surface indicating viral modulations of the actin cytoskeleton [60,61,290,291]. In the region of interest identified in this study, several genes have been classified as involved in cellular movement function such as ARRB2, PLD2 and PFN1 and are known to be involved in actin cytoskeleton reorganization (Figure 3.7) [365]. In addition, some molecules such as KIF1C, PELP1, DERL2 are important in cellular trafficking. Derlins, including DERL1 and DERL2, are ER membrane proteins involved in the degradation of proteins that misfold in the ER [366,367,368,369,370]. KIF1C, a member of the kinesin superfamily, is involved in retrograde vesicle transport from the Golgi-apparatus to the ER [371]. It has been suggested that KIF1C associates with the 14-3-3 protein which regulates cytokinesis and cell cycle arrest due to DNA damage.

Interestingly, our network analysis also included some genes encoding proteins associated with apoptosis and modulating innate and adaptive immune responses to virus infections (Figure 3.7).

These proteins such as ARRB2 are known to modulate chemotatic responses and granule release as well as contribute to anti-apoptotic signaling [372,373,374,375]. In recent years, ARRB2 has been increasingly implicated in modulation of nuclear factor kappa B (NFκB) signaling and interacting with I kappa B alpha (IκBα) and extracellularly-regulated kinases 1 and 2 (ERK1/2) activation by acting as scaffold/adaptor proteins for G protein coupled receptor activation of MAP kinases, respectively, suggesting that ARRB2 is a regulator of innate immune activation and inflammatory gene expression besides its importance as a key component in actin cytoskeleton modulation [373,376,377,378,379,380,381,382,383,384,385]. Phosphatidylcholine-specific phospholipase D (PLD2) produces phosphatidic acid, an intracellular signaling lipid involved in vesicular trafficking and regulation of cytoskeletal organization. PLD2 is also involved in downstream activation of MAPK and cell signaling primarily associated with leukocyte chemotaxis [386]. Furthermore, some genes in the region were associated with the host inflammatory response and innate immunity. CXCL16, also a member of the CXC chemokine family, is expressed as a

soluble form and a transmembrane protein that induces chemotaxis of activated T cells into a site of inflammation [387,388,389]. While the transmembrane form may have receptor activity, the soluble CXCL16 induces inflammatory responses [388,390]. The nucleotide binding and oligomerization, leucine-rich repeat (NLR) family of proteins senses microbial infections and activates the inflammasome, a multiprotein complex critical for activation of caspase-1 and production of proinflammatory cytokines, particularly interleukin (IL)-1β and IL-18 [391]. The NUP88, belongs to nucleoporin proteins [NUPs] essential for the exchange of macromolecules across the nuclear envelope [392]. NUP88 promotes nuclear retention of NFκB and is required for proper nuclear accumulation of key animal and plant immune regulators such as Rel-like transcription factors [393,394]. Thus, depletion of NUP88 in mammalian cells prevents NFκB-dependent target gene expression. Although EAV replicates in the cytoplasm, the EAV nsp1 and N proteins are targeted to the nucleus. In particular, the N protein possibly shuttles between cytoplasm and nucleus and may be engaged in cytoplasmic virus assembly [120]. Thus, NUP88 may play an important role in EAV assembly and cells that are deficient or have an abnormal form of this protein may not be able to produce infectious virus particles.

Finally, the network analysis showed (Figure 3.7) that many molecules encoded by genes found in ECA11 are directly or indirectly related in the ERK1/2 and NFkB signaling pathways. During EAV infection there is increased production of proinflammatory cytokines such as IL-1, IL-6, IL-8 and tumor necrosis factor alpha (TNF-α) [257]. Some viruses ensure their survival by blocking the host anti-infective apoptotic mechanisms with a variety of viral proteins that modulate various stages of the death-signaling pathways. The transcription factor NFkB is activated following stimulation with, for example, the proinflammatory cytokines, TNF-α and IL-1. Many viral proteins disrupt the innate immune responses mediated by NFkB by nullifying signaling cascades that activate NFkB. In this respect, activation of NFkB was shown to facilitate some viral infections by promoting viral replication and preventing virus-induced apoptosis, thus priming the host cell for infection. EAV may utilize such mechanisms to evade the equine immune response and establish persistent infection in the cells of the reproductive tract of the stallion. However, further studies are needed to

investigate potential mechanisms that involve the roles of proteins encoded by genes located in this region of ECA11 in the virus life cycle and host response to EAV infection, as well as to identify the mechanism of establishment of persistent infection in some but not all stallions infected with the virus. The findings from this study can help to develop working hypotheses to decipher novel mechanisms of viral immune evasion, establishment of persistent infection and viral pathogenesis.

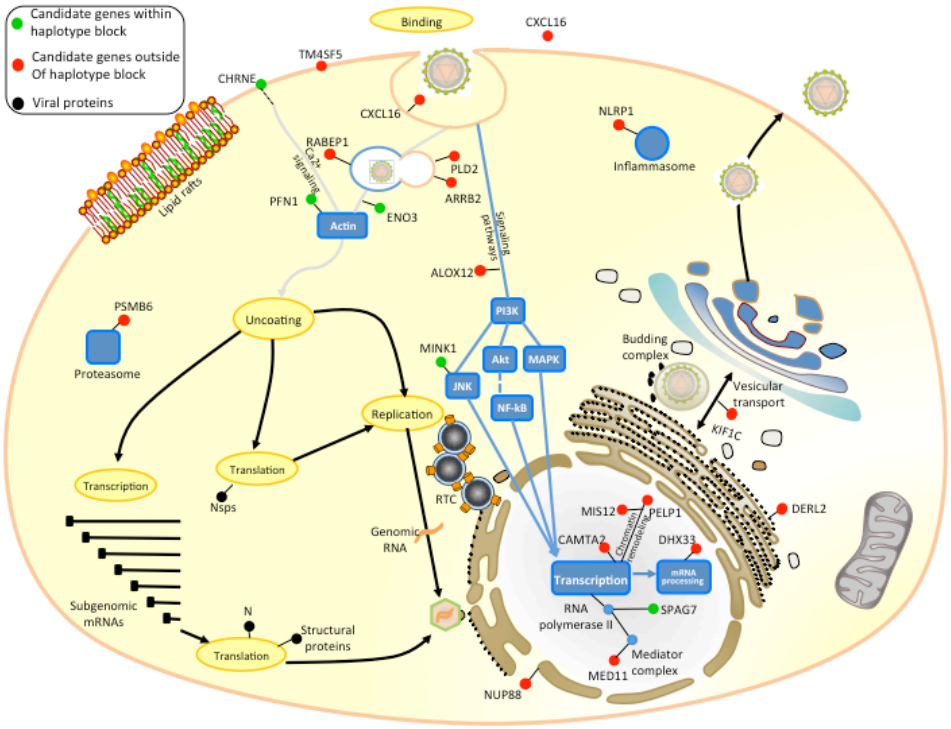

Figure 3.7. Subcellular location of candidate genes and EAV life cycle. The function and subcellular location of candidate molecules were manually curated based on PANTHER, IPA and published literature search. Subsequently, molecules were mapped along with stages of EAV life cycle at the position most likely to interact with virus life cycle. Green circles, molecules encoded by genes located in the haplotype block; red circles, putative molecules encoded by genes found within 500 kb upstream and downstream of the haplotype block; blue circles, molecules in the vicinity interacting with genes located in the region retrieved in the network analysis; black circles, viral proteins.

Table 3.4. List of genes located in the vicinity of the highest associated haplotype block

Gene symbol[§]	NCBI gene ID	Description	Known molecular function	Virus
Receptor Activity				
CHRNE	100146223	Similar to nicotinic acetylcholine receptor epsilon	Acetylcholine receptor activity, ligand-gated ion channel activity	HIV-1
ARRB2	100072892	Similar to beta-arrestin 2	Receptor internalization. Endocytosis	HIV-1
PELP1	100072897	Similar to proline, glutamic acid and leucine rich protein 1	Estrogen receptor coactivator. Receptor activity	
RABEP1	100072805	RAB GTPase binding effector protein 1	Endocytic pathway. Fusion of early endosome and regulation of recycling vesicle formation	
CXCL16*	100061442	Similar to SR-PSOX	Scavenger receptor family. NKT cell and MØ activation	HIV, SARS-CoV, KSHV
Intracellular Vesicle Trafficking				
DERL2	100061027	Derlin-2 (Der1-like protein 2)	Removal of misfolded protein from ER	Murine polyomavirus
KIF1C	100072836	Kinesin family member 1C	Vesicle transport, redistribution of Golgi membrane. Microtubule motor activity	
Actin and Cytoskeleton				
SPAG7	100061215	Similar to Sperm associated antigen 7	Nucleic acid binding, cytoskeleton	Human parvovirus B19
PFN1	100061295	Similar to profilin 1	Actin polymerization. Cytoskeletal signaling pathway	RSV
Innate and Adaptive Immunity				
NLRP1		NLR family, pyrin containing domain 1	Regulation of inflammatory response. Induction of apoptosis	KSHV/HHV8, Myxoma virus, HIV-1
DHX33	100072797	DEAH (Asp-Glu-Ala-His) box polypeptide 33	Putative RNA helicase	HIV-1
NUP88	100061117	Nucleoporin 88kDa	Innate immunity, nuclear export	Hepatitis C and B virus
PSMB6	100072870	Proteasome subunit beta type-6 precursor	Peptidase activity. Involved in antigen presentation by MHCI	
ALOX12	100072916	Similar to 12-lipoxygenase	Oxidoreductase activity. MØ activation. B cell mediated immunity	
CXCL16[¶]	100061442	Similar to SR-PSOX	Scavenger receptor family. NKT cell and MØ activation	HIV, SARS-CoV, KSHV
Transcription Factors				
RPAIN	100061089	RPA interacting protein	Nuclear transporter of RPA	
ZFP3	100061153	Zinc finger protein 3 homolog	DNA binding. Transcription factor	

CAMTA2	100072844	Similar to Calmodulin-binding transcription activator 2	Transcriptional coactivator. DNA binding	
MED11	100072890	Similar to HSPC296	Component of pol II transcription machinery. Transcription initiation complex stabilization	Measles virus
Enzyme Activity				
ENO3	100061187	Hypothetical protein LOC100061187	Lyase activity	
MINK1	100061370	Misshapen-like kinase	SAPK/JNK signal pathway. Kinase activity	
PLD2	100072863	Similar to Phospholipase D2	ERK1/2 signaling pathway. Hydrolase activity	HIV-1
Others				
MIS12	100060987	MIND kinetochore complex component	Chromosome segregation	
C17orf87		Transmembrane protein C17orf87	Transmembrane protein	
L11_049426896	100072818	Hypothetical protein	-	
L11_049471914		Hypothetical protein	-	
INCA1	100072840	Similar to HSD45	Regulation of cell proliferation. Spermatogenesis	
GLTPD2	100072874	Glycolipid transfer protein domain-containing protein 2	Lipid transport	
VMO1	100072878	Vitelline membrane outer layer protein 1 homolog precursor	-	
TM4SF5	100072881	Transmembrane 4 L6 family member 5	-	
ZMYND15	100061402	Zinc finger MYND domain-containing protein 15	-	
L11_049822588		Hypothetical protein	-	

CHAPTER FOUR

Assessment of correlation between *in vitro* $CD3^+$ T cell susceptibility to EAV infection and clinical outcome following experimental infection

Vet Micro. 2011 (accepted for publication)

4.1. SUMMARY

In a recent study, we demonstrated that the experimentally derived EAV VBS could infect *in vitro* a small population of $CD3^+$ T lymphocytes from some but not all horses. In a subsequent genome-wide association study, we demonstrated the putative candidate genes associated with susceptibility/resistance of $CD3^+$ T lymphocytes to EAV are located on horse chromosome 11. In this present study, horses were divided into two groups based on their *in vitro* $CD3^+$ T cell susceptible or resistant phenotype and challenged with recombinant EAV VBS. Following experimental inoculation, both groups of horses were assessed for severity of clinical outcome, virus shedding, as well as production of proinflammatory and immunomodulatory cytokines in peripheral blood mononuclear cells using real-time quantitative RT-PCR. The data showed that there was a significant difference between the two groups of horses in terms of cytokine mRNA expression and an increase in clinical signs in horses possessing the *in vitro* $CD3^+$ T cell resistant phenotype. A correlation was found between the *in vitro* susceptibility or resistance phenotype of $CD3^+$ T lymphocytes and the different clinical/cytokine expression responses observed in horses following infection with EAV. This is the first study to provide direct evidence for a correlation between variation in host genotype and phenotypic differences in terms of the extent of viral replication, nature and severity of clinical signs and cytokine gene expression caused by infection with virulent EAV.

4.2. INTRODUCTION

Equine arteritis virus (EAV) is a small enveloped virus with a positive-sense, single-stranded RNA genome of 12.7 kb that belongs to the family *Arteriviridae* (genus *Arterivirus*, order *Nidovirales*) [7,34]. EAV is the causal agent of equine viral arteritis (EVA) in equids. The vast majority of EAV infections are inapparent or subclinical [76,77,395]. However, some acutely infected horses may develop any combination of the following clinical signs: pyrexia, depression, anorexia, dependent edema (scrotum, ventral trunk, and limbs), conjunctivitis, lacrimation and swelling around the eyes (periorbital or supraorbital edema), respiratory distress, urticaria, and lymphopenia [77,353]. In natural outbreaks of the disease, the virus can cause abortion in pregnant mares with abortion rates varying from 10 to 71%, depending on the virus strain and other factors [77,353]. Following EAV infection, a variable proportion of stallions (30-70%) can become persistently infected and continuously shed the virus in their semen [77,190]. The mechanism of persistence of EAV in the male reproductive tract is not clear. However, studies have established that persistence of EAV in the stallion is testosterone-dependent [217,218].

The clinical signs observed in natural cases of EVA vary considerably between outbreaks and among individual horses. While many of these differences are almost certainly attributable to the virus strain, it is also likely that environmental or management conditions and host factors such as age, immune status and nutritional state play a significant role in determining clinical outcome following exposure to EAV. In addition, it is probable that host genetics may be particularly important although there are no reports linking individual horse genotypes with either susceptibility to EAV or the clinical consequences of infection. However, there are very significant differences in the seroprevalence among different breeds. For example, EAV infections are considered endemic in Standardbred (STB) horses but not in Thoroughbred (TB) horses in the U.S, with 77.5% to 84.3% of all STBs but only up to 5.4% of TBs testing seropositive for this virus [355]. Furthermore, the seroprevalence of EAV infection among Warmblood stallions is also very high in many European countries with 55 to 93% of all Austrian Warmblood stallions possessing antibodies against to this virus. Although management practices could explain some of these dramatic differences (Timoney and McCollum,

1993), it is also possible that certain horse breeds are inherently more susceptible to infection with this virus than others.

In a recent study, we demonstrated that the EAV VBS could infect *in vitro* $CD3^+$ T lymphocytes from some but not all horses [330]. The data suggested that the $CD3^+$ T lymphocyte subpopulation of individual horses varied in their susceptibility to *in vitro* EAV infection. Furthermore, a comprehensive single nucleotide polymorphism analysis using Equine SNP50 Genotype Bead Chip (Ilumina, San Diego, CA) and Sequenom MassARRAY® system (Sequenom Inc., San Diego, CA) has shown that genes associated with susceptibility/resistance of $CD3^+$ T lymphocytes to EAV infection are located on horse chromosome 11 (Go *et al.*, unpublished). As a result of this clearly defined genetic basis, we hypothesized that *in vitro* susceptibility of $CD3^+$ T lymphocytes to EAV infection may correlate with the clinical responsiveness of horses to challenge with virulent strains of EAV. To test this hypothesis, we conducted an *in vivo* study by exposing horses possessing either susceptible or resistant $CD3^+$ T lymphocytes with recombinant viruses derived from the virulent Bucyrus strain (rVBS) of EAV. Following infection, the two horse groups were monitored for clinical signs, duration plus magnitude of virus shedding, and production of proinflammatory/immunomodulatory cytokines at the mRNA level.

4.3. MATERIALS AND METHODS

Cells and viruses

Equine pulmonary artery endothelial cells (EECs) were maintained in Dulbecco's modified essential medium (Mediatech, Herndon, VA) with sodium pyruvate, 10% fetal bovine serum (Hyclone Laboratories, Inc., Logan, UT), 100U/μg per ml of penicillin/streptomycin and 200mM L-glutamine [142]. The high-passage rabbit kidney cells (RK-13; passage 399-409) were grown in Eagle's minimum essential medium (EMEM) with 10% ferritin supplemented bovine calf serum (Hyclone Laboratories, Inc., Logan, UT) and 100U/μg per ml of penicillin/streptomycin (Gibco, Carlsbad, CA). The EAV VBS (ATCC VR-796; American Type Culture Collection, Manassas, VA) was used for *in vitro* infection of equine peripheral blood mononuclear cells (PBMCs) as previously described [330]. The rVBS which has been shown to have similar growth

kinetics in EECs and equivalent capacity for lymphocyte infectivity, was used for experimental inoculation of horses [328,330]. Furthermore, the *in vivo* virulence phenotype of this virus has been previously demonstrated by experimental inoculation of horses [328]. Both viruses were propagated in EECs and tissue culture supernatants were stored at -80°C. Virus titers were determined by plaque assay in high passage RK-13 cells as previously described [291]. The experimental challenge studies were carried out in accordance with an IACUC approved protocol.

Horses

In order to divide horses into two groups based on the *in vitro* susceptibility phenotype of their $CD3^+$ T lymphocytes to the EAV VBS, a large number of horses (n=62) were first screened by dual-color flow cytometry as previously described [330]. A total of 8 mares were selected, 4 in Group A (susceptible) and 4 in Group B (resistant), for use in this study (Table 4.1). All horses were confirmed seronegative for EAV neutralizing antibodies using a previously described protocol [337].

Table 4.1. Horses used in the study.

Group	Horse ID	Breed	Gender	Age
A	E7	TBX	F	7
	F23	Mix	F	6
	F84	TB	G	10
	G13	TBX	F	5
B	F19	Mix	F	6
	F64	TB	F	8
	F83	TB	F	7
	E9	TBX	F	7

Antibodies

The equine $CD3^+$ T lymphocyte monoclonal antibody (MAb) UC F6G was kindly provided by Dr. Jeff Stott, University of California, Davis. The R-PE conjugated $F(ab')_2$ fragment of goat anti-mouse IgG1 (Southern Biotech, Birmingham, AL) was used as the secondary antibody. To detect EAV antigen in infected cells, the Alexa Fluor 488-labeled MAb against EAV nonstructural protein 1 (nsp1; MAb 12A4) was used [306,330].

Dual-color flow cytometry analysis of PBMCs

The susceptibility of $CD3^+$ T lymphocytes to EAV was determined using dual-color flow cytometry analysis. Dual fluorescent antibody staining of PBMC cultures was performed using anti-equine CD3 monoclonal antibody (MAb) specific for $CD3^+$ T lymphocytes as well as an MAb specific for the EAV nsp1 as previously described [330]. Double-stained PBMCs were analyzed using a FACSCalibur (Becton Dickinson, San Jose, CA). The percentage of CD3 surface antigen and intracellular EAV antigen positive lymphocytes were determined by CellQuest™ quadrant statistics (Becton Dickinson, San Jose, CA).

Experimental infection of horses

Horses (Groups A [susceptible; n=4] and B [resistant; n=4]) used in the study were transferred to an experimental facility one week prior to challenge for acclimatization purposes. Pre-inoculation blood samples and PAXGENE® RNA tubes (PreAnalyticX, Valencia, CA) were collected to determine base-line values for complete and differential blood counts and cytokine gene expression in peripheral blood from both groups of horses. All horses were clinically evaluated prior to experimental inoculation with the virus. Both groups of horses were inoculated intranasally with 3×10^6 pfu of the EAV rVBS in 4.0 ml of EMEM using a fenestrated catheter inserted into the area of the posterior nares and the nasopharynx. Horses were monitored for the appearance of clinical signs (cough, nasal discharge, anorexia, depression, edema and urticaria) twice daily (AM and PM) for the first two weeks after inoculation and then once daily for two additional weeks (Figure 4.1).

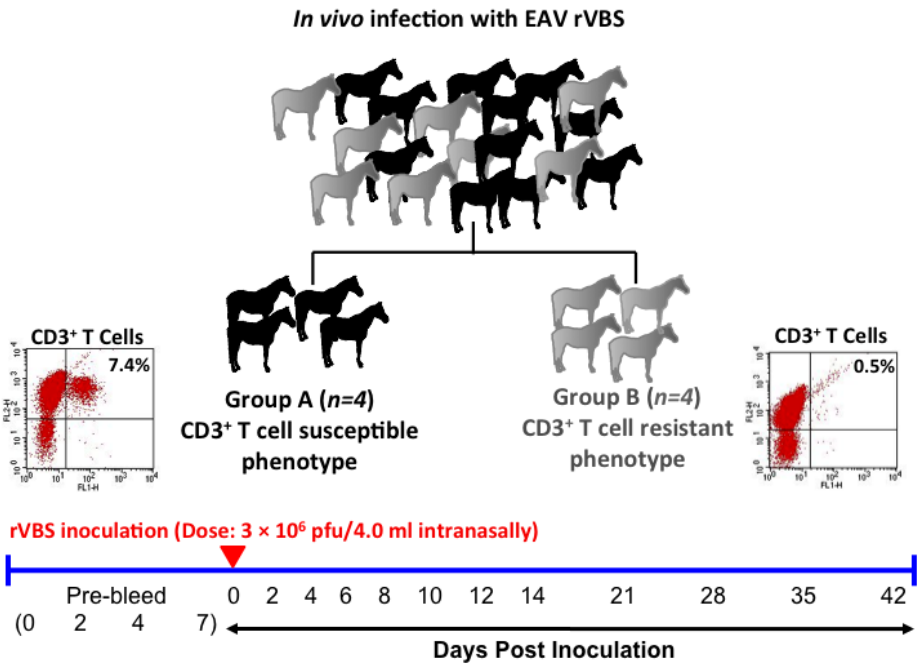

Figure 4.1. Schematic representation of study design and timeline for experimental EAV inoculation and sample collections. Serum, blood for PBMC isolation and PAXGENE® blood samples were collected prior and post challenge on the indicated days. However, PAXGENE® tubes for cytokine mRNA analysis were collected up to 21 DPI, whereas other samples were collected up to 42 DPI. Clinical examinations and nasopharyngeal swab collections were also performed on the same days up to 42 DPI. Representative dot plots of dual-color immunofluorescence flow cytometry data of $CD3^+$ T lymphoctyes are shown for each group with percentage (%) of infected cells indicated on the right hand corner. X-axis of the plot represents relative fluorescence intensity (RFI) of cells stained with EAV nsp1 AF488-conjugated antibody and Y-axis represents the RFI of cells stained with antibody to CD3 surface molecule of equine T lymphocytes.

Blood samples were collected at 0, 2, 4, 6, 8, 10, 12, 14, 21, 28, 35 and 42 days post-inoculation (DPI) for complete blood cell counts. Approximately 3 ml of whole blood was collected on 0, 2, 4, 6, 8, 10, 12, 14 and 21 DPI into PAXGENE® blood RNA tubes (PreAnalyticX, Valencia, CA) for total RNA extraction from peripheral blood [396]. The tubes were equilibrated at room temperature for several hours and then stored at -

20°C until processed. Blood samples were collected every other day during the first two weeks after virus challenge for immediate PBMC isolation and subsequent staining of $CD3^+$ T cells infected with EAV as described above. Nasal swabs were collected at 0, 2, 4, 6, 8, 10, 12, 14, 21, 28, 35 and 42 DPI using sterile rayon swabs (1/2" x 1") with plastic shafts (16"). After collection, the rayon tip of each swab was cut off into 7 ml of virus transport medium (Hank's balanced salt solution with penicillin, streptomycin, gentamicin sulfate and amphotericin B; all from Life Technologies, Carlsbad, CA). Subsequently in the laboratory, individual nasal swabs in transport medium were transferred to the barrel of a 12 ml disposable syringe and expressed through a 0.45 μm syringe filter (Millipore, Billerica, MA). Nasal swab elutes/filtrates were stored at -80°C until tested. The serum neutralizing antibody response to EAV was determined in each horse at 0, 2, 4, 6, 8, 10, 12, 14, 21, 28, 35 and 42 DPI following previously described protocols [337].

Virus isolation

Virus isolation was attempted from PBMCs and nasal swabs as previously described [328,331]. Briefly, confluent monolayers of RK-13 cells in 6-well plates were inoculated with serial 10-fold dilutions (10^0-10^5 in duplicate) and overlaid with RK-13 growth medium containing 0.75% carboxymethylcellulose. The cells were incubated at 37°C in the presence of 5% CO_2 for 5 days and plaques were visualized by staining monolayers with a solution of buffered formalin-crystal violet. A second passage was performed 4 days after the initial passage.

Microneutralization assay

Neutralizing antibody titers of the test sera were determined as described by Senne *et al.* [292,337]. Briefly, serial two-fold dilutions of each sample from 1:4 to 1:512 were made in EMEM (Invitrogen, Carlsbad, CA) containing 10% guinea pig complement (Rockland Immunochemicals, Gilbertsville, PA). Each serum sample was tested in duplicate in 96-well plates. An equal volume of virus dilution containing an estimated 200 $TCID_{50}$ of the modified live virus vaccine strain of EAV (ARVAC®, Pfizer Animal Health, New York, NY) was added to each well, except serum and cell controls.

The plates were shaken to ensure mixing of the well contents and then incubated for 1h at 37°C. A suspension of high passage (P399 to P409) RK-13 cells was added to each well in a volume double that of the serum-virus mixtures and the plates were incubated in 5% CO_2 for 72 h at 37°C until viral cytopathic effect had fully developed in the virus control wells. Antibody titers were recorded as the reciprocal of the highest serum dilution that provided at least 50% protection of the RK-13 cell monolayer.

Proinflammatory and immunomodulatory cytokine mRNA expression in peripheral blood mononuclear cells after experimental inoculation of EAV

The frozen PAXGENE® blood RNA tubes (PreAnalyticX, Valencia, CA) were thawed and total RNA was extracted using the PAXGENE blood RNA extraction kit (Qiagen, Valencia, CA) with an automated QIAcube (Qiagen, Valencia, CA) following the manufacturer's protocol. The RNA concentration was assessed at OD_{260nm} and purity was verified by the OD_{260}/OD_{280} ratio using NanoDrop (Thermo Scientific, Wilmington, DE). The reverse transcription reaction was performed with 0.5 µg of total RNA using random hexamer primers and MultiScribe™ reverse transcriptase enzyme (High Capacity cDNA Reverse Transcription kit with RNase inhibitor [Applied Biosystems, Foster City, CA]) according to the manufacturer's instructions. The reactions were incubated at 25°C for 10 min, 37°C for 120 min and 85°C for 5 min. The cDNA samples were stored at -20°C until further analysis by quantitative RT-PCR (qRT-PCR). Cytokine mRNA expression was measured using equine specific intron-spanning primers/probe sets, except for IFN-α which does not possess introns (Table 4.2)[397,398,399,400,401,402]. Briefly, PCR amplification was carried out using a 10µl reaction mixture containing 4.5 µl of diluted cDNA (1:1 dilution with nuclease-free water), 0.5 µl of 20X assay mix for the primers/probe set of interest (Applied Biosystems, Foster City, CA) and 5 µl of TaqMan® Gene Expression Master Mix (Applied Biosystems, Foster City, CA). Samples were incubated in duplicate wells at 95°C for 10 min followed by 40 cycles at 95°C for 15 s and 60°C for 60 s using an Applied Biosystems 7500 Fast Real-Time PCR System. For each sample, cDNA corresponding to the β-glucuronidase (β-GUS) gene was amplified and used as an endogenous control for relative quantification of sample cDNA. All PCR efficiency values were determined using LinReg [403]. Results were expressed

as relative quantification (RQ) calculated as $2^{-\Delta\Delta Ct}$ where $\Delta\Delta C_t$ = [(Avg. gene of interest C_t – Avg. β-GUS C_t) $_{sample}$ – (Avg. gene of interest C_t – Avg. β-GUS C_t) $_{calibrator}$] [404]. The calibrator was calculated from the mean ΔC_t of pre-inoculation samples of each horse.

Validation of reference genes as internal controls

To determine the effect of the experimental treatment on the expression of candidate internal control genes, four reference genes, β-glucuronidase (β-GUS), equine β-2- microglobulin, β-actin and equine GAPDH were evaluated. PBMC samples were prepared and infected as described previously. The relative amounts of reference genes cDNA were determined by TaqMan real-time quantitative PCR. The relative amounts of the endogenous controls were calculated using the $2^{-\Delta C'T}$ equation where $\Delta C'_T = C_{T,Time\ x} - C_{T,Time\ 0}$ [404].

Statistical analysis

Two-way repeated measures-analysis of variance (ANOVA) (Holm-Sidak method) was used to determine differences in body temperature, absolute lymphocyte counts, virus titers from PBMCs and nasopharyngeal swabs and cytokine gene expression within Group A and B horses. Significant differences were determined at the level of $p < 0.05$. Statistical analysis was performed using SigmaPlot® 11 (Systat Inc., Richmond, CA).

Table 4.2. PCR primers and TaqMan® MGB probes specific for equine cytokines

Cytokine Name[a]	Primers[b] and probe[c]	Sequences (5'-3')
IL-1β [400,401]	EQIL-1B-JN2F	CCGACACCAGTGACATGATGA
	EQIL-1B-JN2R	ATCCTCCTCAAAGAACAGGTCAT
	EQIL-1B-JN2M2	ATTGCCGCTGCAGTAAG
IL-6 [400,401]	EQIL-6-IL6F	GGATGCTTCCAATCTGGGTTCAA
	EQIL-6-IL6R	TCCGAAAGACCAGTGGTGATTTT
	EQIL-6-IL6M2	ATCAGGCAGGTCTCCTG
IL-8	EQIL-8IS-JN1F	GCCGTCTTCCTGCTTTCTG
	EQIL-8IS-JN1R	CCGAAGCTCTGCAGTAATTCTTG
	EQIL-8IS-JN1M2	CAACCGCAGCTTCAC
IL-10 [397]	EQIL10IS-JN2F	AGGACCAGCTGGACAACATG
	EQIL10IS-JN2F	GGTAAAACTGGATCATCTCCGAC
	EQIL10IS-JN2M2	CCAGGTAACCCTTAAAGTC
TNF-α [400,401]	EQTNFAIS-JN2F	TTACCGAATGCCTTCCAGTCAAT
	EQTNFAIS-JN2R	GGGCTACAGGCTTGTCACTT
	EQTNFAIS-JN2M1	CCAGACACTCAGATCAT
IFN-α[d]	EqIL-IFN-α F	TGACCTGCCTCACACCCATA
	EqIL-IFN-α R	TTGTCCCAGGAGCATCAAGAC
	EqIL-IFN-α Pro	CCTGGGCAACACAAG
IFN-γ [398]	EQIFNGIS-JN3F	AGCAGCACCAGCAAGCT
	EQIFNGIS-JN3R	TTTGCGCTGGACCTTCAGA
	EQIFNGIS-JN3M1	ATTCAGATTCCGGTAAATGA
β-GUS [398,399,402]	GUS-GUSF	GCTCATCTGGAACTTTGCTGATT
	GUS-GUSR	CTGACGAGTGAAGATCCCCTTTT
	GUS-GUSM2	CTCTCTGCGGTGACTGG

[a] References are indicated in parenthesis
[b] F-forward primer; R-reverse primer
[c] Pro-Minor groove binding (MGB™) probe labeled with 5' FAM (6-carboxyfluorescein) reporter dye and 3' non-fluorescent quencher dye (NFQ)
[d] New primers and probe were designed and validated for this study

4.4. RESULTS

In vitro CD3$^+$ T lymphocyte susceptible phenotype of horses

As a prerequisite to the *in vivo* infection experiments, PBMCs from horses under consideration for inclusion in the study were subjected to a phenotypic analysis to determine their CD3$^+$ T cell susceptibility following *in vitro* infection with EAV. Based on their T cell phenotype, horses were divided into two distinct groups. Of 62 horses screened, 4 horses with CD3$^+$ T cells that could be infected (susceptible) with EAV VBS were selected and included in Group A and 4 other horses with CD3$^+$ T cells resistant to EAV VBS infection were included in Group B. Dot plots of flow cytometric analysis showing infectivity of CD3$^+$ T cells are shown in Figure 4.2 for each horse included in the study. The percentage of the CD3$^+$ T cell subpopulation susceptible to EAV ranged from 2.3% to 10.3% in Group A horses (Figure 4.2). After assessing the phenotype, horses were challenged intranasally with the EAV rVBS.

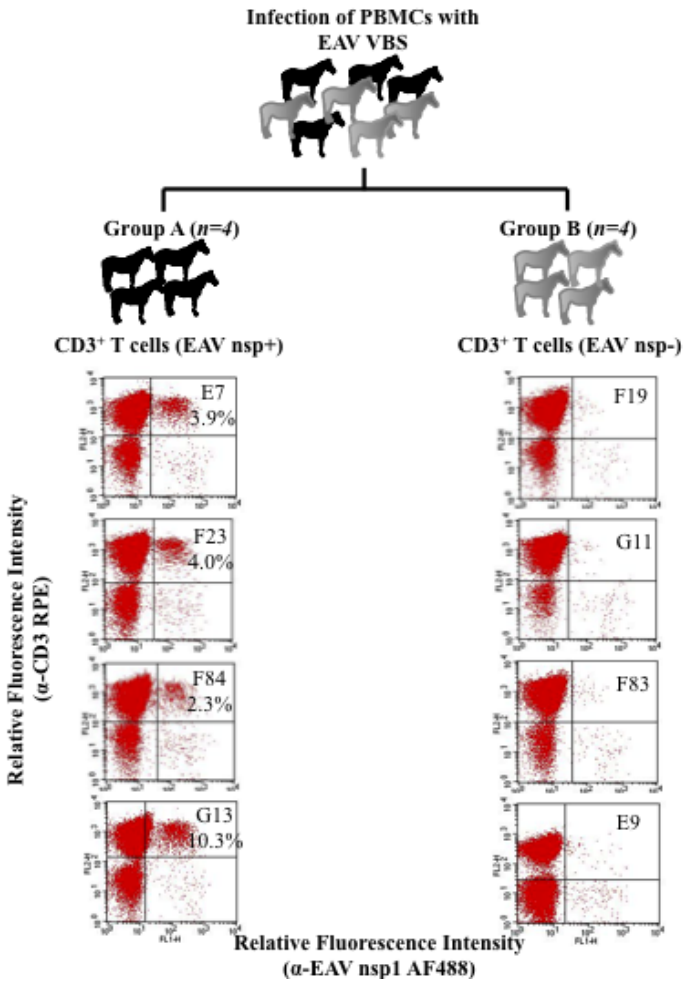

Figure 4.2. Phenotypic analysis of horses used to identify two experimental groups in the study. Horses were divided into Groups A and B based on their susceptibility of $CD3^+$ T lymphocytes to infection with the EAV VBS using dual-color immunofluorescence flow cytometric analysis. Dot plot of VBS infection is shown for each horse used in the study. X-axis of the plot represents relative fluorescence intensity (RFI) of cells stained with EAV nsp1 AF488-conjugated antibody and Y-axis represents the RFI of cells stained with antibody to CD3 surface molecule of equine T lymphocytes. Horse ID and percentage (%) of infected CD3+ T lymphocytes are identified on the right hand corner of each dot plot.

Clinical disease and virus shedding

Following experimental infection with EAV rVBS, febrile responses were observed in all horses from both groups starting at 3 DPI and persisting (5-6 days) until 8 or 9 DPI (Figure 4.3.A). However, there was a consistent trend toward higher body temperatures in Group B horses from 3-8 DPI that culminated in statistically significant increases (p <0.05) in febrile responses compared to all Group A horses at 7 and 9 DPI. The febrile response was also delayed in Group A horses with the peak temperature on 8 DPI which occurred on 7 DPI in Group B. In addition to febrile responses, other clinical signs commonly associated with exposure to EAV were more pronounced in Group B horses. Three out of 4 members of this group had continuous serous nasal discharge lasting 3 to 4 days, with one horse (E9) having particularly severe respiratory distress with labored breathing (respiratory rate >30/min) for 2 days. All Group B horses had congestion coupled with petechial hemorrhages on oral mucous membranes (Figure 4.4.A) from 7-8 DPI and 3 out of 4 of these animals developed mild to moderate hind leg edema, restricted to the fetlocks (Figure 4.4.B). In contrast, a serous nasal discharge was encountered (present for 4 days at 6-9 DPI) in only one horse in Group A (F84). Furthermore, petechial hemorrhages on oral mucous membranes were not seen in any Group A horse, and only one member of this group (F84) developed hind leg edema which was mild compared with that seen in Group B subjects. However, one Group A mare (F23) developed skin eruptions (hives) on the body (Figure 4.4.C), while another mare (E7) in the same group had mild mammary gland edema (Figure 4.4.D) that lasted for more than 10 days. Horses in both groups developed severe lymphopenia between 4-8 DPI (Figure 4.3.B) and although this appeared to be more pronounced in Group B horses between 4-8 DPI, this trend was not confirmed by subsequent statistical analysis.

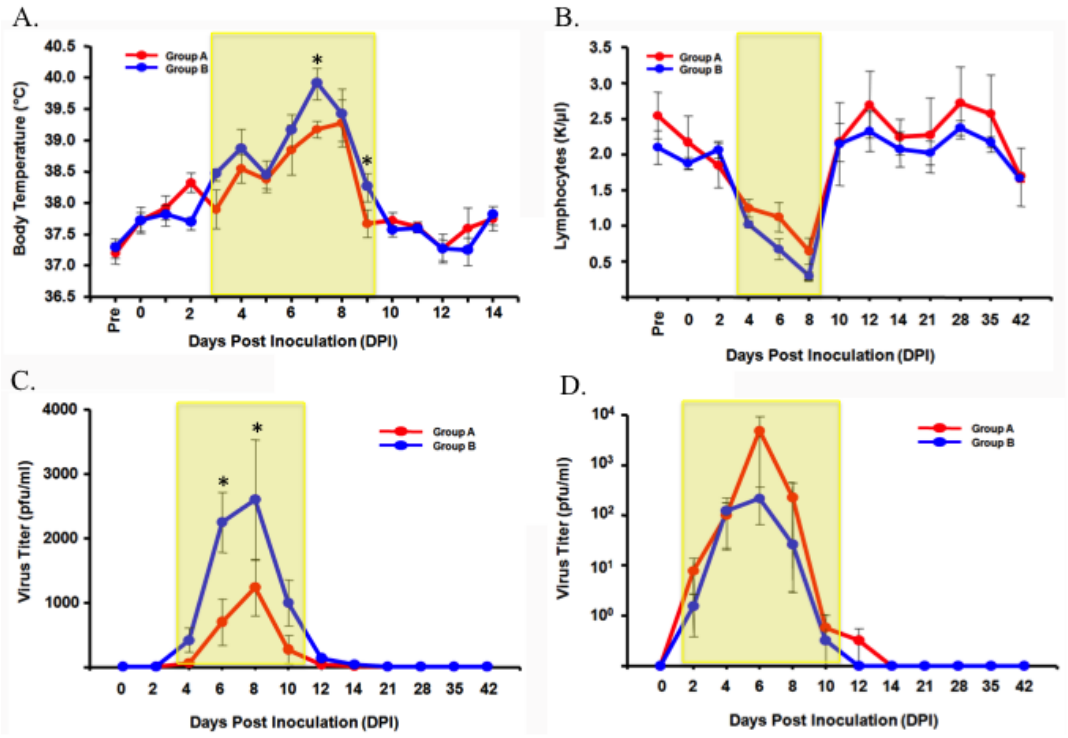

Figure 4.3. The body temperatures, peripheral blood lymphocyte counts, and virus titers in nasal secretions and blood. Rectal temperature (A), peripheral blood lymphocyte counts (B), virus isolation from peripheral blood mononuclear cells (C) and nasal secretions (D) of both groups of horses inoculated with EAV rVBS. The mean and standard deviation are shown in all panels. Days when horses developed maximum clinical outcomes are boxed in yellow.

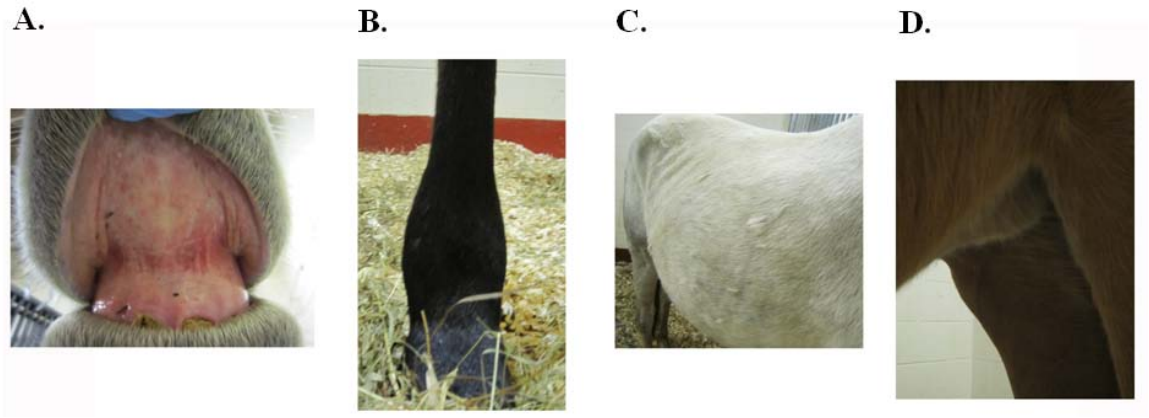

Figure 4.4. Representative examples of clinical signs following experimental inoculation of EAV rVBS. (A) Petechial hemorrhages, (B) limb edema, (C) hives and (D) mammary edema.

Horses from both groups had detectable viremia levels from 4-10 DPI with peak titers occurring at 8 DPI (Figure 4.3.C). As might be predicted from the clear differences in clinical signs, viral titers in PBMCs were statistically significantly higher in Group B compared to Group A horses at 6 and 8 DPI ($p < 0.05$). Although these results appeared to be contradicted by amounts of virus detected in nasal secretions (Figure 4.3.D), the differences between the groups were due entirely to a single horse (F84) in Group A that had a 55-fold higher virus titer in nasal swab material on day 6 post-inoculation compared to the other members of its cohort. This subject was the only Group A recipient to present with a prolonged nasal discharge and interestingly, compared with the other group members, had the lowest percentage of EAV susceptible $CD3^+$ T lymphocytes (2.3%; Figure 4.2). As a result of this one "super-shedder", the viral titers present in nasal swab material were not statistically different between the two groups.

Attempts to detect EAV infected $CD3^+$ T cells in peripheral blood analogous to those observed following *in vitro* infection of PBMCs were conducted using dual-color flow cytometry with antibodies to CD3 surface molecule and EAV nsp1 protein (intracellular staining). Unfortunately, $CD3^+$ T lymphocytes expressing intracellular EAV nsp1

antigen were not detected in any of the horses (either group) during the first 2 weeks of acute infection.

Humoral responses following inoculation with the EAV rVBS were identical between the horses of both groups with serum neutralizing antibody titers being detectable at 8 DPI and increasing to ≥1:512 by 10 DPI (Figure 4.5). The appearance of neutralizing antibodies in peripheral blood was directly correlated with significant decreases in viremia and virus shedding in nasal secretions coupled with a return to normal clinical values.

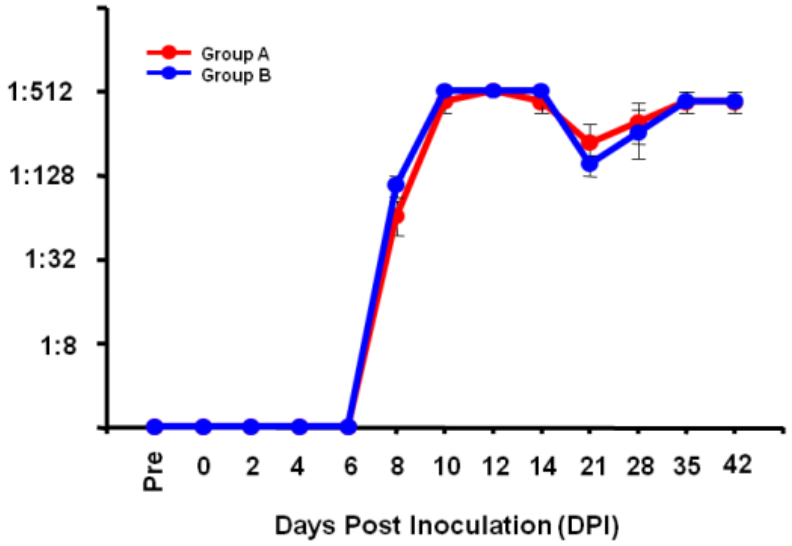

Figure 4.5. Serum neutralizing antibody responses in both groups of horses inoculated with EAV rVBS. The mean and standard deviation of reciprocal antibody titers are shown.

Proinflammatory and immunomodulatory cytokine gene expression in peripheral blood

There were significant differences between Group A and B horses in the level and/or kinetics of cytokine mRNA expression as determined by qRT-PCR analysis (Figure 4.6). Although increased amounts of IL-1β mRNA were observed in all experimental subjects following infection with EAV rVBS, the kinetics were

significantly different between the two groups. In Group A horses, IL-1β mRNA reached maximal levels just 2 days after infection, whereas peak amounts were not observed in Group B horses until 6 DPI (Figure 4.6.A). A very similar kinetic distribution was observed for IL-6 with maximum mRNA levels seen at 2 DPI for Group A horses compared with 4 DPI for Group B (Figure 4.6.B) recipients. Although the kinetics of IL-8 and IFN-γ mRNA expression were broadly similar between groups, with a correlation between maximal levels and peak viral burdens, significantly higher amounts ($p < 0.05$) of mRNAs encoding these cytokines were produced in Group B horses (Figures 4.6 C, F). Of the panel of cytokines investigated, only TNF-α mRNA levels appeared to be similar between Group A and B horses both in terms of the time and the duration of increased expression levels (Figure 4.6.D). Although increases in overall TNF-α mRNA amounts appeared to be higher in Group B horses consistent with their more severe clinical signs, this difference was not confirmed statistically. Somewhat surprisingly, EAV infection did not stimulate significant increases in IFN-α expression in any of the Group A recipients. In contrast, there was substantial induction of IFN-α mRNA synthesis in Group B horses (Figure 4.6.E). Just as with IFN-α mRNA, EAV infection did not stimulate IL-10 gene expression in any of the Group A horses, whereas expression of this gene was up-regulated in the Group B experimental subjects. In all Group B horses, there were significant ($p < 0.05$) increases in IL-10 mRNA levels at 4 and 8 DPI compared with pre-infection amounts and the equivalent Group A post-infection time-points (Figure 4.6.G). In summary, with the exception of TNF-α, there were significant differences between the two groups of horses in expression of both proinflammatory (IL-1β, IL-6 and IL-8) and immunomodulatory (IFN-α, IFN-γ, and IL-10) cytokines indicating that they may influence the clinical outcome along with innate and cellular immune response to EAV.

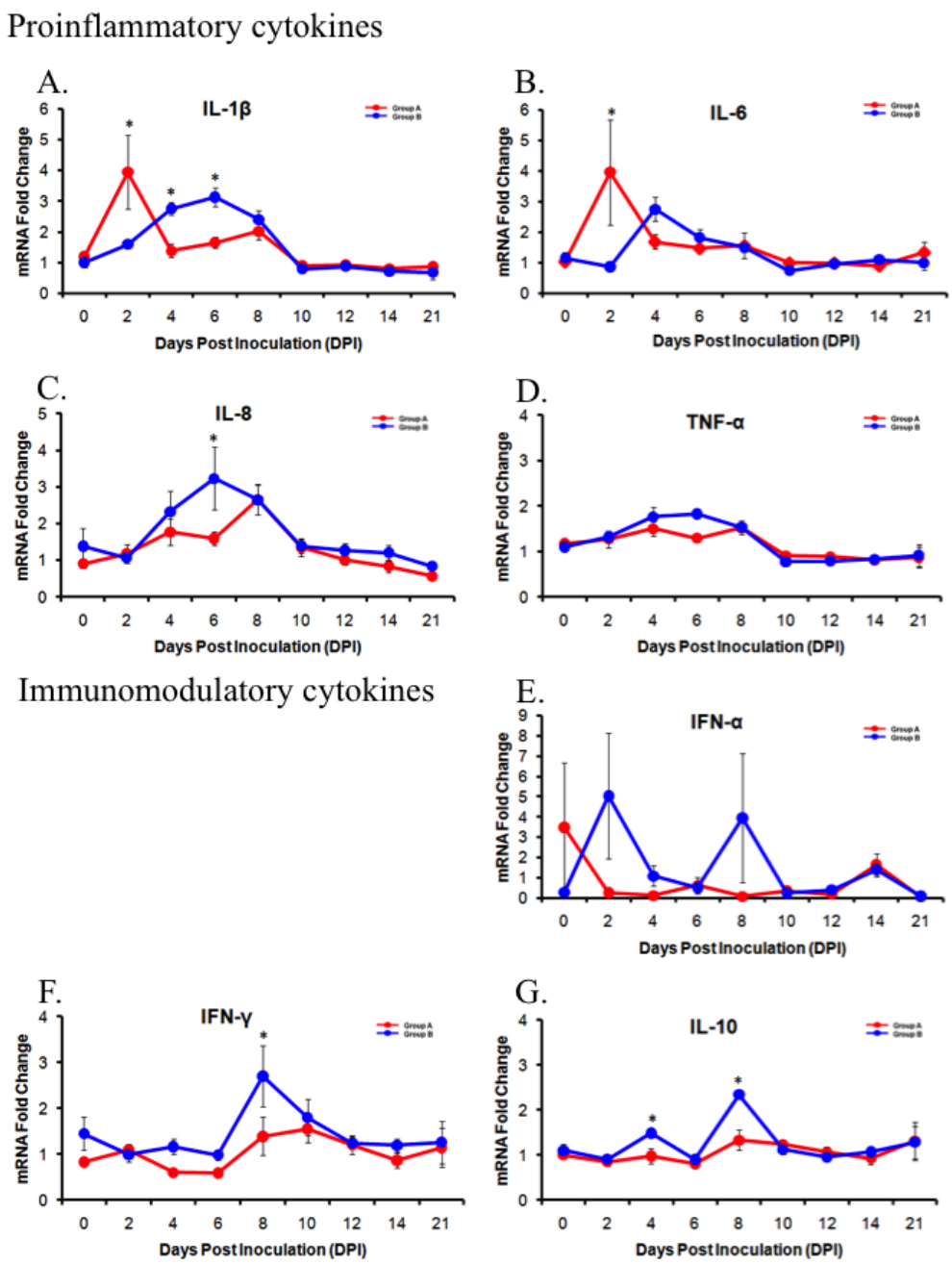

Figure 4.6. Relative quantification (RQ) of proinflammatory and immunomodulatory cytokine mRNA expression in Group A and Group B horses. Mean (±SE) mRNA expression of proinflammatory cytokines (A) IL-1β, (B) IL-6, (C) IL-8, (D) TNF-α and mean mRNA expression of immunomodulatory cytokines (E) IFN-α, (F) IFN-γ and (G) IL-10. Statistically significant difference (p <0.05) between Group A and B horses is indicated with an asterisk (*).

4.5. DISCUSSION

Previous work in our laboratory using an *in vitro* dual-color flow cytometry assay demonstrated that horses could be grouped into two populations based on the susceptibility of $CD3^+$ T lymphocyte subpopulations to infection with EAV [330]. Although progeny virions were not detected [330] suggesting infection of $CD3^+$ T lymphocytes is not fully permissive, it was hypothesized that the presence of virus specific structural and/or non-structural proteins could modify functional characteristics of these cells. Therefore, the objective of this study was to determine if the differences in the susceptibility or resistance of $CD3^+$ T cells *in vitro* correlate with clinical outcome to exposure *in vivo*. These studies were conducted using viruses derived from a virulent infectious EAV cDNA clone to minimize, as far as possible, the effects of variation occurring within the viral population or quasispecies [328]. To our knowledge, there have been no published reports demonstrating an association between clinical outcome following exposure to EAV and specific host factors. The results described here clearly demonstrate that while other environmental and/or host factors are likely to be important as exemplified by the atypical prolonged nasal discharge coupled with high-titer respiratory tract virus shedding seen in the Group A horse (F84), there is a correlation between clinical response to EAV infection *in vivo* and the susceptibility of $CD3^+$ T lymphocytes *in vitro*. Horses with the $CD3^+$ T lymphocyte resistant phenotype (Group B) had higher febrile responses, possessed higher titers of virus in blood, were the only experimental subjects to have petechial hemorrhages on oral mucous membranes and were more likely to suffer hind leg edema or develop serous nasal discharges than horses with the $CD3^+$ T lymphocyte (Group A) susceptible phenotype. However, the overall duration of clinical signs and development of humoral immune responses associated with viral clearance were indistinguishable between horses in these two groups.

In addition to clinical signs, there were significant differences between Group A and Group B horses in proinflammatory cytokine gene expression. At present, the regulatory mechanisms controlling these very different cytokine mRNA expression profiles in these two groups of horses are unknown. However, production of TNF-α, IL-1β and IL-8 by macrophages has been shown to contribute to the pathogenesis of EVA [257] by enhancing macrophage activation and exerting profound effects on endothelial cells

leading to increased vascular permeability with subsequent tissue edema producing clinical signs that are characteristic of severe EVA. Furthermore, IL-6 may contribute to the overall severity of disease by stimulating prostaglandin E2 (PGE2) synthesis leading to increases in febrile responsiveness. Therefore, by comparison with horses in Group A, subjects in Group B have higher levels of mRNA encoding IL-1β, IL-6, IL-8 and possibly TNF-α, all inflammatory cytokines with the potential to augment the pathogenicity of EAV at times when viral burdens attain their highest levels. At present, it is not known if the early (2 DPI) short pulse of increased IL-1β and IL-6 expression seen in Group A horses that is predicted to stimulate for example, the synthesis of acute-phase proteins, has any limiting effects on EAV replication.

Significant differences between Group A and Group B horses following infection with the EAV rVBS were also seen in IFN-α mRNA levels and in expression of the immunomodulatory cytokines IFN-γ and IL-10. The failure to mount a strong IFN-α induction could affect both innate and adaptive immune responses in Group A horses. Specifically, reduced IFN-α production could lead to slow dendritic cell maturation, antigen-specific $CD8^+$ T cell maturation, as well as slow IFN-γ and other cytokine production. Furthermore, EAV infection did not stimulate IL-10 expression compared to pre-infection levels in any Group A horse. In contrast, significant increases in IL-10 mRNA amounts, compared with both pre-infection levels and equivalent time-points for Group A animals, were observed in all group B horses at 4 and 8 DPI (Figure 4.6.G). IL-10 was originally considered as a cytokine that modulates the balance of Th1/Th2 response, in favor of the Th2-type response [405]. It inhibits macrophage activation and antigen presentation, thereby inhibiting T cell function. The IL-10 secreted by regulatory T (Treg) cells reduces T-cell-mediated immune inflammation by inhibiting cytokine production (IL-1, IL-6, IL-12, TNF-α and the chemokine IL-8) in macrophages and Th1 cells (IFN-γ) [406]. As a result, IL-10 can limit and eventually terminate inflammatory responses caused by infectious agents [333]. Therefore, it is likely that IL-10 expression is up-regulated in Group B but not in Group A subjects because of the higher levels and/or different kinetics of inflammatory cytokine expression observed in horses with $CD3^+$ T lymphocytes that are resistant to infection with EAV. Although increased EAV-induced IFN-γ expression was present in PBMCs from some Group A horses,

significantly higher levels of mRNA encoding this cytokine were observed at 8 DPI in Group B horses. Together, these results demonstrate that EAV induces very different cytokine expression profiles in Group A and Group B horses. At present, the mechanism(s) underlying these differences is not known, although the possibility exists that it may be a direct effect caused by EAV infecting and then modifying the functional and/or regulatory properties of specific T-lymphocyte subsets within the $CD3^+$ T lymphocyte population. The fact that nsp1 expressing $CD3^+$ T lymphocytes were not found in peripheral blood samples from EAV infected Group A horses is perhaps not surprising considering the blood volume of a typical horse is approximately 45 L. In addition, it is very likely that most infected T cells will be present within the tissue sites supporting active viral replication rather than in general circulation.

Unfortunately, the small subpopulation(s) of $CD3^+$ T lymphocytes that are susceptible to infection with EAV in PBMCs of Group A horses is unknown at present. During *in vitro* infection experiments with PBMCs harvested from more than 400 horses, the percentage of infected $CD3^+$ T lymphocytes ranged from 2.3 to 20%, depending on the individual animal (data not shown). Previously, we have reported that the majority of $CD3^+$ T lymphocytes infected with EAV are $CD4^+$ rather than $CD8^+$ T cells [330]. Regulatory T cells are a subset of $CD4^+$ T cells with natural immune-suppressive activity [407]. In this respect, we hypothesize that the small subpopulation of $CD3^+$ T lymphocytes infected with EAV could be Treg lymphocytes. Unfortunately, there are no commercial or published antibodies specific for equine Treg cells, such as the antibodies available to the Foxp3 and CD25 Treg markers of other species. However, it may be possible to purify dual labeled nsp1/$CD3^+$ expressing T cells by flow cytometry and characterize them by PCR analysis using primers for transcription factors that are specific for the different T helper cell types (Horohov, personal communication).

Although infection coupled with disruption to the functional properties of specific T-cell subsets might account for all of the observed differences between Group A and B horses following infection with EAV, this could also be just one manifestation of a more general mechanism affecting a range of cell types. In this alternative broad-spectrum model, variation in genotype between Group A and B horses is predicted to induce direct effects in numerous cell-types that fundamentally alter the way in which horses respond

following exposure to EAV in terms of permissiveness for viral replication, clinical responses and cytokine production. Unfortunately, we cannot distinguish between these two alternatives at the present time. The genome-wide analysis reported above has shown the susceptibility or resistance of $CD3^+$ T lymphocytes to infection with EAV is associated with a genetically dominant haplotype on horse chromosome 11 in the region ECA11: 49572804-49643932 (Go *et al.* unpublished data). There are a number of candidate genes within this region that could influence EAV replication or host responses to this virus and that are actively associated with immune (innate and adaptive) and inflammatory responses. As an example, in addition to a role in the chemotatic response, ARRB2, encoded by β-arrestin-2, is believed to control NFκB signaling by interacting with IκBα. Furthermore, this protein may also modulate MAP kinase activity. Another example is the gene encoding the nucleoporin protein (NUP88) that promotes retention of NFκB in the nucleus and is required for the transport of key immune regulators such as the Rel-like transcription factors. Although considerable additional effort is required to fully characterize the structural gene or regulatory sequences involved, there is a very clear genetic correlation between both the susceptibility or resistance of $CD3^+$ T lymphocytes *in vitro* and the different clinical/cytokine expression responses observed in Group A compared to Group B horses following infection with EAV. It is hoped identifying the role of host factors encoded by genes within ECA11: 49572804-49643932 will advance our understanding of the molecular interactions between EAV and its host.

In summary, our findings demonstrate that clinical signs and viremia burdens are more severe in horses with $CD3^+$ T lymphocytes that are resistant (Group B) compared with those that are susceptible (Group A) to EAV infection in an *in vitro* experimental system. Furthermore, these separate groups within the horse population have significantly different cytokine expression profiles following exposure to EAV. At this stage, it is not clear whether higher viremia levels cause these differences or if they are the result of genetically programmed intrinsic responses that for example, in Group B horses may actually promote viral replication and facilitate more severe clinical disease. Although genetic variability is frequently predicted to account for some of the disparities in virus-induced clinical signs observed between individuals, this is the first study to provide direct evidence for a correlation between variation in the genotype of horses and

phenotypic differences in terms of the extent of viral replication, severity of disease and cytokine gene expression caused by exposure to EAV. Although the nucleotide sequences located in ECA11: 49572804-49643932 involved in this phenomenon have yet to be determined, this study provides inroads for explaining at least some of the variation in clinical signs seen among horses after infection with a virulent strain of EAV. It is anticipated that future genetic characterization experiments will increase our understanding of the pathogenesis of EAV, plus contribute towards identification of molecules involved in controlling innate and/or adaptive immune responses. Furthermore, such studies may enable the mechanisms associated with the ability of EAV to persist within certain stallion populations to be elucidated leading to effective treatments or the option to preventive measures to prevent establishment of the carrier state in particular those at higher risk.

CHAPTER FIVE

In vitro susceptibility of $CD3^+$ T lymphocytes to EAV infection reflects genetic predisposition of stallions at risk of becoming carriers

5.1. SUMMARY

Following equine arteritis virus (EAV) infection, a variable proportion of stallions (30-70%) can become persistently infected and continuously shed the virus in their semen. Carrier stallions are the natural reservoir of EAV and ensure the virus is maintained in equine populations between breeding seasons by continuously shedding the virus in their semen. Recent studies in our laboratory have shown that an *in vitro* assay based on dual color flow cytometry analysis of $CD3^+$ T cells could be used to divide the horses into susceptible and resistant groups. In this study, we have extended these previous studies and established a possible correlation between susceptibility of $CD3^+$ T lymphocytes to EAV infection and establishment of persistent infection in stallions. The data showed that carrier stallions that have the susceptible $CD3^+$ T lymphocyte phenotype to EAV infection may represent those at higher risk of becoming persistently infected compared to stallions that do not possess this phenotype.

5.2. RESULTS AND DISCUSSION

Equine arteritis virus (EAV) is a small enveloped virus with a positive-sense, single-stranded RNA genome that belongs to the family *Arteriviridae* (genus *Arterivirus*, order *Nidovirales*) [7,34]. EAV is the causal agent of equine viral arteritis (EVA) which is a respiratory and reproductive disease of horses and other equid species [76,77]. The vast majority of EAV infections are inapparent or subclinical [76,77,395] in nature, but occasional outbreaks occur which are characterized by influenza-like signs in adult horses, abortion and pneumonia in young foals [77,353]. Following EAV infection, a variable proportion of stallions (30-70%) can become persistently infected and continuously shed the virus in their semen [77,190]. Carrier stallions are the natural reservoir of EAV; they ensure the virus is maintained in equine populations between breeding seasons [77,189]. The continued growth in international trade of horses and semen has served as a significant means of dissemination of EAV strains around the world [77,78,188,189,356,408]. Therefore, identification of carrier stallions is of critical epidemiological importance in the prevention and control of EAV infection [76,77,199,354,408]. The mechanism of persistence of EAV in the male reproductive tract is not clear. Studies have established that persistence of EAV in the stallion is testosterone-dependent [217,218]. Although multiple factors may contribute to development of the carrier state, host genetic variation is assumed to explain the individual differences in occurrence of the carrier state as well as virus clearance because such variations exist even after exposure to the same virus. Moreover, the prevalence of EAV infection varies markedly among different breeds of horses strengthening the assumption of genetic influence [77]. Recently, we demonstrated differences in *in vitro* susceptibility of $CD3^+$ T lymphocytes to EAV infection that have a strong association of genetic markers with *de facto* proof that the trait is under genetic control by conducting a genome-wide association study (GWAS; Go *et al.*, in press [chapter 3]). The objective of current study is to establish a correlation between susceptibility of $CD3_+$ T lymphocytes to EAV infection and establishment of persistent infection in stallions. We were fortunate to find stallions that became EAV carriers after natural exposure and stallions that did not became carriers after exposure to EAV (seroconverted by natural exposure and not by vaccination against EVA). To ensure carrier status, isolation of EAV from equine semen

samples was attempted in high passage (P399-409) rabbit kidney-13 (RK-13) cell lines according to the OIE described protocol [292]. Subsequently, PBMCs were collected from carrier (n=7) and non-carrier (n=7) stallions. The susceptible or resistant phenotype of each animal was defined by dual color flow cytometric analysis of *in vitro* EAV infected $CD3^+$ T lymphocytes as described previously [330]. Briefly, 1×10^6 PBMCs isolated from peripheral blood by centrifugation through Ficoll-Paque Plus (Amersham Biosciences, Piscataway, NJ) were infected with the virulent Bucyrus strain (ATCC VR-796) of EAV at an m.o.i of 2. Subsequently, infected PBMCs were incubated with monoclonal antibody (MAb) specific for equine $CD3^+$ T cells and with secondary R-PE-conjugated goat anti-mouse IgG1 (Southern Biotech, Birmingham, AL). Intracellular staining for EAV antigen was performed using Alexa Fluor 488-conjugated anti-EAV nps1 (12A4) MAb. Two-color cytometric acquisition was done using a FACScalibur and data was analyzed by CellQuest software (Becton Dickinson, San Jose, CA). Results were expressed as the percentage of $CD3^+$ T lymphocytes infected with EAV after subtraction of cells stained with mouse IgG1 (MOPC; Sigma, St. Louis, MO) isotype control antibody. Interestingly, $CD3^+$ T lymphocytes from all EAV carrier stallions were susceptible to *in vitro* EAV infection (Figure 5.1.A). The percentage of CD3+ T lymphocytes susceptible to EAV infection ranged from 4% to 17% among carrier stallions. In contrast, none of the EAV non-carrier stallions had the $CD3^+$ T lymphocyte susceptible phenotype (Figure 5.1.B). The data suggested that carrier stallions that have the susceptible $CD3^+$ T lymphocyte phenotype to EAV infection represent those at higher risk of becoming persistently infected compared to stallions that do not possess this phenotype.

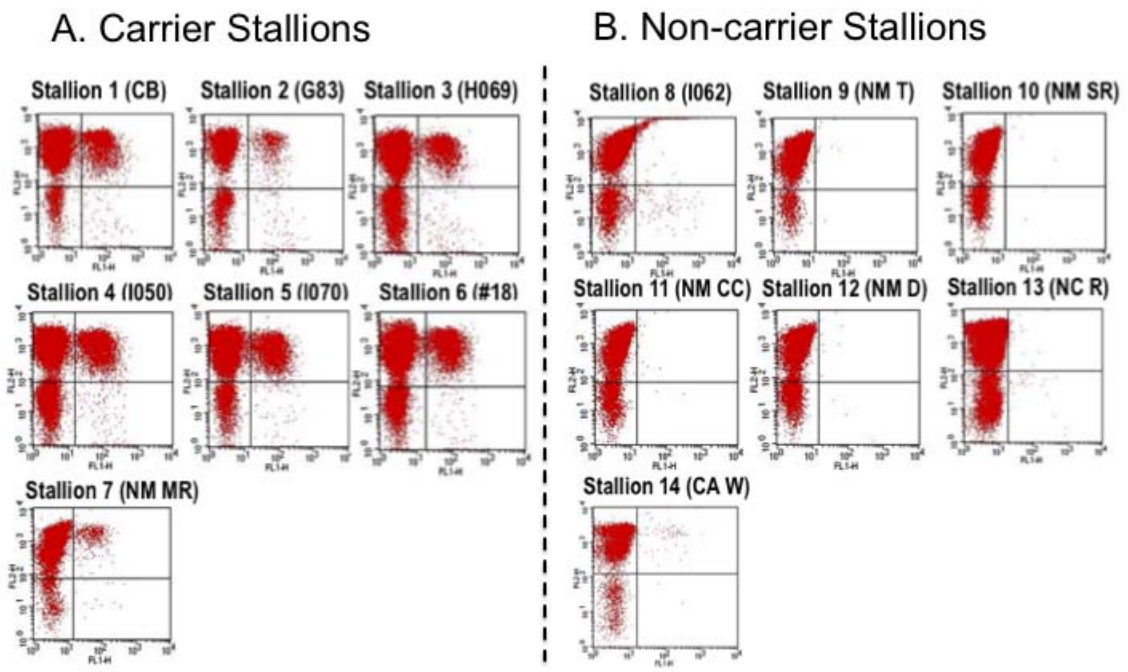

Figure 5.1. Dual-color immunofluorescence flow cytometry analysis of carrier and seropositive non-carrier stallions. (A) Carrier status was confirmed by isolating EAV from semen. **(B)**Non-carrier stallions are seropositive horses with antibodies specific to EAV after natural exposure to EAV and not due to vaccination. Cells double stained with anti-CD3 and anti-nsp1 (12A4) MAbs are shown in the upper right quadrant of each dot plot.

Previously, we have identified a dominant haplotype associated with the susceptible phenotype in a region of equine chromosome 11 (ECA11): 49572804-49643932 by testing four horse breeds (Thoroughbred, Saddlebred, Strandardbred and Quarter horses). The presence of the common haplotype suggested that the trait occurred in a common ancestor of all four breeds that might have segregated among modern horse breeds (discussed in detail in chapter 3 of the dissertation; Go *et al.*, in press). To evaluate whether the same haplotype is associated with carrier and non-carrier status, ECA11: 49572804-49643932 region of stallions included in the study was genotyped using Sequenom MassARRAY® system (Sequenom Inc., San Diego, CA). Briefly, genomic DNA (gDNA) was isolated from PBMCs of each animal using Puregene whole

blood extraction kit (Qiagen, Valencia, CA) following the manufacturer's instructions. DNA from these horses was genotyped for single nucleotide polymorphisms (SNPs) using the EquineSNP50 BeadChip (Illumina, San Diego, CA). Using the option for association studies, the distribution of SNPs was compared between carrier and non-carrier stallions. The SNP data (Table 5.1) showed that five out of seven carrier stallions with the $CD3^+$ T lymphocyte susceptible phenotype had the "GGAGGT" haplotype previously reported to be highly associated with the trait (Go *et al.*, in press [chapter 3]). Unfortunately, the association of the trait with the genetic markers was imperfect since two carrier stallions (CB and I050) were found without the "GGAGGT" haplotype implicated for susceptibility. This emphasizes once again the limitation of low coverage SNPs available for equine and results could be inaccurate. The possibility that the "GGAGGT" haplotype associated with $CD3^+$ T lymphocyte susceptibility is not conserved in all horse breeds, such as Dutch Warmblood and Rocky Mountain Paint, cannot be excluded (Table 5.1).

Table 5.1. Haplotype of carrier and non-carrier stallions for selected SNPs in ECA11: 49572804-49643932

Phenotype	Status	Horse ID	HAP1	HAP2	Breed
Positive	EAV shedder	CB	CACATC	GGAGGC	Dutch Warmblood
Positive	EAV shedder	G83	CACATC	GGAGGT	QH
Positive	EAV shedder	H069	GGAGGT	GGAGGC	Paint
Positive	EAV shedder	I050	GGAGGC	GGAGGC	Rocky Mountain Paint
Positive	EAV shedder	I070	GGAGGT	GGAGGC	TWH
Positive	EAV shedder	#18	GGAGGT	GGAGGT	STB
Positive	EAV shedder	NM-MR	GGAGGT	GGAGGC	QH
Negative	Non-shedder	I062	GGAGGC	GGAGGC	Rocky Mountain X
Negative	Non-shedder	NM-T			TB
Negative	Non-shedder	NM-SR			QH
Negative	Non-shedder	NM-CC			QH
Negative	Non-shedder	NM-D			TB
Negative	Non-shedder	NC-R	GGAGGC	GGAGGC	Dutch Warmblood
Negative	Non-shedder	CA-W	GGAGGT	GGAGGC	Hanoverian

NOTE: The positive and negative phenotype refers to *in vitro* $CD3^+$ T lymphocyte susceptibility and resistance, respectively. The haplotype "GGAGGT" associated with $CD3^+$ T cell susceptibility is highlighted in yellow as described elsewhere (Go *et al.*, in press [chapter 3]). Each haplotype is highlighted with a different color.

Larger numbers of carrier and non-carrier stallions (naturally exposed) are needed to draw definite conclusions about the link between $CD3^+$ T cell susceptibility to EAV infection and the genetic traits of horses at risk to become carrier stallions after exposure to EAV. However, it is a challenge to find a large number of such stallions, especially the non-carrier stallions that have seroconverted due to natural exposure to the virus. Ultimately, results from this study are being confirmed in an *in vivo* study with experimental infection of stallions with susceptible and resistant $CD3^+$ T lymphocyte phenotypes with EAV to see whether stallions with $CD3^+$ T lymphocytes are at higher risk of establishing carrier status compared to those with the resistant phenotype.

The data presented in this study clearly demonstrated that there is a genetic difference between stallions that become carriers after exposure to EAV and those that are able to clear the virus, non-carrier stallions. The trait could be determined by assessing the susceptibility of their $CD3^+$ T lymphocytes to *in vitro* VBS EAV infection which is likely to be the most precise method. However, it is expensive, time consuming and cumbersome to run on a routine or large-scale basis. This study provides the possibility of development of a genetic test to identify stallions that are predisposed to persistent infection. It would allow us to develop new and improved prevention strategies in horses. Eventually, findings from this study will allow us to develop diagnostic tools to predict possible carrier stallions of EAV and prevent further spreading of the virus.

Copyright © Yun Young Go 2011

CHAPTER SIX

Equine arteritis virus does not induce type I interferon α/β production in equine endothelial cells: Identification of nonstructural protein 1 as a main interferon antagonist

6.1. SUMMARY

The primary objective of this study was to investigate the effect of equine arteritis virus (EAV) on type I IFN production. Equine endothelial cells (EECs) were infected with virulent Bucyrus strain (VBS) of EAV at a multiplicity of infection (m.o.i) of 5 and type I IFN (IFN-α/β) expression at mRNA and protein levels were measured by real-time RT-PCR and IFN bioassay using vesicular stomatitis virus expressing the green fluorescence protein (VSV-GFP), respectively. Sendai virus (SeV), a well-known inducer of type I IFN, was used as the positive control for type I IFN induction. IFN-α and IFN-β mRNA levels in EECs infected with EAV VBS were not increased compared to those in mock-infected cells, whereas SeV infection strongly induced production of IFN-α and IFN-β mRNA in the same type of cells at both 3 and 6 h.p.i. Protein levels determined by IFN bioassay provided additional confirmation of this finding. Subsequently, the potential of each of the 12 nonstructural proteins (nsps) of EAV to antagonize type I IFN production was determined by IFN-β promoter luciferase reporter system. The results demonstrated that nsps 1, 2 and 11 had the capability to inhibit type I IFN activity. Of these three nsps, nsp1 exhibited the strongest inhibitory effect by inhibiting IFN synthesis. Collectively, these data demonstrated that failure to induce type I IFN in EAV infected cells may allow the virus to subvert the equine innate immune response. EAV nsp1 may play a critical role in producing this effect.

6.2. INTRODUCTION

Equine arteritis virus (EAV) is the causative agent of equine viral arteritis (EVA), a respiratory and reproductive disease of horses [77]. EAV is a small enveloped virus with a positive-sense, single-stranded RNA genome of ~12.7 kb which belongs to the family *Arteriviridae* (genus *Arterivirus*, order *Nidovirales*), which also includes porcine reproductive and respiratory syndrome virus, simian hemorrhagic fever virus, and lactate dehydrogenase-elevating virus of mice [7,34]. The EAV genome includes nine known functional open reading frames (ORFs 1a, 1b, 2-7) [34,56]. ORFs 1a and 1b are located in the 5'-proximal three-quarters of the genome and are translated to produce replicase polyproteins pp1a and pp1ab (1,727 and 3,175 amino acids, respectively), with the latter being a C-terminally extended version of the former [141]. ORF 1b translation depends on a -1 ribosomal frameshift just before termination of ORF 1a translation [10]. The two replicase precursor polyproteins are cleaved by three different ORF 1a-encoded proteinases yielding at least 13 end products named nonstructural protein (nsp) 1 to 12 (including a recently described nsp7α and 7β) [113]). The three EAV proteinase domains are located in nsp1, nsp2 and nsp4 [34,66]. The remaining eight ORFs (2a, 2b and 3, 4, 5a, 5b and 6-7) are located in the 3' quarter of the genome and encode the structural proteins (GP2, E, GP3, GP4, ORF5a protein, GP5, M and N, respectively) of the virus [57,58,81,137].

The type I interferon (IFN-α/β) is a key component of the host innate immune response to viral infection. Recognition of pathogen-associated molecular pattern (PAMPs) in double-stranded RNA (ds RNA) by intracellular receptors, such as retinoic acid inducible gene I protein (RIG-I) and melanoma differentiation-associated gene product (MDA5) [409] activates protein signaling cascades that result in activation of antiviral transcription factors such as interferon regulatory factor-3 (IRF-3), nuclear factor-κB (NF-κB) and activating protein 1 (AP1) [410]. The IFN-β promoter contains four positive regulatory domains (PRDs), including the binding site for three different transcription factors, IRF-3 (PRDs I and III), NF-κB (PRDII) and AP1 (PRD IV). Activation of these transcription factors triggers the formation of enhanceosomes in the cell nucleus and induces the expression of IFN-α/β . [410,411].

Many viruses have evolved strategies to counteract key elements of the IFN response and prevent development of an antiviral environment in the host. The innate

immune response to EAV infection is poorly characterized. Recently, it had been shown that porcine reproductive and respiratory syndrome virus (PRRSV), a close relative of EAV antagonizes type I IFN production in infected cells [412,413,414,415,416,417]. Based on this finding, we hypothesized that EAV infection may also down regulate type I IFN response in infected cells and that the nsps of the virus may play an important role in subverting the host innate immune response. To test this hypothesis, we investigated the ability of EAV to modulate type I IFN response in infected cells. Specifically, we investigated the mechanisms used by EAV to inhibit type I IFN production in infected cells and the possible role of EAV nsps as modulators of the innate immune response.

6.3. MATERIALS AND METHODS

Virus and cells

Equine pulmonary artery endothelial cells (EECs), baby hamster kidney 21 (BHK-21 [ATCC CCL-10]) and HEK293T cells (kindly provided by Dr. Ying Fang, South Dakota State University, Brookings, SD) were maintained in Dulbecco's modified essential medium (Mediatech, Herndon, VA) with sodium pyruvate, 10% fetal bovine serum (FBS; HyClone Laboratories, Inc., Logan, UT), 100 U/μg per ml penicillin streptomycin, and 200 mM L-glutamine. HeLa (ATCC CCL-2) and MDBK (ATCC CCL-22) cells were grown in Eagle's minimum essential medium with 10% ferritin-supplemented bovine calf serum (Hyclone Laboratories, Inc., Logan, UT) and 100 U/ μg per ml penicillin/streptomycin (Gibco, Carlsbad, CA). The experimentally derived virulent Bucyrus strain (VBS) of EAV was propagated once in EECs to prepare high titered working stocks for the present study as previously described [343,344]. Sendai virus (SeV; Cantell strain) was purchased from American Type Culture Collection (ATCC VR-907; Manassas, VA), propagated once in embryonated chicken eggs to prepare the working virus stock. The virus titer was determined by hemagglutination inhibition assay using chicken red blood cells as described previously [418]. Vesicular stomatitis virus expressing green fluorescent protein (VSV-GFP; [419]) was kindly provided by Dr. Adolfo Garcia-Sastre (Mt. Sinai School of Medicine, New York, NY).

Plasmids

The construction of plasmids for expression of recombinant EAV nsp1 to nsp12 in mammalian cells has been previously described [420]. Briefly, the coding regions of each of the twelve nsps were PCR-amplified from the EAV rVBS full-length infectious cDNA clone [328] and cloned into the pCAGGS eukaryotic expression vector [421]. The nsp5, nsp6, nsp10 and nsp12 were constructed as C-terminal FLAG-tagged fusion protein. Expression of recombinant EAV nsps was performed in BHK-21 cells transfected with individual plasmids containing nsp1 to nsp12 coding regions using Fugene HD (Promega, Madison, WI) according to manufacturer's instructions. The authenticity of each recombinant protein was confirmed by immunofluorescence and Western immunoblotting assays. Reporter plasmids expressing the firefly luciferase under the control of either the IFN-β promoter (p125-Luc) or an artificial promoter containing three IRF3 binding sites (p55-CIB-Luc) were kindly provided by Dr. Takashi Fujita [422]. The pNF-κB-Luc or pISRE-Luc reporter plasmids expressing the firefly luciferase under the control of a promoter with NF-κB-response element or the interferon-stimulated response element (ISRE) was purchased from Stratagene (La Jolla, CA). The pRL-SV40 plasmid that expresses a *Renilla* luciferase under the control of a simian virus (SV40) promoter was purchased from Promega (Madison, WI). The pEFneo-RIG-I, pEFneo-MDA5, and pEFneo-IKKε were kindly provided by Dr. Bin Gotoh [423]. The pcDNA3-TRIF was purchased from Addgene (Cambridge, MA). Construction of pCAGGS-IRF3 plasmid was described previously [415].

Antibodies

To detect EAV antigens in infected cells, MAbs against EAV nonstructural protein-1 (nsp1; MAb 12A4) and nucleocapsid protein (N; Mab 3E2) were used [213,306]. Protein-specific polyclonal rabbit antisera recognizing EAV nsp2 [110], nsp3 (rabbit 98.E3, [84]), nsp4 (a 1:1 mix of anti-nsp4M and anti-nsp4C; [110]), nsp7-8 [110], and nsp10 [87] have been previously described. In addition, antisera against nsp9 and nsp11 were raised by immunizing rabbits with purified full-length recombinant proteins expressed in *E.coli* (J.C. Zevenhoven, D. D. Nedialkova and E. J. Snijder, unpublished data). Commercially available anti-FLAG (Agilent Technologies, Santa Clara, CA)

monoclonal antibody was used to detect FLAG-tagged fusion proteins in immunofluorescence and Western immunoblotting analyses. Rabbit polyclonal antibodies for human IRF3 (Santa Cruz Biotechnology, Santa Cruz, CA) and anti-β-actin (Cell Signaling, Danvers, MA) and monoclonal antibodies for human NF-κB p65 (Santa Cruz Biotechnology) were used. Phosphorylation-specific rabbit polyclonal antibodies for phospho-IRF3 (Ser398; Upstate Millipore, Billerica, MA), and phospho-NF-κB p65 (Ser276; Santa Cruz Biotechnology) were used for immunofluorescence and Western immunoblotting analyses.

RNA extraction and quantitative real time RT-PCR

Total RNA was extracted using MagMAX™-96 Total RNA Isolation kit (Ambion, Austin, TX) according to the manufacturer's recommendations in a MagMAX™ Express-96 magnetic particle processor (Applied Biosystems, Foster City, CA). RNA from each culture was treated with DNase to remove any contaminating genomic DNA (gDNA). The RNA concentration was assessed at OD_{260nm} and purity was verified by the OD_{260}/OD_{280} ratio using NanoDrop (Thermo Scientific, Wilmington, DE). The reverse transcription reaction was performed with 1 μg of total RNA using RT random primers and a MultiScribe™ reverse transcriptase (High Capacity cDNA Reverse Transcription kit with RNase inhibitor [Applied Biosystems, Foster City, CA]) according to the manufacturer's instructions. The following IFN-β primers and probe set were used: EqIL-IFN-βF: 5'-AATGGCCCTCCTGCTGTGT-3', EqIL-IFN-βR: 5'-CCGAAGCAAGTCATAGTTCACAGA-3' and EqIL-IFN-β probe FAM-CTCCACCACGGCTC -NFQ for PCR amplification using an Applied Biosystems 7500 Fast Real-Time PCR System. For each sample, cDNA corresponding to the β-glucuronidase (β-GUS) gene was amplified and used as an endogenous control for relative quantification of a sample cDNA. All PCR efficiency values were determined using LinReg. The relative concentration of target gene mRNA was equal to $2^{-\Delta\Delta Ct}$ where $\Delta\Delta C_t = [(\text{Avg. gene of interest } C_t - \text{Avg. } \beta\text{-GUS } C_t)_{sample} - (\text{Avg. gene of interest } C_t - \text{Avg. } \beta\text{-GUS } C_t)_{calibrator}]$. The calibrator was calculated from the mean ΔC_t of mock-infected samples for each individual gene.

Interferon bioassay

The interferon bioassay was performed using VSV-GFP as previously described [416,424]. Briefly, EEC's were either infected with EAV or SeV alone or dual infected with both EAV/SeV at an m.o.i of 5 and incubated for 24 h at 37°C. Culture supernatants were collected and virus in the supernatants was inactivated by ultraviolet (UV)-irradiation for 30 min. Two-fold dilutions of supernatants were made in DMEM and used in IFN bioassays. MDBK cells were grown in 96-well plates to 70% confluency and incubated with two-fold dilutions of each of the supernatants. After 24 h incubation at 37°C, cells were infected with VSV-GFP at an m.o.i. of 0.1 and further incubated at the same temperature for 16 h. Cells were fixed with 4% paraformaldehyde and expression of green fluorescence protein was examined under an inverted fluorescence microscope.

Confocal microscopy

HEK293 T cells grown on coverslips were transfected with plasmids as indicated previously, washed with PBS and fixed with 4% paraformaldehyde in phosphate-buffered saline (PBS; pH7.4) for 30 min at RT. After washing three times with PBS (pH 7.4) containing 10mM glycine (glycine/PBS), cells were permeabilized with 0.2% Triton X-100 in PBS (pH 7.4) for 10 min. The coverslips were incubated with the appropriate primary monoclonal or polyclonal antibody in PBS containing 5% fetal bovine serum (FBS) for 1 h at RT. After three 10mM glycine/PBS washes, coverslips were incubated with FITC-conjugated or DyLight 549-conjugated goat anti-mouse or anti-rabbit antibody (Southern Biotech, Birmingham, AL and KPL, Gaithersburg, MD, respectively) for 1 h at RT. Coverslips were washed and mounted in 4', 6'-diamidino-2-phenylindole (DAPI) containing aqueous mounting medium (Vector Laboratories, Burlingame, CA) and observed under an inverted fluorescence microscope.

Cell transfection and luciferase reporter assay

HEK293T cells were seeded in 24-well plates and transfected with various combinations of plasmid DNA: the pEFneo-RIG-I, pEFneoMDA5, pEFneo-IKKε, pcDNA3-TRIF, or pCAGGS-IRF3 was mixed with a plasmid encoding the EAV protein

(or empty pCAGGS), luciferase reporter plasmid and SV40-RL. Transfection was performed using HD-FuGENE6 transfection reagent following the manufacturer's instruction (Promega, Madison, WI). For the Sendai virus or IFN stimulation, HEK293T cells were transfected with a plasmid encoding the EAV proteins (or empty pCAGGS, pCAGGS-NS1), reporter plasmids and pSV40- RL. At 20 h post-transfection, cells were infected with Sendai virus at 5000 HA unit/0.5 ml/ well for 12-16 h, or induced by treatment with 2000 IU/0.5 ml/ well of IFN-α or IFN-β for 16 h. Cells were harvested at the indicated time points. Cell lysates were prepared and subjected to reporter gene assay using the dual luciferase reporter system (Promega, Madison, WI) according to manufacturer's instruction. *Firefly* and *Renilla* luciferase activities were measured in a luminometer (Berthold Technologies, Oak Ridge, TN). Values for each sample were normalized using the *Renilla* luciferase values.

6.4. RESULTS

Suppression of type I interferon production by EAV

To investigate the effect of EAV on type I IFN production, IFN-β mRNA expression was analyzed using quantitative real time RT-PCR. Equine pulmonary endothelial cells (EECs) were mock-infected or infected with EAV VBS at an m.o.i of 5 for 8 h, followed by infection with SeV for 3 or 6 hpi. Sendai virus (SeV) was used as a positive control for type I IFN induction and mock-infected cells were used as a negative control. As shown in Figure 6.1.A, IFN-β mRNA was barely detected in cells infected with EAV alone, whereas SeV infection induced a strong expression, approximately 190-200 fold, of IFN-β mRNA in the same cells. Moreover, SeV-induced IFN-β mRNA expression, at both 3 and 6 hpi, was significantly suppressed in cells previously infected with EAV. In parallel with the quantitative measurement for IFN-β mRNA, suppression of IFN production by EAV was confirmed by IFN bioassay using VSV expressing the green fluorescence protein (VSV-GFP; Figure 6.1.B). VSV is IFN sensitive and presence of IFN-α/β blocks VSV replication. EECs were mock-infected, either infected with EAV or SeV alone, or dual infected with both EAV/SeV. Subsequently, MDBK cells were incubated with two-fold serial dilutions of virus inactivated cell culture supernatant fluid for 24 h followed by infection with VSV-GFP at an m.o.i. of 0.1 for 18 h. The VSV

infectivity was determined by monitoring the levels of GFP expression. As shown in Figure 6.1.B, VSV-GFP replicated normally in cell culture supernatant from mock-infected cells while VSV replication was effectively inhibited in supernatant from SeV-infected cells up to a dilution of 1:32. In contrast, VSV replication was not inhibited in cell culture supernatant from cells infected with EAV alone. Consistent with quantitative RT-PCR results, SeV-induced type I IFN production was significantly inhibited by EAV exposure since VSV-GFP replication was detected at a lower sample dilution compared to that of culture supernatant from SeV-infected cells. Together, the data suggest that EAV has an intrinsic ability to prevent induction of IFN in infected cells and suppress IFN production in SeV-infected cells.

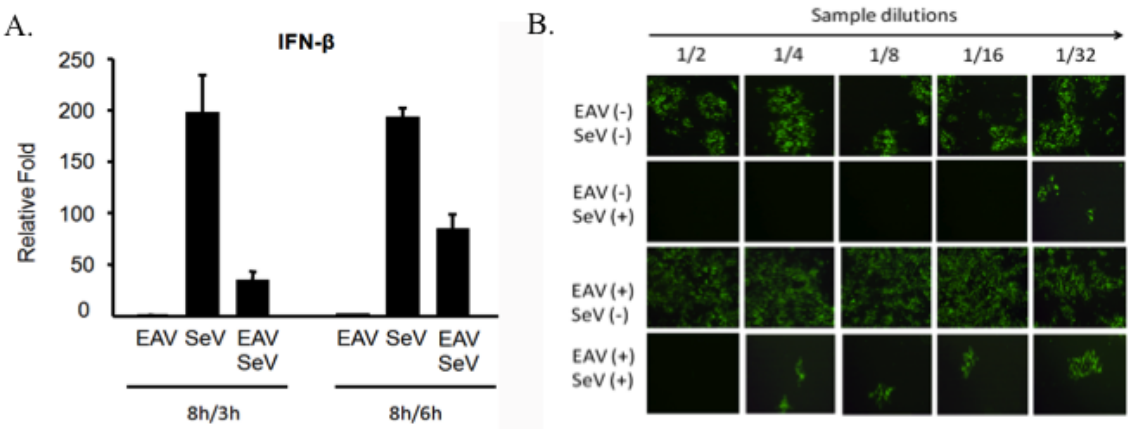

Figure 6.1. Inhibition of type I IFN production after EAV infection. A. EECs were mock-infected or infected with EAV VBS at an m.o.i. of 5 for 8 or 12 h. Subsequently, cells were infected with Sendai virus (SeV; 100 HAU/ml) for 3 h. Total RNA was isolated and real time RT-PCR was performed for the detection of equine IFN-β. The average IFN-β copy numbers ± standard error of the mean (SEM) from three independent experiments is shown. B. VSV bioassay for IFN production. EECs were mock-infected or infected with EAV VBS at an m.o.i. of 1 for 24 h. SeV was used as an IFN stimulator. Cell culture supernatants were collected and UV-irradiated for 30 min prior to use in the assay. MDBK cells were grown in 96-well plates and incubated with 2-fold dilution series of the supernant up to 1/32. After 24 h incubation, cells were infected with VSV-

GFP at an m.o.i. of 0.1, and 18 h after infection, GFP expression was assessed by fluorescence microscopy. Each dilution was tested in duplicate.

The EAV nsp1, nsp2 and nsp11 exhibited strong inhibition of IFN-β promoter activation

To investigate the role of EAV viral proteins as IFN antagonists, we focused on the nonstructural proteins of EAV. The 12 nonstructural proteins derived from an infectious cDNA clone of virulent Bucyrus strain of EAV were cloned individually into a pCAGGS mammalian expression vector. The expression and authenticity of recombinant proteins from the plasmids were verified by immunofluorescence and Western blot using protein-specific rabbit antisera (nsp1-4, nsp7-9 and nsp11) or anti-FLAG antibody (nsp5, nsp6, nsp10, and nsp12; data not shown). To determine the nsp(s) that has an effect on IFN-β activation, we used an IFN-β promoter-luciferase reporter plasmid (p125-Luc) that expresses the firefly luciferase under the control of the IFN-β promoter. HEK293T cells were co-transfected with individual nsp-expressing pCAGGS plasmid, p125-Luc, and a *Renilla* luciferase expression plasmid (pRL-SV40) to normalize expression levels of samples. As a positive control, swine influenza virus NS1 (sw-ns1) gene was used to co-transfect the cells with the reporter plasmid; this has been widely reported to inhibit IFN-β promoter induction. Twenty-four hours after transfection, cells were infected with SeV to induce luciferase production. As shown in Figure 6.2.A, the expression of sw-ns1 significantly inhibited luciferase expression. In contrast, a strong reporter signal was observed in cells transfected with empty pCAGGS plasmid after infection with SeV. IFN-β promoter activation by SeV infection was suppressed to various degrees by expression of several EAV nsps, among which nsp1, nsp2 and nsp11 showed the strongest inhibition of IFN-β promoter-driven luciferase expression. In particular, nsp1 exhibited the strongest inhibitory effect, followed by nsp11 and nsp2. These results suggested that several EAV nsps are capable of suppressing IFN-β promoter activation of which nsp1 had the strongest inhibitory effect, indicating that it may play a major role as a type I IFN antagonist. The nsps expression from plasmids was confirmed by IFA (Figure 6.2.B)

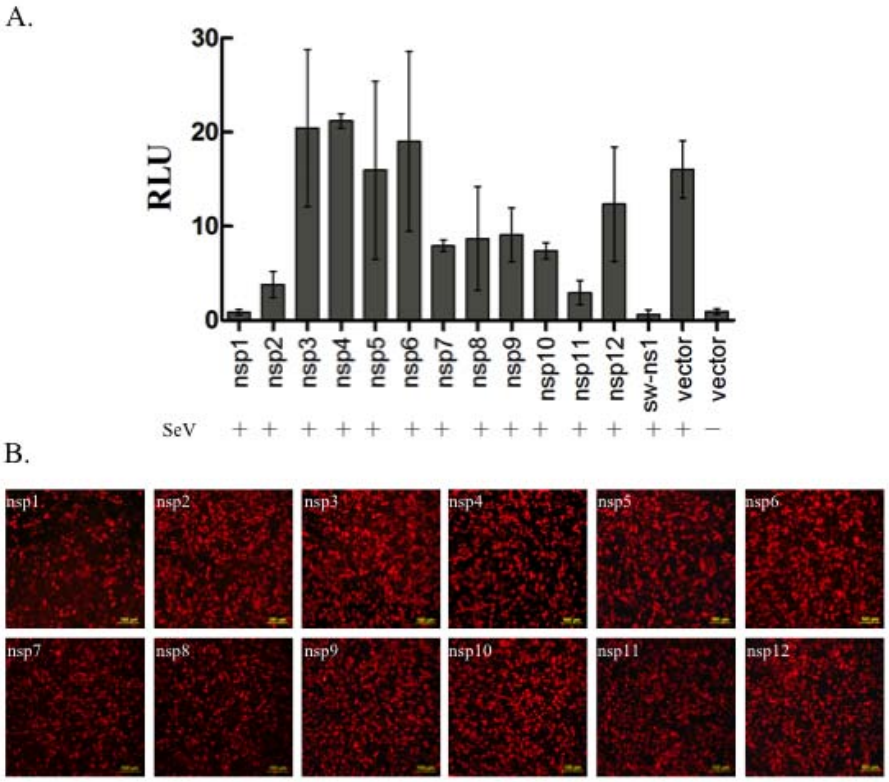

Figure 6.2. EAV nonstructural proteins (nsps) involved in suppression of IFN-promoter activation. A. HEK293T cells were co-transfected with p125-Luc, pRL-SV40 and pCAGGS expressing nsps or pCAGGS empty vector for 24 h. Cells were harvested and measured for firefly and *Renilla* luciferase activities. Relative luciferase activity is defined as a ratio of firefly luciferase reporter activity to *Renilla* luciferase activity. Each data point shown represents a mean value ± standard error of the mean (SEM) from three experiments. B. Expression of nsps in transfected cells detected by indirect immunofluorescence assay. HEK293T cells were transfected with each EAV nsp and fixed at 24 h post-transfection. Cells were stained with EAV protein-specific rabbit antisera or anti-FLAG monoclonal antibody. DyLight 549-conjugated goat anti-rabbit antibody was used as secondary antibody.

EAV nsp1 interferes with IRF3- and NF-κB-mediated IFN-β activation

Since the nsp1 of EAV showed the highest type IFN antagonistic activity, it was decided to further investigate its effect on the specific signaling pathway(s) using AP-1-,

NF-κB- and IRF-3-driven luciferase reporter systems. Cells were co-transfected with control plasmids or with plasmids expressing the EAV nsp1 protein, the plasmid pRL-SV40 and a plasmid containing a firefly luciferase gene under the control of a promoter (pAP-1-Luc) or containing two NF-κB binding sites (pNF-κB-Luc) or with three IRF3 binding sites (p55-CIB-Luc) (Figure 6.3). In cells expressing EAV nsp1 and sw-ns1 proteins (positive control), the level of IRF3-dependent luciferase expression upon SeV stimulation was significantly reduced compared to that of the control plasmid (empty pCAGGS vector). Similarly, NF-κB-dependent luciferase expression was blocked in cells expressing EAV nsp1. In contrast, EAV nsp1 did not affect the AP-1-dependent reporter gene expression after SeV stimulation, whereas sw-ns1 strongly inhibited luciferase expression under control of the promoter containing the AP-1 binding site. Based on these findings, it would appear that EAV nsp1 suppresses IFN-β transcription by interfering with IRF-3 and NF-κB activity but not AP-1 activity.

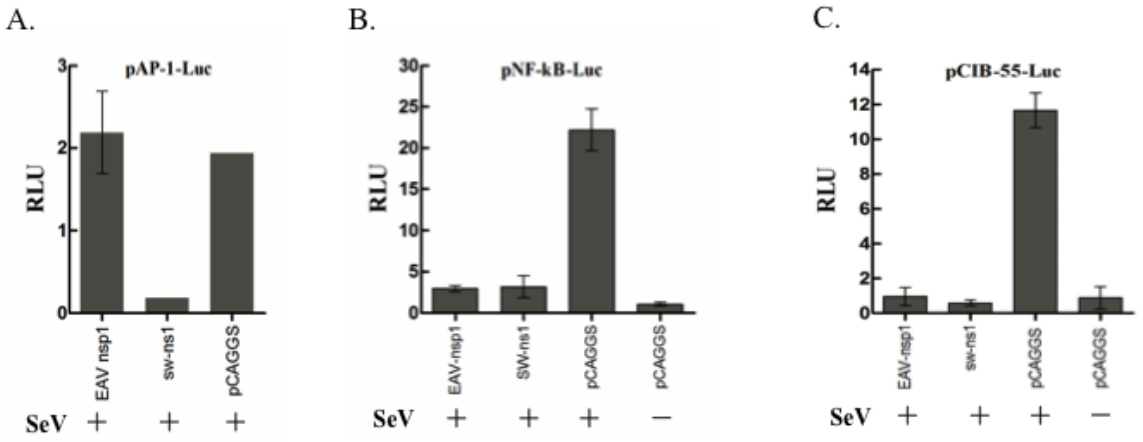

Figure 6.3. EAV nsp1 inhibits both IRF-3 and NF-κB pathways but not AP-1. HEK293T cells were co-transfected with (A) AP-1-Luc, (B) NF-κB-Luc and (C) p55-CIB-Luc, which contains three IRF-3 binding sites, a plasmid that constitutively expresses *Renilla* luciferase, and plasmids expressing EAV nsps or the indicated control plasmids. Cells were infected with Sendai virus (SeV) 24 hpi. Cells were harvested and analyzed for firefly and Renilla luciferase. Data were normalized using the *Renilla* luciferase values. Data are averages ± standard deviation for three experiments.

EAV nsp1 blocked expression of IRF3-dependent reporter genes

We further investigated specific steps that EAV nsp1 could possibly block the IRF-3 signaling pathway. The ability of IRF-3 to activate its DNA binding site was examined using a plasmid construct containing a firefly luciferase gene under the control of a promoter with three IRF-3 binding sites (pCIB-55-Luc). First, we investigated whether the nsp1 was interfering with the mitochondrial antiviral signaling (MAVS) complex activity. Since MDA5 or RIG-1 is associated with the MAVS complex, cells were co-transfected with a plasmid expressing MDA5, RIG-1 or MAVS protein, a plasmid expressing EAV nsp1, the plasmid pRL-SV40 and the p55-CIB-Luc reporter plasmid. As shown in Figure 6.4.A-C, IRF-3-dependent luciferase expression was suppressed in the presence of EAV nsp1. These results suggested that EAV nsp1 might inhibit the MAVS-mediated IFN-β induction or downstream portion of the signaling pathway. Therefore, we further tested the effect of EAV nsp1 on TRIF- and IKKε-mediated IFN-β induction and the results showed that nsp1 had the ability to suppress TBK1 and IKKε mediated reporter gene expression (Figure 6.4.D-E). Similarly, overexpression of IRF3 itself did not activate transcription of the reporter plasmid either (Figure 6.4.F) suggesting that nsp1 blocked the IRF-3. The data suggest that EAV nsp1 might block processes downstream of IRF-3 activation, possibly in the nucleus. Furthermore, we studied the activation of IRF-3 in EAV nsp1 transfected cells by Western blot analysis. Neither expression of EAV nsp1 nor control plasmid increased levels of phosphorylated IRF-3 (pIRF-3) in cells in the absence of SeV stimulus. In contrast, infection of SeV induced phosphorylation of IRF-3 (pIRF-3) to a similar level in cells transfected with EAV nsp1 and the control plasmid. Total levels of IRF-3 were unaltered by expression of nsp1 and the control plasmid or SeV infection (data not shown). Together with the luciferase assay data, these results suggest that the EAV nsp1 has the ability to block induction of IFN-β at a point downstream of activation of IRF-3, since nsp1 expression inhibits the activation of the IFN-β promoter but does not block the activation of IRF-3.

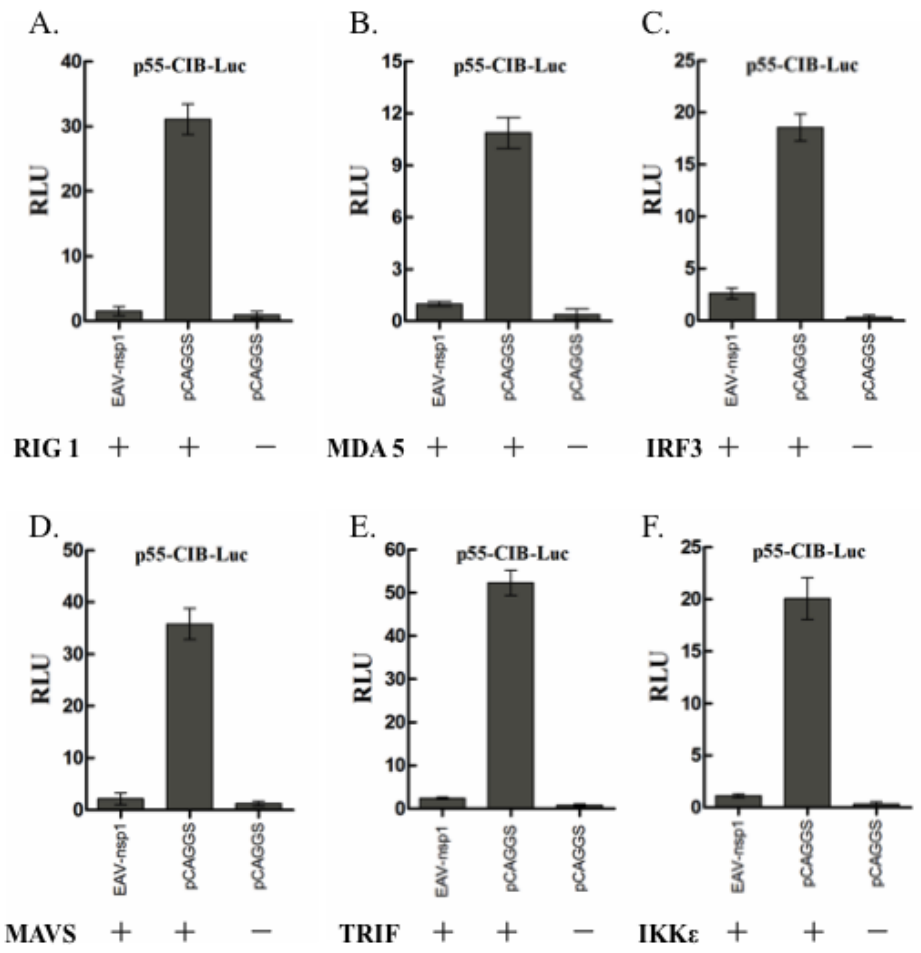

Figure 6.4. EAV nsp1 inhibits the IRF-3 signaling pathway. Suppression of (A) RIG-I (B) MDA-5 (C) IRF-3 (D) MAVS (E) TRIF and (F) IKKε induced IRF-3 dependent reporter gene expression by EAV nsp1 in HEK293T cells. (A-F) Cells cultured in 24-well plates were co-transfected with plasmid pEFneo-RIG-I, pEFneo-MDA-5, pEGFP-N1-MAVS, pcDNA3-TRIF, pEFneo-IKKε, or pCAGGS-IRF3 along with a plCAGGS expressing nsp1 protein or pCAGGS empty vector, pRL-SV40 and a luciferase reporter plasmid, p55-CIB-Luc for 24 h. Cells were harvested and measured for firefly and *Renilla* luciferase activities. Relative luciferase activity is defined as a ratio of firefly luciferase reporter activity to *Renilla* luciferase activity. Mean value ± SEM from three experiments is shown.

EAV nsp1 blocked expression of NF-κB-dependent reporter genes

Next, we investigated the ability of EAV nsp1 to inhibit NF-κB mediated transcription. In the presence of EAV nsp1, NF-κB-dependent reporter gene expression was strongly inhibited (Figure 6.5.A) following stimulation with TNF-α, a potent inducer of the NF-κB signaling,. Subsequently, the effect of EAV nsp1 on the MAVS complex, TRIF and IKKε mediated IFN-β induction was evaluated. Interestingly, overexpression of any of these proteins induced activation of NF-κB-dependent reporter gene expression (Figure 6.5.B-D). Similarly, overexpression of p65, a subunit of the NF-κB complex, itself had no effect on activation of transcription from the NF-κB-driven reporter plasmid (Figure 6.5.E). These data suggested that EAV nsp1 likely blocks processes downstream of the activation of NF-κB complex, possibly somewhere in the nucleus.

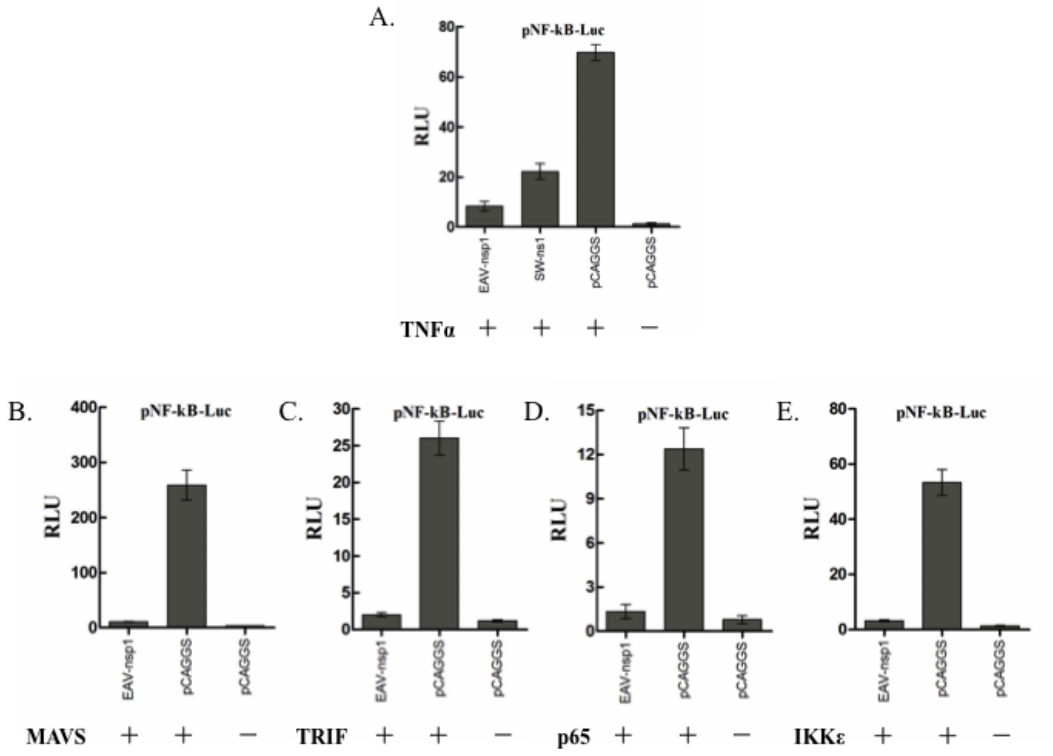

Figure 6.5. EAV nsp1 inhibits the NF-κB signaling pathway. Suppression of (A) TNF-α (B) MAVS (C) TRIF (D) p65 subunit of NF-κB and (E) IKKε induced NF-κB-dependent reporter gene expression by EAV nsp1 in HEK293T cells. (A) Cells cultured in 24-well plates were co-transfected with pNF-κB-Luc, pRL-SV40, and pCAGGS

expressing nsp1 or pCAGGS empty vector for 24 h and subsequently stimulated with TNF-α (20 ng/ml) for 6 h. (B-E) Cells were co-transfected with plasmid pEGFP-N1-MAVS, pcDNA3-TRIF, pEGFP-N1-p65 or pEFneo-IKKε along with a pCAGGS expressing nsp1 protein or pCAGGS empty vector, pRL-SV40 and a luciferase reporter plasmid, pNF-κB-Luc for 24 h. Cells were harvested and measured for firefly and *Renilla* luciferase activities. Relative luciferase activity is defined as a ratio of firefly luciferase reporter activity to *Renilla* luciferase activity. Mean value ± SEM from three experiments is shown.

EAV nsp1 expression blocked the nuclear accumulation of IRF-3 and NF-κB

The mechanism by which EAV nsp1 can reduce IRF-3 and NF-κB-dependent gene expression was examined by assessing the nuclear localization of IRF-3 and p65, respectively, in cells expressing EAV nsp1 by confocal microscopy (Figure 6.6). In mock-infected cells, IRF-3 was localized primarily to the cytoplasm. On the other hand, SeV infection stimulated IRF-3 nuclear translocation in a large number of cells. However, IRF-3 remained in the cytoplasm of cells expressing EAV nsp1 after SeV infection, while IRF-3 was occasionally observed in the nucleus of cells that did not express nsp1. Similarly, NF-κB remained in the cytoplasm of most of the unstimulated cells, whereas TNF-α stimulation induced p65 nuclear accumulation in most cells. In cells expressing EAV nsp1, TNF-α stimulation did not induce complete p65 nuclear translocation since p65 was found in both nucleus and cytoplasm, indicating that EAV nsp1 partially blocks p65 nuclear translocation. Taken together, it appears that IFN-β transcription activation is blocked through inhibition of both IRF-3 and NF-κB nuclear accumulation.

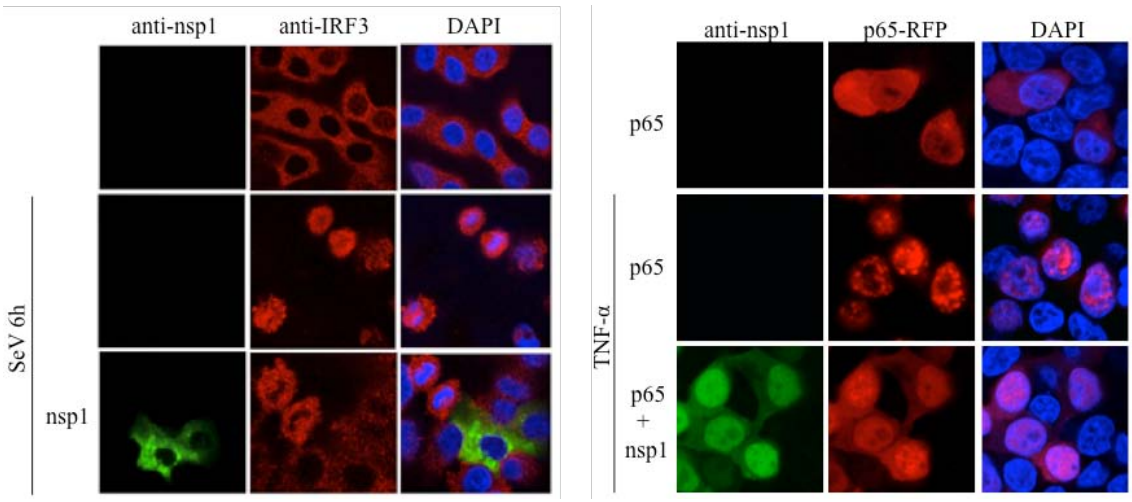

Figure 6.6. Effect of EAV nsp1 in IRF-3 and NF-κB nuclear translocation. (A) HEK293T cells were transfected with EAV nsp1 for 24 h and then infected with Sendai SeV for 6 h. Cells were fixed and stained with Alexa 488 conjugated-anti-EAV nsp1 (12A4) MAb and rabbit anti-IRF3 antibody. (B) HEK293T cells were co-transfected with EAV nsp1 and p65-RFP for 24 h and then stimulated with TNF- α (10 ng/ml) for 2 h. Cells were fixed and stained with anti-EAV nsp1 (12A4) MAb. FITC-conjugated goat anti-mouse was used as a secondary antibody. Cell nuclei were stained with DAPI.

6.5. DISCUSSION

Viruses use different mechanisms to inhibit interferon response in order to evade the host innate immune response. Synthesis and secretion of type I IFN, such as IFN-α and IFN-β with antiviral, anti-proliferative and immunomodulatory functions, are critical aspects of the antiviral immune response [410,425,426]. Thus, many viral proteins that antagonize multiple components of the interferon pathways have been identified. In addition, many viruses encode more than one protein capable of inhibiting the interferon response which act synergistically to ensure complete blocking of interferon activity. Highly pathogenic viruses, such as Ebola, Nipah and SARS-CoV, encode multiple viral proteins capable of inhibiting interferon activity, suggesting important roles for these proteins in pathogenesis and disease outcome [427]. In this study, we investigated whether EAV has the ability to interfere with the host's innate immune response, in

particular, type I IFN production. We showed that EAV infection of equine endothelial cells significantly inhibited type I IFN production at both mRNA and protein levels, whereas infection with SeV stimulated type I IFN production significantly. Furthermore, EAV infection significantly inhibited SeV-induced type I IFN production as well. Based on reporter-gene experiments, three EAV nonstructural proteins, nsp1, nsp2 and nsp11 strongly inhibited activation of the IFN-β promoter indicating that they modulate type I IFN activity. Among these proteins, expression of nsp1 had the strongest inhibitory effect on IFN-β-responsive promoter activation. Similar to our findings, previous studies on PRRSV also demonstrated that nsp1α, nsp1β, nsp2, nsp4 and nsp11 of PRRSV play a role in type I IFN antagonism and inhibit activation of IFN-β promoter [414,415]. The two N-terminal PRRSV replicase cleavage products, nsp1α and nsp1β have the ability to inhibit both IFN synthesis and signaling, while nsp1α strongly inhibits IFN synthesis only. Specifically, nsp1β strongly inhibited IRF-3 dependent gene induction in the signaling pathway leading to IFN-β synthesis. In addition to these nsps, the nuceocapsid protein of PRRSV also inhibits type I IFN production [83,424].

Further examination revealed that EAV nsp1 inhibited two key transcription factors that activate the IFN-β promoter, IRF-3 and NF-κB, but not AP-1. EAV nsp1 expression strongly inhibited IRF-3- and NF-κB-dependent gene induction in the signaling pathway that leads to IFN-β synthesis. Both IRF-3 and NF-κB activation are regulated by MAVS which functions downstream of RIG-I and MDA5 and upstream of the IKK complex and TBK1/IFF-I [428,429,430,431]. Among the various factors involved in type I IFN production, IRF-3 plays a critical role. IRF-3 is expressed in most cell types and resides in the cytoplasm in an inactive form. When stimulated, IRF-3 becomes phosphorylated and undergoes conformational changes, leading to dimerization with the exposed nuclear localization signal. In the nucleus, IRF-3 recruits co-activator CBP/p300 and forms a complex to bind IRF-3 responsive elements (PRD I/III) of the IFN-β promoter [410]. In addition to IRF-3, NF-κB is also a critical regulator of host innate and adaptive immunity. It plays an important role in the regulation of cell proliferation as well as cell survival. Through evolution, viruses can either activate or inhibit the NF-κB pathway in order to survive in host cells. Viruses such as African swine fever virus and influenza A virus block NF-κB activation to counter the host innate

immune response [432,433]. In contrast, viruses such as hepatitis C virus, reovirus and herpes simplex virus have developed mechanisms to directly activate NF-κB to support production of progeny viruses and intracellular spreading [434,435,436]. Overexpression of components of the pathway by which IRF-3 and NF-κB are activated in response to SeV infection and TNF-α, respectively, showed that EAV nsp1 acts downstream of all tested steps in both signaling pathways. Therefore, we postulated that EAV nsp1 may have an effect on nuclear accumulation of these transcription factors or formation of the transcription enhanceosome on the IFN-β promoter inside the nucleus. Our results showed that nsp1 inhibits nuclear accumulation of both IRF-3 and NF-κB. Furthermore, both IRF-3- and NF-κB-dependent gene expressions were blocked by EAV nsp1. Interestingly, IRF-3 and p65 activation by SeV and TNF-α, respectively, were not affected, but their nuclear accumulation was inhibited. However, the exact mechanism that EAV nsp1 uses to inhibit IRF-3 and NF-κB nuclear accumulation is unclear at this time. It is possible that EAV nsp1 mediates the sequestration of these activated proteins in the cytoplasm and affects enhanceosome assembly in the cell nucleus. Recent studies have shown that PRRSV nsp1 modulates type I IFN response by blocking dsRNA–induced IRF-3 and IFN promoter activities, but IRF-3 phosphorylation and its nuclear translocation occur normally in the presence of the nsp1. It has been reported that PRRSV nsp1 blocks the IRF-3 activation by degrading the CREB (cyclic AMP response element binding)-binding protein (CBP) and subsequently inhibiting formation of enhanceosomes in the nucleus [416].

In summary, EAV proteins with interferon antagonistic activity have been identified for first time in this study. Our data indicated that several EAV replicase proteins including nsp1, nsp2 and nsp11 have IFN antagonistic activity and regulate the host innate immune response. Among these proteins, nsp1 may play a key role as interferon antagonist by inhibiting nuclear accumulation of activated IRF-3 and NF-κB. However, further studies are needed to map the exact step(s) at which EAV nsp1 protein acts on the IFN induction pathway.

Copyright © Yun Young Go 2011

CHAPTER SEVEN

A newly discovered ORF5a protein is critical for virus production in equine arteritis virus

This work was included in Firth *et al.* J. Gen. Virol. 2011, 92: 1097-1106

Reprinted with permission

7.1. INTRODUCTION

The members of the family *Arteriviridae* (order *Nidovirales*) include equine arteritis virus (EAV), lactate dehydrogenase elevating virus (LDV) of mice, porcine respiratory and reproductive syndrome virus (PRRSV) and simian hemorrhagic fever virus (SHFV). The arterivirus genome consists of a positive-sense, single-stranded RNA molecule. The genome organization and expression strategy of arteriviruses share similarities with those of coronaviruses and it is presumed that their key replicative enzymes have a common ancestry [7,8,9]. Therefore, arteriviruses and coronaviruses were united in the order *Nidovirales*, which was recently expanded by addition of roniviruses, toroviruses and bafiniviruses [8]. The arterivirus genome consists of at least nine known open reading frames (ORFs). The 5'-proximal ORFs 1a and 1b encode the non-structural polyproteins, pp1a and pp1ab precursors, that are processed into at least 13 mature non-structural proteins [66,83]. The 3'-proximal end of the genome contains overlapping ORFs 2 to 7 that are expressed via synthesis of a set of subgenomic mRNAs [89,91]. These ORFs encode seven structural proteins: the nucleocapsid (N) protein and six envelope proteins, the glycoproteins (GP) GP2, GP3, GP4 and GP5, and the non-glycosylated envelope (E) and membrane (M) proteins [34,93]. The genome organization of the EAV ORFs2-7 region is extremely compact, where the termini of the ORFs are overlapping with neighboring genes and with transcription-regulatory sequences (TRS) located upstream of each ORF for sg mRNA synthesis [89,91]. The compact EAV genome organization is a result of the strong selective pressure that RNA virus genomes are under to encode the maximum amount of information into a limited sequence space. Therefore, overlapping coding sequences can be easily found in RNA

viruses, although they can be difficult to detect when they are short. A recent in-depth comparative computational analysis revealed conservation of an additional AUG-initiated ORF in the arteriviruses, termed ORF5a, which overlaps the 5' end of ORF5 [81]. The newly identified ORF5a protein, conserved in all arteriviruses, was first detected in a comparative alignment of PRRSV-NA sequences. A similar ORF5a was found in PRRSV-EU as well as in LDV, SHFV and EAV. The new coding sequence has 51 or 46 codons in PRRSV-NA, 43 codons in PRRSV-EU, 47 codons in LDV, 64 codons in SHFV and 59 codons in EAV. The pattern of substitutions across sequence alignments indicated that ORF5a is subject to functional constraints at the amino acid level, while an analysis of substitutions at synonymous sites in ORF5 revealed a greatly reduced frequency of substitutions in the portion of ORF5 that is overlapped by ORF5a. The ORF5a protein and GP5 are likely expressed from the same subgenomic mRNA, via a translation initiation mechanism involving leaky scanning. The objective of this study was to confirm the biological relevance of ORF5a in the EAV life cycle using the EAV reverse genetics systems. The effect of ORF5a knockout mutant was independently confirmed using two molecular clones, the pEAV515 and pEAVrVBS of the virulent Bucyrus strain (VBS) of EAV. In addition to BHK-21 cells, natural host cells, equine pulmonary artery endothelial cells (EECs), were included in the study.

7.2. MATERIALS AND METHODS

Cells

Equine pulmonary artery endothelial cells (EECs) [343] were maintained in Dulbecco's modified essential medium (DMEM, Mediatech, Herndon, VA) with sodium pyruvate, 10% fetal bovine serum (Hyclone Laboratories, Inc., Logan, UT), 100U/μg per ml of penicillin/streptomycin and 200mM L-glutamine [154,213,328]. The baby hamster kidney cells (BHK-21; ATCC CCL10; American Type Culture Collection, Manassas, VA) were grown in Eagle's minimum essential medium with 10% ferritin supplemented bovine calf serum (Hyclone Laboratories, Inc., Logan, UT) and 100U/ μg per ml of penicillin/streptomycin (Gibco, Carlsbad, CA).

Infectious cDNA clones

The ORFX2b mutant viruses were constructed by introducing site-specific mutations into two EAV infectious cDNA clones. Specifically, the pEAV515 clone was derived from a cell culture adapted attenuated strain of EAV (pEAV030; [64]) and the pEAVrVBS clone was derived from the EAV VBS [328].

Generation of EAV515/ORFX2b and rVBS/ORFX2b mutant viruses

Briefly, a shuttle vector (pM92128[rVBS]ORFX2b) containing a *BamH*I (9,150)-*Xho*I (12,726) fragment of the pEAVrVBS infectious cDNA clone was used to mutate the putative ORFX2b [328]. Site-specific nucleotide substitutions were introduced into the start (UAU > UAC) and stop (UGG >UAG) codons of the ORFX2b in the pM92128[rVBS]ORFX2b shuttle vector using a standard site-directed mutagenesis protocol described by Landt *et al.* [437]. The engineered mutations in the pM92128[rVBS]ORFX2b shuttle vector were confirmed by sequence analysis and subsequently, the *BamH*I-*Xho*I fragment was transferred back into the full-length pEAVrVBS infectious cDNA clone using *BamH*I and *Xho*I restriction sites and confirmed by sequencing.

Run-off RNA transcripts were generated *in vitro* as previously described from each mutant infectious cDNA clones (pEAV515/ORFX2b and prVBS/ORFX2b), as well as their respective parental infectious cDNA clones (pEAV515 and prVBS) following linearization with restriction enzyme *Xho*I [64,327]. Briefly, 3 µg of each plasmid DNA were digested with *Xho*I and purified by standard phenol-chloroform extraction and ethanol precipitation procedures, and dissolved in nuclease-free water. The *in vitro* transcription reactions were performed in 50 µl reactions by adding 2 µg of each *Xho*I-linearized plasmid DNA, rNTP (10mM each), 1mg/ml BSA, 100mM DTT, 5X T7 transcription buffer, 10mM cap analog (New England Biolabs, Ipswich, MA), RNAguard RNase inhibitor and T7 polymerase (Promega, Madison, WI). The transcription reactions were incubated at 37°C for 3 h. The *in vitro* transcribed RNA was stored at -80°C until further use. Each of the full-length capped RNA transcripts were transfected into either BHK-21 cells or EECs by electroporation as previously described [327]. Briefly, subconfluent monolayers of BHK-21 and EEC cells were trypsinized, washed, and

resuspended in ice-cold phosphate-buffered saline (PBS; pH 7.4) at a concentration of 1×10^7 cells. Freshly thawed 50 µl (80 µg) aliquots of each IVT RNA were placed into cuvettes (0.4 cm, electrode gap; BioRad, Hercules, CA) and 600 µl of 5×10^6 of BHK-21 or 1×10^7 of EEC cells were added. Two pulses of 850 V, infinite ohms (pulse controller), and 25-mF capacitance were given with a Gene Pulser II electroporator unit (BioRad, Hercules, CA). After electroporation was complete, cells were set aside at room temperature for a 10 minute "recovery period". Subsequently, the BHK-21 and EEC cells were resuspended in 10 ml of appropriate complete cell culture medium and seeded into T-25cm^2 tissue culture flasks (Corning, Corning, NY), and incubated at 37°C in a 5% CO_2 incubator for 48-120 h until 90-100% cytopathic effect (CPE) was observed. Cell culture supernatant was harvested at 18, 24, 48, 72, 96 and 120 h post-transfection and centrifuged at 1,600 ×*g* for 10 min at 4°C. The supernatant was stored at –80°C in single-use aliquots.

Virus titrations and plaque morphology

Virus titers and the plaque morphology of the recombinant viruses were determined by plaque assays. Briefly, confluent monolayers of EECs and BHK-21 cells in 6-well culture plates were infected with 10-fold serial dilutions of recombinant EAV515, EAV515/ORFX2b, rVBS and rVBS/ORFX2b viruses in duplicates. Following a 1 h incubation, 0.75% CMC (caboxymethyl cellulose)-DMEM was added to each well and cells were incubated at 37°C for 96 h (McCollum, 1962). Plaques were stained with 1% crystal violet solution containing 1% formaldehyde at 96 h post-infection and titers were expressed as PFU/ml.

7.3. RESULTS

Using reverse genetics systems, mutants from two molecular clones, pEAV515 and pEAVrVBS, were generated with ORF5a-inactivating nucleotide substitutions. The pEAV515 is a derivative of pEAV030 which was based on an EAV isolate that was extensively adapted to cell culture (over 300 passages) [64]. Recombinant EAV derived from this clone causes very mild clinical signs upon experimental infection of horses [327]. In contrast, pEAVrVBS derived from EAV VBS, can cause severe disease in

horses [328]. In both mutants, the ORF5a translation initiation codon (AUG to ACG: U-11113→C) was mutated and a premature termination codon was introduced at the 6th codon of ORF5a (G-11128→A) (Figure 7.1). The introduced mutations were carefully designed to be translationally silent with the overlapping GP4 coding sequence.

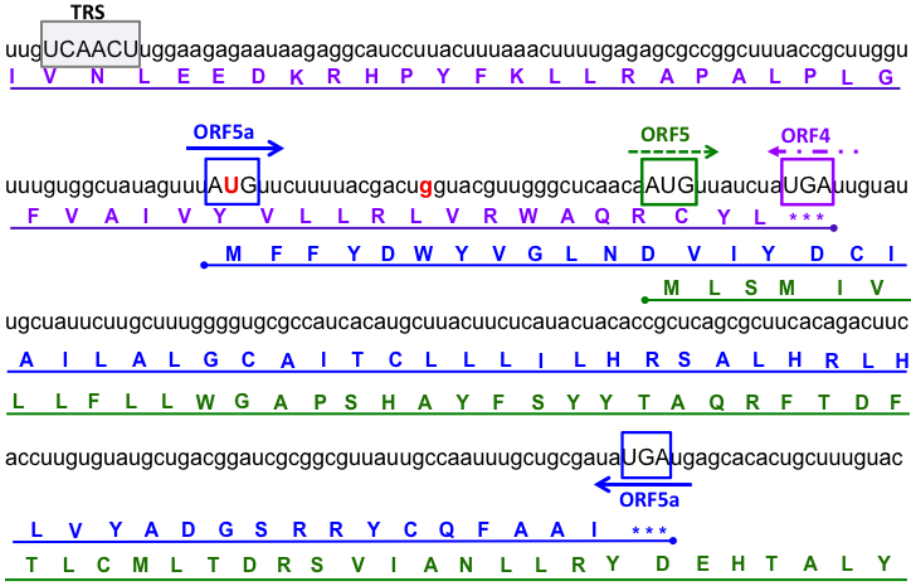

Figure 7.1. Schematic representation of ORF5a expression in EAV. Translated ORF5a (blue) is overlapping with both ORFs encoding GP4 (purple) and GP5 (green). The start and stop codons of relevant ORFs are boxed. The "U" and "g" nucleotides represent the mutations introduced to knockout ORF5a in the mutant Δ5a-2 viruses. The TRS (grey box) for sg RNA5 synthesis is located far upstream and includes the ORF5a start codon and thus, the ORF5a is possibly expressed from the same sg mRNA as GP5 by leaky ribosomal scanning. Modified from Firth *et al.* [81]

In vitro-transcribed full-length RNAs were electroporated into both BHK-21 and equine pulmonary artery endothelial cells (EECs). Immunofluorescence staining with monoclonal antibody to nsp1 protein was performed to verify transfection efficiency at the early phase of virus replication (data not shown). Virus titers in the medium of transfected cells were determined by plaque assay (Figure 7.2). ORF5a knockout mutants showed a reduction in virus titer of at least two logs and a tiny plaque size indicating the

progeny viruses of ORF5a knockout mutants had severely crippled phenotypes compared to the wild-type virus. Therefore, this comparative study confirmed that the expression of ORF5a is critical for efficient EAV amplification irrespective of virus strain where the molecular clones are derived and cell lines used for analysis.

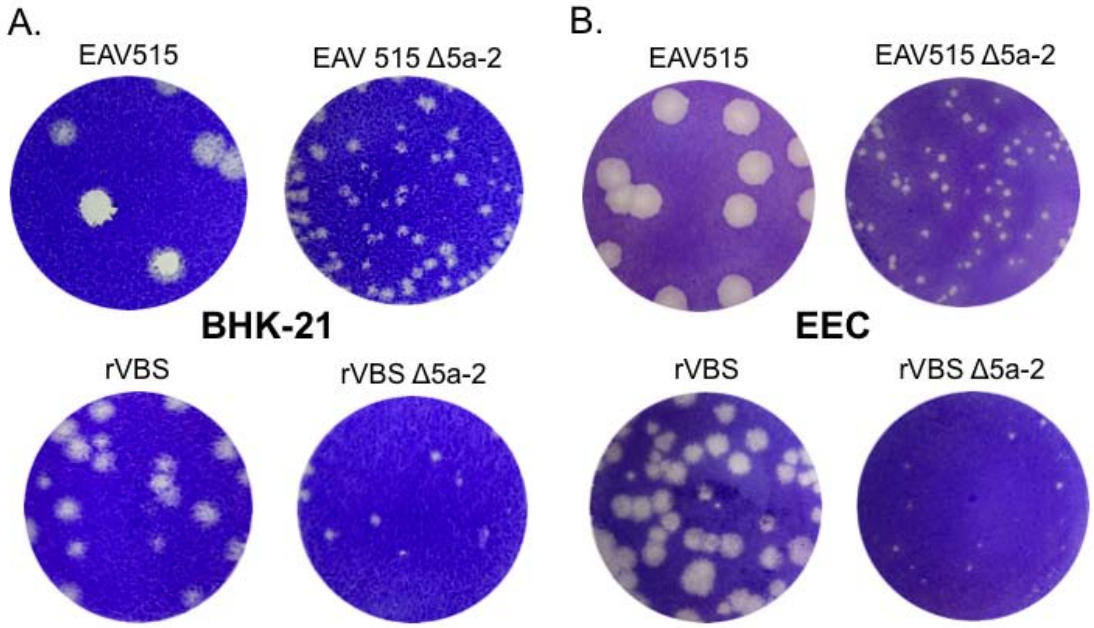

Figure 7.2. Comparison of plaque morphology of wild-type EAV and ORF5a knockout mutants. (A) Plaque morpohology on BHK-21 cells and (B) on equine endothelial (EEC) cells. In both molecular clones, Δ5a-2 plaque sizes and titers are severely reduced compared to those of the corresponding parental virus. Modified from Firth *et al.* [81]

7.4. DISCUSSION

In this study, we described evidence for the presence, conservation and biological significance of a novel short coding sequence in the 3'-proximal end of all arterivirus genomes. The ORF5a and the overlapping GP5 gene are likely to be expressed from a bicistronic sg mRNA. The mutational inactivation of ORF5a in EAV has shown that ORF5a mutant has severely impaired replication indicating that its expression is important for virus life cycle. To independently confirm the effect of the ORF5a knock out, we used two molecular clones derived from EAV strains with different virulence.

EAV strains can differ significantly in the severity of the disease they induce [15,328]. The EAV515 was based on an EAV isolate that was extensively passaged in cell culture while the pEAVrVBS was based on EAV isolate, VBS, that causes severe disease in horses. Regardless of the virus backbones used to inactivate ORF5a expression, the Δ5a-2 mutants had a severely crippled phenotype with tiny plaque sizes and lower virus titers. In addition to BHK-21 cells, EECs of equine origin were also used to evaluate the replication of the mutant viruses in a more natural host cell. In conclusion, these assays have independently confirmed that the expression of ORF5a is required for efficient EAV amplification, regardless of the background of the molecular clone and cell type used for analysis.

Discovery of the new ORF5a protein drives arterivirus researchers to question whether any previous attempts to engineer EAV-based vectors could have been affected, inadvertently, by the presence of ORF5a. For example, in a construct created by de Vries *et al.* [325] the overlap between ORF4 and ORF5 was removed and 24 nt were inserted to create an insertion site for foreign sequences. Fortunately, the insertion site is in-frame with ORF5a and the change appears to be tolerated. Similarly, spontaneous insertion of 12 nt into ORF5a of PRRSV-NA after passaging in cell culture 70 times seems to be tolerated [438]. In contrast, attempts to insert any other foreign sequences encoding GFP [439] or ectodomain of GP5 protein of other arteriviruses [147] into EAV-based vectors failed, possibly due to the disruption of ORF5a. Therefore, the reason for crippled or non-viable phenotypes of some of previously reported constructs could be, at least partially, attributed to the disruption of ORF5a protein expression. Thus, it would be important to engineer any arterivirus-based vector with care not to disrupt the expression of functional ORF5a protein.

Unfortunately, the function of the ORF5a protein could not been determined in this study. Several attempts to raise polyclonal antisera against the ORF5a using synthetic peptides containing the non-hydrophobic domain of this protein were unsuccessful. Therefore, it was not possible either to confirm the presence of the ORF5a protein in virus particles or to perform a subcellular localization study in the infected cells. However, in a parallel but independent study performed by Johnson *et al.* [440], the expression of the novel protein in cells infected with PRRSV was confirmed using

proteomic analysis. This paper also described the production of antibodies recognizing the PRRSV ORF5a protein in infected pigs [440]. Therefore, both PRRSV-NA and EAV studies together strongly suggest that the ORF5a protein is the eighth structural protein of the arteriviruses, although further studies are needed to obtain more detailed information into its yet unknown function.

CHAPTER EIGHT

Development of a fluorescent-microsphere immunoassay for detection of antibodies specific to equine arteritis virus and comparison with the virus neutralization test

Clin Vaccine Immunol. 2008, 15(1): 76-87

Reprinted with permission.

8.1. SUMMARY

The development and validation of a microsphere immunoassay (MIA) to detect equine antibodies to the major structural proteins of equine arteritis virus (EAV) is described. This was based on cloning and expression of full-length individual major structural proteins ($GP5_{1-255}$; M_{1-162}; and N_{1-110}) as well as the partial sequence of each structural protein ($GP5_{1-116}$; $GP5_{75-112}$; $GP5_{55-98}$; M_{88-162}; and N_{1-69}) that comprise putative antigenic regions of these proteins. Purified recombinant viral proteins expressed in *E. coli* were covalently bound to fluorescent polystyrene microspheres and analyzed with the Luminex xMap 100 instrument. Of the eight recombinant proteins, the highest concordance with the virus neutralization test (VNT) results was obtained with the partial $GP5_{55-98}$ protein. The latter assay was validated by testing a total of 2,500 equine serum samples previously characterized in the VNT. With use of an optimal cutoff value of 992 mean fluorescence intensity (MFI), the sensitivity and specificity of the assay were 92.6% and 92.9%, respectively. The $GP5_{55-98}$ MIA and VNT test outcomes correlated significantly (r = 0.84; p-value<0.0001). Although the $GP5_{55-98}$ MIA is less sensitive than the standard VNT, it has the potential to provide a rapid, convenient, and more economical test for screening equine sera for the presence of antibodies to EAV, with the VNT then being used as a confirmatory assay.

8.2. INTRODUCTION

Equine arteritis virus (EAV) is the causative agent of equine viral arteritis (EVA), a respiratory and reproductive disease of horses [77]. EAV is a small enveloped virus with a positive-sense, single-stranded RNA genome of 12.7 kb and belongs to the family *Arteriviridae* (genus *Arterivirus*, order *Nidovirales*), which also includes porcine reproductive and respiratory syndrome virus, simian hemorrhagic fever virus, and lactate dehydrogenase-elevating virus of mice [7,34]. The EAV genome includes nine functional open reading frames [34,56]. Open reading frames (ORF) 1a and 1b encode two replicase polyproteins (pp1a and pp1ab) [34,56,100], and the remaining seven ORFs (2a, 2b and 3-7) encode structural proteins of the virus. These include four membrane glycoproteins GP2 (25 kDa), GP3 (36-42 kDa), GP4 (28 kDa) and GP5 (30-44 kDa), respectively encoded by ORFs 2b, 3, 4, and 5, two unglycosylated membrane proteins E (8 kDa) and M (17 kDa) encoded by ORFs 2a and 6, and the phosphorylated nucleocapsid protein N (14 kDa) encoded by ORF7 [57,58,137]. The major envelope glycoprotein GP5 expresses the known neutralization determinants of EAV. The two major envelope proteins, GP5 and M, form a disulfide-linked heterodimer in the virus particle, and this association is critical for their maturation and for the expression of some of the neutralization epitopes in authentic form [67,68,73].

Serological and clinical studies indicate that EAV is widely distributed in equine populations around the world [173,175,176]. Although there is considerable variation in the sequence of the GP5 protein of field strains of the virus, there is only one known serotype of EAV, and all strains evaluated thus far are neutralized by polyclonal antiserum raised against the prototype Bucyrus strain of EAV [69,70,71,72,74,75,76,158]. Both natural and experimental infections of horses with either virulent or avirulent strains of EAV result in long-lasting immunity against all strains of the virus [264,265,266]. Equine arteritis virus infection in horses induces antibodies against the three major viral structural proteins, GP5, M, and N [76,221,268]. Virus neutralizing (VN) antibodies are detectable between 1 to 2 weeks after primary infection, and their appearance usually coincides with the onset of clearance of virus from the circulation [240,441]. However, virus does persist in the male reproductive tract of certain stallions for long periods of

time despite the presence of high titers of virus-specific neutralizing antibodies in their serum.

Serologic diagnosis of acute EAV infection of horses is based on demonstration of seroconversion or a $\geq$ 4 -fold increase in neutralizing antibody titer to the virus in paired (acute and convalescent) serum samples using the virus neutralization test (VNT). The VNT is the principal serological assay used to detect evidence of EAV infection by most laboratories around the world, and it continues to be the current World Organisation for Animal Health (OIE) prescribed standard test for EVA [77,292,442,443,444]. The assay is used for diagnostic, epidemiological surveillance, international trade, and vaccination monitoring purposes. The number of equine sera tested annually by a diagnostic laboratory can vary considerably, from several hundred to thousands of samples per year [443,444,445]. Although the VNT is currently the most highly sensitive and specific serodiagnostic test for this infection, it is expensive, labor-intensive, and time-consuming to perform. In addition, results tend to vary among laboratories, when adequate attention is not paid to standardization of both test reagents and procedure. Moreover, serum cytotoxicity caused by anti-cellular antibodies directed against rabbit kidney-13 (RK-13) cells can be mistaken for viral cytopathic effect and can give rise to difficulties in test interpretation at lower serum dilutions. To overcome these disadvantages, several laboratories have developed and evaluated enzyme-linked immunosorbent assays (ELISAs) to detect antibodies to EAV using whole virus, synthetic peptides, or recombinant viral proteins (e.g., GP5, M, and N) as antigens [70,75,254,274,275,304,305,306,446]. The various studies have shown that the source of antigen as well as the sera evaluated can markedly influence the results obtained with EAV protein specific ELISAs and competitive ELISA [76,80]. None of these ELISAs has yet been shown to be of equivalent sensitivity and specificity to the VNT.

Recent developments in particle array technology have made it possible to perform immunoassays using microspheres (microbeads). The best-established microsphere assay system is the Luminex xMap system (Luminex Corp., Austin, TX), which incorporates three well-developed technologies: bioassays, solution phase microspheres, and flow cytometry. The microsphere assay technology developed by Luminex is ideally suited to a wide range of applications in drug discovery and diagnostics, as well as basic research.

Immunoassays based on this particle array technology can overcome the problems associated with the traditional VNT and ELISAs. Some of the distinct advantages of microsphere immunoassay (MIA) over traditional ELISAs include accuracy; high sensitivity, specificity, and reproducibility; high-throughput sample analysis; and multiplexing capability. MIAs are becoming increasingly popular for the serologic diagnosis of autoimmune and infectious diseases of humans and animals [447,448,449,450,451]. The primary objective of the present study was to develop a reliable immunological assay to detect antibodies to EAV in horses, using Luminex xMap technology, and to compare its performance with that of the VNT. The MIA could be suitable to detect antibodies to EAV in equine sera and the specificity and sensitivity of this assay should be equivalent to that of the standard VNT.

8.3. MATERIALS AND METHODS

Cells

High-passage (P399 to P409) rabbit kidney-13 (RK-13) cells were propagated and maintained in Eagle's minimum essential medium (EMEM; Mediatech, Herndon, VA) supplemented with 10% fetal calf serum (FCS; Hyclone, Logan, UT), 100U/ml penicillin, 100μg/ml streptomycin, 1μg/ml amphotericin B and 0.06% sodium bicarbonate at 37°C [452].

Equine sera

A total of 2,500 diagnostic equine serum samples were evaluated for the presence of anti-EAV antibodies by the MIA and VNT. The sera used in the study were selected randomly from those submitted for serological testing to the OIE EVA Reference Laboratory, Gluck Equine Research Center (n = 1,500) and the Livestock Disease Diagnostic Center (n = 1,000), University of Kentucky, Lexington, Kentucky. Panels of EAV antibody-positive and antibody-negative sera from the Gluck Equine Research Center were selected and used to establish normal MIA ranges for negative and positive samples. In addition to these sera, archived sequential serum samples collected from 18 experimentally infected horses were evaluated with respect to the EAV specific antibody response by both VNT and MIA. The horses were divided into four groups and each

group was inoculated with a different strain of EAV (rVBS: n = 4; 030H: n = 2; KY84: n = 7; and CA95G: n = 5) [154,224,327,453]. Blood samples were collected at 0, 2, 4, 6, 8, 10, 12, 14, 21, 28, 35, and at 42 days post infection (dpi) for the EAV rVBS-inoculated horses; at 0, 2, 4, 6, 8, 10, 12, 14, and 21 dpi for the EAV 030H-inoculated horses; at 0, 2, 4, 6, 8, 10, 12, 14, 21, and 28 dpi for the EAV KY84-inoculated horses, and at 0, 2, 4, 7, 9, 14, 21, 28, and 35 dpi for the EAV CA95G-inoculated horses. Sera were aliquoted and stored at -20°C.

PCR amplification, cloning, and sequencing of full-length and truncated versions of ORFs 5, 6, and 7 of EAV

The oligonucleotide primers for amplification of the coding sequences of the GP5, M, and N proteins (ORFs 5, 6, and 7, respectively) as well as the corresponding partial-length proteins were designed according to the published sequence of the EAV VBS (GenBank accession number: DQ846750) [453]. The nucleotides 5'-CACC-3' were added at the 5' end of each primer for directional cloning into the pET TOPO® vector (Invitrogen, Carlsbad, CA; Table 8.1). The full-length ORFs 5, 6, and 7 (that respectively encode full-length GP5, M, and N proteins), as well as the coding region for the amino-terminal ectodomain (aa 1-116) and two antigenic regions (aa 55-98 and aa 75-112) of the GP5 protein [70,274,446], the antigenic carboxyl terminal (aa 88-162) of the M protein [280], and the antigenic amino terminal (aa 1-69) region of the N protein [275], were PCR-amplified from the plasmid containing the complete genomic sequence of the EAV VBS strain (pEAVrVBS; GenBank accession number DQ846751) [453] using *Pfu* DNA polymerase enzyme (La Jolla, Stratagene, CA). PCR amplification was performed according to the manufacturer's instructions. The individual PCR products were concentrated using a Centricon (Ultracel YM-30; Millipore, Billerica, MA) and purified using a commercial kit (Qiagen, Valencia, CA). The individually amplified cDNA fragments encoding EAV ORFs 5, 6, 7 and their respective truncated forms were then directly cloned into the pET100 Directional TOPO® vector according to the manufacturer's instructions (Champion™ pET100/D-TOPO® Expression kit; Invitrogen, Carlsbad, CA). The pET100/D-TOPO allows expression of a

Table 8.1. Primer pairs used for PCR amplification of full-length and partial-length segments of ORFs 5, 6, and 7.

ORF	Protein	Sense	Sequence[a]	Nucleotide position	Size (bp)	Recombinant plasmid
5	$GP5_{1-255}$	+	5'-CACCATGTTATCTATGATTGTATTG-3'	11146-11166	772	pET-$GP5_{1-255}$
		-	5'-CTATGGCTCCCATACCTCAG-3'	11913-11894		
	$GP5_{1-116}$	+	5'-CACCATGTTATCTATGATTGTATTG-3'	11146-11166	355	pET-$GP5_{1-116}$
		-	5'-CTAGAATTCACGGCCATAGTAA-3'	11493-11475		
	$GP5_{55-98}$	+	5'-CACCTACAATTGTTCCGCCAGTAAAAC-3'	11308-11330	139	pET-$GP5_{55-98}$
		-	5'-CTACGGTCCATGCGCCTGTTCC-3'	11439-11421		
	$GP5_{75-112}$	+	5'-CACCACGTTTGGAACCGATTG-3'	11368-11384	121	pET-$GP5_{75-112}$
		-	5'-CTAATAGTAAATAAAAGGGGGCATGTC-3'	11481-11458		
6	M_{1-162}	+	5'-CACCATGGGAGCCATAGATTC-3'	11901-11917	493	pET-M_{1-162}
		-	5'-TCATTGTAGCTTGTAGGCTGTCG-3	12389-12367		
	M_{88-162}	+	5'-CACCATGCCTCGTCTTCGGTCC-3'	12162-12179	232	pET-M_{88-162}
		-	5'-CTATTGTAGCTTGTAGGCTGTCGCCG-3'	12386-12364		
7	N_{1-110}	+	5'-CACCATGGCGTCAAGACGATCACG-3'	12313-12332	337	pET-N_{1-110}
		-	5'-TTACGGCCCTGCTGGAGGCGC-3'	12645-12625		
	N_{1-69}	+	5'-CACCATGGCGTCAAGACGATCACG-3'	12313-12332	211	pET-N_{1-69}
		-	5'-CTAGTTCGACGAAAGGGTGGCGCG-3'	12519-12499		

[a] Underline indicates the overhang sequence to enable directional cloning to pET TOPO® vector

recombinant protein with an Xpress™ epitope and a polyhistidine (6×His)-tag at the amino terminus of each recombinant protein. Plasmids containing individual ORFs were transformed into One Shot® competent *E. coli* (Invitrogen, Carlsbad, CA). Following transformation and purification, individual plasmids were identified and characterized by restriction enzyme analysis for correct orientation of the insert. The authenticity of each ORF and of each truncated version was confirmed by automatic sequencing as previously described [80].

Expression and purification of full length GP5, M, N and their respective partial-length recombinant proteins

Plasmids pET-$GP5_{1-255}$, pET-$GP5_{1-116}$, pET-$GP5_{75-112}$, pET-$GP5_{55-98}$, pET-M_{1-162}, pET-M_{88-162}, pET-N_{1-110} and pET-N_{1-69} were purified and used to transform the BL21 Star™ (DE3) strain of *E. coli* for expression of the recombinant proteins. The *E. coli* strain BL21 Star™ (DE3) is especially designed for expression of genes regulated by the T7 promoter. Following transformation with each expression plasmid, a single colony was grown for approximately 3 h at 37°C in 2 ml of Luria-Bertani liquid medium supplemented with 200 μg/ml of carbenicillin (LBC). Thereafter, 50 μl of the culture was plated out on a LBC agar plate and incubated overnight at 37°C. On the next day, bacterial colonies on the agar plate were scraped off with a sterile tissue culture scraper and added to a 2-L flask containing 500 ml of LBC medium. Cultures were grown to a density of 0.5-0.7 at $OD_{600.}$ Protein expression was induced with 0.5mM isopropyl-β-D-thiogalactopyranoside (IPTG). Bacterial cells were harvested 5 h after induction, by centrifugation at 3000 ×*g* for 15 min at 4°C. Cell pellets were either stored at -80°C or immediately used for further processing.

The recombinant $GP5_{1-255}$, $GP5_{1-116}$, $GP5_{75-112}$ and $GP5_{55-98}$ proteins were purified using a Ni-NTA purification system (Invitrogen, Carlsbad, CA) under hybrid conditions. Briefly, individual cell pellets were resuspended in guanidinium lysis buffer (6M guanidine HCl, 20mM sodium phosphate, 500mM NaCl; pH7.8) containing lysozyme (1mg/ml) and proteinase inhibitors (Halt Proteinase Inhibitor Cocktail kit, Pierce, Rockford, IL) and slowly mixed on a rocker for 10 min at room temperature. After incubation, cell pellets were lysed by sonication with shortwave pulses of 10 sec at

high intensity (output 5). Subsequently, the crude lysates were centrifuged at 3000 ×*g* for 15 min at 4°C to remove bacterial cellular debris. The supernatant was loaded onto a Ni-NTA agarose column and allowed to bind for 1 h at room temperature. After binding, the agarose containing column was washed twice with denaturing binding buffer (8M urea, 20mM sodium phosphate, 500mM NaCl; pH7.8) and twice with denaturing wash buffer (8M urea, 20mM sodium phosphate, 500mM NaCl; pH6.0), to wash off non-specifically bound proteins. Subsequently, protein-bound agarose was washed four times with native wash buffer (50mM NaH_2PO_4, 0.5M NaCl, 10mM imidazole; pH8.0). Finally, each recombinant protein was eluted from the column with 2-ml fractions of native elution buffer pH8.0 (50mM NaH_2PO_4, 0.5M NaCl, 250mM imidazole; pH8.0).

Unlike the GP5 recombinant proteins, the recombinant full-length M_{1-162}, M_{88-162}, full-length N_{1-110}, and N_{1-69} proteins were purified under native conditions. Briefly, individual cell pellets were resuspended in native binding buffer (50mM NaH_2PO_4, 0.5M NaCl; pH8.0) containing lysozyme (1mg/ml) and proteinase inhibitors (Halt Proteinase Inhibitor Cocktail kit, Pierce, Rockford, IL) and incubated on ice for 30 min. After incubation, cell pellets were lysed by sonication with shortwave pulses of 10 sec at high intensity (output 5). Subsequently, the crude sonicates were centrifuged at 3000 ×*g* for 15 min at 4°C to remove cellular debris. The supernatant was loaded onto a Ni-NTA agarose column and allowed to bind for 2 h at 4°C. The recombinant proteins were eluted in native elution buffer (pH8.0) as described above.

Fractions containing the same recombinant protein were pooled together and centrifuged at 3,000 ×*g* for 45 min, with an Amicon® Ultra 5K (Millipore, Billerica, MA) centrifugal filter device used to increase recombinant protein concentration. After concentration, individual proteins were dialyzed against phosphate-buffered saline (PBS; pH=7.4) overnight at 4°C. Final protein concentration was determined using a BCA protein assay (Pierce, Rockford, IL), and the proteins were stored at -80°C.

Western immunoblotting assay

The authenticity of the purified recombinant proteins was confirmed by Western immunoblotting assay as previously described [75,151]. Briefly, proteins were mixed with an equal volume of 2X Laemmli sample buffer (Bio-Rad, Hercules, CA) containing

62.5 mM Tris-HCl, pH 6.8, 2% SDS, 25% glycerol, 0.01% bromophenol blue, and 200mM of dithiothreitol (Pierce, Rockford, IL) and incubated for 15 min at room temperature. Denatured samples were loaded onto sodium dodecyl sulfate-12% polyacrylamide resolving gels and a 5% stacking gel. Following electrophoresis, recombinant proteins were transferred onto a PVDF membrane (Bio-Rad, Hercules, CA). Immunoblotting was performed by using 5% nonfat dried milk powder in Tris-buffered saline with 0.05% Tween 20 (pH7.6) as the blocking solution. Expression and authenticity of each recombinant protein were confirmed using antibodies against the N-terminal 6×His tag as well as individual EAV protein-specific monoclonal antibodies MAb 6D10 for GP5 [75]; MAb 3E2 for N [213] and rabbit anti-EAV M #7888 for M protein [268]. Bound antibodies were detected by enhanced chemiluminescence, as previously described [75].

Virus neutralization test (VNT)

The neutralizing antibody titers of the test sera were determined as described by Senne *et al.* [292,337]. Briefly, serial two-fold dilutions of each sample from 1:2 to 1:256 were made in MEM (Invitrogen, Carlsbad, CA) containing 10% guinea pig complement (Rockland Immunochemicals, Gilbertsville, PA). Each serum sample was tested in duplicate in 96-well plates. An equal volume of a working dilution of virus containing an estimated 200 $TCID_{50}$ of the modified live virus strain of EAV (ARVAC®, Ft. Dodge Animal Health) was added to each well, except the serum controls. The plates were shaken to ensure mixing of the well contents and then incubated for 1h at 37°C. A suspension of high passage (P399 to P409) RK-13 cells was added to each well in a volume equivalent to that of the serum-virus mixtures and incubated for 72 h at 37°C, until viral cytopathic effect had fully developed in the virus control wells. The titer of a sample was recorded as the reciprocal of the highest serum dilution that provided at least 50% neutralization of the reference virus.

Coupling of recombinant proteins to microspheres

Approximately 50 μg of each recombinant protein were covalently conjugated to carboxyl groups on the surface of xMap Multi-Analyte COOH Microspheres according

to the manufacturer's protocol (Luminex Corp, Austin, TX). Each recombinant protein was attached to 6.25 X 10^6 microspheres, and the microspheres were counted with a hemocytometer so that equivalent quantities of each specific bead set were incorporated into the assay.

Development of microsphere immunoassay

A 96-well 1.2 μm filter plate was blocked for 2 min with 100 μl of PBS (pH7.4) with 1% bovine serum albumin and 0.02% sodium azide (PBN buffer) and then washed once with 190 μl of PBS (pH7.4) with 0.05% Tween 20 (PBS-T buffer). Wells were kept moist by addition of 20 μl of PBN buffer. Equine sera (50 μl, diluted 1:100 in PBN buffer) were added to each well of the filter plate. Approximately 2,500 recombinant antigen-conjugated microspheres per protein were added to each well in 50 μl of PBN buffer. The plate was incubated on a shaker in the dark for 30 min at 37°C and then washed three times with PBS-T using a vacuum manifold. Affinity-purified biotin-labeled goat anti-equine IgG (50 μl of a 1:1000 dilution in PBN) was added, and the plate was incubated on a shaker in the dark for 30 min at 37°C and then washed twice with PBS-T. Streptavidin-conjugated with R-phycoerythrin (50 μl of a 1:100 dilution in PBN buffer) was added, and the plate was incubated on a shaker in the dark for 30 min at 37°C and then washed twice with PBS-T using a vacuum manifold. The microspheres were then resuspended in 125 μl of PBN per well, and 75 μl of suspension were transferred to a clear polystyrene 96-well plate. Microspheres were aspirated through the flow cell of a dual-laser Luminex 100 instrument. The median fluorescence intensity (MFI) of 100 microspheres of each specific protein was recorded for each well.

Statistical analysis

A comparison of the diagnostic performance of the tests, VNT and MIA based on the $GP5_{55-98}$ and N_{1-110} proteins, was conducted using nonparametric density estimation and receiver operating characteristic (ROC) analysis. An ROC curve provides a graphical measure of the accuracy of a continuous diagnostic test. It represents a plot of the true positive fraction (TPF) versus the false positive fraction (FPF) across all possible cutoff values that can be used to dichotomize the data into positive or negative outcomes. In

addition to the ROC curve, a related parameter of interest is the area under the curve (AUC). For continuous tests, the AUC equals the probability that a randomly selected diseased individual has a test score that is greater than that for a randomly selected non-diseased individual. A diagnostic test that perfectly discriminates between non-diseased and diseased individuals has an ROC curve that is expressed by the horizontal line TPF=1 with the corresponding AUC=1. Diagnostic tests that are purely random, and hence are worthless, have a ROC curve expressed by the 45 degree angle line with a corresponding AUC=0.5 [454].

Cross-sectional data were obtained from a dual test study design in which both tests were carried out on sera from 2,500 horses, and where the true infection status of each horse was determined using the definitive gold-standard test, the VNT. The Pearson's correlation coefficient was estimated for the $GP5_{55-98}$ based MIA and VNT. A Bayesian bivariate normal analysis of the log transformed joint ($GP5_{55-98}$, N_{1-110}) outcomes was used to estimate ROC curves and area under the curve (AUC) based on methods developed by Choi *et al.* [455]. Specifically, data derived using sera from infected horses were modeled as a bivariate normal with unknown mean vector, ($\mu_{GP555-98}$, μ_{N1-110}), and an unknown covariance matrix that contained three parameters, namely, the (marginal) variances for the $GP5_{55-98}$ test and for the N_{1-110} test, and the correlation between $GP5_{55-98}$ and N_{1-110} test values. Independent diffuse normal prior distributions with a mean of 0 and variance of 100 were placed on $\mu_{GP555-98}$ and μ_{N1-110}, and independent inverse gamma priors with a mean of 1 and a variance of 1000 were used for the variances. The correlation was assigned a uniform prior ranging from -1 to 1. A bivariate normal distribution was also used to model the data for non-infected horses, with the same prior specification as used for infected horses.

Results from the ROC analysis were used to determine an optimal cutoff value for the purpose of classifying horses as EAV antibody-positive or –negative, based on the outcome of the $GP5_{55-98}$ MIA test. The sensitivity and specificity of the $GP5_{55-98}$ MIA test were then estimated at this cutoff value using Bayesian methods. The analysis was performed in S-Plus (Insightful Corp., Seattle, WA) and WinBUGS [456].

The sensitivity for each recombinant EAV structural protein-based MIA was calculated with: (number of true positives/[number of true positives + number of false

negatives]) × 100. Test specificities were calculated using the following equation: (number of true negatives/[number of true negatives + number of false positives]) × 100.

8.4. RESULTS

Cloning, expression, and purification of recombinant proteins

Following PCR amplification, all major structural protein genes and their corresponding partial-length ORFs were individually cloned into the pET100/D-TOPO vector. The recombinant protein from each construct was expressed as a bacterial fusion protein with an N-terminal tag containing the Xpress epitope and a 6×His tag (Figure 8.1 A). Various temperatures and IPTG concentrations were evaluated, to optimize the conditions for protein expression. With the exception of recombinant $GP5_{1-255}$ and its partial-length proteins ($GP5_{1-116}$, $GP5_{75-112}$ and $GP5_{55-98}$), all expressed recombinant proteins were present in the soluble fraction of the *E. coli* lysate. The insoluble GP5 recombinant proteins had to be purified under hybrid conditions instead of native conditions, which were successful for the soluble recombinant proteins (M_{1-162}, M_{88-162}, N_{1-110}, and N_{1-69}).

The expression and authenticity of the recombinant proteins were confirmed by Western immunoblotting assays. EAV structural protein-specific antibodies strongly reacted with their respective recombinant proteins (Figure 8.1.B). In addition, the attachment of a 6×His tag to the expressed proteins was demonstrated by Western immunoblotting with HRP-labeled anti-HisG antibody (data not shown).

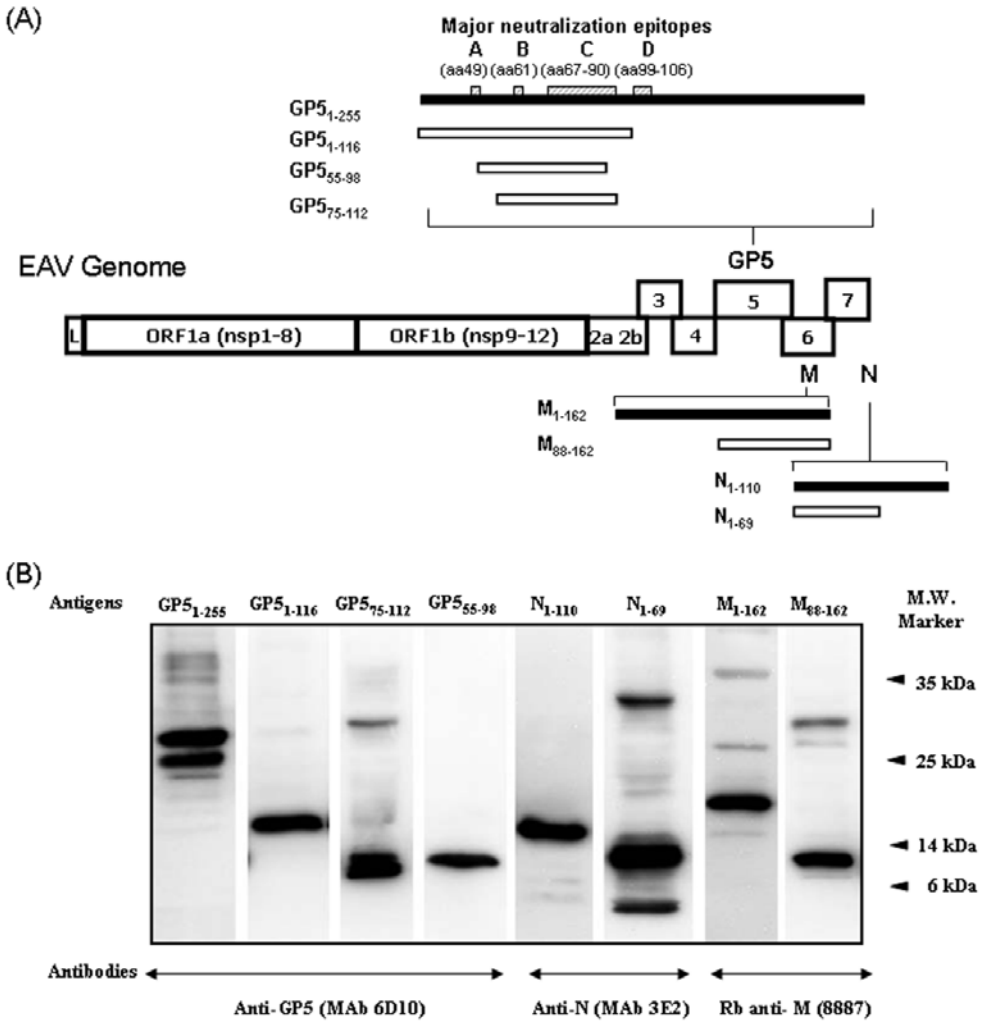

Figure 8.1. Recombinant EAV structural proteins expressed in *E. coli*. (A) Schematic representation of various EAV structural proteins expressed in *E. coli*. The recombinant full-length proteins derived from EAV ORFs 5, 6, 7 and their respective truncated versions are depicted. The black bars denote full-length proteins and the open bars denote partial-length proteins. The putative major neutralization sites A (aa 49), B (aa 61), C (aa 67-90) and D (aa 99-106) located in the N-terminal ectodomain of GP5 protein are indicated by hatched boxes. (B) Western blot analysis of purified bacterial recombinant proteins with EAV protein-specific MAbs and rabbit antisera. Monoclonal or rabbit EAV-specific antibodies used to detect each recombinant protein are indicated at the bottom of the figure. The MW marker is indicated on the right. The molecular masses of recombinant $GP5_{1-255}$, $GP5_{1-116}$, $GP5_{75-112}$, $GP5_{55-98}$, N_{1-110}, N_{1-69}, M_{1-162} and M_{88-162} proteins were 32, 17, 7, 8, 15.3, 10.6, 20.6 and 11kDa, respectively.

Virus neutralization test

Of the 2,500 equine serum samples tested, 1,750 were negative for VN antibodies to EAV (titers <1:4). A total of 750 sera were positive for antibodies to EAV, with titers ranging from 1:4 to ≥1:512.

In addition to the diagnostic samples, a panel of 192 archived sequential sera from 18 horses experimentally infected with different strains of EAV was evaluated using the VNT. The horses experimentally inoculated with EAV rVBS, 030H and KY84 strains developed VN antibodies to EAV after 7-10 days post-exposure (Figure 8.2.A, B, and C). Sera from horses inoculated with EAV rVBS and KY84 had VN antibody titers ranging from 1:128 to 1:1024. The majority of horses in these two groups of horses maintained a titer of ≥1:512 throughout the study. Horses infected with EAV 030H laboratory strain developed lower antibody titers ranging from 1:32 to 1:64. In contrast, horses inoculated with the avirulent CA95G strain developed detectable serum antibody titers from 14 dpi to 35 dpi (Figure 8.2.D). Neutralizing antibody titers in sera from the CA95G inoculated horses were generally lower than those in horses inoculated with the other 3 virus strains, ranging only from 1:4 to 1:16. Only one horse in this group developed a high antibody titer (1:256).

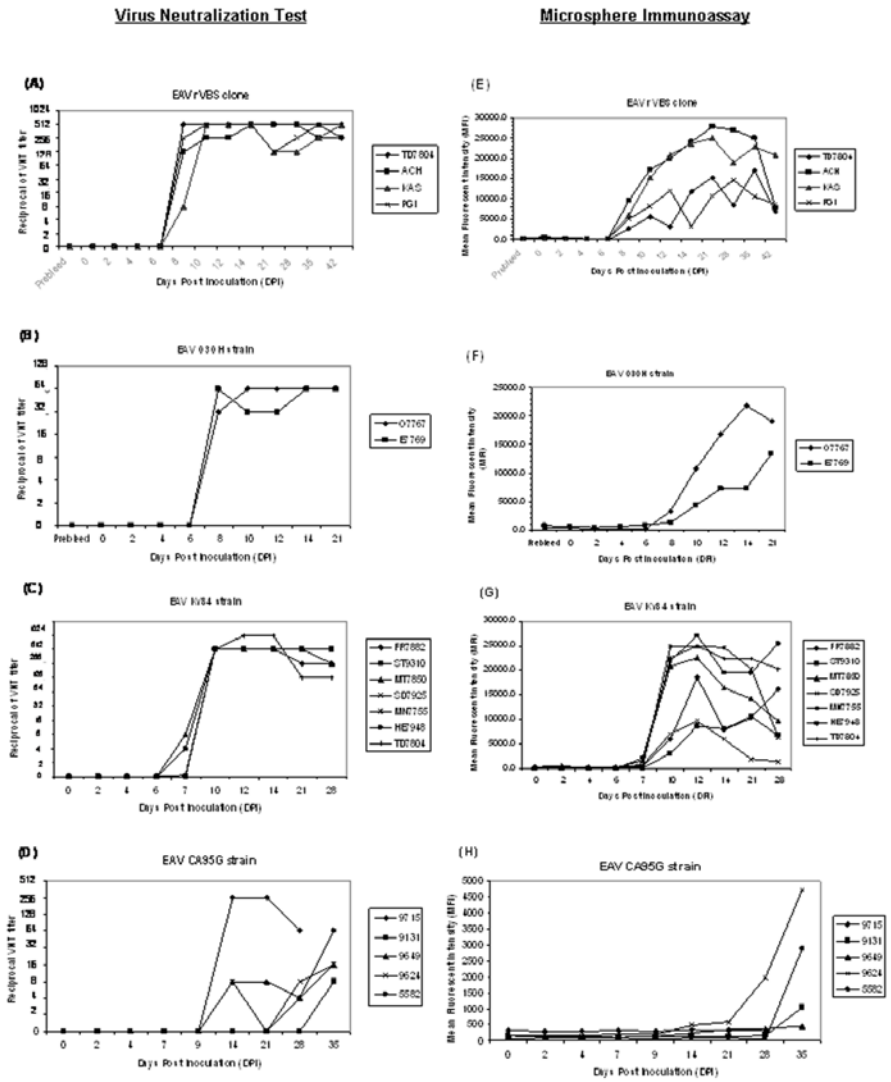

Figure 8.2. Comparison of antibody response to EAV as determined by $GP5_{55-98}$ MIA and VNT using sequential serum samples from experimentally infected horses. The reciprocal VN titers and MFI values of horses inoculated with different EAV strains, EAV rVBS (A, E), EAV 030H (B, F), EAV KY84 (C, G), and CA95G (D, H) are plotted against days post inoculation (dpi). Virus neutralizing antibody response in horse experimentally infected with EAV rVBS (n = 4), EAV 030H (n = 2), EAV KY84 (n = 7), and EAV CA95G (n = 5) measured by standard VNT (A, B, C and D). Virus antibody response in horsed experimentally infected with EAV rVBS (4), EAV 030H (n = 2), EAV KY84 (n = 7), and EAV CA95G (n = 5) measured by $GP5_{55-98}$ MIA (E, F, G and H).

Development of EAV recombinant structural proteins-based MIAs

Eight expressed recombinant proteins were used to coat polystyrene microbeads in development of the MIAs. The optimal dilution of the test sera to be used in the MIAs was predetermined by the use of known strong positive titer (≥1:512) and negative (<1:4) equine sera. The optimal working dilution was considered the serum dilution with lowest background activity from non-specific reactions. At a serum dilution of 1:100, the maximal dynamic range was attained for all the recombinant proteins; this was defined as the optimal serum dilution in the case of each protein (Figure 8.3).

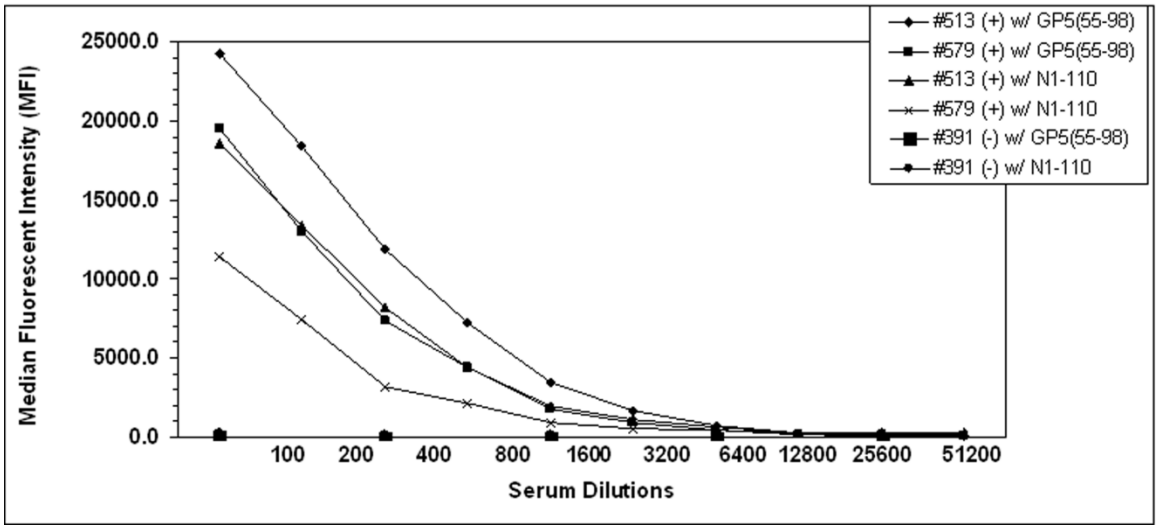

Figure 8.3. $GP5_{55-98}$ and N_{1-110} MIA analyses of serially diluted serum samples. Sera from horses with EAV neutralizing antibodies and negative control equine serum were serially diluted and evaluated in the $GP5_{55-98}$ and N_{1-110} MIAs. The median fluorescent intensity (MFI) for each dilution of standard was determined. Results are reported as MFI per 100 microspheres.

To establish cutoff levels for the MIAs specific for each EAV recombinant protein, 20 equine sera from known EAV-seronegative horses were used. The MIA positive cutoff for each protein was established at three standard deviations above the mean microsphere MFI of the known VNT negative sera. The mean MFI for $GP5_{1-255}$ was 279.5 (SD, 345) with an assay cutoff of 1315; the mean MFI for $GP5_{1-116}$ was 237.9

(SD, 321) with a cutoff of 1202; the mean MFI for $GP5_{75-112}$ was 220.8 (SD, 160.4) with a cutoff of 702; the mean MFI for $GP5_{55-98}$ was 263.1 (SD, 245) with a cutoff of 998; the mean MFI for M_{1-162} was 344.7 (SD, 209.4) with a cutoff of 973; the mean MFI for M_{88-162} was 377.3 (SD, 228.4) with a cutoff of 1063; the mean MFI for N_{1-110} was 432.1 (SD, 161.7) with a cutoff of 917; and the mean MFI for N_{1-69} was 216.6 (SD, 166.5) with a cutoff of 716. Samples with MFI values above the cutoff value were designated as positive, and those below that value were considered negative. Subsequent analysis of 125 positive (VNT titers ranging from 1:4 to >1:512) and 125 neutralizing antibody negative sera tested in parallel in the VNT allowed evaluation of the performance of each recombinant protein (n = 250) in the MIA. MIAs based on recombinant GP5 proteins had high specificity. The specificity of $GP5_{1-255}$, $GP5_{1-116}$, and $GP5_{75-112}$ based-MIAs was 98.4%, with only two false positive results out of 125 VNT antibody-negative samples. The $GP5_{55-98}$-based MIA had a slightly lower specificity, 97.6%, than did the other GP5-based MIAs. The sensitivities of the $GP5_{1-255}$ and $GP5_{1-116}$ based MIAs were the lowest among all of the proteins (3.2% and 5.6%, respectively), detecting only 4/125 and 7/125 VNT-positive samples. The sensitivities of the recombinant $GP5_{75-112}$ and $GP5_{55-98}$ based MIAs were higher (41.6% and 77.6%, respectively) and with detection of 52/125 and 97/125 VNT-positive sera, respectively. Both M protein-based MIAs, (M_{1-162} and partial M_{88-162}), had a high specificity (97.6% and 98.4% respectively), and correctly detected 122/125 and 123/125 VNT seronegative samples. However, both had very low sensitivity (6.4%) and only detected anti-EAV antibodies in 8/125 VNT-positive sera. The sensitivity of the recombinant N_{1-69} based MIA was also very poor; it only detected anti-EAV antibodies in 10/125 (8.0%) VNT-positive sera. In contrast, full-length N_{1-110} detected anti-EAV antibodies in 77/125 VNT-positive sera resulting in a significantly higher sensitivity (61.6%). In summary, these results confirm that MIAs based on $GP5_{1-255}$, $GP5_{1-116}$, $GP5_{75-112}$, N_{1-69}, M_{1-162} and M_{88-162} were markedly less sensitive than the N_{1-110} and $GP5_{55-98}$ MIAs (61.6% and 77.6%, respectively) in detecting anti-EAV antibodies in equine sera, as compared to the VNT (Table 8.2). Accordingly, the MIAs based on recombinant proteins that showed poor sensitivity were excluded from further study, and only $GP5_{55-98}$ and N_{1-110} protein-based MIAs were selected for further development and validation.

Table 8.2. Sensitivities and specificities of MIAs using individual recombinant EAV structural proteins

Recombinant EAV structural protein	Sensitivity (%)[a]	Specificity (%)[b]
$GP5_{1-255}$	3.2	98.4
$GP5_{1-116}$	5.6	98.4
$GP5_{75-112}$	41.6	98.4
$GP5_{55-98}$	77.6	97.6
M_{1-162}	6.4	97.6
M_{88-162}	6.4	98.4
N_{1-110}	61.6	91.2
N_{1-69}	8	97.6

[a],[b] Based on testing of 125 VNT-positive and 125 VNT-negative serum samples

Validation of the $GP5_{55-98}$ and N_{1-110} based MIAs

The same panel of 2,500 diagnostic equine sera evaluated in the VNT was analyzed for the presence of EAV-specific antibodies using $GP5_{55-98}$ and N_{1-110}-based MIAs. Of the 750 VNT-positive sera, only 698 were determined to be positive by the $GP5_{55-98}$ MIA. The $GP5_{55-98}$ MIA failed to detect anti-EAV antibodies in 52 serum samples that were confirmed to be seropositive in the VNT (52 false negatives). Furthermore, only 1644 of the 1,750 VNT-negative sera gave negative results with the $GP5_{55-98}$ MIA assay. This indicated that $GP5_{55-98}$ gave 106 false positive results compared to the VNT. The overall sensitivity and specificity of the $GP5_{55-98}$ MIA were 93.1% and 93.9%, respectively. Similarly, the N_{1-110} MIA gave 256 false negatives (only 494/750 were positive) and 374 false positive (1376/1750 were negative) results, as compared to the VNT. The sensitivity and specificity of the N_{1-110} MIA were 65.9% and 78.6%, respectively.

As mentioned previously, the cutoff values were assigned on the basis of three standard deviations above the mean MFI of 20 EAV antibody-negative equine sera. However, the cutoff value calculated according to this method varied slightly for each of the protein-coated bead sets; this could be a factor contributing to the differences in

sensitivity observed between the MIA and standard VNT. Moreover, a statistical approach using the negative reference population assumes a normal distribution of the test variable and does not consider the sensitivity of the assay [457]. Both sensitivity and specificity are important parameters when a diagnostic test is applied to a given population and an alternative approach to determination of the cutoff value is to consider both the negative and positive reference populations [458,459,460]. Such an approach was adopted in this study by using nonparametric ROC analysis to define the cutoff value with the entire equine serum data set derived from the study. Such an approach to tabulation of results is recommended in comparative studies of this type, in order to eliminate variability in the day-to-day performance of the assay [461]. By using the ROC analysis, a recalculated optimal cutoff value to classify sera as positive or negative was 992 MFI. With this cutoff, the sensitivity and specificity of $GP5_{55-98}$ MIA were 92.6% and 92.9% respectively, as compared to the VNT (Table 8.3). The cutoff value that maximizes the tradeoff between sensitivity and specificity of the N_{1-110} based MIA was 1261.43. At this cutoff, the estimated sensitivity and specificity were 88.3% and 54.7%, respectively.

Table 8.3. Sensitivity and specificity of VNT and $GP5_{55-98}$ MIA for determination of antibodies to EAV

Total no. of samples	VNT		$GP5_{55-98}$			
	Negative	Positive	Negative[a]	Positive[a]	Sensitivity[b] % (95% CI)[c]	Specificity[b] % (95% CI)[c]
2500	1750	750	1694	806	92.6 (90.1-94.3)	92.9 (91.7-94.1)

[a] Determined according to the optimal cutoff 992 MFI

[b] Sensitivity and specificity calculated using Bayesian analysis.

[c] CI, credible interval

The results from both recombinant protein-based MIAs were subjected to Bayesian analysis. The area under the ROC curve for both $GP5_{55-98}$ and N_{1-110} MIAs was

compared to that for the VNT. The area under curve (AUC) for the $GP5_{55-98}$ MIA was higher (AUC=0.983 with a 95% credible interval, the Bayesian analog of a confidence interval, of 0.979 to 0.986) than the AUC for the N_{1-110} MIA (AUC=0.772 with a 95% credible interval of 0.751 to 0.793; Fig. 8.4.). This result confirms that the diagnostic accuracy of the $GP5_{55-98}$ based MIA is significantly higher than the N_{1-110} based MIA; it can reliably detect anti-EAV antibodies in equine sera.

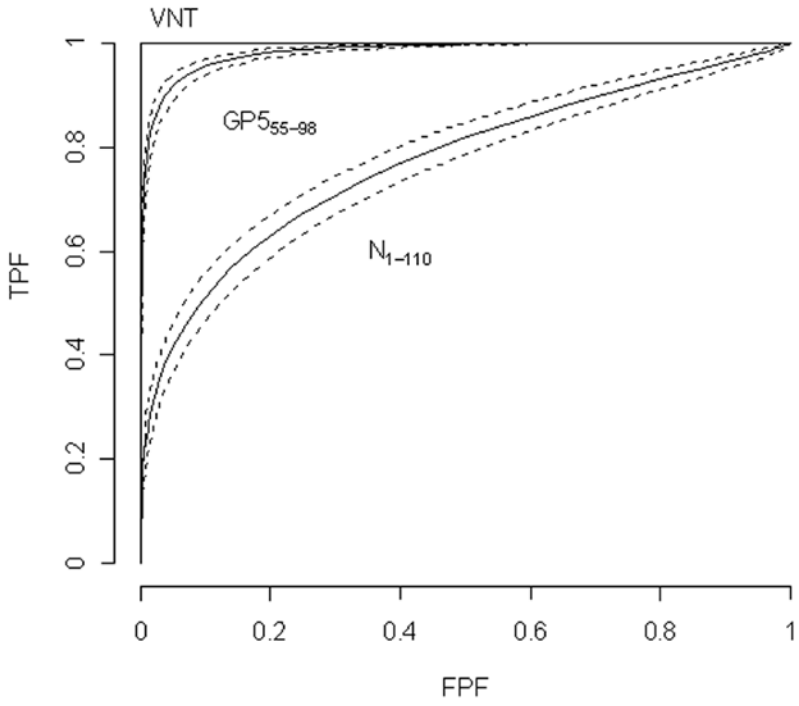

Figure 8.4. ROC curves depicting the sensitivity and specificity of the $GP5_{55-98}$ and N_{1-110} MIAs compared to the VNT. An ROC curve represents a plot of the true positive fraction (TPF) versus the false positive fraction (FPF) across all possible cutoff values that can be used to dichotomize the data into positive or negative outcomes. In addition to the ROC curve, a related parameter of interest is the area under the curve (AUC). Estimated ROC curves (solid lines) with pointwise 95% credible bands (dashed lines) for the $GP5_{55-98}$ MIA and N_{1-110} MIA are indicated.

A correlation analysis was performed between the $GP5_{55-98}$ MIA and the VNT. This indicated that there was a significant correlation between the outcomes of the $GP5_{55-98}$ MIA and the standard VNT (r = 0.84; p-value<0.0001; Figure 8.5).

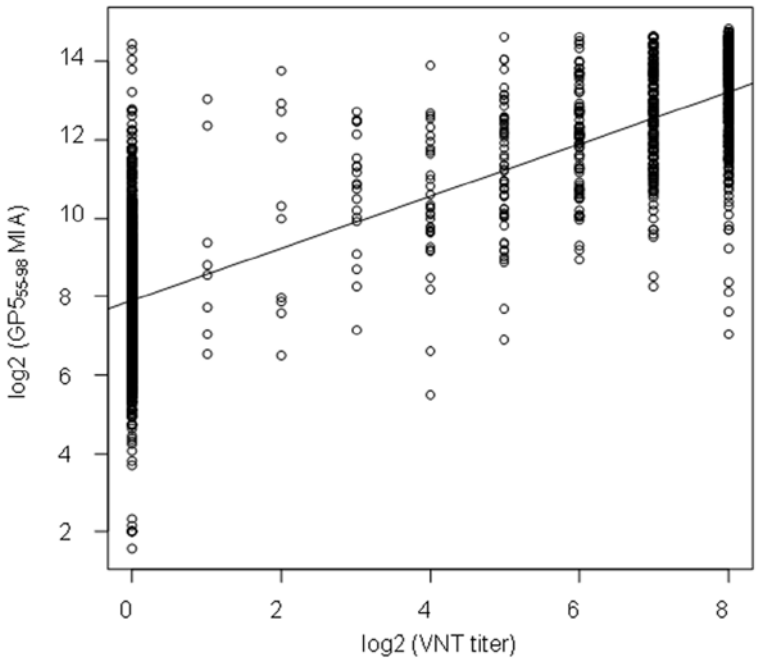

Figure 8.5. Analysis of the correlation analysis between the $GP5_{55-98}$ MIA and the VNT for detection of anti-EAV antibodies in equine sera. $GP5_{55-98}$ MIA scatter plot versus VNT using 2,500 equine sera is depicted on the $\log_2$ scale. The VNT data were plotted on the X-axis and the MIA data were plotted on the Y-axis.

Comparison of the sensitivity of the $GP5_{55-98}$ MIA and VNT using sequential serum samples from experimentally inoculated horses

A panel of 192 archived sequential serum samples from 18 horses comprising four groups, each inoculated with a different strain of EAV, was used to compare the antibody response detected by the $GP5_{55-98}$ MIA and the VNT [154,327,453].

Analysis of sera collected from EAV rVBS (n = 4) and EAV 030H (n = 2) inoculated horses gave a reactive signal in the $GP5_{55-98}$ MIA from day 8 pi. The MFI values for sera collected from day 8 to 42 were positive, with values ranging respectively for the two strains from 2,541 to 27,736 (Figure 8.2.E) and from 1,295 to 21,874 (Figure

8.2.F). Seroconversions detected by the $GP5_{55-98}$ MIA were in full agreement with the VNT results, where neutralizing antibodies were also detected from day 8 (Figure 8.2.A and 8.2.B). Similarly, reactive signals were detected in sera from horses inoculated with EAV KY84 (n = 7) from dpi 7 (two horses) and dpi 10 (other horses). The MFI values in sera from horses inoculated with EAV rVBS, 030H and KY84 ranged from 1,648 to 27,142. The only discrepancy between the results of the $GP5_{55-98}$ MIA and the VNT involved serum from one horse (SD7925), which had a threshold neutralizing antibody titer (1:4) on day 7 (Figure 8.2.C); this sample was not positive in the MIA (Figure 8.2.G). In general, the pattern of antibody development determined with the $GP5_{55-98}$ MIA correlated very well with the pattern found using the standard VNT. Both assays detected EAV-specific antibodies in samples collected after 10 dpi. If consideration is given to the fact that the two tests measure antibodies on different scales, there was greater variability in results using the MIA than the VNT. Despite this, the sensitivity of the MIA was not affected by this variability.

In contrast, when 44 sequential serum samples from 5 horses inoculated with the highly attenuated EAV CA95G strain were used to compare the $GP5_{55-98}$ MIA and the VNT, the $GP5_{55-98}$ MIA failed to give consistent positive reactive signals (Figure 8.2.H). The earliest reactive signal detected by the $GP5_{55-98}$ MIA was on 28 dpi for horse 9624, whereas the latter had detectable low levels of neutralizing antibodies from 14 dpi when tested by the VNT (Figure 8.2.D). Similarly, horse number 5582 had a threshold neutralizing antibody titer (1:4) on day 28 in the VNT; this was not detected by the $GP5_{55-98}$ MIA which only had reactive signals from 35 dpi. Horse number 9131 developed a low neutralizing antibody titer (1:8) by 35 dpi which was detected by the $GP5_{55-98}$ MIA. Horses number 9715 and 9649 did not show reactive signals at all whereas VN antibodies were detected at low levels from 14 dpi. The MFI values of the antibody-positive sera from CA95G inoculated horses ranged from 1,055 to 4,688.

8.5. DISCUSSION

This study evaluated a newly developed MIA based on $GP5_{55-98}$ as an alternative diagnostic procedure for the detection of antibodies to EAV. Evaluation of various forms of recombinant viral structural proteins (e.g., full-length proteins, and partial-length

proteins containing the antigenic regions) allowed identification of the best recombinant protein antigen for use in the MIA. Previous reports have shown that two bacterial fusion proteins (aa 1-116 and 55-98) and a synthetic peptide (aa 81-106), both based on GP5 of EAV, can be used as effective diagnostic antigens in ELISAs [274,446]. It has been previously demonstrated that horses immunized with portions of GP5 expressed either in bacteria (aa 55-98) or as a synthetic oligopeptide (aa 75-97) developed EAV-neutralizing antibodies [70,446]. Chirnside *et al.* (1995) used a series of recombinant bacterial fusion proteins derived from EAV ORF7 to define the immunoreactive region of the viral nucleocapsid (N) protein [275]. These studies indicated that the major N-protein epitope that reacts with anti-EAV equine sera is located within the aa residue segment 1-69 in the terminal region of the protein. Similarly, it has been demonstrated that only the carboxyl terminal sequence (aa 88-162) of the M-protein is necessary to identify equine serum antibodies specific to the EAV M protein; it was further suggested that this region should be useful for the serodetection of EAV infected horses [280]. On the basis of the foregoing, it was decided to express the full-length $GP5_{1-255}$, M_{1-162} and N_{1-110} and various antigenic regions of the GP5 (aa 1-116, 75-112 and 55-98), M_{88-162} and N_{1-69} proteins as bacterial fusion proteins to be used in MIAs to detect antibodies to EAV. When the sensitivity and specificity of these different MIAs and the VNT were compared, all of the MIAs with the exception of the MIA based on $GP5_{55-98}$ bacterial fusion protein, were of a very low specificity and sensitivity; accordingly, they were considered unsuitable as sero-diagnostic assays for EVA.

The low immunoreactivity of MIAs incorporating three of the GP5 proteins, ($GP5_{1-255}$, N-terminal ectodomain $GP5_{1-116}$, and $GP5_{75-112}$), as well as M (M_{1-162} and M_{88-162}), and N (N_{1-110} and N_{1-69}) proteins may result from misfolding and aggregation of the *E.coli*-expressed recombinant proteins. Despite the fact that the GP5 N-terminal ectodomain contains the major neutralization epitopes of EAV, the three MIAs incorporating GP5, the full-length $GP5_{1-255}$, the N-terminal ectodomain $GP5_{1-116}$, and $GP5_{75-112}$ had markedly low sensitivity. It has been reported that in the absence of the M protein, the recombinant GP5 protein tends to form large protein aggregates that are neither immunogenic nor immunoreactive [76,221]. Similarly, it has been shown that the GP5 protein, when expressed by baculovirus or mammalian expression systems, is not

processed properly and is easily misfolded [154]. As the length of the recombinant GP5 was reduced, the sensitivity of the MIA increased significantly; this would indicate that a reduction in length allows exposure of some of linear epitopes present in the antigenic region of the recombinant GP5 protein.

There was very good agreement between the results of the $GP5_{55-98}$ based MIA and the VNT. However, the $GP5_{55-98}$ MIA was found to have lower sensitivity and specificity than the VNT. Many factors could adversely affect the sensitivity of the $GP5_{55-98}$ MIA. (i) The short length of the GP5 protein incorporated into the assay could have targeted antibodies that are only specific for linear epitopes present in the region of aa 55-98, but not for any conformational epitopes. In addition, failure of the $GP5_{55-98}$ MIA to detect some sera that possessed VN antibodies to EAV could be also due to the lack of two major neutralization sites located outside of this region, neutralization sites A (aa 49) and D (aa 99-106), and/or lack of conformational interaction of the four neutralization sites (A-D) in the N-terminal ectodomain of GP5 as shown previously [69]. (ii) Recombinant proteins expressed in *E. coli* differ from the virion-associated GP5 protein, due to the lack of secondary structural folding and post translational modifications. (iii) The VNT putatively detects antibodies to the GP5 major envelope glycoprotein, which carries the known neutralization determinants of EAV [76]. Although there is only one known serotype of EAV, the GP5 protein has been shown to be the most variable of the EAV structural proteins among field strains of the virus [151,158]. Antigenic variation among EAV field strains could reduce sensitivity of the assay. It should be noted that the cloned GP5 amino acid sequence (aa 55-98) was derived from the EAV VBS, and field strains of EAV have been shown to differ significantly in this region; this could result in significant differences in neutralization phenotype among viral isolates using polyclonal equine sera. (iv) The lower sensitivity of the $GP5_{55-98}$ MIA could also be associated with dilution of the test samples. Previously, it has been documented that recombinant proteins expressed by bacteria can exhibit high background reactivity with equine serum [274,275,446]. In the present study, we determined 1:100 to be the optimal serum dilution for minimization of the non-specific binding of antibodies to the bacterial recombinant proteins. At this dilution, the majority of sera with low antibody titers (1:4 to 1:8) in the VNT gave false negative results in the

$GP5_{55-98}$ MIA (Table 8.4). It should be emphasized, therefore, that the MIA can only reliably detect sera with moderate to high antibody titers (≥ 1:16) to EAV.

Table 8.4. Distribution of numbers of samples giving false negative results in $GP5_{55-98}$ MIA (*n*=750)

Virus Neutralizing titer	No. of false negative in MIA / Total no. of VNT positive (%)
1:4	5 / 7 (71.4)
1:8	4 / 10 (40.0)
1:16	6 / 21 (28.6)
1:32	10 / 34 (29.4)
1:64	11 / 58 (18.9)
1:128	4 / 76 (5.3)
1:256	5 / 162 (3.1)
≥1:512	6 / 382 (1.6)

On testing sera from horses experimentally exposed to rVBS, 030H and KY84 strains of EAV, there was excellent concordance between the $GP5_{55-98}$ MIA and the VNT for detection of the antibody response to the virus. While the EAV 030H and KY84 strains of EAV had one and four substitutions, respectively, between aa 55 and 98 compared to the cloned $GP5_{55-98}$, sera from horses exposed to these virus strains did not give any false negative reactions in the $GP5_{55-98}$ MIA. In contrast, sera from the EAV CA95G strain-inoculated horses failed to give a consistent positive signal in the $GP5_{55-98}$ MIA. On comparative amino-acid sequence analysis, EAV CA95G virus strain had six aa substitutions in this region, five of which were located between aa 79 and 90 (Figure 8.6). This would indicate that amino-acid substitutions located in the region of aa 79-90 could have a significant effect on the sensitivity of the $GP5_{55-98}$ MIA. Furthermore, comparative amino-acid analysis of GP5 showed that some other field strains of EAV (e.g., WA97 and IL93) had multiple amino acid substitutions between aa 79 and 90 (Figure 8.6). Accordingly, horses exposed to EAV strains that have significant number of amino acid substitutions in this region may well give false negative results in the $GP5_{55-98}$ MIA. To

maximize sensitivity of a GP5-based MIA, it may be necessary to include a cocktail of $GP5_{55-98}$ amino acid sequences comprising multiple sequences representative of known phenotypically different strains of EAV rather than depend on a single $GP5_{55-98}$ sequence from one strain.

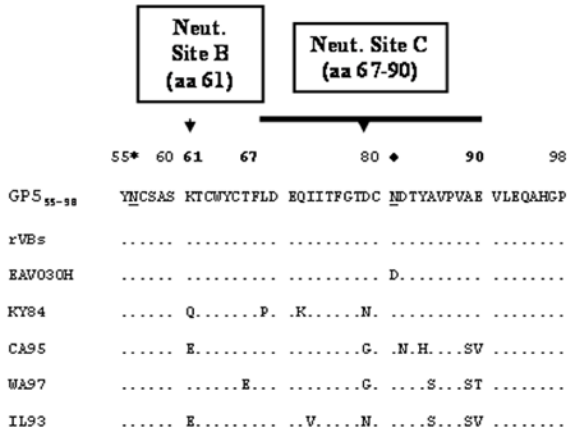

Figure 8.6. Aligned deduced amino acid sequences of GP5 55-98 proteins from various laboratory (rVBS and 030H) and field (KY84, CA95G, WA97 and IL93) strains of EAV. Dots indicate the same amino acid as that in the sequence at the top. Letters indicate the amino acid substitution at each site. The predicted N-linked glycosylation sites are underlined. The respective conserved and variable glycosylation sites are indicated by * and ◆.Neut., neutralization.

ELISA assays targeting whole virus or recombinant GP5, M, and N proteins have been investigated for the serological diagnosis of EAV infection [221,254,268,274,275,304,305,306,446]. An ELISA procedure incorporating an ovalbumin-conjugated synthetic peptide representing aa 81-106 of GP5 has been previously described for the detection of anti-EAV antibodies in equine sera [446]. That ELISA had a slightly higher sensitivity and specificity (96.75% and 95.6% respectively) than the MIA based on $GP5_{55-98}$ used in this study. Similarly, an ELISA based on a cocktail of three major structural proteins (GP5, M, and N) expressed by baculovirus was able to detect antibodies in most equine sera that were positive in the VNT following

natural or experimental infection (92.3% sensitivity and 100% specificity) [221]. It should be stressed that the latter two studies [221,446] were undertaken using a limited number of EAV VNT antibody-positive (n = 400 and n = 73 respectively) and antibody-negative (n = 400 and n = 111 respectively) equine sera. By comparison, the sensitivity (92.6%) and specificity (92.9%) of the $GP5_{55-98}$ MIA were evaluated based on testing 2,500 diagnostic equine sera.

The MIA based on $GP5_{55-98}$ has several advantages over the VNT as well as over various ELISAs. ELISAs that utilize whole viral antigen preparations can give rise to a large number of false-positive reactions, when sera are derived from horses vaccinated with tissue culture-derived vaccines. Such animals can develop antibodies to cell culture proteins remaining in the EAV whole-virus antigen preparation [462]. Furthermore, these cell protein-specific antibodies cause cytotoxicity at the lower serum dilutions that in turn can interfere with interpretation of the VNT results [463]. The $GP5_{55-98}$ MIA circumvents both of these problems, since it utilizes a recombinant protein that represents the immunodominant GP5 protein of EAV. Furthermore, the $GP5_{55-98}$ MIA is not subjective in interpretation, is less time-consuming, is less expensive, and uses a smaller sample volume. Accordingly, the $GP5_{55-98}$ MIA can be considered a more convenient and rapid serologic testing procedure for EAV infection, especially for screening large numbers of sera. The MIA can be completed within a few hours; in comparison the VNT takes 72 h. The MIA does not require the use of live virus and so does not require virus containment facilities.

In summary, we have developed and validated several MIAs that use recombinant EAV structural proteins to detect antibodies to EAV in equine serum. Among eight recombinant proteins, the highest concordance with the VNT results using selected equine sera was obtained with the partial GP5 protein, $GP5_{55-98}$. The $GP5_{55-98}$ MIA and the VNT outcomes correlated significantly (r = 0.84; p-value<0.0001). Although the $GP5_{55-98}$ MIA is less sensitive than the VNT, it has the potential to provide an accurate, rapid, convenient and more economical test for screening equine sera for the presence of antibodies to EAV with the VNT used as a confirmatory assay.

CHAPTER NINE

Characterization of Equine Humoral Antibody Response to the Nonstructural Proteins of Equine Arteritis Virus

Clin Vaccine Immunol. 2011, 18(2): 268-79

Reprinted with permission

9.1. SUMMARY

Equine arteritis virus (EAV) replicase consists of two polyproteins (pp1a and pp1ab) that are encoded by open reading frames (ORFs) 1a and 1b of the viral genome. These two replicase polyproteins are post-translationally processed by three ORF1a-encoded proteinases to yield at least 13 nonstructural proteins (nsp 1-12, including nsp7α and 7β). These nsps are expressed in EAV-infected cells but the equine immune response they induce has not been studied. Therefore, the primary purpose of this study was to evaluate the humoral immune response of horses to each of the nsps following EAV infection. Individual nsp-coding regions were cloned and expressed in both mammalian and bacterial expression systems. Each recombinant protein was used in an immunoprecipitation assay using equine serum samples from horses (n=3) that were experimentally infected with three different EAV strains (VB, KY77 and KY84), stallions (n=4) that were persistently infected with EAV, and horses (n=4) that were vaccinated with the modified live virus (MLV) vaccine strain. Subsequently, protein-antibody complexes were subjected to Western immunoblotting analysis with individual nsp-specific rabbit antisera, mouse anti-His antibody, or anti-FLAG-tagged antibody. Nsp2, nsp4, nsp5 and nsp12 were immunoprecipitated by most of the sera from experimentally or persistently infected horses, while sera from vaccinated horses did not react with nsp5 and reacted weakly with nsp4. However, serum samples from vaccinated horses were able to immunoprecipitate nsp2 and nsp12 proteins consistently. Information from this study will assist ongoing efforts to develop improved methods for the serologic diagnosis of EAV infection in horses.

9.2. INTRODUCTION

Equine arteritis virus (EAV) is the causative agent of equine viral arteritis (EVA), a respiratory and reproductive disease of horses [77]. EAV is a small (approximately 40-60 nm in diameter) enveloped virus with a positive-sense, single-stranded RNA genome of ~12.7 kb and belongs to the family *Arteriviridae* (genus *Arterivirus*, order *Nidovirales*), which also includes porcine reproductive and respiratory syndrome virus, simian hemorrhagic fever virus, and lactate dehydrogenase-elevating virus of mice [7,34]. The EAV genome includes nine known functional open reading frames (ORFs 1a, 1b, 2-7) [34,56]. ORFs 1a and 1b are located in the 5'-proximal three-quarters of the genome and are translated to produce replicase polyproteins pp1a and pp1ab (1,727 and 3,175 amino acids, respectively), with the latter being a C-terminally extended version of the former [141]. ORF 1b translation depends on a -1 ribosomal frameshift just before termination of ORF 1a translation [10]. The two replicase precursor polyproteins are cleaved by three different ORF 1a-encoded proteinases (see below) yielding at least 13 end products named nonstructural protein (nsp) 1 to 12 (including a recently described nsp7α and 7β; [113]). The three EAV proteinase domains are located in nsp1, nsp2 and nsp4 [34,66]. The remaining seven ORFs (2a, 2b and 3-7) are located in the 3' quarter of the genome and encode the structural proteins (GP2, E, GP3, GP4, GP5, M and N, respectively) of the virus.

EAV infection in horses induces long-lasting immunity that protects against reinfection with all strains of the virus [76,195,264,265,266]. Resistance to reinfection is assumed to be mediated by neutralizing antibodies directed against glycoprotein 5 (GP5), the major envelope protein of the virus [69,74,76,145,148,149,151,152,279,327]. The serum neutralization test, which principally detects antibodies to GP5, remains the most sensitive assay to detect EAV-specific antibodies in horse serum. The antibody response of horses to individual EAV proteins differs markedly depending on the interval after infection, the infecting virus strain, the individual horse, and the specific serological assay used [76]. Until now, the characterization of the humoral antibody response of the horse to EAV has been mainly based on the structural proteins of the virus [143,150,221,254,268,274,275,276,280,304,305,306,462,464]. The serologic response of horses to the individual structural proteins of EAV has been extensively characterized by

Western immunoblotting, enzyme-linked immunosorbent (ELISA), competitive ELISA (cELISA) assays, and microsphere immunoassay (Luminex) using recombinant GP5 and membrane (M) proteins and the nucleocapsid (N) protein [143,150,221,254,268,274,275,276,280,304,305,306,462,464]. Immunoblotting studies confirmed that infected horses respond to a number of viral structural proteins, and that sera from horses other than carrier stallions most consistently recognized the conserved carboxy-terminal region of the M protein [268]. However, little is known about the equine humoral immune response to the non-structural proteins of EAV. The nsps of EAV are the first viral proteins synthesized in cells infected with EAV and are essential to the viral replication cycle [26,93]. Thus, it is reasonable to predict the antibodies directed against nsps might appear early in the course of EAV infection based on their level of abundance and immunogenicity. Therefore, it is hypothesized that a distinct antibody response, similar to the immune response to structural proteins of EAV, may be generated to some of the nsps. The current study aimed to determine the humoral immune response of EAV-infected horses to each of the nsps encoded by the ORF 1a and ORF 1ab region of the viral genome (the proteolytic cleavage products derived from pp1a and pp1ab). Specifically, in the present study the recombinant nsps expressed in mammalian cells and *E. coli* were utilized in combined immunoprecipitation and Western immunoblotting analyses to establish the specificity of the antibody response of EAV-infected or vaccinated horses to the nsps of EAV.

9.3. MATERIALS AND METHODS

Cells

High-passage (P399 to P409) rabbit kidney-13 (KY RK-13) and baby hamster kidney-21 (BHK-21 [ATCC CCL-10]; P61-P80) cells were cultured and maintained in Eagle's minimum essential medium (EMEM; [Mediatech, Herndon, VA]) supplemented with 10% fetal calf serum (FCS; Hyclone, Logan, UT), 100U/ml penicillin, 100μg/ml streptomycin, 1μg/ml amphotericin B and 0.06% sodium bicarbonate at 37°C.

Antibodies

Monoclonal antibodies specific for nsp1 of EAV (12A4) have been previously described [306]. Similarly, mono-specific polyclonal rabbit antisera recognizing EAV nsp2 [110], nsp3 (rabbit 98.E3, [84]), nsp4 (a 1:1 mix of anti-nsp4M and anti-nsp4C; [110]), nsp7-8 [110], and nsp10 [87] have been previously described. In addition, we used previously unpublished antisera against nsp9 and nsp11 that were both raised by immunizing rabbits with full-length expression products purified from *E.coli* (J.C. Zevenhoven, D. D. Nedialkova and E. J. Snijder, unpublished data). Commercially available anti-FLAG (Agilent Technologies, Santa Clara, CA) and anti-His (Invitrogen, Carlsbad, CA) monoclonal antibodies were used to detect FLAG and His-tagged fusion proteins in Western immunoblotting analyses, respectively.

Equine sera

Sera from 11 horses that were seropositive for antibodies to EAV by virus neutralization assay were used to characterize the equine humoral immune response to the EAV nsps (Table 9.1). The panel consists of three serum samples from horses that were experimentally inoculated with virulent Bucyrus (VB) strain or the KY77 and KY84 strains of EAV, four serum samples from stallions confirmed to be persistently infected carriers of EAV (stallions D, E, G and R; [80,224,327]) and four serum samples from horses vaccinated with the modified live virus vaccine strain of EAV (ARVAC®; formerly Fort Dodge Animal Health Laboratories [now Pfizer Animal Health, New York, NY]). Two equine serum samples negative for neutralizing antibodies to EAV were included as controls.

Table 9.1. Serologic response of horses to EAV nsps following experimental infection, vaccination, and in cases of persistent virus infection.

Horse No.	§Breed	Status/ PI	SN⌘ titer	Proteins										
				nsp1	nsp2	nsp3	nsp4	nsp5	nsp7	nsp8	nsp9	nsp10	nsp11	nsp12
Acutely infected horses														
1462 (VB,KY53)	TB	2 mo PI	≥1:1024	-	+	-	$+_w$	+	-	-	-	-	-	+
77E853 (KY77)	TB	2 mo PI	1:1024	-	+	-	+	+	-	-	-	-	-	+*
198/199 (KY84)		42 DPI	1:1024	-	+	-	+	+	-	-	-	-	-	$+_w$
Persistently infected stallions														
D		Shedder	1:512	-	-	-	$+_w$	$+_w$	-	-	-	-	-	$+_w$
E		Shedder	1:256	-	+	-	+	+	-	-	-	-	-	+
R	DWB	Shedder	≥1:512	-	+	-	+	$+_w$	-	-	-	-	-	$+_w$
G	STB	Shedder	1:256	-	+	-	+	-	-	-	-	-	-	$+_w$
Vaccinated horses														
SR-10258 (#800)	TB		≥1:512	-	$+_w$	-	$+_w$	-	-	-	-	-	-	+
94-593	TB	128 DPV	1:512	-	$+_w$	-	$+_w$	-	-	-	-	-	-	+
508	STB	8 mo PV	1:256	-	$+_w$	-	$+_w$	-	-	-	-	-	-	+
478	STB	8 mo PV	1:128	-	$+_w$	-	$+_w$	-	-	-	-	-	-	+

§TB=Thoroughbred; DWB=Dutch Warmblood; STB=Standardbred

⌘SN=Serum neutralization

$+_w$ Immunoprecipitation protein signal was weaker compared to other positive sera in Western immunoblotting analysis

+* Protein expressed in both mammalian and bacterial cells were immunoprecipitated with equine sera

Virus neutralization (VN) test

The neutralizing antibody titers of the test sera were determined as described by Senne *et al.* [292,337]. Briefly, serial two-fold dilutions of each sample from 1:4 to 1:512 were made in MEM (Invitrogen, Carlsbad, CA) containing 10% guinea pig complement (Rockland Immunochemicals, Gilbertsville, PA). Each serum sample was tested in duplicate in 96-well plates. An equal volume of a virus dilution containing an estimated 200 $TCID_{50}$ of the modified live virus vaccine strain of EAV (ARVAC®, Ft. Dodge Animal Health) was added to each well, except the serum controls. The plates were shaken to ensure mixing of the well contents and then incubated for 1h at 37°C. A suspension of high passage (P399 to P409) RK-13 cells was added to each well in a volume double that of the serum-virus mixtures and the plates were incubated for 72 h at 37°C, until viral cytopathic effect had fully developed in the virus control wells. The titer of a sample was recorded as the reciprocal of the highest serum dilution that provided at least 50% neutralization of the reference virus.

Construction of plasmids for expression of recombinant EAV nsp1 to 12 in mammalian cells and *E. coli*

The twelve nonstructural proteins (nsp1 to nsp12) of EAV were PCR-amplified from the EAV rVBS full-length infectious cDNA clone containing plasmid (pEAVrVBS; GenBank accession number DQ846751; [328]) using the primer pairs listed in Table 9.2.

Table 9.2. Primers used to for PCR amplification of individual nsps for cloning into pCAGGS vector

Protein(aa)	Nucleotide location[c]		Primer sequences (5'-3')[a,b]	Recombinant plasmid	Predicted MW(kDa)
nsp1 (260)	255-1004	F	ttcGAATTCaccATGGCAACCTTCTCCGCTACTGG	pCAGGS-nsp1	28.6 (28.6)
		R	ttcCTCGAGttaGCCGTAGTTGCCAGCAGGCAA		
nsp2 (571)	1005-2717	F	ttcGAATTCaccATGGGCTACAATCCACCAGGGGAC	pCAGGS-nsp2	61.4 (61.5)
		R	ttcCTCGAGttaACCTATCAGCCGGAACCCCGGA		
nsp3 (233)	2718-3416	F	ttcGAATTCaccATGGGATGGATTTATGGGATATGC	pCAGGS-nsp3	25 (25.1)
		R	ttcCTCGAGttaTTCAAACACCATCCCGCCCTC		
nsp4 (204)	3417-4028	F	ttcGAATTCaccATGGGGCTATTCAGGTCACCGAAGG	pCAGGS-nsp4	21 (21.2)
		R	ttcCTCGAGttaCTCTCTATTGGATAAGCCATC		
nsp5 (162)	4029-4514	F	ttcGAATTCaccATGAGCAGCCTTTCTGGACCTCAG	pCAGGS-nsp5-FLAG	18.1 (19.3)
		R	ttcCTCGAGtta**CTTATCGTCGTCATCCTTGTAATC**CTCCAGGAAGTATTTCATCATG		
nsp6 (22)	4515-4580	F	ttcGAATTCaccATGGGAGGAGTGAAAGAGAGTGTCACC	pCAGGS-nsp6-FLAG	2.3 (3.4)
		R	ttcCTCGAGtta**CTTATCGTCGTCATCCTTGTAAT**CCTCCTGGGTAATTGGTTTGC		
nsp7 (225)	4581-5255	F	ttcGAATTCaccATGAGTCTCACTGCAACATTAGC	pCAGGS-nsp7	25.2 (25.4)
		R	ttcCTCGAGttaTTCATAGCTCCCCTTGCCCAGC		
nsp8 (50)	5256-5405	F	ttcGAATTCaccATGGGCCTAGATCAGGACAAAGTG	pCAGGS-nsp8	5.5 (5.6)
		R	ttcCTCGAGtcaGTTTAACTGATTCACTGCCTC		
nsp9 (693)	5256-7333	F	ttcGAATTCaccATGGGCCTAGATCAGGACAAAGTG	pCAGGS-nsp9	76.8 (76.9)
		R	ttcCTCGAGttaCTCATACTGCTTGGTGCGGAAG		
nsp10 (467)	7334-8734	F	ttcGAATTCaccATGAGTGCCGTGTGCACAGTTTGTGG	pCAGGS-nsp10-FLAG	50.5 (51.6)
		R	ttcCTCGAGtta**CTTATCGTCGTCATCCTTGTAATC**TTGCTTTTCCCAGCCACAG		
nsp11 (219)	8735-9391	F	ttcGAATTCaccATGTCCAACAAAATTTCGTGCCTC	pCAGGS-nsp11	24.2 (24.3)
		R	ttcCTCGAGttaCTCTTGGACATAAAAGGTCGC		
nsp12 (119)	9392-9748	F	ttcGAATTCaccATGGGTGTTGATGCAGTTACATCAGC	pCAGGS-nsp12-FLAG	12.5 (13.6)
		R	ttcCTCGAGtta**CTTATCGTCGTCATCCTTGTAATC**CACGGGCCCAATGACTGAACC		

[a] The restriction enzyme sites used for cloning are underlined (EcoRI –GAATTC; XhoI-CTCGAG).
[b] The C-terminal FLAG tag in the nsp5, nsp6, nsp10, nsp12 reverse primers are indicated in bold face.
[c] The nucleotide positions for the primers are based on GeneBank accession number DQ846751

The PCR amplification was performed with high fidelity *Pfu* DNA polymerase enzyme (Agilent; Santa Clara, CA) according to the manufacturer's protocol. The nsp5-, nsp6-, nsp10-, and nsp12-coding regions were amplified using reverse primers with the FLAG-tag coding sequence followed by a downstream stop codon. Subsequently, the individual PCR products were gel purified, digested with restriction enzymes *EcoRI* and *XhoI,* and cloned into the pCAGGS eukaryotic expression vector (generously donated by Dr. Brenda Hogue, Arizona State University, Tempe, AZ [421]). To remove the ORF1a/ORF1b ribosomal frameshift site in the nsp9-coding sequence and allow full-length nsp9 expression, mutations were introduced into the pCAGGS-nsp9 construct with site-directed PCR mutagenesis using the Quick Change® II XL Site-Directed Mutagenesis kit (Agilent, Santa Clara, CA) following manufacturer's instructions. Specifically, the ORF1a/ORF1b ribosomal frameshift site had been removed by mutating nucleotide A-5404 to C and inserting a C between G-5399 and T-5400 ([65]; numbered according to GenBank accession # DQ846751). Plasmids containing individual nsp-coding sequences were transformed into *E. coli* (DH5α) and grown at 37°C overnight. Plasmids were purified from overnight cultures of *E. coli* using the QIAprep Spin Miniprep plasmid extraction kit (Qiagen, Valencia, CA). Following purification, individual plasmids were identified and characterized by restriction enzyme analysis for correct orientation of the insert. The nucleotide identity of each construct was confirmed by automatic BigDye terminator cycle sequencing (Eurofins MWG-Operon, Huntsville, AL). The plasmids containing individual nsps 1-12 were identified as pCAGGS-nsp1 to pCAGGS-nsp12, respectively.

For generating bacterial expression plasmids for EAV nsp1 to nsp12, each nsp-coding sequence was amplified from pEAVrVBS using the primers listed in Table 9.3.

Table 9.3. Primers used for PCR amplification of individual nsps for cloning into pQE-TriSystem His-Strep 2 vector.

Protein (aa)	Nucleotide location[b]		Primer sequences (5' - 3')a	Recombinant plasmid	Predicted MW (kDa)
nsp1 (260)	225-1004	F	ttcGAATTCtATGGCAACCTTCTCCGCTACTGG	pQE-rVBSnsp1	28.6 (32.5)
		R	ttcCTCGAGGCCGTAGTTGCCAGCAGG		
nsp3 (233)	2718-3416	F	ttcGAATTCtGGATGGATTTATGGGATATGC	pQE-rVBSnsp3	25 (28.8)
		R	ttcCTCGAGTTCAAACACCATCCCGCCCTC		
nsp4 (204)	3417-4028	F	ttcGAATTCtGGGCTATTCAGGTCACCGAAGG	pQE-rVBSnsp4	21 (24.9)
		R	ttcCTCGAGCTCTCTATTGGATAAGCCATC		
nsp6 (22)	4515-4580	F	ttcGAATTCtGGAGGAGTGAAAGAGAGTGTCACC	pQE-rVBSnsp6	2.3 (6.1)
		R	ttcCTCGAGCTCCTGGGTAATTGGTTTGC		
nsp7 (225)	4581-5255	F	ttcGAATTCtAGTCTCACTGCAACATTAGC	pQE-rVBSnsp7	25.2 (29.1)
		R	ttcCTCGAGTTCATAGCTCCCCTTGCCCAGC		
nsp8 (50)	5256-5405	F	ttcGAATTCtGGCCTAGATCAGGACAAAGTG	pQE-rVBSnsp8	5.5 (9.6)
		R	ttcCTCGAGGTTTAACTGATTCACTGCCTC		
nsp10 (467)	7334-8734	F	ttcGAATTCtAGTGCCGTGTGCACAGTTTGTGG	pQE-rVBSnsp10	50.5 (54.4)
		R	ttcCTCGAGTTGCTTTTCCCAGCCACAG		
nsp12 (119)	9392-9748	F	ttcGAATTCtGGTGTTGATGCAGTTACATCAGC	pQE-rVBSnsp12	12.5 (16.4)
		R	ttcCTCGAGCACGGGCCCAATGACTGAACC		

[a] The restriction enzyme sites used for cloning are underlined (EcoRI - GAATTC; XhoI - CTCGAG).

[b] The nucleotide positions for the primers are based on GenBank accession number DQ846751.

Subsequently, PCR products were gel purified, digested with *EcoRI* and *XhoI*, and cloned into the pQE-TriSystem His·Strep 2 vector (Qiagen, Valencia, CA) which has promoters for expression in *E. coli*, insect cells and mammalian cells, allowing expression of His·Strep-tagged proteins from a single vector. Each construct containing nsp1-12 was designated as pQE-rVBSnsp1 through pQE-rVBSnsp12. Following transformation and purification, individual plasmids were identified and characterized by restriction enzyme analysis for correct orientation of the insert. The nucleotide identity of each construct was confirmed by automatic BigDye terminator cycle sequencing (Eurofins MWG-Operon, Huntsville, AL).

Expression of recombinant nsp1 to nsp12 in mammalian cells

Expression of recombinant EAV nsps was performed in BHK-21 cells transfected with individual plasmids containing nsp1-12 coding regions using Fugene® HD (Promega) according to manufacturer's instructions. Briefly, BHK-21 cells were plated the day before transfection at a density of 5×10^5 cells into a 100 mm cell culture dish in 17 ml of complete growth medium. A total of 19 µg of each plasmid was mixed with Fugene® HD reagent (Promega) and the complex was incubated for 10 min at room temperature (RT). Subsequently, each mixture was added onto confluent monolayers of BHK-21 cells and incubated at 37°C in a 5% CO_2 incubator. At 24 h post-transfection, cells were lysed in NP40 cell lysis buffer (50mM Tris, [pH 7.4], 250mM NaCl, 5mM EDTA, 50mM NaF, 1mM Na_3VO_4, 1% Nonidet P40 [NP40] and 0.02% NaN_3) supplemented with 1X proteinase inhibitor cocktail (Pierce) and 1mM phenylmethanesulphonyl fluoride (PMSF). Insoluble materials were removed by centrifugation at 4°C for 10 min at 13,000 ×*g* in a microcentrifuge. Cleared cell lysates were stored at -80°C for further use. The expression and validity of each recombinant protein were confirmed by indirect immunofluorescence and Western immunoblotting analyses.

Expression and purification of recombinant EAV nsp1 to nsp12 expressed in bacterial cells

Plasmids pQE-rVBSnsp1, nsp3, nsp4, nsp6, nsp7, nsp8, nsp10 and nsp12 were transformed in an expression strain of *E. coli*, M15[pREP4], and a single colony was

used to inoculate 10 ml of Luria-Bertani (LB) medium containing both ampicillin (100 µg/ml) and kanamycin (25 µg/ml). The culture was grown overnight, diluted 1:20 in fresh LB medium with ampicillin and kanamycin, and subsequently grown at 37°C until an OD_{600} of 0.6 was reached. Recombinant protein expression was induced by addition of 1mM of isopropyl-β-D-thiogalactopyranoside (IPTG). Bacterial cells were harvested 4 h after induction by centrifugation at 4000 ×*g* for 20 min at 4°C and stored at -20°C. Individual recombinant fusion proteins containing 8× His-tag were purified with the Ni-NTA (Qiagen, Valencia, CA) agarose-affinity isolation procedure. Briefly, induced bacterial cell pellets were resuspended in buffer B (100mM NaH_2PO_4, 10mM Tris base and 8M urea, pH 8.0) and incubated for 1 h at RT with gentle mixing. The lysates were clarified at 10,000 ×*g* for 30 min at RT. The supernatant containing recombinant protein was decanted into 50% Ni-NTA slurry and rotated gently for 1 h at RT. After binding, the agarose containing column was washed twice with buffer C (100mM NaH_2PO_4, 10mM Tris base and 8M urea, pH 6.3). Elution was performed in 0.5-ml fractions of buffer D (100mM NaH_2PO_4, 10mM Tris base and 8M urea, pH 5.9) four times followed by elution in 0.5-ml fractions of buffer E (100mM NaH_2PO_4, 10mM Tris base and 8M urea, pH 4.5) four times. Fractions containing the same recombinant protein were pooled together and stored at -80°C for further use.

Immunofluorescence assays

For the indirect immunoflurorescence assay (IFA), BHK-21 cells grown on glass cover-slips in 24-well plates were transfected with 0.55 µg of each nsp expression plasmid (nsp1 to nsp12) using Fugene® HD (Promega, Madison, WI) according to the manufacturer's instructions. At 18 h post-transfection, cells were fixed in 4% paraformaldehyde in phosphate-buffered saline (PBS; pH7.4) for 30 min at RT and washed three times with PBS (pH 7.4) containing 10mM glycine (glycine/PBS). After permeabilization with 0.2% Triton X-100 in PBS (pH 7.4) for 10 min, cover-slips were incubated with the appropriate nsp-specific monoclonal or polyclonal antibody, or with anti-FLAG tag MAb (1:200), in PBS containing 5% fetal bovine serum (FBS). After three 10mM glycine/PBS washes, coverslips were incubated with FITC-conjugated goat anti-mouse or anti-rabbit IgG (Southern Biotech, Birmingham, AL) for 1 h at RT. Cover-

slips were washed and mounted in 4', 6'-diamidino-2-phenylindole (DAPI) containing aqueous mounting medium (Vector Laboratories, Burlingame, CA) and observed under an inverted fluorescence microscope.

Western immunoblotting

The solubilized proteins were mixed with 5X reducing sample buffer containing 100mM dithiothreitol (DTT; Pierce, Rockford, IL) and incubated for 10 min at RT. Samples were resolved in a SDS-12% polyacrylamide gel (PAGE). The gel was transferred to a PVDF membrane (Bio-Rad, Hercules, CA). Blocking was performed in 5% skim milk powder dissolved in TBS-T (10mM Tris-HCl [pH 7.6], 150mM NaCl, 0.05% Tween 20). Blots were incubated with primary antibody for 1 h at RT followed by biotinylated goat anti-mouse or anti-rabbit antibodies (Invitrogen, Carlsbad, CA) for 1 h. Subsequently, the blots were incubated with streptavidin-horseradish peroxidase tertiary antibody (Invitrogen, Carlsbad, CA) and detected using an enhanced chemiluminescence reaction (ECL, Amersham, Piscataway, NJ).

Immunoprecipitation

Immunoprecipitation of individual EAV nsps was performed using Dynabeads® Protein G (Invitrogen, Carlsbad, CA) Immunoprecipitation kit following manufacturer's instructions. Briefly, 10 µl of equine antiserum was added to the Dynabeads® Protein G and incubated with rotation for 10 min at RT allowing antibody binding to the beads via their Fc region. The bead-bound antibody complex was washed with binding buffer. EAV nsp-containing cell lysate was mixed with the bead-bound antisera complex and incubated for 30 min at RT with constant rotation. Then, the bead-antibody-antigen complex was washed 3 times with washing buffer. The immunoprecipitated target antigen was eluted in elution buffer and mixed with 5X reducing sample buffer containing DTT (Pierce, Rockford, IL) and heated for 5 min at 70°C. Subsequently, denatured samples were resolved by SDS-12% PAGE and subjected to Western immunoblotting analysis as described previously.

9.4. RESULTS

Characterization of EAV nonstructural proteins expressed in mammalian cell

cDNA fragments corresponding to twelve nonstructural proteins (nsp1-nsp12) of the VB strain of EAV were cloned and expressed in BHK-21 cells. Due to lack of protein specific-antisera, recombinant proteins nsp5, nsp6, nsp10 and nsp12 were expressed as C-terminal FLAG-tagged fusion proteins from each construct. The expression and validity of each recombinant protein was confirmed by indirect immunofluorescence (IFA) and Western immunoblotting analyses with protein-specific rabbit antisera and monoclonal anti-FLAG antibody (Figures 9.1.A and 9.1.B). All twelve proteins, except for nsp6 (a very short peptide of 22 amino acids) which was expressed only in few cells, were expressed at high levels and detected by IFA (Figure 9.1.A). Consistent with the IFA result, nsp6 could not be detected in the Western immunoblotting assay indicating that expression of this protein is either insufficient or it may be lost during SDS-PAGE and Western immunoblotting due to its extremely small size (3.4 kDa after modification). As shown in Fig. 1B, all of the recombinant proteins migrated according to their predicted sizes, listed in Table 9.2.

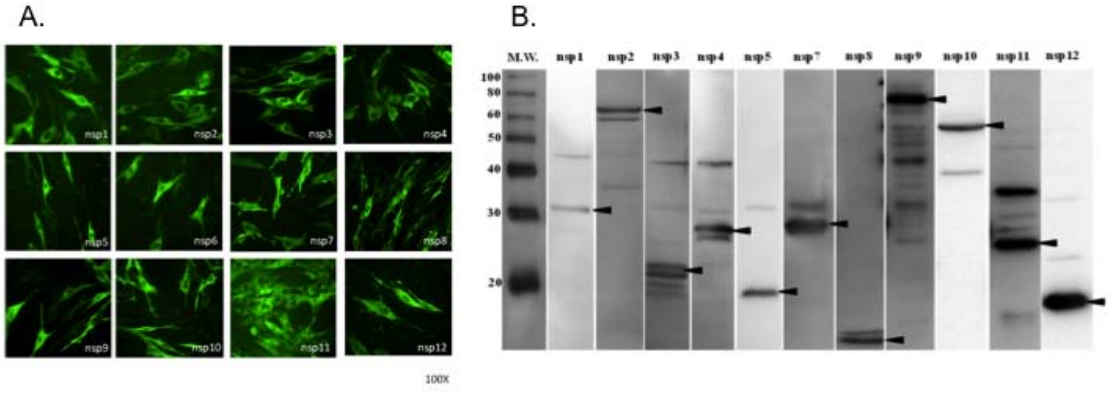

Figure 9.1. Expression of EAV nonstructural proteins in mammalian cells. (A) Expression of EAV nonstructural proteins in BHK-21 cells as detected by immunofluorescence assay. For this purpose, BHK-21 cells were transfected with plasmids encoding individual nsps and examined at 24 h post-transfection by IFA. Protein-specific monoclonal antibody 12A4 (nsp1), protein-specific rabbit anti-peptide

sera (nsp2, nsp3, nsp4, nsp7-8, nsp9, and nsp11) or anti-FLAG monoclonal antibody (nsp5, nsp6, nsp10 and nsp12) and FITC-conjugated goat anti-mouse or rabbit IgG (H+L) were used for detection of each protein. Each recombinant protein is identified at the bottom of each panel. (B) Western immunoblotting analyses of recombinant EAV nsps expressed in mammalian cells, performed with protein-specific monoclonal antibodies as specified for panel (A). Sizes of the molecular weight markers are shown on the left hand side of the figure and nsps are identified above each lane. Arrows indicate the position of each recombinant protein.

Characterization of EAV nonstructural proteins expressed in *E. coli*

As an alternative to the use of a mammalian expression system, we employed a bacterial expression system with a C-terminally 8× His-tagged vector as a secondary/purification strategy. This system is more convenient for production of larger amounts of protein, which could be used as antigen in future diagnostic tests. Segments of the EAV genome containing the sequences of nsp1, nsp3, nsp4, nsp6, nsp7, nsp8, nsp10, and nsp12 were successfully inserted into the pQE-TriSystem His·Strep 2 expression vector. When *E. coli* were transformed with each plasmid expressing individual nsp and induced with IPTG, bands migrating at a position corresponding to nsp1, nsp4, nsp7, nsp8, nsp10 and nsp12 with a molecular size of approximately 32 kDa, 26 kDa, 29 kDa, 9 kDa, 55 kDa and 16 kDa respectively, as indicated in Table 9.3, were observed on Western blots (Figure 9.2). Although the predicted molecular mass of nsp4 is 21 kDa, nsp4 was detected as an approximately 30 kDa product, as documented previously [110]. Nsp1 and nsp12 were expressed at high concentrations in both soluble and insoluble fractions of cell lysates. In contrast, larger amounts of nsp3, nsp4, nsp6, nsp7, nsp8 and nsp10 could be recovered from insoluble fractions of cell lysates compared to soluble fractions. Therefore, proteins were purified under denaturing conditions using an immobilized-metal affinity chromatography procedure with the Ni-NTA resin column. Although expression of nsp3 and nsp6 proteins was confirmed in a Western immunoblotting analysis before purification, these proteins could not be recovered after purification using Ni-NTA resin columns. Accordingly, bacterially

expressed nsp3 and nsp6 could not be further evaluated in the study. Furthermore, nsps 2, 5, 9 and 11 were toxic and could not be expressed in M15[pREP4] *E. coli* using pQE-TriSystem His·Strep 2 vector.

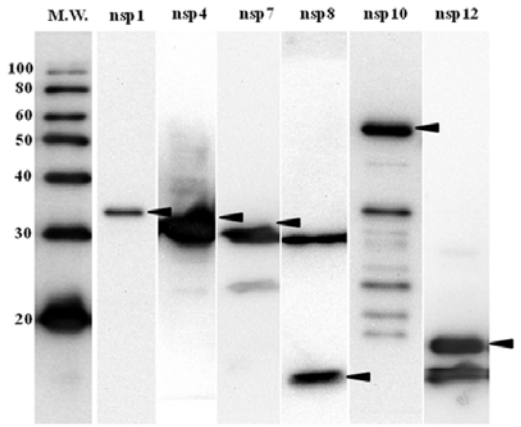

Figure 9.2. Western immunoblotting analyses of recombinant nsp4, nsp7, nsp8, nsp9 nsp10 and nsp12 of EAV expressed in *E. coli.* Samples were total lysates from IPTG-induced cultures of *E. coli* M15[pREP4] cells transformed with pQE-TriSystem Strep·His2. Total bacterial cell lysate was bound to Ni-NTA resin column. The bound individual recombinant proteins were eluted in elution buffer and subjected to Western immunoblotting analysis. Recombinant proteins were detected using anti-His monoclonal antibody. Sizes of the molecular weight markers are shown on the left hand side of the figure and nsps are identified above each lane. Arrows indicate the position of the protein.

Immunoprecipitation of EAV nsps 1 to 12 expressed in mammalian cells with equine serum

To determine the equine antibody response to nonstructural proteins of EAV, recombinant proteins nsp1 to nsp12 expressed in mammalian cells were subjected to immunoprecipitation using 11 serum samples containing antibodies to EAV. The VN antibody titers of these serum samples varied between 1:128 and ≥1:1024 (Table 9.1).

Individual recombinant nsps expressed in mammalian cells were immunoprecipitated using well-characterized equine serum samples from experimentally and persistently infected horses plus sera from horses vaccinated with the commercial modified live virus vaccine (ARVAC®, Fort Dodge Animal Health Laboratories [now Pfizer Animal Health Inc., New York, NY]). Briefly, total solubilized proteins derived from nsp-transfected (nsp1 to nsp12) or pCAGGS-empty vector-transfected BHK-21 cells were immunoprecipitated with equine sera and the immunoprecipitated proteins were subjected to SDS-polyacrylamide gel electrophoresis. As a control, two equine serum samples negative for EAV antibodies were included in these assays. Individual nsps in the immunoprecipitates were then identified with an nsp-specific monoclonal antibody (nsp1), a specific rabbit antiserum (nsp2, nsp3, nsp4, nsp7, nsp8, nsp9, nsp11), or an anti-FLAG monoclonal antibody (nsp5, nsp6, nsp10 and nsp12) by Western immunoblotting analysis. All three sera from horses that were previously experimentally infected with EAV strains VB, KY77, and KY84 precipitated recombinant nsp2 expressed in mammalian cells. Also three out of four serum samples from persistently infected horses recognized nsp2, although serum from stallion G gave a weak precipitation reaction as compared to the others. In contrast, all four serum samples from vaccinated horses weakly immunoprecipitated nsp2 as detected by Western immunoblotting assay (Figure 9.3.A). Similarly, all three sera from horses experimentally infected with different EAV strains reacted strongly with recombinant nsp5 expressed in mammalian cells. Interestingly, sera from persistently infected horses did not consistently immunoprecipitate nsp5. Sera from stallion E gave a strong immunoprecipitation reaction with nsp5 (comparable to sera from experimentally infected horses) while sera from stallions D and R reacted very weakly and serum from stallion G did not react at all. In contrast, none of sera from vaccinated horses were able to immunoprecipitate nsp5 (Figure 9.3.B).

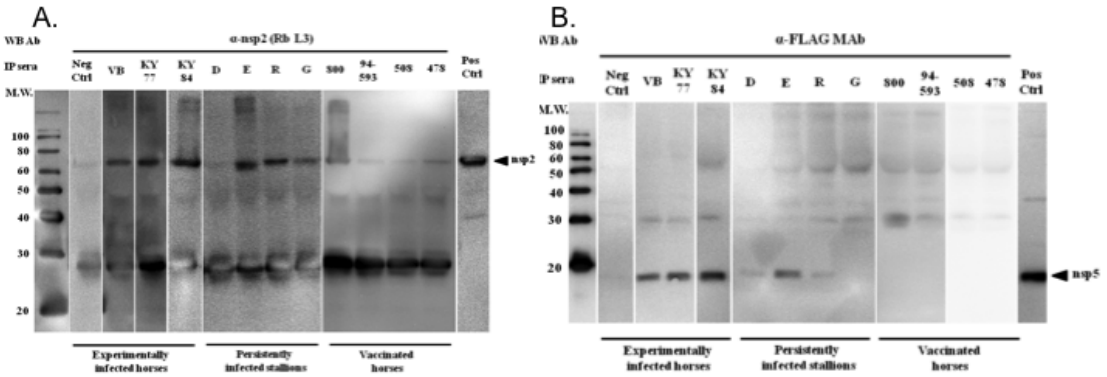

Figure 9.3. Immunoprecipitation analyses of (A) nsp2 and (B) nsp5 using sera from experimentally infected, vaccinated and persistently infected horses. Nsp2 and nsp5 expressed in mammalian cells were immunoprecipitated using equine sera and detected by Western immunoblotting analysis with an anti-nsp2 rabbit serum and the anti-FLAG tag monoclonal antibody, respectively. Sizes of the molecular weight markers are shown on the left hand side of the figure and serum samples used for immunoprecipitation are identified above each lane. Extreme right hand lanes contain corresponding recombinant proteins expressed in mammalian cells as the control.

All of the sera from experimentally infected horses gave a very weak immunoprecipitation reaction with nsp12 (Figure 9.4). Equine serum from the horse experimentally inoculated with the KY77 strain strongly immunoprecipitated nsp12 compared to sera from two other horses experimentally inoculated with the VB and KY84 strains of EAV. None of the sera from persistently infected stallions and vaccinated horses recognized nsp12 expressed in mammalian cells. Interestingly, none of the 11 equine serum samples evaluated in this study were able to immunoprecipitate nsp1, nsp3, nsp4, nsp7, nsp8, nsp9, nsp10, and nsp11 expressed in mammalian cells (Table 9.1). Based on these results using recombinant proteins expressed in mammalian cells, only nsp2 and nsp5 were consistently recognized by equine antiserum. As expected, none of the proteins were immunoprecipitated by the two negative control sera, confirming the specificity of EAV nsp recognition. Furthermore, none of the equine sera reacted with the solubilized cellular proteins from pCAGGS-empty vector-transfected BHK-21 cells (data not shown).

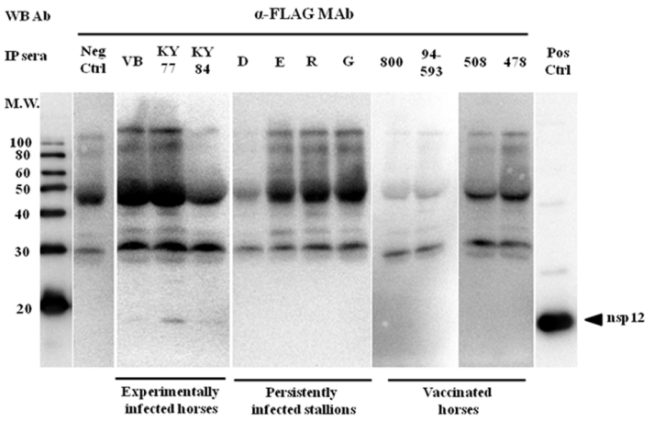

Figure 9.4. Immunoprecipitation analysis of nsp12 using sera from experimentally infected, vaccinated and persistently infected horses. Nsp12 expressed in mammalian cells was immunoprecipitated using equine sera and detected by Western blot analysis with the anti-FLAG tag monoclonal antibody.

Immunoprecipitation of EAV nonstructural proteins expressed in *E. coli* with equine serum

In order to verify whether equine serum from acutely (experimentally) infected, persistently infected, and vaccinated horses can react with bacterially expressed antigens similar to antigens expressed in mammalian cells, purified nsp1, nsp3, nsp4, nsp7, nsp8, nsp10 and nsp12 proteins were subjected to immunoprecipitation analyses with equine antisera. Consistent with the immunoprecipitation results using antigens expressed in mammalian cells, none of tested sera recognized nsp1, nsp3, nsp7, nsp8, and nsp10 antigens. Interestingly, sera from horses used in this study immunoprecipitated nsp4 and nsp12 expressed in bacterial cells although they did not previously immunoprecipitate the same proteins expressed in mammalian cells (Figures 9.5.A and 9.5.B). With the exception of serum from one persistently infected stallion, other sera from persistently infected stallions and all three experimentally infected horses strongly immunoprecipitated nsp4 expressed in *E. coli.* Serum sample from the persistently infected stallion D gave a weak immunoprecipitation reaction as compared to other

samples (Figure 9.5.A). Interestingly, the serum samples from vaccinated horses were only able to weakly immunoprecipitate nsp4. Previously, most tested sera did not react or reacted weakly with nsp12 expressed in mammalian cells. In contrast, most sera reacted strongly with bacterially-expressed nsp12 antigen (Figure 9.5.B). Sera from VB- and KY77-inoculated horses and stallion E reacted strongly with the bacterially expressed nsp12 antigen, while the rest of the sera (KY84, stallions D, R and G) only reacted weakly with this antigen in immunoprecipitation assays. Additionally, all four sera from vaccinated horses were also able to strongly immunoprecipitate nsp12. Based on these results, horses consistently mount an immune response to EAV nsp4 and nsp12. Equine antisera from experimentally infected and vaccinated horses, as well as persistently infected stallions were unable to immunoprecipitate nsp1, nsp7, nsp8, and nsp10 expressed in *E. coli*. As expected, none of the proteins were immunoprecipitated with negative control sera, confirming the specificity of our approach.

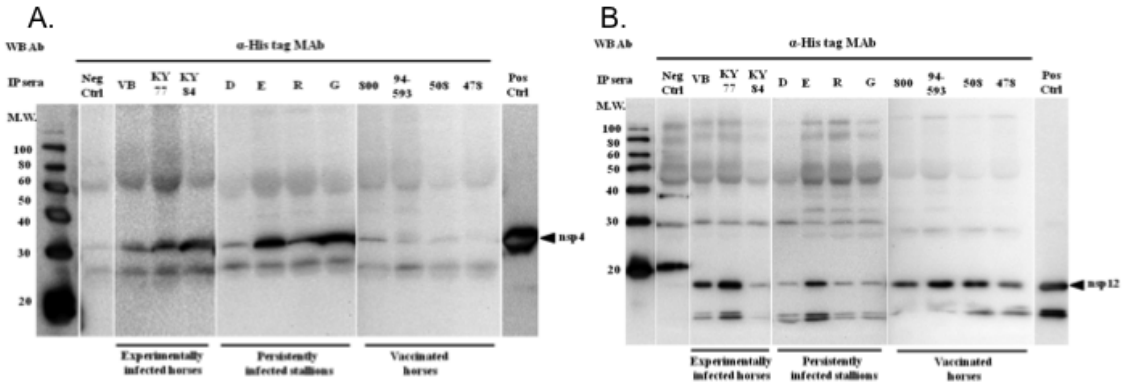

Figure 9.5. Immunoprecipitation analyses of (A) nsp4 and (B) nsp12 using sera from experimentally infected, vaccinated and persistently infected horses. Nsp4 and nsp12 expressed in *E. coli* were immunoprecipitated using equine sera and detected by Western immunoblotting analysis with the anti-His monoclonal antibody. For molecular weight markers and controls, see the legend to Figure 9.3.

9.5. DISCUSSION

In this study, we generated recombinant EAV nsp1 to nsp12 using mammalian and *E. coli* expression systems. Most of the proteins migrated at the predicted molecular size as indicated in Tables 9.2 and 9.3. However, several nsps expressed in mammalian cells showed nonspecific protein bands on the membrane that were also recognized by protein-specific rabbit antisera, e.g. nsp2, nsp3, nsp4, nsp9 and nsp11 (Figure 9.1.B). This observation was just considered to be background bands or possible instability/degradation of expressed proteins. Previous studies have shown that nsp2, nsp3 and nsp5 contain predicted membrane-spanning domains which may serve to anchor nsps to the modified intracellular membranes with which the viral replication complex is presumed to be associated [87]. Incomplete disassociation of these nsps from cellular proteins during SDS-PAGE could have caused some of these extra bands with higher molecular weights. Consistent with previous reports, the recombinant nsp4 (predicted as 21 kDa and 25 kDa with modifications in mammalian and bacterial expression systems, respectively) migrated as a protein of approximately 30 kDa, a phenomenon described as aberrant migration of this protein during SDS-PAGE [114,465]. Additionally, the two bands of nsp4 visible by Western immunoblotting analysis using nsp4-specific rabbit antisera have been reported earlier [465].

The difficulties encountered during expression of recombinant nsp2, nsp5, nsp9 and nsp11 and purification of nsp3 and nsp6 in *E. coli* were likely related to the inherent toxicity, codon-usage differences between bacterial and mammalian cells and/or misfolding of these proteins when expressed from the pQE-TriSystem vector. Although expression of nsp3 and nsp6 was confirmed in pilot experiments, these proteins could not be recovered by Ni-NTA purification. It is plausible that misfolding of these proteins masked their 8× His-tag and prevented binding to the Ni-NTA resin. Specifically, nsp2 and nsp5, which showed high immunoreactivity against equine sera when expressed in mammalian cells, may need to be expressed using a different expression vector and *E. coli* strain to generate recombinant proteins that could be used in diagnostic assays in the future.

Previous studies on characterization of the equine humoral immune response to EAV focused mainly on detection of antibodies to major viral structural proteins,

especially GP5, M and N proteins [148,150,221,254,268,274,277,306,462]. To further characterize the host immune response to EAV proteins, individual recombinant nsps expressed in both mammalian and bacterial cells were immunoprecipitated with EAV antibody positive and negative sera and identified with individual protein specific monoclonal antibodies or protein-specific rabbit antisera by Western immunoblotting analyses. These viral proteins synthesized during early phase of infection in host cells are degraded in the cytoplasm by the proteasome, and the resulting peptides are translocated into the endoplasmic reticulum, where they are loaded onto major histocompatibilty complex (MHC) class molecules [281]. It has been suggested that during antigen processing, antigenic sites buried in native form, such as hydrophobic regions are exposed to the immune system and make them more immunogenic [466,467]. The data showed that nsp2, nsp4, nsp5, and nsp12 are the most immunogenic proteins among all twelve nsps (Table 9.1) and that horses tend to mount an immune response to these viral proteins. All three sera from experimentally infected horses consistently recognized nsp2, nsp4, nsp5, and nsp12. In contrast, the antibody response to nsp2, nsp4, and nsp12 in persistently infected stallions was somewhat variable. In addition, nsp5 was the only protein which consistently reacted with sera from carrier stallions. These data suggested that the serologic response of horses against nsps which clear the virus following acute infection might be different from that of persistently infected horses. It is possible that horses mount a strong immune response to viral nsps in the acute-phase (when virus replication is active) which remains until late convalescent-phase but decreases over time. In the presence of high titer neutralizing antibodies in the serum during persistent infection, EAV is harbored in the ampulla of the reproductive tract of the stallion [188]. Therefore, it could be postulated that virus replicates in immunologically privileged cells in the stallion's reproductive tract preventing (or reducing) the exposure of nsps to the host immune system. However, some of the nsps may still be able to induce a limited immune response during prolonged persistent infection in the reproductive tract of the stallion. Moreover, all nsps may not be equally immunogenic and this may also vary among different strains of EAV. This could explain the difference between serologic response to nsps in vaccinated animals as compared to the horses experimentally inoculated with more virulent field strains (VB, KY77, and

KY84 strains). The response of vaccinated horses with the MLV vaccine strain (ARVAC®) was also different from that of experimentally and persistently infected horses. Sera from vaccinated horses recognized nsp2 and nsp12 while nsp4 and nsp5 reacted very weakly or did not react at all. Furthermore, different horses may also respond differently to EAV nsps during infection. It has been previously shown that immune response to EAV structural proteins differ with the infecting virus strain and duration of infection [268]. The M protein was most consistently recognized by various serum samples, whereas the response to the N and GP5 proteins was variable [221,268].

Interestingly, the equine humoral immune response to nsp4 and nsp12 differed depending on whether the protein was expressed in mammalian or bacterial cells. Most sera, except for those from vaccinated horses, strongly reacted with nsp4 expressed in bacteria. However, none of the sera immunoprecipitated nsp4 when expressed in mammalian cells. Similarly, the equine sera from experimentally infected horses or persistently infected stallions were either only weakly immunoprecipitated or did not precipitate the nsp12 expressed in mammalian cells while they strongly reacted and immunoprecipitated the nsp12 expressed in *E. coli*. The reason for this difference in recognition of the same antigen expressed in a different expression system might be due to the failure of antigenic epitopes to be presented in their native form to be recognized by the equine antibodies. It is also possible that nsp4 and nsp12 proteins, when expressed in a mammalian expression system, are not processed properly or misfolded; this may lead to obscuring both the conformational and linear epitopes recognized by equine antibodies. However, the proteins expressed in *E.coli* are denatured during the purification process and this may well expose the linear epitopes recognized by equine antibodies and facilitate immunoprecipitation of both nsp4 and nsp12 proteins.

In porcine reproductive and respiratory syndrome virus (PRRSV) infection in pigs, nsp1, nsp2, and nsp7 were found to be the most immunogenic nsps of the virus [468,469,470]. Subsequently, PRRSV nsp1 α/β and nsp7, and also nsp2, have been explored as potential antigens for the development of serological diagnostic assays. However, our data strongly suggest that horses do not mount a strong humoral antibody response to EAV nsp1 and nsp7 as compared to pigs infected with PRRSV. In our hands, it appears that EAV nsp1 is toxic in both mammalian and bacterial cells as expression of

this protein was not highly efficient as compared to other nsps. Therefore, suboptimal antigen concentration provided for immunoprecipitation assay could have adversely affected the result. As in PRRSV, there is significant variation in EAV nsp2 [63,164]. However, unlike the PRRSV nsp2, until now, no B cell or T cell epitopes have been identified in this protein in the case of EAV [469,471,472].

The virus neutralization (VN) test is the OIE (World Animal Health Organization) prescribed regulatory test for serologic detection of EAV infection of the horse [292]. However, this assay is expensive, labor-intensive, and time-consuming to perform. Results of the assay tend to vary among laboratories when insufficient attention is paid to standardization of both test reagents and procedures. To address this problem, we previously developed a microsphere immunoassay (MIA) using recombinant structural proteins of EAV. However, the sensitivity and specificity of the assay was 92.6% and 92.9%, respectively, compared to the VN test [464]. In this current study, we identified the key EAV nsps recognized by horses during acute and persistent infection, as well as following vaccination. Thus, the recombinant nsps (nsp2, nsp4, nsp5, and nsp12) identified in this study in combination with the structural proteins could be used in a new MIA to further improve the specificity and sensitivity of the assay. Moreover, nsp5 could be a potential candidate to be used as antigen in a companion differential diagnostic test to distinguish horses vaccinated with current modified live virus vaccine (ARVAC®) from naturally infected horses. Once we develop this new MIA, it will be used to further characterize the antibody response to EAV by testing sequential serum samples from experimentally inoculated and vaccinated horses [224,327,328,331]. We also plan to evaluate this MIA with a large panel of equine sera determined to be positive and negative for EAV antibody by VN test.

In summary, data presented in this study showed that the equine humoral immune response to EAV nsps is directed against the nsp2, nsp4, nsp5, and nsp12. None of the horse sera recognized nsp1, nsp3, and nsp6 through nsp12 when recombinant antigens were used in immunoprecipitation assays. Among these proteins, nsp2 and nsp12 were consistently recognized by either experimentally and persistently infected horses or vaccinated horses. In contrast, nsp4 and nsp5 were recognized efficiently only by sera from experimentally and persistently infected horses but not by vaccinated horses.

Therefore, this study suggests that these antigens can be used for serodiagnostic testing of EAV infection. Incorporation of the immunogenic nsps in a new MIA, along with structural proteins as antigen, might greatly improve the sensitivity and specificity of the previously developed MIA. An improved MIA assay is already under development in our laboratory. Thus, a multiplex MIA including the most immunogenic structural and nonstructural proteins of EAV could become a potential alternative to the standard VN test.

SUMMARY OF DISSERTATION

The nature of the interaction between the virus and the host is cirtical not only for viral replication, but also in determining the virulence and pathogenesis of the pathogen concerned. The goal of this study was to better understand how cellular proteins interact with viral RNA or viral proteins, and the role they play in viral infection. Furthermore, it was hoped to characterize more clearly the mechanisms of EAV pathogenesis and viral persistence in stallions using contemporary molecular biology techniques and host genomic analysis via a genome-wide association study (GWAS).

The viremia that is present in horses acutely infected with EAV is primarily associated with the buffy coat cells in the blood (peripheral blood mononuclear cells [PBMCs]). Currently, detailed information of the target cells and the role of viral proteins in infection of PBMCs is lacking. A specific objective was to characterize the EAV target cell population in equine PBMCs and the interaction between the targe cell population and the virus. This was accomplished using two strains of EAV, the virulent Bucyrus (VB) strain and the attenuated modified live virus (MLV) vaccine strain of EAV. The VB strain of EAV primarily infects $CD14^+$ monocytes and a small subpopulation of $CD3^+$ T lymphocytes (predominantly $CD4^+$ T) as determined by dual-color flow cytometry. In contrast, the MLV vaccine strain of EAV has significantly reduced ability to infect $CD14^+$ monocytes and has lost its capability to infect $CD3^+$ T lymphocytes. **Using infectious cDNA clones of EAV and reverse genetic systems, it was shown that interactions between GP2, GP3, GP4, GP5 and M envelope proteins of the VB strain play a major role in determining the $CD14^+$ monocyte tropism while the tropism of $CD3^+$ T lymphocytes is determined by GP2, GP4, GP5 and M envelope proteins but not the GP3 protein.** This altered tropism correlated with amino acid variations mostly located in the ectodomain of major and minor envelope proteins of the virus which occurred during extensive cell culture passage of the Bucyrus strain of EAV; this resulted in the highly attenuated MLV strain. This may have direct and/or indirect effects on interaction with host cell receptor(s). Specifically, changes in the MLV genome could potentially influence its attachment and entry properties, as well as reducing viral replication and production of progeny virus in host lymphocytes. Infection of $CD14^+$ monocytes with EAV is perhaps not surprising in view of the fact that members of the

Arteriviridae family are monocyte/macrophage tropic; however, it provided the first evidence that $CD3^+$ T lymphocytes may play a role in the pathogenesis of EVA when horses are infected with virulent strains of EAV. During the course of this study, we found a clear difference among horses in terms of the susceptibility of their $CD3^+$ T lymphocytes to *in vitro* infection with the VB strain of EAV. Horses could be categorized into two groups, the first arbitrarily designated Group A were those in which almost one third of the monocytes along with $CD3^+$ T lymphocyte (mainly $CD4^+$ T cells) subpopulations were susceptible to infection with the VB strain of EAV. The second group designated Group B, were those in which monocyte susceptibility was only half that observed in Group A horses and all $CD3^+$ T lymphocyte subpopulations were resistant to EAV VB strain infection. Based on this finding, we had to presume that the horse's intrinsic genetic make-up may play a role in determining the clinical outcome of infection with EAV. To investigate the possible hereditary basis of this trait, we conducted a genome-wide association study (GWAS) using the Illumina Equine SNP50 chip to compare horses of susceptible or resistant phenotypes. **This study led to the identification of a common, genetically dominant haplotype associated with the putative equine susceptible phenotype in the region ECA11: 49572804-49643932. The presence of a common haplotype indicates that the trait occurred in a common ancestor of all four breeds that were studied, suggesting that it may be segregating among other modern horse breeds.** Subsequently, biological pathway analysis revealed several cellular genes within this region encoding proteins associated with virus attachment and entry, cytoskeletal organization and NF-κB pathways that may be associated with the trait responsible for the *in vitro* susceptibility/resistance of $CD3^+$ T lymphocytes to EAV infection. However, further studies are needed to investigate potential mechanisms that involve the roles of proteins encoded by genes located in this region of ECA11 in the virus life cycle and the host response to EAV infection. The findings from this study can help in developing working hypotheses to decipher novel mechanisms of viral immune evasion, viral pathogenesis, and establishment of persistent infection in stallions. Consistent with these findings, we hypothesized that the *in vitro* susceptibility of $CD3^+$ T lymphocytes to EAV infection correlates with the clinical responsiveness of horses following exposure to the virus. To test this hypothesis, we

selected horses that were either susceptible or resistant based on their *in vitro* $CD3^+$ T cell phenotype and challenged them with the recombinant VB strain of EAV. The study findings revealed a difference between the two groups of horses in terms of cytokine mRNA expression and evidence of possible increased frequency in clinical signs in individuals possessing the *in vitro* $CD3^+$ T cell resistant phenotype (Group B**). An inverse correlation was found between the *in vitro* susceptibility or resistance phenotype of $CD3^+$ T lymphocytes and the different clinical/cytokine expression responses observed in horses following infection with EAV. This was the first study to provide direct evidence of a correlation between variation in host genotype and phenotypic differences in terms of the extent of viral replication, nature of clinical signs and cytokine gene expression following infection with a recombinat virulent strain of EAV.** Determining the basis for differences in outcome to virus infection and cytokine gene expression in horses may be key in the animals's control of infection. We extended these studies by investigating the possible correlation between susceptibility of $CD3^+$ T lymphocytes to EAV infection and establishment of persistent infection in stallions. **Data from this study showed that stallions that possess the susceptible $CD3^+$ T lymphocyte phenotype to EAV infection may be at higher risk of becoming persistently infected compared to stallions that do not possess this phenotype.** Identification of specific gene(s) or a chromosome region associated with establishment of persistent infection is under investigation. Hopefully, findings from this study will allow us to develop a genetic diagnostic tool to predict stallions at higher risk of EAV persistence with the potential to reduce the reservoir of the virus and thereby restrict spread of the virus.

Based on the findings of studies conducted to date, there is evidence that both virus and host factors are likely to influence the clinical outcome of EAV infection. One of the major shortcomings of these studies, however, is failure to identify the small subpopulation(s) of $CD3^+$ T lymphocytes that are susceptible to infection with VB strain of EAV in PBMCs of Group A horses. Whether susceptibility of T lymphocytes to infection with the VB strain of the virus has a determining role in the pathogenesis of infection with this strain of EAV remains unknown at this time and warrants further investigation.

The host immune response facilitates viral clearance and is a key determinant of the outcome of infection. To investigate this in greater detail, a study was undertaken to determine the precise effect of EAV on the immune system of horses, innate and humoral immunities. Many viruses have evolved strategies to counteract key elements of the type I interferon (IFN) response and successfully prevent development of an antiviral environment in the host that would inhibit their persistence in their host. This strategy of evading the host immune system is commonly seen in persistent viral infections. *In vitro* investigations in an equine endothelial cell line provided evidence that EAV inhibits type I IFN production in infected cells. **Among EAV nonstructural (nsps), nsps 1, 2 and 11 had the capability to inhibit type I IFN activity. Of these three nsps, nsp1 appeared to have the strongest inhibitory effect on IFN synthesis. Collectively, these data demonstrated that failure to induce type I IFN in EAV infected cells may allow the virus to subvert the equine innate immune response and facilitate establishment of persistent infection in the stallion.** Further studies are needed, however, to map the exact step(s) at which EAV nsp1 protein acts on the IFN induction pathway.

It is a fundamental fact that the host immune system is capable of detecting invading foreign pathogens. Until now, research emphasis has mostly been on the humoral immune response to the structural proteins of EAV. One of the final objectives of these studies, therefore, was to evaluate the humoral immune response of horses to each of the nsps following EAV infection. **Among 12 nsps, nsp2, nsp4, nsp5 and nsp12 were immunoprecipitated by most of the sera from experimentally or persistently infected horses, while sera from vaccinated horses did not react with nsp5 and only reacted weakly with nsp4. However, serum samples from vaccinated horses were able to immunoprecipitate nsp2 and nsp12 proteins consistently. Information from this study hopefully will assist ongoing efforts to develop improved methods for the serologic diagnosis of EAV infection in horses.**

The host-virus interaction is in a continuous process of evolution where both entities develop strategies to overcome the effects of the other. The outcome of interaction between EAV and the horse have evolved such that the virus can persist in the stallion's reproductive tract despite the presence of high neutralizing antibody titers in its bloodstream. In the range of studies that were carried out, we tried to integrate aspects of the interaction of EAV with

its host. Our focus was initially on the virus and then on those aspects of the host that are important for the successful interaction of the virus with the host. Special attention was paid to those aspects that are important for clearance of virus from the host. The data presented in this dissertation suggest new directions for future EAV research using genomic and proteomic approaches to study host cell factors involved in EAV attachment and entry and establishment of persistent infection in the stallion.

APPENDIX 1

List of Abreviations

aa	Amino acid
AMΦ	Alveolar macrophage
Asn	Asparagine
BHK-21	Baby hamster kidney-21
BMΦ	Blood macrophage
bp	base pair
CAVV	Cavally virus
CD	Cluster of differentiation
cDNA	Complementary deoxyribonucleic acid
CF	Complement fixation
CMI	Cell mediated immunity
CoV	Coronavirus
CPE	Cytopathic effect
CTL	Cytotoxic T lymphocyte
Cys	Cysteine
DMV	Double membrane vesicle
DNA	Deoxyribonucleic acid
Dpi	Days post infection
Ds	Double stranded
E	Envelope protein
EAV	Equine arteritis virus
ED	Equine dermal
EDTA	Ethylenediaminetetraacetic acid
EEC	Equine endothelial cells
eGFP	Enhanced green fluorescence protein
ELISA	Enzyme linked immunosorbent assay
EPAEC	Equine pulmonary artery endothelial cells
ER	Endoplasmic reticulum
ERGIC	ER-Golgi intermediate complex
EToV	Equine Torovirus
EU	European
EVA	Equine viral arteritis
GAV	Gill-associated virus

GFP	Green fluorescent protein
GP	Glycoprotein
GWAS	Genome-wide association study
HEK	Human embryonic kidney
HK	Horse kidney
IFN	Interferon
Ig	Immunoglobulin
IMP	Immunoprecipitation
IVT	*In vitro* transcription
kDa	kilodalton
LDV	Lactase dehydrogenase-elevating virus
M	Membrane protein
MAb	Monoclonal antibody
MDBK	Madin-Darby bovine kidney
MGB	Minor-groove binding
MIA	Microsphere immunoassay
MLV	Modified live virus
Mn	Manganese
MOI	Multiplicity of infection
mRNA	Messenger RNA
MW	Molecular weight
N	Nucleocapsid protein
NA	North American
NC	Nucleocapsid
NF-κB	Nuclear factor-kappa B
NMR	Nuclear magnetic resonance
Nsp	Nonstructural protein
NTPase	Nucleoside triphosphatase
OIE	World Organisation for Animal Health
ORF	Open reading frame
PAM	Pulmonary alveolar macrophage
PBMC	Peripheral blood mononuclear cells
PCP	Papain-like cysteine protease
PCR	Polymerase chain reaction
PFU	Plaque forming unit
PMO	Phosphorodiamidate morpholino oligomers
pp	Polyprotein

PPMO	Peptide-conjugated phosphorodiamidate morpholino oligomers
PRRS	Porcine reproductive respiratory syndrome
PRRSV	Porcine reproductive respiratory syndrome virus
qrRT-PCR	quantitative real-time reverse-transcription PCR
RdRp	RNA-dependent RNA polymerase
RFS	Ribosomal frameshift
RK	Rabbit kidney
RK-13	Rabbit kidney-13
rMLV	recombinant MLV
RNA	Ribonucleic acid
RT-PCR	Reverse transcription-polymerase chain reaction
rRT-PCR	Real time reverse transcription-polymerase chain reaction
rVBS	recombinant VB strain
SARS	Severe acute respiratory syndrome
SARS-CoV	Severe acute respiratory syndrome coronavirus
SDS-PAGE	Sodium dodecyl sulfate polyacrylamide gel electrophoresis
sg mRNA	Subgenomic mRNA
SHFV	Simian hemorrhagic fever virus
SNP	Single nucleotide polymorphism
ss	Single stranded
T reg	Regulatory T cells
TCF	Tissue culture fluid
TCID50	50% tissue culture infective dose
TRS	Transcription regulation sequence
UTR	Untranslated region
VB	Virulent Bucyrus
VBS	Virulent Bucyrus strain
VI	Virus isolation
VN	Virus neutralization
VNT	Virus neutralization test
VRP	Venezuelan equine encephalitis virus replicon particle
YHV	Yellow head virus
ZBD	Zinc-binding domain
ZF	Zinc finger

APPENDIX 2

Experimental Methods

TISSUE CULTURE MEDIA RECIPES

EPAEC (EQUINE PULMONARY ARTERY ENDOTHELIAL CELLS):

DMEM (with high glucose [4.5 g/L], without L-glutamine; Cellgro 15-013-CM)	1L
Fetal bovine serum (FBS, 10%; Hyclone SH30396.03)	110mL
Penicillin and streptomycin (10,000 U/ml and μg/ml; Gibco 15140-122)	11mL
0.1 mM Non-essential amino acids (10 mM [100X] Gibco 11140-050)	11mL
2 mM L-glutamine (200 mM [100X] Gibco 25030)	10 mL

HEK293T (HUMAN EMBRYONIC KIDNEY 293T CELLS):

DMEM (with high glucose [4.5 g/L], without L-glutamine; Cellgro 15-013-CM)	500 mL
Fetal bovine serum (FBS, 10%; Hyclone SH30396.03)	50 mL
Penicillin and streptomycin (10,000 U/ml and μg/ml; Gibco 15140-122)	5 mL
200 mM L-glutamine (200 mM [100X] Gibco 25030)	5 mL

A594 (HUMAN ALVEOLAR BASAL EPITHELIAL CELLS: ATCC CAT. # CCL-185):

F-12 Kaighn's modification (Hyclone SH30526.01)	500 mL
Fetal bovine serum (FBS, 10%; Hyclone SH30396.03)	50 mL
Penicillin and streptomycin (10,000 U/ml and μg/ml; Gibco 15140-122)	5 mL

PBMC (PERIPHERAL BLOOD MONONUCLEAR CELLS):

RPMI 1640 (without L-glutamine; Gibco 21870)	500 ml
Fetal bovine serum (FBS, 10%; Hyclone SH30396.03)	50 mL
Penicillin and streptomycin (10,000 U/ml and μg/ml; Gibco 15140-122)	5 mL
200 mM L-glutamine (200 mM [100X] Gibco 25030)	5 mL
55 μM 2-mercaptoethanol (55 mM [1000X]; Gibco 21985-023)	0.5 ml

RABBIT KIDNEY 13 HIGH PASSAGE AND LOW PASSAGE (P207) FROM BILL MCCOLLUM, UKY:

Laboratory Designated Name: RK-13 HP# (High passage), RK-13 LP# (Low passage)

EMEM (With Earle's salts and L-glutamine; GIBCO 11095-080	500 ml
Cosmic calf serum 10% (Hyclone SH30087.03)	50 ml
Penicillin and Streptomycin (GIBCO 15140-122)	5 ml

RABBIT KIDNEY 13 (ATCC CATALOG NO. CCL-37):

Laboratory Designated Name: CCL-37-RK13

Minimum Essential Medium (EMEM;	
With Earle's salts and L-glutamine; GIBCO 11095-080	500 ml
Fetal Bovine Serum 10% (Hyclone SH30396.03)	50 ml
Penicillin and Streptomycin (GIBCO 15140-122)	5 ml
1.0 mM Sodium pyruvate (100 mM [100x] GIBCO 11360-070)	5 ml
0.1 mM Nonessential amino acids (10 mM [100x] GIBCO 11140-050)	5 ml

RABBIT KIDNEY 1 (ATCC CATALOG NO. CCL-106):
Laboratory Designated Name: LLC-RK1

Medium 199 (GIBCO 11150-059)	500 ml
Horse serum 10% (Hyclone SH30074.03)	50 ml
Penicillin and Streptomycin (GIBCO 15140-122)	5 ml

VERO 76 (ATCC CATALOG NO. CRL-1587):
Laboratory Designated Name: VERO 76

DMEM (With high glucose [4.5g/L] and L-glutamine; GIBCO 11965-092)	500 ml
Fetal Bovine Serum 10% (Hyclone SH30396.03)	50 ml
Penicillin and Streptomycin (GIBCO 15140-122)	5 ml

VERO C1008 (ATCC CATALOG NO. CRL-1586):
Laboratory Designated Name: VERO C1008

EMEM (With Earle's salts and L-glutamine; GIBCO 11095-080	500 ml
Fetal Bovine Serum 10% (Hyclone SH30396.03)	50 ml
Penicillin and Streptomycin (GIBCO 15140-122)	5 ml
1.0 mM Sodium pyruvate (100 mM [100x] GIBCO 11360-070)	5 ml
0.1 mM Nonessential amino acids (10 mM [100x] GIBCO 11140-050)	5 ml

BHK-21 (C-13; ATCC CATALOG NO. CCL-10):
Laboratory Designated Name: BHK-21

EMEM (With Earle's salts and L-glutamine; GIBCO 11095-080	500 ml
Fetal Bovine Serum 10% (Hyclone SH30396.03)	50 ml
TPB (Tryptose phosphate broth)	50 ml
Penicillin and Streptomycin (GIBCO 15140-122)	5 ml

EQUINE DERM CELLS (NBL-6; ATCC CATALOG NO. CCL-57):
Laboratory Designated Name: ED (Equine derm)

Minimum Essential Medium (EMEM;	
With Earle's salts and L-glutamine; GIBCO 11095-080	500 ml
Fetal Bovine Serum 10% (Hyclone SH30396.03)	50 ml
Penicillin and Streptomycin (GIBCO 15140-122)	5 ml
1.0 mM Sodium pyruvate (100 mM [100x] GIBCO 11360-070)	5 ml
0.1 mM Nonessential amino acids (10 mM [100x] GIBCO 11140-050)	5 ml

MDBK (BOVINE KIDNEY CELLS; ATCC CATALOG NO. CCL-22)
Laboratory Designated Name: MDBK

EMEM (With Earle's salts and L-glutamine; GIBCO 11095-080)	500 ml
Horse Serum 10% (Hyclone SH30396.03)	50 ml
Penicillin and Streptomycin (GIBCO 15140-122)	5 ml
1.0 mM Sodium pyruvate (100 mM [100x] GIBCO 11360-070)	5 ml
0.1 mM Nonessential amino acids (10 mM [100x] GIBCO 11140-050)	5 ml

FETAL EQUINE KIDNEY PRIMARY CELLS (FEK-XX1) FROM BILL MCCOLLUM, UKY
Laboratory Designated Name: FEK

EMEM (With Earle's salts and L-glutamine; GIBCO 11095-080)	500 ml
Fetal Bovine Serum 10% (Hyclone SH30396.03)	50 ml
Penicillin and Streptomycin (GIBCO 15140-122)	5 ml

EQUINE PULMONARY ARTERY ENDOTHELIAL CELL MEDIUM (ECMM)
Laboratory Designated Name: EPAEC

DMEM (With high glucose [4.5g/L], *without* L-glutamine; Cellgro 15-013-CM)	1 L
Fetal Bovine Serum 10% (Hyclone SH30396.03)	110 ml
Penicillin and Streptomycin (GIBCO 15140-122)	11 ml
L-glutamine (200 mM; GIBCO	10 ml
0.1 mM Nonessential amino acids (10 mM [100x] GIBCO 11140-050)	11 ml

CELL LINES GROWN WITH EMEM 10% FSCS IN INCUBATOR WITHOUT CO_2

BHK-21 (Baby Hamster Kidney 21: C-13; ATCC Cat. # CCL-10); RK-13 (Rabbit Kidney 13 Low passage [P194-P204] from Bill McCollum, KY); RK-13 (Rabbit Kidney 13 High passage [P399-P409] from Bill McCollum, KY); Vero 76 (African Green Monkey Kidney: ATCC Cat. # CRL-1587); MDBK (Bovine Kidney cells: ATCC Cat. # CCL-22); ED (Equine Dermal cells: NBL-6; ATCC Cat. # CCL-57)

LARGE SCALE (10 L) CELL CULTURE MEDIA, EMEM 10% FSCS:

Materials

1. EMEM (NEAA, L-glutamine; Mediatech #50-011-PB; 10L/bt) — 10L/bottle
2. Ferritin supplemented calf serum (FSCS; Hyclone SH30072.03) — 1000 mL
3. Penicillin and streptomycin (10,000 U/ml and µg/ml; Gibco 15140-122) — 100 mL
4. Fungizone (Sigma A-9528, one vial) — 10 mL
   - Fungizone — 50 mg
   - Sterile distilled water — 50 ml

   Dissolve fungizone in dH_2O and dispense in 10 ml aliquots. Store at -20°C. Unreconstituted vial should be stored at 4°C.
5. Sodium bicarbonate ($NaHCO_3$; Sigma Cat. # S5761-500g) — 6 g
6. Glass fiber prefilter (Millipore Cat. # AP2012450)
7. Durapore® membrane filters (045 µm; Millipore Cat. # HVLP14250)
8. 12 L bottle and stir bar

Method

EMEM	96.1g
$NaHCO_3$	6.0 g
Penicillin/Streptomycin	100 ml
Fungizone (Amphotericin 1,000µg/ml)	10 ml
Serum –ferritin supplemented calf serum (FSCS)	1000 ml
dH2O (tissue culture grade water)	q.s. to 10,000 ml

1. Add 8 L dH2O to 12 L bottle with stir bar.
2. Place on stirrer/hotplate and turn stirrer to setting #3.
3. Add EMEM bottle (rinse twice with water) and mix until dissolved, about 15 min.
4. Add sodium bicarbonate (color should change from yellow to red), penicillin/streptomycin (p/s), fungizone (f), and serum (rinse each container twice with water).
5. Final concentration of penicillin/streptomycin 100 U/ml and 100µg/ml and fungizone 1 µg/ml.
6. Add water to 10 L and mix 5 min.
7. In cell culture room, filter through sterile Millipore filter unit using a prefilter. Dispense 1 L/sterile 1 L bottle.
8. Perform sterility check. Store at 4°C.

CARBOXYMETHYLCELLULOSE (CMC) OVERLAY MEDIA (1.3X EMEM 10% FSCS):

Materials

1. Carboxymethylcellulose, medium viscosity (Sigma C-4888) 6.0 g
2. Distilled water 140 ml

Method

1. Add water to a 1 L bottle, swirl while adding 0.75% carboxymethylcellulose (CMC) and then shake if necessary.
2. Let stand overnight at room temperature (shake occasionally).
3. Autoclave for 20 min at 121°C (liquid setting).
4. When cooled to approx. 40°C, add 1.3X EMEM 10% FSCS to the 800 ml mark.

1.3X EMEM 10% FSCS:

EMEM	96.1g
$NaHCO_3$	6.0 g
Penicillin/Streptomycin	100 ml
Fungizone (Amphotericin 1,000µg/ml)	10 ml
Serum –ferritin supplemented calf serum (FSCS)	1000 ml
dH2O (tissue culture grade water)	q.s. to 7,800 ml

Prepare same as for EMEM 10% FSCS except start with 6 L dH2O and q.s. to 7.8 L.

5. Perform sterility check. Store at 4°C.
6. Before using, add 0.8 ml gentamicin/bottle (working concentration – 50 µg/ml).

VIRUS TRANSPORT MEDIUM:

Hanks's Balanced Salt Solution w/ Phenol Red 1X (Invitrogen; 14170112)	500 ml
HEPES Buffer (final concentration 25 mM; Invitrogen; 15630080)	20 ml
Bovine Serum Albumin V (final concetration 0.5%; Sigma: A9647)	2.5 g
Antibitic-Antimycotic (100X, Peniillin, Steptomycin & Amphotericin B; Invitrogen; 15240112)	5 ml
Gentamicin Sulfate (final concentration 250 mg/L) Cellgro; 30-005-CR	2.5 ml

NET BUFFER (PH 7.5) FOR RESUSPENSION OF VIRUS PELLET:

Materials

50 mM Tris hydrochloride (500 ml dH_2O)	3.938 g
50 mM Tris base (500 ml dH_2O)	3.029 g
5 mM EDTA	0.95 g
150 mM NaCl	4.383 g

Method

1. Add Tris base to Tris-hydrochloride until the mixture reaches pH 7.5. (Add about 100ml of 50mM Tris-Base to 500ml of 50mM Tris-HCl to get pH 7.5)
2. Add 5 mM EDTA and 150 mM NaCl to above 50 mM Tris-HCl pH 7.5
3. Filter and store at 4°C.

DULBECCO'S PHOSPHATE-BUFFERED SALINE (PBS):

PBS (Gibco 21600-069)	95.5 g (1 bottle)
Sterile distilled water	q.s. to 10,000 ml

1. Add 9 L dH_2O to 12 L bottle with stir bar. Place on stirrer/hotplate and turn stirrer to setting #3.
2. Add PBS bottle (rinse twice with water) and mix for 10 min.
3. Add 800 ml to each 1 L bottles. Autoclave for 20 min at 121°C (liquid setting).
4. Cool to room temperature before tightening caps and labeling. Perform sterility check. Store at room temperature.

TRYPSIN EDTA SOLUTION:

PBS (sterile 1X)	180 ml
Trypsin EDTA (no phenol red [10X]; Gibco 15400-054)	20 ml

FREEZING MEDIA:

Dimethylsulfoxide (DMSO; Sigma D-2650)	10%
EMEM 10% FSCS	90%

Or

Recovery™ Cell Culture freezing medium (Gibco; 12648-010)

GUINEA PIG COMPLEMENT:
100 ml/bottle, (Rockland Cat # C300-0100). Thaw and dispense (on ice) into 1 or 2 ml volumes and store at -70°C.

MISCELLANEOUS:

0.5% Trypsin EDTA (no phenol red [10X]; Gibco 15400-054)
Phosphate buffered saline (PBS, pH 7.4, without calcium chloride/magnesium chloride; Gibco 10010)
Dulbecco's Phosphate buffered saline (PBS 10L/bottle, Gibco 10010)
HEPES buffer solution (1M; Gibco 15630)

ANTIBIOTICS FOR CELL CULTURE

Gentamicin:
Gentamicin sulfate, 50 mg/ml, 10 ml/vial **(**Mediatech 30-005-CR). Store at 4°C.

Pen-Strep:
Penicillin and streptomycin (10,000 U/ml and µg/ml; Gibco 15140-122)

Antibiotic-Antimycotic:
Anti-Anti (100X; Gibco 15240)

Fungizone:
Amphotericin B Solubilized (Sigma A-9528)

BACTERIAL MEDIA RECIPES

LIQUID MEDIA

LB Medium (Luria-Bertani Medium; 500 ml):

Deionized water	500 ml
Bacto-tryptone	5 g
Bacto-yeast extract	2.5 g
NaCl	5 g

1. Stir until the solutes have dissolved. Adjust the pH to 7.0 with 5N NaOH.
2. Sterilize by autoclaving for 20 minutes on liquid cycle.

Psi Broth (500 ml):

Bacto-tryptone	5.0 g
Bacto-yeast extract	2.5 g
NaCl	2.5 g
4 mM MgSO4	
10 mM KCl	
dH2O	to 500 ml

1. Autoclave liquid cycle 30 min.

MEDIA CONTAINING AGAR

LB Agar Plates:

Deionized water	500 ml
Bacto-tryptone	5 g
Bacto-yeast extract	2.5 g
NaCl	5 g

1. Prepare LB medium according to the above recipe. Just before autoclaving, add 7.5 g of Bacto agar. Sterilized by autoclaving for 20 minutes on liquid cycle.
2. When the medium is removed from the autoclave, swirl it gently to distribute the melted agar throughout the solution (need to be very careful, the media may boil over when swirled). Allow the medium to cool to 45-50^{0}C before adding antibiotics*.
3. To avoid air bubbles, mix the medium by swirling. Pour 20-25 ml of medium in a petri dish (use the tissue culture hood and fluorescent light should be off).
4. When medium has hardened completely, invert the plates and wrap in aluminum foil and store them at 4°C until needed. The plates should be removed from storage 1-2 hours before they are used and allow them to dry.

*Antibiotics solutions

Antibiotic	**Working concentration**
Ampicillin	50 μg / ml
Streptomycin	50 μg / ml
Tetracycline	50 μg / ml
Kanamycin	50 μg / ml
Carbenicillin	60 μg / ml
Chloramphenicol	170 μg / ml

Stock solutions should be stored at -20^{0}C. Avoid repeated freeze thawing and exposure to light. Magnesium ions are antagonists of tetracycline. Use media without magnesium salts for selection of bacteria resistant to tetracycline.

STORAGE MEDIA FOR BACTERIA

Cultures Containing Glycerol:

1. Aliquot 0.85 ml of bacterial culture in to a freezing vial and add 0.15 ml of sterile glycerol (sterilized by autoclaving for 20 minutes on liquid cycle). Vortex the culture to disperse glycerol evenly. Freeze the culture in ethanol-dry ice or liquid nitrogen, and then transfer the tube to -70°C.
2. To recover the bacteria, scrape the frozen surface of the culture with a sterile inoculating needle, and then immediately streak the bacteria that adhere to the needle onto the surface of an LB agar plate containing the appropriate antibiotics. Incubate the plate at 37°C. Return the frozen culture to storage at -70°C.

COMMONLY USED SOLUTIONS AND BUFFERS FOR MOLECULAR BIOLOGY

0.5 M EDTA (pH 8.0)

Deionized water	115 ml
EDTA (di-sodium)	27.918 g
5N NaOH	15,825 µl

Bring the volume to 150 mls with deionized water

5.0 M Sodium chloride

29.22 g of NaCl in 100 mls of distilled water

10% SDS

10 g in of SDS in 100 mls of deionized water

3.0 M Sodium acetate (pH 5.2)

Dissolve 24.609 g of sodium acetate in 60 mls of deionized water. Adjust the pH to 5.2 with glacial acetic acid (approximately 25.6 mls). Bring the volume to 100 mls with deionized water.

10 M Ammonium Acetate (50 ml)

Ammonium acetate	38.5 g
Deionized water to	50 ml

1 M $MgCl_2$ (100 ml):

$MgCl_2$ $6H_20$	20.3 g
Deionized water to	100 ml

1 M Dithiothreitol (DTT; 10 ml)

DTT	1.55 g
10 mM Sodium acetate (pH 5.2) to	10 ml

Store at -20^{0}C

1M Tris HCl (pH 8.0)

Tris HCl	Tris base	Molarity
4.44 g / l	2.65 g / l	0.05 M
88.8 g / l	53.0 g / l	1.0 M
8.88 g / 100 mls	5.30 g / 100 mls	1.0 M
17.76 g / 200 mls	10.6 g / 200 mls	1.0 M

1M Tris HCl (per liter)

Tris Base 121.1g

Add deionized water to 800 ml

Desired pH	Volume of HCl
pH 7.4	70 ml
pH 7.6	60 ml
pH 8.0	42 ml

Add deionized water to 1 liter

TE BUFFER

pH 8.0
10 mM Tris HCl (pH 8.0)
1 mM EDTA (pH 8.0)

pH 7.6
10 mM Tris HCl (pH 7.6)
1 mM EDTA (pH 8.0)

pH 7.4
10 mM Tris HCl (pH 7.4)
1 mM EDTA (pH 8.0)

TAE (Tris-acetate; 50X concentrated stock solution [per liter])

Tris base	242 g
Glacial acetic acid	57.1 ml 0.5
0.5 M EDTA (pH 8.0)	100 ml
Deionized water	q.s.

Working concentration 1X (dilute 10 ml in 490 ml of deionized water)

Proteinase K 2X Buffer

Reagent	**Final concentration**	**To make 100 mls of buffer**
Tris HCl (pH 8.0)	0.2 M	20 ml of 1.0 M Tris HCl (pH 8.0)
NaCl	0.3 M	6.0 ml of 5.0 M NaCl
EDTA (pH 8.0)	25 mM	5.0 ml of 0.5 M EDTA (pH 8.0)
SDS	2.0%	20 ml of 10% SDS
Deionized water		49 ml

Ethidium Bromide (EtBr; 10 mg/ml)

1. Add 1 g of EtBr to 100 ml of deionized water.
2. Stir on a magnetic stir for several hours to ensure that the dye has dissolved.
3. Wrap the container in aluminum foil or transfer the solution to a dark bottle and store at room temperature.
4. Final concentration to be used: 0.5 µg/ml

Method

1. EtBr in agarose: 5.0 µl of EtBr (10 µg/µl) solution per 100 ml of agarose
2. EtBr staining solution (1× TAE with 0.5 µg/ml EtBr): 25 µl of EtBr stock solution in 500 ml of 1× TAE buffer

Gel Loading Buffer (6X)
0.25% bromophenol blue (MW 691.9)
30% glycerol
Dissolved in 1X TAE solution

To make 40 ml 6X loading buffer:

0.25% bromophenol blue (MW 691.9)	0.1 g
30% glycerol	12 ml
1X TAE solution	to 40 ml

Preparation of 25 bp DNA ladder (Invitrogen Cat. # 10597-011)

100 bp DNA ladder (1 µg/µl)	50µl
6× loading buffer	100 µl
Nuclease free water	450 µl

Preparation of 100 bp DNA ladder (Invitrogen Cat. #)

100 bp DNA ladder (1 µg/µl)	50µl
6× loading buffer	100 µl
Nuclease free water	450 µl

Preparation of 1 kb plus DNA ladder (Invitrogen Cat. # 15615-024)

1 kb plus DNA ladder (1 µg/µl)	50 µl
6× loading buffer	100 µl
Nuclease free water	450 µl

Preparation of low DNA mass ladder (Invitrogen Cat. # 10068-013)

Low DNA mass ladder	100 µl
6× loading buffer	100 µl
Nuclease free water	400 µl

Preparation of PCR products

PCR products	10 µl
6× loading buffer	2 µl

Preparation of PCR products to estimate concentration

PCR products	2 µl
6× loading buffer	2 µl
Nuclease free water	8 µl

BUFFERS AND REAGENTS FOR WESTERN IMMUNOBLOTTING

10X SDS-PAGE RUNNING BUFFER (4 LITERS)

Glycine	580 g
Tris base	120 g
SDS	40 g
Distilled water to	4 liters

TRANSFER BUFFER FOR WESTERN IIMMUNOBLOTTING (FOR PROTEINS <80,000 M.W)

	1 Liter	4 Liters
Tris base 25 mM	2.9 g	11.6 g
Glycine 190 mM	14.5 g	58.0 g
Methanol 20%	200 ml	800 ml

Make up to 1 liter or 4 liters with distilled water (800 or 3200 mls)

WASHING BUFFER FOR WESTERN IMMUNOBLOTTING (TBS-T/ TRIS BUFFERED SALINE WITH 0.05% TWEEN 20; pH 7.6)

	1 Liter	4 Liters
Tris base	2.42 g (20 mM)	9.68 g
NaCl	8.0 g (137 mM)	32.0 g
6N HCl	3.8 ml	10.4 ml
Tween 20 (0.05%)	500 µl	2 ml
Deionized water to	1 liter	4 liters

ANTIBODY DILUTION BUFFER (ADB) FOR WESTERN IMMUNOBLOTTING

Nonfat dry milk	10 g
Sodium azide (NaN_3)	0.1 g
NaCl	9.0 g
Na_2HPO_4	4.5 g
NaH_2PO_4	0.5 g
PBS (1X)	1 L

AVIDIN-HRP CONJUGATE DILUTION BUFFER IN PBS FOR WESTERN IMMUNOBLOTTING

PBS (1X)	500 ml
1% Nonfat dry milk	5g
0.05% Tween 20	250 µl

BLOCKING AGENT FOR WESTERN IMMUNOBLOTTING

5% Nonfat dry milk in TBS-T (25 g for 500 ml)
(Use nonfat dry milk for horse serum to reduce the high background. Generally BSA can be used as a blocking agent for western immunoblotting).

MOLECULAR WEIGHT MARKERS AND SAMPLE BUFFER

BenchMark™ Pre-stained protein ladder (Invitrogen; Cat. #10748-010)

MagicMark™ XP Western protein standard (20-220kDa; Invitrogen; Cat. #LC5602)

Lane Marker Reducing sample buffer (5X) (Thermo Scientific Pierce; Cat. # 39000)

Laemmli sample buffer (2X) (BioRad; Cat. # 161-0737)

SOLUTIONS AND REAGENTS

1.5 M Tris HCl, pH 8.8 (BioRad; Cat. # 161-0798)

0.5 M Tris HCl, pH 6.8 (BioRad; Cat. # 161-0799)

SDS solution 10% w/v (BioRad; Cat. # 161-0416)

TEMED (N, N, N', N'-Tetra-methylethylenediamine) (BioRad; Cat. # 161-0801)

Blocking grade blocker non-fat dry milk (BioRad; Cat. # 170-6404)

COMMONLY USED STAINS

Crystal violet stain (stock solution):

Crystal violet (Mallinckrodt 8839)	12g
Methanol (Fisher A412-20)	600 ml

Crystal violet stain (working solution):

1 part of above stock solution
9 parts 10% buffered formalin (Fisher 23-245-685)

Coomassie Blue R protein stain

Brilliant blue R	0.41 g
Glacial acetic acid	50 ml
95% Ethanol	225 ml
Distilled water	225 ml

0.2% Trypan Blue for cell counting

Trypan blue	0.2 g
PBS	100 ml

Sterile filter.

ANTIBODIES

EAV SPECIFIC ANTIBODIES

Specificity	Clone	Species Origin	Specifity
EAV GP5	6D10	Mouse (MAb)	EAV GP5
EAV GP5	FP55	Rabbit	EAV GP5
EAV M	8887	Rabbit	EAV M
EAV N	3E2	Mouse (MAb)	EAV N
GP2	4033	Rabbit	EAV GP2
GP3	3509	Rabbit	EAV GP3
GP4	7466	Rabbit	EAV GP4
EAV nsp1	12A4	Mouse (MAb)	EAV nsp1
EAV nsp2	L3	Rabbit	EAV nsp2
EAV nsp3	98E	Rabbit	EAV nsp3
EAV nsp4	T1	Rabbit	EAV nsp4
Nsp7 and 8	D (M1)	Rabbit	EAV nsp7 and nsp8
α-EAV antibody[†]	11412	Rabbit	EAV

CONJUGATED-EAV SPECIFIC ANTIBODIES

Specificity	Clone	Species Origin	Conjugated Form	Specifity
Rabbit 8887 PB IgG	Rabbit polyclonal	Rabbit	Alexa Fluor 488	Prebleed
EHV-1	Monoclonal	Mouse (MAb)	Alexa Fluor 488	EHV-1
EAV anti-nsp1	12A4	Mouse (MAb)	Alexa Fluor 488	EAV nsp1
EAV anti-N	3E2	Mouse (MAb)	Alexa Fluor 488	EAV N

CELL SURFACE ANTIGEN

Specificity	Clone	Species Origin	Company	Catalog #	Species Specifity	Working Dilution	Isotype
B cells	E18A	Mouse	VMRD	E18A	Horse	50 µl at 15 µg/ml	IgG2a
B cells	6Dw19	Mouse	Cornell	N/A	Horse	50 µl/ 5×10^5 cells	IgG1
CD11a/CD18	CVS9	Mouse	Serotec	MCA1081	Horse	1:10	IgG1
CD13	CVS19	Mouse	Serotec	MCA1084	Horse	1:10	IgG1
CD14	Big10	Mouse	Alexis	ALX-804-496	Human, pig, dog, horse	1:10	IgG1
CD14-105		Mouse	Cornell	N/A	Horse	1:4	IgG1
CD172a (SWC3)	DH59B	Mouse	VMRD	DH59B	Many species	50 µl at 15 µg/ml	IgG1
CD2	Mac288	Rat	Serotec	MCA1278	Horse	1:200	IgG2a
CD3	UC F6G	Mouse	UCD	N/A	Horse	1:20 (1×10^6 cells/tube)	IgG1
CD4	CVS4	Mouse	Serotec	MCA1078	Horse	1:10	IgG1
CD4	BH2	Mouse	UCD	N/A	Horse	1:25 to 1:50 (2×10^6 cells)	IgG1
CD44	CVS18	Mouse	Serotec	MCA1082	Horse	1:10	IgG1
CD5	CVS5	Mouse	Serotec	MCA1079	Horse	1:10	IgG1
CD8	CVS8	Mouse	Serotec	MCA2385	Horse	1:10	IgG1
CD8	KH8	Mouse	UCD	N/A	Horse	1:25 to 1:50 (2×10^6 cells)	IgG1
CD8α	73/6.9.1	Mouse	VMRD	73/6.9.1	Horse	50 µl at 15	IgG3

						µg/ml	
MHC I	N/A	Mouse	VMRD	H58A	Horse		IgG2a
MHC II (HLA-DP)		Mouse	VMRD	H42A	Horse		IgG2a
CD163							

CELL SURFACE ANTIGEN- CONJUGATED ANTIBODIES

Specificity	Clone	Species Origin	Company	Catalog #	Isotype
CD3-FITC	CD3-12	Rat	Serotec	MCA1477F	IgG1
CD3-DyLight 649		Mouse	UCD	UC-F6G-DyLight	N/A
CD86 (B70/B7-2)-R-PE	IT2.2	Mouse	BD	555665	IgG2b, κ
CD206 (MMR)-PE	3.29B1.10	Mouse	Beckman	PN IM2741	IgG1
CD83-PE	HB15a	Mouse	Beckman	PN IM2218U	IgG2b
CD21-PE	N/A	Mouse	BD Pharmingen	555422	N/A

ISOTYPE CONTROL ANTIBODIES

Specificity	Clone	Species Origin	Company	Catalog #	Species Specifity	Isotype
IgG1	MOPC-21	Mouse	Sigma	M5284	Mouse	IgG1
IgG	Polyclonal	Rabbit	BD	550875	Rabbit	IgGl
IgG2a	G155-178	Mouse	BD	553454	Mouse	IgG2a, κ
IgG3	A112-3	Mouse	BD	553486	Mouse	IgG3, κ
PE-IgG1, κ	MOPC-21	Mouse	BD	556650	Mouse	IgG1, κ
IgG2a, κ	RTK275	Rat	Biolegend	400501		IgG2a, κ
Rabbit Ig Fraction	N/A	Rabbit	Dako	X0936	Rabbit	N/A

SECONDARY CONJUGATED ANTIBODIES

Specificity	Conjugate Form	Company	Catalog #
Goat $F(ab')_2$ Anti-mouse IgG1	FITC	SouthernBiotech	1072-02
Goat $F(ab')_2$ Anti-mouse IgG1	R-PE	SouthernBiotech	1072-09
Goat Anti-mouse IgG (H+L chain specific)	Texas Red® (TXRD)	SouthernBiotech	1031-07
Goat $F(ab')_2$ Anti-rat IgG (H+L chain specific)	FITC	SouthernBiotech	3052-02
Goat Anti-horse IgG (H+L chain specific)	FITC	Jackson ImmunoResearch	108-096-003
Goat Anit-guinea Pig IgG (H+L)	FITC	Vector Laboratories	FI-7000
Goat Anti-rabbit IgG (H+L)	Texas Red®	Vector Laboratories	TI-1000
Goat Anti-horse IgG (H+L)	Biotin	Vector Laboratories	BA-8000
Goat Anti-horse IgG (H+L)	Peroxidase	Jackson ImmunoResearch	108-035-003
Donkey $F(ab')_2$ Anti-goat IgG (H+L chain specific)	Allophycocyanin	Jackson ImmunoResearch	705-136-147

Goat Anti-mouse IgG	Alexa Fluor 488	Invitrogen	A31561
Goat Anti-rabbit IgG (H+L)	DyLight 549	KPL	072-04-15-16
Goat F(ab')$_2$ Anti-mouse IgG (H+L chain specific)	PE-Cy5.5	Caltag (Invitrogen)	M35018
Goat F(ab')$_2$ Anti-mouse IgG (H+L chain specific)	R-PE	Caltag (Invitrogen)	M35004-1
Goat F(ab')$_2$ Anti-rabbit IgG (H+L chain specific)	R-PE	Caltag (Invitrogen)	L43001
Goat F(ab')$_2$ IgG	Unlabeled (UNLB)	Southern Biotech	0110-01
Goat F(ab')$_2$ Anti-mouse IgG (H+L chain specific)	Alexa Fluor 488	Invitrogen	A11017
Goat F(ab')$_2$ Anti-mouse IgG (H+L chain specific)	R-PE	Invitrogen	A10543
Goat α-rabbit IgG (H+L)	Biotin-XX	Invitrogen	B2770
Goat α-mouse IgG (H+L)	Biotin-XX	Invitrogen	B2763
Goat α-rabbit IgG (H+L)	HRP	Southern Biotech	4050-05
Goat α-mouse IgG (H+L)	HRP	Southern Biotech	1031-05

ANTIBODIES FOR INTERFERON PATHWAY ANALYSIS

Specificity	**Clone**	**Species Origin**	**Company**	**Catalog #**
Anti-human interferon alpha	MMHA-2	Mouse	PBL InterferonSource	21100-1
Anti-human interferon beta	MMHB-3	Mouse	PBL Biomedical Laboratories	21400-1
Anti-human interferon gamma	MMHG-2	Mouse	PBL Biomedical Laboratories	21550-1
Anti-STAT1α p91	c-111	Mouse	Santa Cruz Biotechnology	Sc-417
Anti-phospho-STAT1 (Tyr701)			Cell Signaling	9171S
Anti-STAT2	A-7	Mouse	Santa Cruz Biotechnology	Sc-1668
Anti-phospho-STAT2 (Tyr689)		Rabbit	Upstate (Millipore)	07-224
Anti-NF-κB p65	F-6	Mouse	Santa Cruz Biotechnology	Sc-8008
Anti-phospho-NF-κB p65 (Ser276)		Rabbit	Santa Cruz Biotechnology	Sc-101749
Anti-IRF3	FL-425	Rabbit	Santa Cruz Biotechnology	Sc-9082
Anti-phospho-IRF3 (Ser398)		Rabbit	Upstate (Millipore)	07-581
Anti-human IL-2 Rα (CD25)		Goat	R&D	AF-223-NA
Anti-FLAG M2		Mouse	Agilent	200472-21
Anti-His antibody		Mouse	Invitrogen	372900
β-actin		Rabbit	Cell Signaling	4967

MITOGENS AND RECOMBINANT CYTOKINES

MITOGENS

Name	Description	Company	Catalog #
ConA	Concanavalin A	Sigma	C5275
LPS	Lipopolysaccharide	Sigma	L2630
PWM	Pokeweed mitogen	Sigma	L8777
PHA-P	Phytohemagglutinin	Sigma	L1168
PMA	Phorbol 12-myristate 13-acetate	Sigma	P1585
IL-2	Human Interleukin-2	Sigma	I2644

CYTOKINES

Name	Description	Company	Catalog #
reIL-2 (Cys141Ser)	Recombinant IL-2	R&D	1613-IL
Human TNF-α	Human tumor necrosis factor-α	Cell Signaling	8902SF
Equine IFN-α1	Equine interferon-α1	KingFisher Biotech	RP0142E-005

REAGENTS FOR INTRACELLULAR CYTOKINE STAINING USED FOR FLOW CYTOMETRY

Name	Description	Company	Catalog #
7-AAD	7-Aminoactinomycin D	Invitrogen	A1310
PI	Propidium Iodide	BD Pharmingen	51-66211E
Ionomycin	Ionomycin calcium salt	Sigma	I3909
Brefeldin A	Brefeldin A	Sigma	B5936

TISSUE CULTURE TECHNIQUES

PROPAGATION OF CONTINUOUS CELL LINES (RK-13, BHK-21 AND VERO CELLS)

Materials

1. Trypsin EDTA (keep in the water bath for few minutes, at 37^0C)
2. Confluent T-75 flask of cells
3. Appropriate cell culture medium

Method

1. Cells must be confluent (3-7 days old).
2. Pour off media.
3. Rinse cells 2-3 times with PBS (pH 7.4)
4. Add 1 ml (25 cm^2 flask), 2 ml (75 cm^2 flask), 4 ml (150 cm^2 flask) trypsin-EDTA, and rock gently for 30 seconds, then let the flask(s) sit at RT for 1 min
5. Pour off trypsin-EDTA (optional) and incubate the flask(s) another 7-8 minutes at 37°C.
6. Add appropriate amount of media EMEM + 10% FSCS + p/s/f for 1:5 split.

Once a week split cells: 1-150 cm^2 flask with confluent RK-13 cells is made up to approx. 300-335 ml EMEM 10% FSCS.

10 ml is added to 25 cm^2 flask,
30 ml to 75 cm^2 flask,
60 ml to 150 cm^2 flask

Note

To get a confluent monolayer within 24-36 hours transfer 2 ml of cell suspension into a T-75 flask and add 20 ml of complete medium to the flask (1:5 split).
Generally one T-75 flask is sufficient to seed five 96 well plates for neutralization or microtitration assays. For specific cell lines:

One T-75 flask of BHK-21 cells (confluent) is sufficient for 5-10, 96 well plates.
One T-75 flask of Vero cells (confluent) is sufficient for 3-4, 96 well plates.
One T-75 flask of RK-13 cells (confluent) is sufficient for 3-4, 96 well plates.

COUNTING OF CELLS

Manual method

1. Trypsinize the cells and add 10 ml of complete medium.
2. Centrifuge and resuspend the cells in 10 ml of complete medium.
3. Make a 1:10 dilution of cell suspension (100 µl in 900 µl of complete medium). Take 0.5 ml of diluted cell suspension into a snap cap tube and add 0.5 ml of 0.2% Trypan blue (1:2 dilution). Load the hemocytometer and count the cells in each of the four large squares. Some cells will be touching the outside borders. Count only those cells touching two of the outside borders (e.g., the upper and left). Determine the average number of cells per 10^{-4} ml (cells / ml = average number of cells per large square × 10^4 / ml × dilution factor).

Automated method using cell viability analyzer, ViCell XR (Beckman Coulter)

Materials

ViCell XR Quad reagent pak (Beckman Coulter Cat. # 383722)
4 ml sample cup 120/bag (Beckman Coulter Cat. # 383721)

1. Make 1 ml of 1:10 dilution of cell suspension (100 µl in 900 µl of complete medium)
2. Place 1 ml in a 4 ml sample cup (Beckman Coulter Cat. # 723908)

3. Place the sample cup in the machine (position 1-10)
4. Log in sample: position, sample ID, cell type, dilution factor. OK or next sample when done.
5. Start queue
6. "Camera image" provides cell image while counting and "Autosample queue" provides average of number of counted cells and viability

FREEZING CELLS

Materials

1. Freezing medium
2. Cells in log phase of growth
3. Trypsin EDTA (keep in the water bath for few minutes, at 37^0C)
4. Nalgene™ Cryo 1°C freezing container (Nalgene Cat. # 5100-0001)

Method

1. Pour off the media.
2. Add 3-4 ml of trypsin EDTA solution and rinse the cells (this is to remove the fetal bovine serum).
3. Add 3-4 ml of fresh trypsin EDTA solution and leave it for 3-4 min. (preferably at 37^0C) and bang on the flask to detach the cells from the surface.
4. Add 10-12 mls of complete medium (the medium contain 10% fetal bovine serum and this will inhibit trypsin) and pour into a 50 ml conical tube.
5. Centrifuge at 1100 or 1300 rpm (200 ×g) in a table top centrifuge for 5 minutes at 25^0C.
6. Aspirate the supernatant and resuspend the cell pellet in freezing medium at approx. 10^7 cells / ml. Freeze in 2 ml vials (1 ml per vial).
7. Freeze cells first in Nalgene™ Cryo 1°C freezing container with isopropanol at -80°C for 1 day
8. Transfer frozen cell vials to liquid nitrogen container

RECOVERY OF FROZEN CELLS

Material

1. Frozen cells (-70°C) in aliquots.
2. Growth medium

Method:

1. Rapid thawing of the cells is necessary. Thaw the cells in the water bath at 37°C, by swirling the tube (do not submerge the lid to avoid contamination of the cells).
2. Resuspend in 15 ml of growth medium and centrifuge at 1200 or 1300 rpm (200 ×*g*) in a table top centrifuge for 5 minutes at 25°C.
3. Aspirate the supernatant and resuspend the cells in 10 ml of growth medium. Transfer the cell suspension into a T-75 flask and add 10 ml of medium. Incubate at 37°C for 2-3 days.

ISOLATION OF EQUINE DERMAL FIBROBLASTS

Materials

Skin biopsy punches (5mm; Miltex Cat. # 33-35)
Hanks' balanced salt solution (HBSS; Gibco 14175)
PBS (pH 7.4)
Petri dishes and coverslips

Methods (modified from "Isolation and characterization of fibroblasts from diabetic patient with chronic vascular disease by Megan Francis, Illinois Institute of Technology [IIT])

1. Skin biopsy is harversted from chest area of horse
2. Place tissue in a sterile PBS and gentamicin (200 g/ml)

3. Each specimen is washed 3X with sterile HBSS (10mM) in Petri dishes and then turn with the skin side to the glass bottom for careful dissection. Small pieces of dermal connective tissue is harvested from the tissue.
4. The pieces are rinsed with HBSS and transferred to Petri dishes (65 mm × 15 mm). 4-5 pieces per dish. A smaller Petri dish (35 mm × 10 mm) is placed on the tissue pieces to keep the tissue in place during medium changes. To avoid floating of tissue, place a sterile coverslip on to each piece of tissue until fibroblasts get attached on the plate.
5. Wells are filled with pre-warmed DMEM containing 10% (v/v) FBS, 200 g/ml gentamicin, 1.25 g/ml fungizone and 2 mM gluctamine and incubated at 37°C, 5% CO_2.
6. After 2 days of culturing, the medium is replaced DMEM containing 10% (v/v) FBS, 50 g/ml gentamicin, and 2 mM glutamine.
7. Regular medium changes are performed every 2 days.
8. Cell growth is monitored with an inverted microscope.

ISOLATION OF PERIPHERAL BLOOD MONONUCLEAR CELLS FROM EQUINE BLOOD

Isolation of PBMCs

1. Collect blood via venipuncture into tubes with EDTA. Invert several times to mix and keep on ice at farm. Need one 15 ml conical tube w/Ficoll-Paque Plus for two 10 ml EDTA tubes.
2. Wait approximately 20~30 min. until RBC has settled down, leaving cloudy, yellow plasma layer on top of RBC layer.
3. Using a pipet, carefully aspirate plasma from EDTA tube, stopping aspiration when reach the RBC layer. Layer plasma on to 4ml Ficoll-Paque Plus in 15 ml conical tube. Cap tube when finished. Keep at room temperature and harvest all plasma layers from tubes collected from same horse.
4. Centrifuge at 500 g, 30 min, 20°C
5. Aspirate plasma layer above gradient down to cloudy band of PBMC. Discard into sterile beaker. With same pipet, aspirate PBMC at interface and place into 50 ml conical tube. Combine PBMC from 4 gradient (15 ml conical) tubes into one 50 ml tube for washing.
6. (<u>For platelets removal</u>) Add at least 3 volumes of PBS to the lymphocytes in the tube. Mix by pipetting.
7. Centrifuge at 100 g for 10 min at 20°C. Remove the supernatant.
8. Repeat same washing procedure once more.
9. Resuspend the pellet in adequate quantity of 10% cRPMI and count cells (<u>Approx. ten of 10 ml EDTA tubes give about 3 – 4 × 10^7 cells per ml</u>)

Separation of adherent and non-adherent PBMCs

1. Count the cells and resuspend them at 1 × 10^7/ml in complete RPMI (cRPMI). The objective is to get at least 2 × 10^8 PBMC to plate out into one of 150mm culture dish.
2. Place 20ml PBMC preparation into 1 × 150mm diameter, treated tissue culture dishes (1 × 10^7 PBMC/ml; total volume 25ml). Avoid over crowding of the plate to give enough space for the adherent cells to attach.
3. Incubate for 4h at 37°C/ 5% CO_2
4. Gently tilt the dish and aspirate off the supernatant containing non-adherent cells. Pellet non-adherent cells by centrifuging at 1900 rpm 15 min.
5. Wash adherent cells twice with 20ml of PBS (pH7.4). Rinse down the dish in 4 different angles (5ml/angle). Aspirate and save the PBS after each wash in a tube and pellet them down for cell counting.
6. Resuspend the cell pellets (non-adherent cells and PBS wash) in 10 ml of plain RPMI for each pellet and count cells.
7. To calculate approx. number of adherent cells, subtract the number of non-adherent cells and cells from PBS wash.

GENERATION OF MONOCYTE-DERIVED DENDRITIC CELLS

Materials

1. EDTA (purple top, 15% EDTA liquid, Kendall Cat. #8881 311743) vacutainer tubes
2. Ficoll-Paque Plus (GE Health Care, Cat. #17-1440-02)
3. 15ml centrifuge tubes (Corning, Cat. #430052)
4. Complete RPMI 1640 (Gibco, Cat. #21870)
5. Plain RPMI 1640 (Gibco, Cat. #21870)
6. 1× PBS (pH 7.4, Gibco, Cat. #10010)
7. Corning® treated tissue culture dishes (Corning, 100 mm Cat. # 430167, 150 mm Cat. # 430599)
8. Differentiation medium

a. Complete RPMI with GM-CSF (Sigma, Cat. #G5035) and IL-4 (R&D Cat. #1809-EL); see below

9. Nycoprep (Accurate Chemical, Cat. #AN-223510)
10. 6-well tissue culture plate (Costar, Cat. #3506)

Collection and processing of blood

1. Collect 300ml of horse blood in 30 EDTA containing vacutainer tubes (10ml × 30). Isolate PBMC by layering plasma onto Ficoll-Paque Plus. Plasma from 20ml of blood (2 × 10mls tubes) can be layered onto one 15 ml conical tube containing 4 ml of Ficoll.

   - This gives approx. 5×10^7/ml viable PBMCs (Total number of cells 1.5×10^9 cells/300ml)
   - It is known that generally 100 ml of blood give 2×10^8 PBMC. Out of these cells 1-2% will be monocytes

2. Count the cells and resuspend them at 1×10^7/ml in complete RPMI (cRPMI). The objective is to get at least 2×10^8 PBMC to plate out into one of 150mm culture dish. Expect yield of 1.5% DC:PBMC.

Separating blood derived monocytes

8. Place 20ml PBMC preparation into 1 × 150mm diameter, treated tissue culture dishes (1×10^7 PBMC/ml; total volume 25ml). Avoid over crowding of the plate to give enough space for the adherent cells to attach.
9. Incubate for 4h at 37°C/ 5% CO_2
10. Gently tilt the dish and aspirate off the supernatant containing non-adherent cells
11. Wash adherent cells twice with 20ml of PBS (pH7.4). Rinse down the dish in 4 different angles (5ml/angle).
12. Aspirate and discard the PBS after each wash.
13. Add 25ml of differentiation medium to the dish.

✓ **Preparation of stock and working GM-CSF (Sigma; Cat # G5035, Lot 027K1018)**
- Vial contains 5µg of lyophilized GM-CSF
- Reconstitute with 5ml of sterile pyrogen-free distilled water which will give a **stock concentration of 1µg/ml**. Aliquot in 50µl each tube and store at -20°C.
- **Recommended working concentration** is **0.1ng/ml of cRPMI**

Working conc.	Working vol./ ml	20ml media
0.1ng	0.1 µl	2 µl
1ng	1 µl	20 µl
10ng	10 µl	200 µl

✓ **Preparation of stock and working IL-4 (R&D; Cat #1809-EL, Lot MFM016021)**
- Vial contains 20 µg of lyophilized rEqIL-4
- Reconstitute with 2 ml of sterile distilled water which will give a **stock concentration of 10 µg/ml**. Aliquot in 200µl each tube and store at -20°C.

- **Working concentration** is **100ng/ml**

Working conc.	Working vol./ ml	20ml media
100ng	10 µl	200 µl
200ng	20 µl	400 µl

14. Incubate the culture dishes in differentiation medium for 4 days at 37°/ 5% CO_2.

Collection of cultured cells

1. During differentiation the cells round up and detach, so they are no longer adherent. Harvest the cells with a pipette and transfer the entire volume into centrifuge tubes.
2. Pellet the cells (150 ×g , 10min) and resuspend each pellet in 10ml plain RPMI
3. Overlay each 10ml aliquot onto 4ml Nycoprep (1.068g/ml) in separate 15 ml centrifuge tubes
4. Spin at 500 ×g for 15 min with no brake
5. Harvest and pool the interfaces and wash once with PBS
6. Count the cells

CLASSICAL VIROLOGY TECHNIQUES

PROCESSING OF NASAL SWABS FOR VIRUS ISOLATION

Materials

10 ml syringes
Autoclaved plastic forceps
0.45 µm syringe filter (Corning Cat. # 431220 or Millipore, Millex™ Cat. # SLHA033SB)
1.7 ml screw cap tubes (Sardstedt Cat. # 72.694.996 [color cap], #72.694.006 [clear cap])
15 ml conical tubes

Methods

1. Thoroughly swab the nasopharyngeal area with a sterile rayon swabs (1/2" x 1") with plastic shafts (16").
2. After collection, the rayon tip of each swab is cut off into 7 ml of virus transport medium (Hank's balanced salt solution with penicillin, streptomycin, gentamicin sulfate and amphotericin B; all from Life Technologies, Carlsbad, CA).
3. Squeeze the swab to recover maximum amount of media and centrifuge at 300 ×g for 10 min to remove debris.
4. Transfer individual nasal swabs in transport medium to the barrel of a 12 ml disposable syringe and express through 0.45 µm syringe filter (Millipore).
5. Collect the filtrate into a 15 ml conical tube. Bring up the sample volume to 7 ml with plain MEM to normalize samples (e.g. after filtration usually approx. 6 ml is recovered). Leave approximately 2.0 ml for virus isolation and aliquot the remaining filtrate (approximately 1 ml × 2) into tubes. Freeze at -70°C until tested.
6. Aspirate off media from confluent RK-13 cells in 6-well plates and inoculate 500 µl specimen/well in duplicate.
7. Incubate plates at 37°C in presence of 5% CO_2 for 1-2 hours.
8. Add 10ml CMC overlay to each flask and incubate at 37°C in the presence of 5% CO_2 for 5 days.
9. Do second passage on day 4 using the same cells. Stain cells on day 5 with crystal violet. Archive the TCF at -80°C.

SERUM PROCESSING

Materials

Vacutainer needles
Vacutainer adapters (Termuno, Venoject II Cat. # P-1316R)
15 ml BD Vacutainer tubes (Kendall Monoject [no additive] Cat. # 8881 301819)
1.7 ml screw cap tubes (Sardstedt Cat. # 72.694.006)
Transfer disposable pipets for serology (Samco scientific Cat. # 202-1S)

Methods

1. Collect blood into vacutainer tubes via jugular venipuncture (about 15 ml blood).
2. Transport blood tubes to the lab. Spray tubes with diluted Roccal-D (1:200). Rinse tubes and dry with paper towel. Let stand at room temperature for 4-5 hours or for 1 hour at 37°C (water bath works faster).
3. Sediment blood cells at 2000 rpm (300 ×g) for 10 min.
4. Collect serum and aliquot into tubes (1.4 ml × 4). Freeze at -20°C until tested for virus or antibody.
5. Proceed as in steps 5-8 above for virus isolation.

BUFFY COAT PROCESSING FOR VIRUS ISOLATION (WITHOUT GRADIENT PURIFICATION)

Methods

1. Draw blood by venipuncture into vacutainer tubes containing sodium citrate or EDTA and mix thoroughly.
2. Allow blood to stand for 1-2 hours or sediment at 600-700 rpm (100 ×g) for 10 min. Remove plasma layer and sediment at 2000 rpm for 10 min. The few red blood cells in pellet cause no apparent concern.
3. Aspirate off supernatant; resuspend pellet in 5 ml EMEM 10% FSCS and vortex thoroughly. (If desired, pellet can be washed with PBS before resuspending in EMEM media). Freeze or inoculate.
4. Proceed as in steps 5-8 above.

PERIPHERAL BLOOD MONONUCLEAR CELLS (PBMCS) PROCESSING FOR VIRUS ISOLATION

Materials

15 ml BD vacutainer tubes w/ACD (Citrate-dextrose solution; Sigma C3821- 50ML)
Ficoll-Paque Plus (GE Healthcare Cat#17-1440-03)
15 ml conical tubes
50 ml conical tubes
1.7 ml screw cap tubes (Sardstedt Cat. # 72.694.006)

Preparation of Vacutainer tubes with Acid Citrate Dextrose (ACD)

Using a small gauge needle and a 10 ml syringe, add 1.5 ml ACD to each 15 ml vacutainer tube. Mark tubes to identify that they contain ACD. Store at 4°C.

Preparation of Ficoll-Paque Plus gradients in 15 ml conical bottom polypropylene tubes

Place 4.0 ml Ficoll-Paque Plus in each tube (will need 15 ml tube per 20 ml vacutainer of collected blood). Centrifuge briefly to pull all of Ficoll-Paque Plus to bottom of the tube. Store at 4°C but warm to room temperature before use.

Methods

1. Collect blood via venipuncture into tubes with ACD (about 13.5 ml blood and the final volume is about 15 ml per tube). Invert several times to mix. Keep on ice at farm.
2. Transport blood tubes to the lab. Spray tubes with dilute Roccal. Rinse tubes and dry with paper towel. Invert tubes several times to re-mix blood (prevents PBMC from settling on top of RBC too much). Keep at room temperature.
3. Wait approximately 20-30 min until RBC has settled again, leaving cloudy, yellow plasma layer on top of RBC layer.
4. Layering plasma onto Ficoll-Paque Plus using transfer disposable pipet.
5. Using serological pipet, carefully aspirate plasma of one Vacutainer tube, stopping aspiration as reach the RBC layer (a few RBCs are OK but try not to pull lost of RBCs into pipet). Layer plasma onto Ficoll-Paque Plus in conical tube. Plasma from one 20 ml vacutainer of blood should approximately fill the Ficoll-Paque Plus tube to 14-15 ml height in tube. Cap tube when finished. Keep at room temperature. Continue, using the same pipet, and harvest all plasma layers from the vacutainers collected from one horse.
6. Centrifuge at 500 ×g (2800 rpm), 30 min, 25°C.
7. Harvesting PBMC from gradient:
    - Aspirate plasma layer above gradient down to cloudy band of PBMC. Discard into sterile beaker. With same pipet, aspirate PBMC at interface (approx. 2-3 ml/15 ml tube) and place into 50 ml polypropylene centrifuge tube. Continue removing plasma, harvesting interfaces. Combine PBMC from 4 gradient (15 ml conical) tubes into a 50 ml tube for washing.

8. Cell washing steps:
    - Add sterile PBS (pH 7.4) to bring the volume to 40 ml. Cap tube and mix cells by inverting tube 5 times (or tapping tube with the index finger).
    - Centrifuge for 15 min at 500 ×g (2800 rpm), 4°C.
    - Aspirate the supernatant without disturbing the cell pellet.
    - Add sterile PBS to bring the volume to 40 ml and cap tube. Mix cells by tapping the tube with the index finger or by vortexing.
    - Centrifuge for 10 min at 500 ×g (2800 rpm), 4°C.
    - Aspirate the supernatant without disturbing the cell pellet.
    - Resuspend the pellet in 8.0 ml of 10% EMEM (this gives about $1.5 \times 10^7 – 3.0 \times 10^7$ cells per ml). Leave 2.0 ml of buffy coat cells in the conical tube for virus isolation and aliquot the remaining cells (approximately 1.2 ml × 5) into tubes.
    - Freeze the remaining cells at -80°C.

ISOLATION OF EAV FROM SEMEN

1. Thaw 15 ml tube containing semen sample in warm tap water, then place on ice.
2. Label 8 flasks ($25cm^2$) [4 RK-14 (KY) "high pass" and 4 RK-13 (ATCC-CCL37) "low pass"]/semen, 2×10^{-1}, 1×10^{-2}, 1×10^{3} for high pass, 2×10^{-1}, 1×10^{-2}, 1×10^{3} for low pass.
3. Sonicate (output 20, #4.5 on dial) samples on ice 3 ×15 sec.; let set on ice for 15 sec. 1 min between sonications (dilute small volumes to 5 ml). Clean sonicator probe with 95% EtOH 2X between each sample. Spin 300 ×g (1900 rpm) for 10 min to remove sperm and debris, save and use supernatant (SSP).
4. Set up 3 tubes (10^{-1} to 10^{-3}) for each sample, 4.5 ml EMEM 10% FSCS per tube.
5. Aspirate off media from 25 cm^2 (3-6 day old RK-13 monolayers). Do not rinse! Make 10^{-1} (0.5 ml sample in 4.5 ml diluent), vortex; with new pipet add 0.5 ml of 10-1 to tube #2 (10^{-2}) and 1 ml to each of 4 flasks marked 10^{-1}. Continue the same way with dilutions 10^{-2} and 10^{-3} (2 flasks each).
6. Incubate all flasks at 37°C in air incubator (incubator without CO_2) with caps closed for 1 hour (2 hours maximum).
7. Add 10 ml of CMC overlay to each flask and incubate at 37°C in air incubator (incubator without CO_2) with caps closed.
8. Check for CPE on day 4.
   If bacterial contamination occurs, redo after bacteriological examination and sensitivity testing to find out which antibiotics to used in the TC media. Repeat test as above and also note contamination. Specimen may be filtered through a 0.45 µm filter using a 5 or 10 cc syringe, if necessary.
9. If negative, a second passage is performed on day 4. (See 2nd passage)
10. If sample is toxic this material is passages as is (2nd passage).
11. If positive, supernatant is usually harvested from a 10-2 flask showing viral activity (store at -20°C) and a reverse SN-test is performed against known positive and negative sera (See reverse SN-test).
12. After 5 days harvest supernatant from flasks and stain flasks with crystal violet using 2 ml crystal violet in buffered formalin. Stain 1-24 hours, remove stain, rinse flasks with tap water and read.
13. All semen samples are placed in freezer zip lock storage bags and stored at -70°C.
14. Permanently store negative SSP at -20°C and positive SSP at -70°C.

Second passage

1. Aspirate media from 2 "high pass" and 2 "low pass" confluent 3-5 day old RK-13 cells in 25 cm^2 flasks for each negative semen sample.
2. From 2 flasks of 10^{-1} passage #1 take up 0.5 ml from each with same pipet (1ml) and add 1 ml to 1 new flask for each high and low pass. Do the same for 10^{-2} passage #1, taking up 1 ml from each. Do 10^{-1} and 10^{-2} only. Close caps and incubate at 37°C for 1-2 hours (minimum 1 hour) in air incubator.

3. Add 10 ml of CMC overlay to all flasks, close caps, and incubate at 37°C in air incubator (without CO_2).
4. Read after 3-4 days.
5. After 4 days, harvest media and stain flasks (See passage #1).

MAKING WORKING VIRUS STOCKS

Materials

1. EAV
2. Five confluent monolayers of RK-13 cells in T-150 flasks
3. EMEM
4. RK-13 medium
5. 50 ml conical centrifuge tubes
6. Freezing vials

Method

1. Inoculate monolayers with EAV at an m.o.i. of 1. Resuspend the virus in approximately 50 ml of serum free MEM and add 10 ml per T-150 flask.
2. At the same time mock infect one T-75 flask of RK-13 cells.
3. Adsorb for 1 hour at 37°C. .
4. Add 40 ml of complete RK -13 medium / T-150 flask. Incubate at 37°C for 48 hours or until 95% - 100% CPE.
5. Centrifuge at 5000 g (or 3000 rpm in the table top centrifuge) at 4°C for 15 minutes.
6. Make 1.8 ml and 0.5 ml aliquots of supernatant and store at -70°C.
7. Use one 0.5 ml frozen vial to titrate the virus.

PREPARATION OF HIGH TITER VIRUS STOCKS

Methods

1. Seed cells into 3, triple-deck flasks and grow until confluency.
2. Remove the medium and leave approx. 50 ml of complete medium containing 10% fetal bovine serum. Add 500 µl-1 ml of virus per flask. If the titer of the virus is known use an m.o.i of 1 (higher m.o.i will may produce deletion mutant).
3. Adsorb for 1 hour at room temperature on the orbital shaker.
4. Add 20-40 ml of complete medium containing 10% fetal bovine serum and incubate at 37°C for 3-4 days. Check for signs of infection 2 days after the start of infection.
5. Pellet down the cellular debris (3000 rpm / 4°C / 15 minutes) and aliquot into freezing vials and store at 4°C (stable for up to 6 months) and / or -70°C (for long term storage). Virus should be stored away from the fluorescent lights since the virus titer appears to decrease when exposed to fluorescent light for prolonged period of time.
6. Determine the virus titer using the plaque assay procedure.

CONCENTRATION OF EQUINE ARTERITIS VIRUS BY USING A 20% SUCROSE CUSHION

Materials

1. 20% sucrose in NET buffer
2. SF-MEM
3. RK-13 Medium
4. NET buffer

Method

1. Five T-150 flasks with 3 days old confluent monolayers of RK-13 cells.
2. Inoculate EAV PP^3 P^3 at an m.o.i. of 5. Use approximately 2 vials (1 ml / vial) / T-150 flask. 10 vials of virus for five T-150 flasks.
3. Dissolve the virus in SF-MEM.

1. 10 mls / T-150 × 5 = 50 mls
2. Take 40 mls of SF-MEM and add 10 ml of virus
3. Add 10 mls / T-150 flask
4. At the same time mock infect one T-75 flask of RK-13 cells.
5. Adsorb for 1 hour at 37^0C. .
6. Add 20 ml of complete RK -13 medium / T-150 flask. Incubate at 37^0C for 48 hours or until 95% - 100% CPE.
7. Collect the supernatant and centrifuge at 5000 g (or 3000 rpm) / 4°C / 15 minutes to remove cellular debris.
8. Filter the supernatant through 4.5µm bottle-top filter (optional) and overlay on to approx. 3-5 ml of 20% sucrose cushion placed in ultracentrifuge clear tubes. Place each tube into ultracentrifuge bucket and balance to equal weight.
9. Pellet the virus by ultra-centrifugation [36,000 rpm (155,300 g) / 4°C / 4 hours in AH 650 rotor]. Remove brake.
10. Aspirate the supernatant and resuspend the virus pellet in 300-500 µl PBS (pH 7.4). Sonicate for 15/15 sec on and off for three times
11. Store at -80°C.
12. It is better to collect following samples for micro-titration assay to determine the efficiency of purification.

MICROTITRATION ASSAY TO ESTIMATE EQUINE ARTERITIS VIRUS TITERS

Materials:

1. 96 Wells microtitration plates (Falcon® 3072)
2. Sterile snap cap tubes (Fisher or Falcon® 2054)
3. Multi channel pipette (8 or 12 channels)
4. Antiserum or ascitic fluid (Monoclonal antibodies)
5. Negative control serum or control ascitic fluid
6. EMEM (BioWhittaker®)
7. Complete RK-13 medium
8. Confluent RK-13 cells (one T-75 flask is sufficient for 5 ninety six well plates)
9. Equine arteritis virus stock to be titrated
10. Crystal violet staining / fix solution

Method:

1. Each test virus is done in triplicate. Label the 96 well plates with cell controls.
2. Dilute the test virus from 10^{-1} to 10^{-8} in EMEM (ten fold serial dilution). Use 200 µl of virus + 1800 µl of EMEM.
3. Add 50 µl of EMEM to all the wells except to control wells (column 10, 11 and 12) where 100 µl of EMEM should be added.
4. Trypsinize a confluent T -75 flask of RK-13 cells and resuspend the pellet in 10 ml of RK-13 medium. Take 2 ml of the cell suspension and resuspend in 10 ml (1:5) of RK-13 medium (or 4 ml in 20 ml would be better. This gives enough volume to work).
5. Add 50 µl of diluted virus to test wells in triplicate. Start with the highest dilution (10^{-8}) and go to the lowest dilution (10^{-1}; therefore, can use the same pipet tip)
6. Add 100µl of resuspended RK-13 cells to each well. Incubate at 37°C for four days.
7. Feed the plates with 50 µl of growth media on day 2 and day 3 (if necessary) to maintain monolayers.
8. When CPE occurs (usually 4 days), dump out the media in sink and stain with 1% crystal violet solution/fix for 20-30 minutes (it is easy to leave the plate(s) in a bucket containing 1% crystal violet/fix solution because the 1% crystal violet/fix solution can be reused.) and then wash gently with tap water to remove excess Crystal violet (three times). Air dry plates and determine EAV titer by Reed and Munch method.

9. 50% end point values, by Read and Munch Method: Under lined numbers indicate logarithmic characteristic of end point dilution. Triplicates;

3 - 2 - 0 - 0 = 0.25	3 - 1 - 2 - 0 = 0.5
3 - 2 - 1 - 0 = 0.5	3 - 1 - 3 - 0 = 0.2
3 - 2 - 2 - 0 = 0.0	3 - 0 - 0 - 0 = 0.5
3 - 2 - 3 - 0 = 0.3	3 - 0 - 1 - 0 = 0.7
3 - 1 - 0 - 0 = 0.75	3 - 0 - 2 - 0 = 0.8
3 - 1 - 1 - 0 = 0.0	3 - 0 - 3 - 0 = 0.0

10. Report virus titers as $TCID_{50}$ per 50 µl.

PLAQUE ASSAY

Materials:

6 well plates
RK-13 cells
Carboxymethylcellulose (CMC) overlay media (1.3X EMEM 10% FSCS)
Virus for titration

METHOD:

1. Prepare RK-13 in 6-well plates.
2. Make virus dilution (10^{-1} to 10^{-8}) in complete 10% EMEM growth media.
3. Aspirate the medium and add 200 µl of diluted virus to each well in duplicate(Start from 10^{-8} and go to 10^{-1}). Mix gently by rocking the plate.
4. Incubate the plate at 37°C for 1 hour to allow virus particles to adsorb into cells.
5. Following 1 hour incubation period, overlay cells with 4 ml (per well) of CMC overlay media adding to the side of the plate.
6. Allow plates to sit undisturbed on a leveled surface for 4 days until visible plaques develop.
7. After 4 days, discard supernatant and stain with crystal violet staining solution.
8. Count >10 to <100 plaques per well.
9. PFU/ml = (# of plaques in each well [duplicate]/2) × (highest dilution that gives # of plaques) × (dilution factor)
10. e.g. $[(25 + 30)/2] \times 10^{-5} \times 5$ (200 µl) $= 137.5 \times 10^{-5} = 1.37 \times 10^{-7}$ pfu/ml

SEROLOGY

VIRUS NEUTRALIZATION TEST (VNT)

Methods

1. Inactivate sera at 56°C for 30 minutes
2. Put 25µl of serum diluent (10% GP complement in EMEM 10% FSCS [keep on ice until used]) in all wells.
3. Put 25µl of test serum to the first well of two rows (No row for checking toxicity*). Dilute with 25 µl multichannel pipettor.
4. Add 25 µl of virus (200 $TCID_{50}$) diluted in EMEM 10% FSCS to all wells except controls ("See controls").
5. Incubate plates at 37°C (5% CO_2 incubator) for one hour.
6. Add 125 µl of trypsinized cells (prepared as directed below) to every well.
7. Seal plates and incubate at 37°C (5% CO_2 incubator). Read after 48, read and final at 72 hours.

Controls: cell controls, known positive and negative sera, and virus titration controls.
Cell controls: add 50 µl serum diluent to 2 wells.
Serum controls: add 25 µl serum diluent to 1 well/each test serum, add 25 µl test serum.
Known positive serum and known negative serum are set up the same way as test sera.

Virus titration: Add 25 µl serum diluent into each of 4 wells for cell controls (Row #1).
Add 25 µl of working virus dilution to each of 4 wells (Row #2).
Add 25 µl of 1:10 dilution of working virus in EMEM 10% FSCS to each of 4 wells (Row #3).
Add 25 µl of 1:100 dilution of working virus in EMEM 10% FSCS to each of 4 wells (Row #4).
Add 25 µl of 1:100 dilution of working virus in EMEM 10% FSCS to each of 4 wells (Row #5).
Add 125 µl of trypsinized cells to all 20 wells.

*If serum is toxic in serum control well (1:4 dilution), then repeat test with a row to check for toxicity.

REVERSE SN-TEST FOR EAV VERIFICATION – confirmation test

Materials

1. Known positive serum, inactivated and diluted 1:4 in PBS (should come from field sample(s), not from vaccinated horses).
2. Known negative serum inactivated and diluted 1:4 in PBS.
3. Stock virus (Bucyrus)
4. Unknown virus isolate

Methods

1. Add 0.3 ml of known negative serum to 4 tubes for each virus sample to be tested (including stock virus).
2. Add 0.3 ml of known positive serum to 3 tubes for each virus sample to be tested (including stock virus).
3. Make up 1:10 dilution of guinea pig complement in EMEM + 10% FSCS + antibiotics (10 ml for each sample).
4. Make up 10^{-1} to 10^{-5} dilutions of all virus samples to be tested using 1.8 ml of media in #3 and 0.2 ml of virus (It may be necessary to dilute stock virus to 10^{-3} before starting these dilutions).
5. To positive serum (3 tubes) add 0.3 ml of 10^{-1}, 10^{-2} and 10^{-3} virus dilutions.
6. To negative serum (4 tubes) add 0.3 ml of 10^{-2}, 10^{-3}, 10^{-4} and 10^{-5} virus dilutions.

7. Incubate serum-virus mixture for 1 hour at 37°C.
8. 14 flasks 25 cm^2 [7 RK-13 (KY) "high pass", 7 RK-13 (ATCC-CCL37) "low pass"] are used for each virus to be tested. Aspirate off media from 3-5 day RK-13 flasks and add 0.25 ml of above serum-virus mixture to 2 flasks/dilution.
9. Incubate for 2 hours at 37°C (closed caps, no CO2), rock flasks after 1hour.
10. Add 10 ml of CMC overlay/flask. Incubate for 4-5 days according to development of CPE, remove media, and stain with crystal violet plaque stain.

TREATMENT OF SERUM WITH TOXICITY DUE TO (DUVAXYN) ANTIBODIES TO RK-13 CELLS

This procedure has been used successfully to eliminate (or reduce to readable at 1:4) toxicity from serum samples demonstrating the vaccine-induced "European" toxicity at 1:4 and greater in the EAV SNT. These horses have been vaccinated with Duvaxyn EHV 1,4 (the EHV-1 component is made in RK-13 cells). Always treat a known negative and a known positive serum whenever this treatment is performed on toxic serum specimens. Preferably, use serum that has not been previously inactivated. Use sterile technique for the following steps:

Methods

1. Decant growth media from as flask of 7-10 day old RK-13 (KY) cells (P399-409). Wash flask 3X with 10 ml Dulbecco's PBS. Add 1 ml trypsin EDTA/flask, rotate to spread over cell monolayer, then incubate approximately 6-8 min at 37°C.
2. When cells have detached, add 2 ml EMEM with 10% FSCS/flask. Mix well with 5 ml pipet, then divide between three 1.5 ml microcentrifuge tubes.
3. Spin tubes at 2,0000 rpm for 15 sec in microcentrifuge. Use a Pasteur pipet to remove and discard all supernatant.
4. Add 0.5 ml of toxic serum or control serum per tube; mix with pipet until cells are resuspended; label tube appropriately. Incubate for 1 hour at 37°C. Flick tubes after 30 min to resuspend.
5. Spin 2,500 rpm for 15 sec. Use a Pasteur pipet to transfer each serum to a new, labeled 1.5 ml microcentrifuge tube.
6. Inactivate at 56°C for 30 min if serum has not been inactivated previously. Proceed with EAV SNT test, running sera (toxic, negative, positive) as usual and in pre-seeded (planted 18-24 hours prior) plates.

ENZYME LINKED IMMUNOSORBENT ASSAY (ELISA)

Materials

1. Microtiter plates for ELISA
2. Coating buffer
3. ELISA wash buffer
4. Biotinylated anti-mouse IgG
5. Enzyme substrate
6. Substrate stopping solution
7. Blocking solution
8. Antibody dilution buffer (ADB)
9. Conjugate dilution buffer
10. Substrate (e.g., OPD)
11. 1% SDS
12. Test serum or culture supernatant
13. Positive control serum
14. Negative control serum
15. Multichannel pipette
16. Wash bottle

Method

1. Coat the ELISA plates with the antigen as previously described (see antigen preparation for coating ELISA plates) and store the plates overnight at 4^0C. It is advisable to include negative control antigen (e.g., 1% BSA in coating buffer) in the plate.
2. Aspirate coating antigen solution and block unbound sites on the plastic by incubation with 150 µl blocking solution (1% BSA, gelatin, ovalbumin, casein, milk powder) or with antibody dilution buffer (ADB) per well for 30 minutes
3. Wash off unbound protein three times with 150 µl ELISA wash buffer (PBS-Tween [0.05%] also known as TPBS; add 0.5 ml of Tween 20 to 1 liter of PBS, pH 7.5) per well.
4. Add 50 µl of primary antibody diluted in ADB (need to titrate the antibody to find out the best dilution to be used). If tissue culture supernatant is used add 50-100 µl straight. Include some wells with known positive antibody and known negative antibody. Incubate for one hour at room temperature.
5. Wash off unbound antibody three times with 150 µl ELISA wash buffer per well.
6. Add 50 µl of Biotinylated secondary antibody (Biotinylated anti mouse IgG 1:2000 dilution in ADB). Incubate for one hour at room temperature.
7. Wash off unbound secondary antibody three times with 150 µl ELISA wash buffer per well.
8. Add 50 µl of 1:2000 dilution of Avidin-HRP in conjugate dilution buffer (PBS pH 7.5, 0.5% BSA, 0.05% Tween 20). Incubate for 15 minutes at room temperature.
9. Wash off unbound Avidin-HRP three times with 150 µl ELISA wash buffer per well.
10. Add 100 µl of substrate and let react until BSA control just becomes visible, 1 to 20 minutes (10 mls substrate per plate - 0.1M Citrate pH 4.5, 3.3 µl of H_2O_2, 10 mg OPD substrate). If needed terminate reaction with 50 µl of 1% SDS.
11. Assess the color intensity visually or quantitatively in a spectrophotometer designed to read microtitre plates (ELISA) reader.

MOLECULAR BIOLOGY/ RECOMBINANT DNA TECHNIQUES

DESIGNING OF PRIMERS

The approach for designing of specific and efficient primers remains somewhat empirical; there are no hard and fast rules. With experience and by using a good primer designing program (e.g., MacDNASIS v3.5; Hitachi) the majority of the primers can be made to work. Following are some guidelines to design specific and efficient primers.

1. Where possible, select primers with an average G+C content of around 50%.
2. Where possible, select primers with a random base distribution. Try to avoid primers with stretches of polypurines, polypyrimidines, or other unusual sequences.
3. Melting temperature (T_m) should be between 55-75°C.
4. Increasing the T_m, therefore, the annealing temperature enhances discrimination against incorrectly annealed primers and reduces misextension of incorrect nucleotides at the 3' end of the primers. Therefore, increasing the annealing temperature will help to increase the specificity. An applicable annealing temperature is 5°C below the true T_m of the amplification primer. The best annealing temperatures is in the range of 55-72°C. Quick way to calculate annealing temperature is:
5. Annealing temp. (°C) = (# of A and T [A+T] $\times$ 2 + # of G and C [G+C] $\times$ 4) - 5°C.
6. Try to design both positive and negative primers with same T_m (1-2^{0}C difference will not matter).
7. Make sure the primer ends (3') with a G or C.
8. Primer length should be between 19 and 30 bases (19 to 22 bases are preferred).
9. If possible select a unique area of the genome to design the primer.
10. Avoid sequences with significant secondary structure (computer programs are very useful for this).
11. Check the primers against each other for complementarily. Avoiding primers with 3' overlaps will reduce the incidence of "primer-dimer" artifacts.
12. If possible do a simple homology matching (compare the primers with the whole genome using a computer program) and see whether primer(s) have <50% homology in the area closer to be amplified (or to the desired area). This will reduce the number of nonspecific products of same size.

AGAROSE GEL ELECTROPHORESIS

Materials

1. Agarose (SEAKEM® LE agarose; FMC Bio Products).
2. 50X TAE buffer (Tris Acetate EDTA, pH 8.0).
3. Gel casting plate.
4. Gel sealing tape
5. Buffer tank.

Method

1. Make 1000 ml of 1X TAE, by measuring 20 ml of 50X stock into a 1000 ml graduated cylinder and q.s. to 1000 ml mark with deionized distilled water.
2. Weigh 1.0 g of agarose (for 1% gel) and dissolve it in 100 ml of 1X TAE. Melt agarose solution in microwave until completely dissolved. Let stand at room temperature (or at 45°C in a water bath) to remove air bubbles but not enough to solidify.
3. Prepare gel-casting plate by taping the ends with gel sealing tape. Place the sample comb in the proper position on the plate.
4. Pour 100 ml of 1% agarose on to the gel casting plate slowly and allow it to solidify (volume of agarose needed depends on the size of the gel casting plate). The gel should be between 0.3 and 0.5 cm thick. After gel has set, final gelling carried out at 4°C for 30 minutes. There should not be any air bubbles in the gel.
5. Remove the tapes and keep the gel plate in the buffer tank. Add 1X TAE buffer into the reservoirs until it covers the surface of gel at a depth of 3-4 mm.
6. Slowly remove the sample comb and load the samples into the wells (Mix 1-20µl of RNA or DNA with 6X gel loading buffer; loading volume depends on the sample and make sure gel loading buffer get diluted to 1X with sample).

7. Voltage 70V for 2-3 hours (95V for 45-60 minutes) or until the first band has migrated at least 2.5 inches away from the wells. The voltage must never exceed 100V. For low melt Agarose use low voltage (70V). Always run the gel in constant voltage.
8. Stain gel in ethidium bromide, letting it sit for 5-10 min. Destain gel by placing in deionized distilled water for 5 min.
9. Transfer the gel onto a UV light source. Usually a trans illuminator is used to facilitate this step. Place a piece of plastic wrap between the gel and surface of the illuminator. Use a face shield, gloves, and body shield to minimize the UV exposure. Take a picture for records.
10. Locate the DNA or RNA bands and excise by using a sharp scalpel blade (e.g. to obtain the desired band)

Note: Range of separation in gels containing different concentrations of agarose.

% of agarose (%[w/v])	**Efficient range of separation of linear** DNA molecules (Kb)
0.3	5-60
0.6	1-20
0.7	0.8-10
0.9	0.5-7
1.2	0.4-6
1.5	0.2-3
2.0	0.1-2

REAL TIME RT-PCR MEASURING EQUINE CYTOKINE GENE EXPRESSION

Materials

A. Total RNA extraction
1. MagMAX 96™ Total RNA isolation kit (Applied Biosystems [ABI]; Cat# 1830)
2. Isopropanol (Sigma; I9516-500 ml)
3. Absolute ethanol (Decon Labs Inc.; Cat #2716)
4. Sterile round bottom 96-well plate (Corning; #3799)
5. 96-well Magnetic-Ring Stand (ABI; AM10050)
6. 1.5ml sterile microcentrifuge tubes
7. AluminaSeal™ (Diversified Biotech; Cat #ALUM-1000)
8. MagMAX™ Express-96, 96-well Deep Well volume (ABI; Cat# 4400077)
9. MagMAX Express 96 deep well tip combs (ABI; Cat #4388487)
10. MagMAX Express 96 standard plates, 200 µl (ABI; Cat #4388475)
11. MagMAX Express 96 deep well plates (ABI; Cat #4388476)

B. Reverse Transcription
1. High Capacity cDNA Reverse Transcription Kit with RNase Inhibitor, 200 reactions (Applied Biosystems [ABI] Cat# 4374966)
2. Twin.tec PCR plate 96, skirted (96 × 150 µl [Eppendorf; Cat# 0030 128.656])
3. PCR film (Eppendorf; Cat# 0030 127.480)
4. Epgradient Master Cycler (Eppendorf thermal cycler)
5. Nuclease free water (Ambion; Cat #AM9937)

C. Real Time PCR
1. TaqMan® Gene Expression Master Mix (Applied Biosystems [ABI], Cat# 4369016)
2. 20X Gene Expression Assays (Custom designed primers and probe, see below for Order #)
3. Automated Liquid Handling System (Corbett; CAS-1200)
4. 50 µl tips, filtered, liquid sensing (Qiagen; Cat #990512)
5. MicroAmp® Fast Optical 96-Well Reaction Plate with Barcode, 0.1 ml (ABI, Cat# 4346906)
6. MicroAmp® Optical Adhesive Film (ABI, Cat# 4311971)
7. Applied Biosystems 7500 Fast Real-Time PCR System

Methods

A. RNA extraction

1. Extract RNA using MagMAX™-96 Total RNA Isolation Kit. It lyses up to 2×10^6 cells. Cells can be stored in 140µl of Lysis/Binding Solution at -80C until RNA extraction.
   Note: If you stored RNA at -80C, prior to RT heat the sample to 70C for 2 min in a thermal cycler and put on ice to denature RNA.
2. Measure RNA concentration using NanoDrop and adjust to 0.5 µg or 1 µg (in 19.8 µl [final 30 µl reaction] or 26.4 µl [final 40 µl reaction]) depending on samples of the study.

B. Reverse Transcription

1. Prepare 2X reverse transcription master mix, mix and centrifuge briefly.

Final total volume =30 µl

Components	**Volume (µl) n=1**		**Volume (µl) (32 samples + 3 extra)**		**Volume (µl) (28 samples + 3 extra)**	
	30 µl	**40 µl**	**30 µl**	**40 µl**	**30 µl**	**40 µl**
10X RT buffer	3	4	105	140	93	124
25X dNTP Mix (100mM)	1.2	1.6	42	56	37.2	49.6
10X RT Random primers	3	4	105	140	93	124
MultiScribe RTase	1.5	2	52.5	70	46.5	62
RNase inhibitor	1.5	2	52.5	70	46.5	62
Total	10.2	13.6	357	476	316.2	421.6
(Optional) Water						

2. Pipette 10.2 µl of 2X RT master mix into each tube or 96-well plate. Keep on ice.
3. Pipette 19.8 µl of RNA (0.5 µg) sample into each well pipetting up and down two times to mix (NOTE: volume can be adjusted with H_20 based on the RNA conc.).
4. Seal plates with PCR film.
5. Centrifuge briefly to remove bubbles and spin down the contents.
6. Place the place on ice until ready to load on to the thermal cycler.
7. Load the reactions into the thermal cycler and start the reverse transcription run (under Yun Young's folder - High Capacity RT)

Step	**Temp (°C)**	**Time**
1	25	10 min
2	37	120 min
3	85	5 min
4	4	∞

8. Store at -20 or use immediately for PCR amplification.
9. If you are using -20C/80C frozen cDNA, immediately after thawing, heat the samples to 70C for 2 min in a thermal cycler to denature the cDNA and cool on ice.
10. For real time PCR, dilute cDNA samples 1:1 with RNase free water (pool duplicate cDNA samples in one tube and add 60 µl of RNase free water).

C. Real Time PCR

Components	Volume (µl)
TaqMan® Gene Expression Master Mix	5
20X Gene Expression Assays	0.5
1:1 diluted cDNA template	4.5
Total	10

1. Use automated pipettor (Corbett) to dispense both reaction mix and cDNA samples.
2. Turn on the robot and open "1-06-10 YYG.CAS4" program (see Real time plate plan)
3. Prepare reaction mix in 1.5 ml eppendorf tube.

- Mix 70 µl of TaqMan Gene Expression Mix + 7 µl of 20X Gene Expression Assays
- For a 96-well plate I am running 7 cytokines + B-GUS (8 eppendorf tubes)
- The program is setup to load 5.5 µl of each reagent mix into corresponding well

4. Place the reagent mix containing tube in the reagent rack and place a new 96-well real time PCR plate in the robot.
5. Press Run (10 minutes).
   NOTE: If cannot proceed to sample loading immediately, wrap the plate with parafilm and store at 4C until sample loading.
6. Meanwhile prepare cDNA samples in a 1.5 ml eppendorf tube for sample loading.

- Transfer 97 µl of 1:1 diluted cDNA into 1.5 ml eppendorf tube
- For a 96-well plate, I am running 3 samples + NTC + Positive control

7. When reaction mix loading is complete, open "1-06-2010 sample load YYG.CAS4"
8. Place sample tubes on the reagent rack.
9. Program is setup to load 4.5 µl of cDNA sample into corresponding well and mix twice.
10. Press Run (20 minutes)
11. Seal the plate with optical adhesive film
12. Centrifuge the plate briefly to remove air and bubbles.
13. Load the plate into the ABI 7500 Fast PCR Cycler (RQ plate – standard mode – 1:30h duration)

Step	Temp (°C)	Time	Cycle
1	50	2 min	1
2	95	10 min	2
3	95	15 sec	40
4	60	1 min	

Applied Biosystems 20X Gene Expression Assay Order Number:

Order Number	Order Name*	Order Number	Order Name
1749300	EQIL-1B-JN2		
1918058	EquineIL-2-JN2		
1798106	EQIL4IS-JN2	3065515	EqIL-4
50414323	EQIL-6		
1833786	EQIL-8IS-JN1		
50442836	EQIL10IS-JN2		
1649196	IL-12	3065515	EqIL-12p40
1947516	EQIFNA-4-SITER	3053604	EqIFNAlpha
1947516	EQIFNBETA-SITER	3053604	EqIFNBeta
50442836	EQIFNGIS-JN3		
1787254	EQTNFAIS-JN2		
1725506	GUS		

*Probe labeled with 5'-FAM and 3'-NFQ

PREPARATION OF COMPETENT BACTERIA CELLS - DH5α

Materials

1. Large, autoclave tray with ice for the ice/water bath.
2. 40 sterile microcentrifuge tubes.
3. Glycerol
4. LB agar plates without ampicillin.
5. Autoclave centrifuge bottles, microcentrifuge tubes. Dry cycle. 30 min.
6. Chill these: centrifuge bottle, 15 ml conical tube, 0.1 M $MgCl_2$ and $CaCl_2$ solutions.

Perform all procedures using sterile plasticware and solutions.
Solutions

1. 100 ml of 0.1 M $MgCl_2$ prepared from 1 M $MgCl_2$ stock.
2. 100 ml of 0.1 M $CaCl_2$ prepared from 1 M $CaCl_2$ stock.
3. Stock solutions can be sterilized by autoclaving and stored at room temperature. 0.1M solutions should be prepared fresh.
4. LB (10g Bacto-tryptone, 5g yeast extract, 5g NaCl for 1000 ml LB) supplemented with 1 g/L glucose. Autoclave.

Preparation of solutions

1. Glucose-supplemented LB medium (500 ml)

Bacto-tryptone		5.0 g
Bacto-yeast extract		2.5 g
NaCl		2.5 g
Glucose		0.5 g
dH_2O	to	500 ml

Autoclave. Liquid cycle 30 min. Store at 4C.

2. Glycerol 100 ml
Autoclave. Liquid cycle 30 min. Store at 4C.

3. 1 M $MgCl_2$ stock (100 ml)

$MgCl_2 \cdot 6H_2O$ (FW 203.30)		20.33 g
dH2O	to	100 ml

Autoclave. Liquid cycle 30 min. Store at Room temperature.

4. 1 M $CaCl_2$ stock (100 ml)

$CaCl_2 \cdot 2H_2O$ (FW 47.02)		14.70 g
dH2O	to	100 ml

Autoclave. Liquid cycle 30 min. Store at Room temperature.

5. 0.1 M $MgCl_2$ working solution (100 ml) and 0.1 M $CaCl_2$ working solution (100 ml)

Method

1. Streak out bacteria (DH5α or other strain) on an LB agar plate (without antibiotics). Allow to grow overnight at 37°C.
2. The next day, pick a single colony and grow in 2 ml of LB medium (without antibiotics), shaking (250 rpm) at 37°C overnight. Best to do this in the late afternoon.
3. Take 0.5 ml of the prepared LB medium to use as a blank for the OD. Transfer overnight bacterial prep to a 2L flask containing 500 ml of **glucose-supplemented LB medium**. Incubate at 37°C with vigorous shaking. During this time chill all solutions and centrifuge bottles on ice and turn on spectrophotometer, set wavelength at 550. After several hours (2.5-3 h), remove 0.5 ml of bacteria

using a sterile pipet and check OD_{550} (use LB/glucose as blank). Continue to check the culture until the OD_{550} reaches 0.5 (bacteria double about every 20 min). As soon as the correct OD is achieved immediately transfer the culture flask from the shaker to an ice/water bath. Constantly swirl flask for 5 min until the whole sample is uniformly chilled. Pour the bacteria into the chilled centrifuge bottle and spin at 4000 rpm, 4°C for 20 min.

4. Decant supernatant and place bottle with bacteria pellet on ice. Resuspend in 10 ml of ice cold 0.1 M $MgCl_2$ using sterile 10 ml pipet. Once resuspended, add the remaining 90 ml of chilled 0.1 M $MgCl_2$. Sit on ice for 5 min and spin for 20 min at 4000 rpm 4°C.
5. While spinning, transfer 8.6 ml of 0.1 M $CaCl_2$ to a 15 ml conical tube. Add 1.4 ml glycerol. Mix well and let sit on ice.
6. Decant supernatant and place bottle on ice. Resuspend in 10 ml of ice cold 0.1 M $CaCl_2$ using sterile 10 ml pipet. Once resuspended, add the remaining 81.4 ml of ice cold 0.1 M $CaCl_2$. Sit on ice for 20 min and spin in the centrifuge for 20 min at 4000 rpm 4°C.
7. Decant supernatant well and place bottle on ice. Resuspend bacteria in a chilled solution of 8.6 ml 0.1 M $CaCl_2$ /1.4 ml glycerol. Mix well and transfer 0.25 ml aliquots to microcentrifuge tubes that have been placed in dry ice or drop tubes into liquid nitrogen. Quick freeze and store bacteria at -80°C until use. Once thawed, the cells should not be frozen

TRANSFORMATION OF DH5α

Materials

1. Water bath at 42°C
2. Warm SOC medium to RT
3. Warm 3 LB plates w/ampicillin
4. Thaw **on ice** 1 vial of competent cells (DH5α) for each transformation

Methods

1. Thaw on ice, one vial of competent cells per transformation.
2. Add all ligated product to 100ul of competent cell and mix by stirring gently with the pipette. Do not mix by pipetting up and down.
3. Incubate on ice for 30 min
4. Heat-shock the cells for 45 seconds at 42°C without shaking
5. Immediately transfer the tubes on ice 2min
6. Add 900ul of RT SOC medium
7. Cap the tube tightly and shake the tube horizontally at 37°C for 1 h (240rpm)
8. After incubation at 37C for 1h. Transfer the culture to microcentrifuge tube. Decant the supernatant leaving about 100ul of media. Resuspend the bacterial pellet.
9. Spread 100ul from each transformation on a prewarmed LB agar plate (w/ampicillin) and incubate overnight at 37°

PREPARATION OF COMPETENT BACTERIA CELLS - M15 [pREP4]

Materials

1. M15[pREP4] cells (Qiagen)
2. LB medium-kanamycin (25 µg/ml)
3. LB agar-kanamycin (25 µg/ml)
4. TFB1
5. TFB2
6. Kanamycin stock solution (25 mg/ml in H_2O, sterile filter, store in aliquots at -20°C)
7. Large, autoclave tray with ice for ice/water bath
8. 40 sterile microcentrifuge tubes (Label them and place at -80°C at the beginning of the day)

9. Autoclave centrifuge bottles. Dry cycle 30 min. Chill centrifuge bottle and 15 ml conical tube and TFB1, TFB2 buffers.
10. Dry ice

Buffers

TFB1 (500ml)	MW	500 ml
100 mM Rubidium Chloride (RbCl)	120.9	6.05 g
50 mM Manganese Chloride ($MnCl_2$)	197.9	4.95 g
30 mM Potassium acetate	98.14	1.47 g
10 mM Calcium Chloride ($CaCl_2$)	147.0	0.735 g
15% (w/v) Glycerol		75 ml

Adjust pH to 5.8. Sterilize by filtration.

TFB2 (100ml)	MW	100 ml
10 mM MOPS	209.3	0.21 g
10 mM Rubidium Chloride (RbCl)	120.9	0.12 g
75 mM Calcium Chloride ($CaCl_2$)	147.0	1.10
15% (w/v) Glycerol		15 ml

Adjust pH to 6.8 with KOH. Sterilize by filtration.

LB Medium-kanamycin (final concentration 25 µg/ml)

Method

1. Streak out a trace of M15 [pREP4] cells from the vial with a sterile inoculating loop on LB-kanamycin agar plate.
2. Incubate at 37°C overnight.
3. Pick a single colony and inoculate 10 ml of LB-kanamycin (25 µg/ml). Grow overnight at 37°C.
4. Add 2 ml overnight culture to 200 ml prewarmed LB-kan medium in a 500 ml flask, and shake at 37°C until an OD_{600} of 0.5 is reached (approximately 90-120 min). Use LB-kan media as blank. Turn on the centrifuge and keep it cool (4°C).
5. Cool the culture on ice for 5 min. Constantly swirl the flask for 5 min until the whole sample is uniformly chilled. Transfer the culture to a sterile, centrifuge bottle.
6. Collect the cells by centrifugation at low speed (5 min, 4000x g, 4°C).
7. Discard the supernatant carefully. Always keep the cells on ice.
8. Resuspend the cells gently in cold (4°C) TFB1 buffer (30 ml for a 100 ml culture) and keep the suspension on ice for an additional 90 min.
9. Collect the cells by centrifugation (5 min, 4000 x g, 4°C).
10. Discard the supernatant carefully. Always keep the cells on ice.
11. Resuspend the cells carefully in 4 ml ice-cold TFB2 buffer.
12. Prepare aliquots of 220 µl in sterile microcentrifuge tubes and freeze in liquid nitrogen or a dry-ice. Store the competent cells at -80°C.

TRANSFORMATION OF COMPETENT M15 CELLS

Materials

1. Water bath at 42°C
2. Psi broth (LB medium, 4 mM MgSO4, 10 mM KCl)
3. LB-agar plates containing 100 µg/ml ampicillin and 25 µg/ml kanamycin

Method

1. Transfer an aliquot of the ligation mix or plasmid (10 µl or less) into a cold sterile 15 ml Falcon tube.
2. Thaw an aliquot of frozen competent M15[pREP4] cells on ice.

3. Gently resuspend the cells and transfer 100 µl of the cell suspension into the tube with the ligation mix (or plasmid).
4. Transfer the tube to a 42°C water bath for 90 sec.
5. Add 500 µl Psi broth to the cells and incubate for 60-90 min at 37°C in a shaking incubator.
6. Plate out 100 µl on LB-agar plates containing 25 µg/ml kanamycin and 100 µg/ml ampicillin. Incubate the plates at 37°C overnight.

RAPID SCREENING OF SMALL EXPRESSION CULTURES

Method

1. Pick single colonies of transformants into 1.5 ml of culture media containing both ampicillin (100 µg/ml) and kanamycin (µg/ml). Inoculate one extra culture to serve as a noninduced control. Grow the cultures overnight.
2. Inoculate 10 ml of prewarmed medium (including antibiotics) with 500 µl of the overnight cultures, and grow at 37°C for 30 min, with vigorous shaking, until the OD_{600} is 0.5-0.7.
3. Induce expression by adding IPTG to a final concentration of 1 mM (do not add IPTG to the culture to be used as a noninduced control).
4. Grow the cultures for an additional 4-5h, and transfer to microcentrifuge tubes. Harvest the cells by centrifugation for 1 min at 15,000 x g, and discard supernatants.
5. Resuspend cells in Lysis buffer (Use B-PER from Pierce).

Ni-NTA BASED RECOMBINANT PROTEIN PURIFICATION

A. UNDER NATIVE CONDITIONS

Materials

Ni-NTA purification system (Invitrogen, K950-01)

Method

I. Preparing cell lysates under native conditions

1. Harvest cells from a 50 ml culture by centrifugation (5,000 rpm for 5 min). Resuspend the cells in 8 ml of Native binding buffer.
2. Add 8 mg lysozyme and 1X proteinase inhibitors (Pierce) and incubate on ice for 30 min.
3. Using a sonicator, sonicate the solution on ice using six 10-sec bursts at high intensity with a 10-sec cooling period between each burst.
4. Centrifuge the lysate at 3,000 × g for 15 min to pellet the cellular debris. Transfer the supernatant to a fresh tube.
5. Remove 5 µl of the lysate for SDS-PAGE analysis. Store the remaining lysate on ice or freeze at -20°C.

II. Preparing Ni-NTA column and purification under native conditions

1. Resuspend the Ni-NTA agarose in its bottle by inverting and gently tapping the bottle repeatedly.
2. Pipet 1.5 ml of the resin into a 10 ml purification column.
   Allow the resin to settle completely (5-10 min). Gently aspirate the supernatant.
3. Add 6 ml sterile, distilled water and resuspend the resin by alternately inverting and gently tapping the column.
4. Allow the resin to settle using gravity and aspirate the supernatant.
5. For purification under Native conditions, add 6 ml Native binding buffer.
6. Resuspend the resin by alternately inverting and gently tapping the column.

7. Allow the resin to settle using gravity and gently aspirate the supernatant. Repeat this step one more time.
8. Add 8 ml lysate prepared under native conditions to a prepared purification column.
9. Bind for 2h at 4°C using gentle agitation to keep the resin suspended in the lysate solution.
10. Settle the resin by gravity and carefully aspirate the supernatant. Save supernatant at 4°C for SDS-PAGE analysis.
11. Wash with 8 ml Native wash buffer. Settle the resin by gravity and carefully aspirate the supernatant. Save supernatant at 4C for SDS-PAGE analysis.
12. Repeat step 11 three more times.
13. Clamp the column in a vertical position and snap off the cap on the lower end. Elute the protein with 8-12 ml Native elution buffer. Collect 1 ml fractions and analyze with SDS-PAGE.
14. Store the eluted fractions at 4C.

B. UNDER HYBRID CONDITIONS

Method

I. Preparing cell lysates under denaturing conditions

1. Equilibrate the Guanidium Lysis Buffer, pH 7.8 to 37°C
2. Harvest cells from a 50 ml culture by centrifugation (5,000 rpm for 5 min)
3. Resuspend the cell pellet in 8 ml of Guanidium Lysis Buffer from step 1. Add 8mg of lysozyme and 1X proteinase inhibitor cocktail.
4. Slowly rock the cells for 10 min at RT to ensure thorough cell lysis
5. Sonicate the cell lysate on ice with three 5-sec pulses at high intensity
6. Centrifuge the lysate at 3,000 × g for 15 min to pellet the cellular debris. Transfer the supernatant to a fresh tube.
7. Remove 5 µl of the lysate for SDS-PAGE analysis. Store the remaining lysate on ice or at -20°C. When ready to use, proceed to the hybrid protocol.

II. Preparing Ni-NTA column and purification under hybrid conditions

1. Resuspend the Ni-NTA agarose in its bottle by inverting and gently tapping the bottle repeatedly.
2. Pipet 2 ml of the resin into a 10 ml purification column supplied with the kit. Allow the resin to settle completely by gravity (5-10 min). Gently aspirate the supernatant.
3. Add 6 ml of sterile, distilled water and resuspend the resin by alternately inverting and gently tapping the column.
4. Allow the resin to settle using gravity and aspirate the supernatant.
5. For purification under Denaturing conditions, add 6 ml of Denaturing binding buffer.
6. Resuspend the resin by alternately inverting and gently tapping the column.
7. Allow the resin to settle using gravity and gently aspirate the supernatant. Repeat the step one more time.
8. Add 8 ml lysate to a prepared purification column.
9. Bind for 1h at RT using gentle agitation to keep the resin msuspended in the lysate solution. Settle the resin by gravity or low speed centrifugation and carefully aspirate the supernatant.
10. Wash the column with 4 ml Denaturing binding buffer by resuspending the resin and rocking for two min. Settle the resin by gravity and carefully aspirate the supernatant. Save supernatant at 4°C for SDS-PAGE analysis. Repeat this step one more time.
11. Wash the column with 4 ml Denaturing wash buffer (pH 6.0) by resuspending the resin and rocking for 2 minutes. Settle the resin by gravity and aspirate the supernatant. Save supernatant at 4°C for SDS-PAGE analysis. Repeat this step one more time.
12. Wash the column with 8 ml Native wash buffer by resuspending the resin and rocking for 2 min. Settle the resin by gravity and aspirate the supernatant. Save supernatant at 4°C for SDS-PAGE analysis. Repeat this step 3 more times for a total of 4 native washes.
13. Clamp the column in a vertical position and snap off the cap on the lower end. Elute the protein with 8 ml Native elution buffer. Collect 2 ml fractions and analyze with SDS-PAGE.

PURIFICATION OF RECOMBINANT PROTEINS (pQE-TriSystem - QIAGEN)

PROTEINS UNDER DENATURING CONDITIONS

Methods

I. Growth of E. coli expression culture (100 ml)

1. Inoculate 10 ml of culture medium containing both ampicillin (100 ug/ml) and kanamycin (25 ug/ml) in a 50 ml flask. Grow the cultures at 37°C overnight.
2. Inoculate 100 ml of prewarmed media (with antibiotics) with 5 ml of the overnight cultures and grow at 37°C with vigorous shaking until an OD_{600} of 0.6 is reached (30-60 min).
3. Take a 1 ml sample immediately before induction.
4. Induce expression by adding IPTG to a final concentration of 1 mM.
5. Incubate the cultures for an additional 4-5 h. Collect a second 1 ml sample.
6. Harvest the cells by centrifugation at 4000 ×g for 20 min.
7. Freeze the cells overnight at -20°C.

II. Preparation of cleared *E.coli* lyasates under denaturing conditions

1. Thaw the cell pellet for 15 min on ice and resuspend in buffer B at 5 ml per gram wet weight.
2. Stir cells for 15-60 min at RT or lyse them by gently vortexing, taking care to avoid foaming. Lysis is complete when the solution becomes translucent.
3. Centrifuge lysate at 10,000 ×g for 20-30 min at RT to pellet the cellular debris. Save supernatant (cleared lysate).

III. Batch purification of 6xHis-tagged proteins from E. coli under denaturing conditions

Materials

1. Cleared lysate
2. Ni-NTA resin
3. Empty columns
4. Buffers B-E

Methods

1. Add 1 ml of the 50% Ni-NTA slurry to 4 ml lysate and mix gently by shaking (on a rotary shaker) for 15-60 min at RT.
2. Load-lysate-resin mixture carefully into an empty column with the bottom cap still attached.
3. Remove the bottom cap and collect the flow-through.
4. Wash twice with 4 ml buffer C.
5. Elute the recombinant protein 4 times with 0.5 ml buffer D, followed by 4 times with 0.5 ml buffer E. Collect fractions and analyze by SDS-PAGE.

Buffers for purification under denaturing conditions (Use molecular grade water)

Buffer B (Lysis Buffer)

Components	MW	1 L	500 ml	100 ml
100 mM NaH_2PO_4	119.96 g/mol	11.9 g	5.99 g	1.19 g
10 mM Tris Base	121.1 g/mol	1.2 g	0.6 g	0.12 g
8 M Urea	60.06 g/mol	480.5 g	240.25 g	48.05 g
Adjust pH to 8.0 using NaOH				

Buffer C (Wash Buffer)

Components	MW	1 L	500 ml	100 ml
100 mM NaH_2PO_4	119.96 g/mol	11.9 g	5.99 g	1.19 g

10 mM Tris Base	121.1 g/mol	1.2 g	0.6 g	0.12 g
8 M Urea	60.06 g/mol	480.5 g	240.25 g	48.05 g
Adjust pH to 6.3 using HCl				

Buffer D (Elution Buffer)

Components	MW	1 L	500 ml	100 ml
100 mM NaH_2PO_4	119.96 g/mol	11.9 g	5.99 g	1.19 g
10 mM Tris Base	121.1 g/mol	1.2 g	0.6 g	0.12 g
8 M Urea	60.06 g/mol	480.5 g	240.25 g	48.05 g
Adjust pH to 5.9 using HCl				

Buffer E (Elution Buffer)

Components	MW	1 L	500 ml	100 ml
100 mM NaH_2PO_4	119.96 g/mol	11.9 g	5.99 g	1.19 g
10 mM Tris Base	121.1 g/mol	1.2 g	0.6 g	0.12 g
8 M Urea	60.06 g/mol	480.5 g	240.25 g	48.05 g
Adjust pH to 4.5 using HOH				

Important Note: Due to the dissociation of urea, the pH of Buffers B, C, D, and E should be adjusted immediately prior to use. Do not autoclave.

PROTEIN ANTIGEN DIALYSIS

Materials

1. Slide-A-Lyzer MW 3.5K (Pierce; Cat# 66333)

Methods

1. Hydrate Membrane
   - Remove the cassette from its pouch and slip into the groove of the buoy
   - Immerse cassette in dialysis buffer
   - Hydrate the 3.5K cassettes for 30sec
   - Remove cassette from buffer and remove excess liquid by tapping the edge of the cassette gently on paper towels.
2. Add sample * Do NOT allow the needle to contact the membrane
- Fill the syringe with the sample, leaving a small amount of air in the syringe
- Insert the tip of the needle through one of the syringe ports located at a top corner of the cassette
- Inject sample slowly (Avoid foaming)
- Withdraw air by pulling up on the syringe piston
- Remove the syringe needle from the cassette while remaining air in the syringe
3. Dialysis
- Slip the cassette into the groove of a buoy and float this assembly in the dialysis buffer (Use the dialysis buffer at 500 times the volume of the sample
- Dialyze for 2 hours at 4°C
- Change the dialysis buffer and dialyze for another 2 hours
- Change the dialysis buffer and dialyze O/N at 4°C

4. Sample Removal
- Fill syringe with a volume of air at least equal to the sample size (For low volume samples, fill syringe with a volume of air approximately equal to two times the sample volume)
- Penetrate the gasket with the needle through a top, unused syringe guide port.
- Discharge air into cassette cavity to separate membranes
- Turn the unit so that needle is on the bottom and allow the sample to collect near the port
- Withdraw the sample into the syringe

BCA PROTEIN ASSAY (adapted for Nanodrop use)

The BCA Assay requires a standard curve to be generated each time it is run

Materials
BCA protein assay (Pierce; Cat# 23225)

Method
1. Prepare diluted albumin (BSA) standards.

- Dilute the contents of one BSA ampule into several clean vials. Preferably use the same diluent as the sample(s). Each 1 ml ampule of 2.0 mg/ml BSA is sufficient to prepare a set of diluted standards.

Working range = 20-2,000 ug/ml

Vial	Volume of Diluent	Volume and Source of BSA	Final BSA concentration
A	0	300ul of Stock	2,000 ug/ml *
B	125ul	375ul of Stock	1,500 ug/ml *
C	325ul	325ul of Stock	1,000 ug/ml *
D	175ul	175ul of vial B dilution	750 ug/ml
E	325ul	325ul of vial C dilution	500 ug/ml *
F	325ul	325ul of vial E dilution	250 ug/ml
G	325ul	325ul of vial F dilution	125 ug/ml *
H	400ul	100ul of vial G dilution	25 ug/ml
I	400ul	0	0ug/ml= Blank

If nanodrop allows only 5 standard points use these concentrations (*) to make the standard curve

2. Prepare the BCA Working Reagent (WR)

- Use the following formula to determine the total volume of WR required:

(# standards + # unknowns) × (# replicates) × (volume of WR per sample) = total volume WR required

3. Prepare WR

- Mix 50 parts of BCA reagent A with 1 part of BCA reagent B (50:1, Reagent A:B)

4. Regular assay (using a 20:1 reagent/sample volume ratio).

- Pipet 4 ul of sample in 80 ul of BCA reagent into a 1.7 ml centrifuge tube and mix well.
- Incubate tubes at 37°C for 30 minutes (working range = 20- 2,000 ug/ml). It is better to use water bath.
- Cool all tubes to RT.

5. Measure protein concentration using Nanodrop.

- A blank must be measured before the standard curve may be generated.
- Step 1: Measure the blank (BCA reagent – a “0” standard)
- Step 2: Up to 5 standards can be measured
- Step 3: Measure samples

ANTIBODY PURIFICATION FROM ASCITES

Materials

1. Zeba Desalt Spin Columns (2ml, Thermo Scientific #89889; 5ml #89891)
2. Melon Gel IgG Spin Purification Kit (Thermo Scientific # 45206)
3. Ascites Conditioning Reagent (Thermo Scientific #45219)
4. Variable-speed centrifuge
5. 15 ml conical tubes
6. Buffer for exchange
7. Serum samples

8. Pipettes and tips

Methods

A. Ascites Conditioning

1. Measure the volume of the sample and transfer to a centrifuge tube
2. Place one half the sample volume of 1 X Gel Purification Buffer into a tube and add 40 µl of the Ascites Conditioning Reagent for every 1 ml of original sample volume. Pulse vortex for 10 sec.
3. While mixing the sample, slowly add the buffer containing the Ascites Conditioning Reagent.
4. Rock or rotate sample for 10 min at RT. (Mixture appears opaque after conditioning)
5. Centrifuge sample at 5,000 ×g for 10 min. Take the supernatant and discard the pellet.
6. Desalt sample using Zeba Desalt Spin Columns pre-equilibrated with 1X Melon Gel Purification Buffer. (For best results, use a sample volume less than 10% of the total Zeba Column volume) Follow the manufacter's instructions about "Procedure for Protein Desalting".

B. IgG Purification from Ascites

1. Equilibrate the Melon Gel IgG Purification Support and Buffer to RT
2. Swirl bottle containing the Purification Support (don't vortex) to obtain an even suspension. Dispense 500µl of slurry into a Spin Column placed in a microcentrifuge tube. Swirl the bottle of gel slurry before pipetting each sample to maintain the gel suspension.
3. Centrifuge the uncapped column/tube for 1 min at 2,000-6,000 × g, then remove the spin column and discard flow-through.
4. Add 10 µl of 5X Regenerant per 1 ml of sample to the conditioned ascites and mix. Add 100 µl of the mixture to the gel, cap column, and incubate for 5 min at RT with end-over-end mixing.
5. Remove the bottom cap from the column, loosen top cap and re-insert spin column in the collection tube.
6. Centrifuge for 1 min to collect the purified antibody in the microcentrifuge tube. Repeat steps 5-7 for the second batch.
7. The antibody may be directly used or stored at -20°C

NOTE: Discard or regenerate the gel. For gel regeneration, perform the following steps:

1. Add 1.5 times the gel-bed volume of Melon Gel 1X Regenerant, mix for 5 min with end-over-end mixing, centrifuge and discard flow-through. Repeat this process a total of three times.
2. Wash gel with 10 times the gel-bed volume of water.
3. For storage, wash column with 10 times the gel-bed volume of 1X Melon Gel Purification Buffer. For storage longer than 1 week, add a final concentration of 0.02% sodium azide to the buffer used to wash the column.

IgG ANTIBODY PURIFICATION FROM SERUM

Materials

1. Zeba Desalt Spin Columns (2ml, Thermo Scientific #89889; 5ml #89891)
2. Melon Gel IgG Spin Purification Kit (Thermo Scientific # 45206)
3. Variable-speed centrifuge
4. 15 ml conical tubes
5. Buffer for exchange
6. Serum samples
7. Pipettes and tips

Methods

A. Procedure for buffer exchange

1. Twist off the column's bottom closure and loosen cap. Place column in a collection tube.

2. Centrifuge column at 1,000 × g for 2 min to remove storage solution. Place a mark on the side of the column where the compacted resin is slanted upward. Place column in centrifuge with the mark facing outward in all subsequent centrifugation step.
3. Add 1ml of Melon Gel Purification Buffer to the column. Centrifuge at 1,000 × g for 2 min to remove buffer.
4. Repeat step 3 two additional times, discarding buffer from the collection tube.
5. Place column in a new collection tube, remove cap and slowly apply 200-700 µl sample to the center of the compact resin bed.
6. To ensure maximal protein recovery from low-volume samples, apply a stacker of ultrapure water or buffer to the resin bed after the sample has fully absorbed (40 µl stacker for samples <350µl)
7. Centrifuge at 1,000 × g for 2 min to collect the sample. Discard column after use.

B. Spin-column procedure for antibody purification

1. Equilibrate the Melon Gel IgG Purification Support and Purification Buffer to RT (~ 15 min)
2. Swirl bottle containing the Purification Support (don't vortex) to obtain an even suspension. Dispense 500µl of slurry into a Spin Column placed in a microcentrifuge tube. Swirl the bottle of gel slurry before pipetting each sample to maintain the gel suspension.
3. Centrifuge the uncapped column/tube for 1 min at 2,000-6,000 × g, then remove the spin column and discard flow-through.
4. Add 300 µl of Purification Buffer to the column, pulse centrifuge for 10 sec and discard flow-through. Repeat this wash once. Place the bottom cap on the column.
5. Add 10-100 µl of buffer exchanged serum to the column. Cap column and incubate for 5 min at RT with end-over-end mixing.
6. Remove the bottom cap from the column, loosen top cap and re-insert spin column in the collection tube.
7. Centrifuge for 1 min to collect the purified antibody in the microcentrifuge tube. Repeat steps 5-7 for the second batch.
8. The antibody may be directly used or stored at -20°C.

NOTE: Discard the used gel support. If the gel must be used again, it can be regenerated by adding 500µl of 5M NaCl or 0.5N NaOH, mix for 5 min, centrifuge, and discard flow-through. Wash gel five times by adding 500µl Purification Buffer, centrifuge and discard flow-through. Add 500µl Purification Buffer and store at 4°C. The gel may be regenerated three times without significant loss of selectivity.

MONOCLONAL ANTIBODY ISOTYPING

Antigen-Independent Protocol

For each antibody sample to be tested, this method uses a set of 10 microplate wells corresponding to one negative control, one positive control, and the eight different class/subclass-specific specific primary antibodies (rabbit anti-mouse) supplied in the kit.

In the antigen-independent protocol, the first step is coating the microplate with anti-mouse Ig (G+A+M) polyclonal antibody; therefore, only the mouse IgG, IgA and IgM subclasses that are recognized by this coated antibody are detected.

Materials

1. Monoclonal antibody Isotying kit (Thermo Scientific #37501)
2. Flat-bottom high binding 96-well ELISA plate
3. PBS
4. Coating buffer (10mM sodium bicarbonate, pH 9.4; Cat. #28382)
5. Coating Antibody working solution: add 1 drop (~50 µl) of Coating Antibody (supplied) to 5 ml of Coating Buffer (prepare immediately before use in step 1).
6. 1X Blocking Solution: add 1 drop (~50 µl) of 50X Blocking Solution (supplied) to 2.5 ml of PBS

7. Wash Buffer: add 1 drop (~50 µl) of 50% Tween 20 (supplied) to 50 ml of PBS
8. HRP-GAR IgG (secondary antibody): add 1 drop (~50 µl) of HRP-Conjugated Goat Anti-Rabbit IgG (supplied) to 2.5 ml of wash buffer (prepared immediated before use in step 8)
9. 1X ABTS Substrate Buffer: add 5 drops (~250 µl) of the 10X ABTS Substrate Buffer concentrate (supplied to 2.5 ml of ultrapure water)
10. 1X ABTS Substrate Solution: add 1 drop (~50 µl) of 50X of ABTS Substrate (supplied) to 2.5 ml of 1X ABTS Substrate Buffer (prepare immediately before to use in step 10 of procedure)

Methods

1. Coat wells of a microplate with Coating Antibdoy by adding 50 µl of Coating Antibody Working Solution into 10 wells for each antibody sample to be assayed. Cover and incubate plate at 4°C overnight or at RT for 2 hr.
2. Empty the wells; add 125 µl of 1X Blocking Solution to coated wells; cover and incubate microplate at 37°C for 1 hr.
3. Empty wells and wash four times with 125 µl of Wash Buffer.
4. Add 50 µl of each antibody sample to wells #1 - #9 of each coated plate 10-well set; add 1 drop (50 µl) of Positive Control (supplied) to well #10 of each 10-well set; cover and incubate microplate at 37°C for 1 hr.
5. Empty wells and wash four times with 125 µl of Wash Buffer.
6. Add 1 drop (50 µl) of each specific anti-mouse antibody (8 total) to corresponding wells #1- #8 or each 10-well set.
   Add 1 drop (50 µl) of Normal Rabbit Serum (negative control) to well #9 of each 10-well set.
   Add 1 drop (50 µl) of the Anti-Mouse IgG1 Antibody to well #10 of each 10-well set.
   Record pattern of these primary antibody additions using the data template.
   Cover and incubate microplate at 37°C for 1hr.
7. Empty wells and wash four times with 125 µl of Wash Buffer.
8. Add 50 µl of HRP-GAR IgG (secondary antibody) to each well; cover and incubate microplate at 37°C for 1 hr.
9. Empty wells and wash four times with 125 µl of Wash Buffer.
10. Add 100 µl of 1X ABTS Substrate Solution to each well; cover and incubate microplate at RT for approximately 30 min. until color development is sufficiently complete.
11. Evaluate results qualitatively by spectrophotometry at 405nm. Positive wells typically have absorbance ranging from 0.8 to 1.2.

ALEXA FLUOR 488 PROTEIN LABELING (Molecular Probe)

Materials

1. 0.5ml of IgG solution at 2mg/ml
2. Handheld UV lamp
3. Ringstand
4. Alexa Fluor 488 Protein Labeling Kit (Molecular Probe #A10235) – 3 labelings
5. Autoclaved deionized water

Methods

A. Labeling the protein
1. Prepare a 1M solution of sodium bicarbonate by adding 1mL of dH20 to the provided vial of sodium bicarbonate (component B). Vortex until fully dissolved. It can be stored at 4°C for up to 2 weeks.
2. If the protein concentration if greater than 2mg/ml, dilute the protein to 2mg/ml in PBS.
3. To 0.5mL of the 2mg/ml protein solution, add 50µl of 1M bicarbonate.
4. Allow a vial of reactive dye to warm to RT. Transfer the protein solution from step 3 to the vial of reactive dye. This vial contains a magnetic stir bar. Cap the vial and invert a few times to fully dissolve the dye. Stir the reaction mixture for 1 hr at RT.

B. Purifying the Labeled Protein

1. Assemble the column and position it upright: attach a funnel to the top of a column. Gently insert the column through the X-cut in one of the provided foam holders to avoid damaging the column. Using the foam holder, secure the column with a clamp to a ringstand. Carefully remove the cap from the bottom of the column.
2. Prepare the elution buffer by diluting the RT 10X stock (component D) 10-fold in dH2O. Typically, less than 10 ml is required for each purification.
3. Using one of the provided pipets, stir the purification resin (component C) thoroughly to ensure a homogeneous suspension. Pipet the resin into the column, allowing excess buffer to drain away into a small beaker or other container. Resin should be packed into the column until the resin is ~3cm from the top of the column.
4. Allow the excess buffer to drain into the column bed. Do not worry about the column drying out, since the matrix will remain hydrated. Make certain the buffer elutes through the column with a consistently even flow prior to adding the reaction mixture. If the flow of buffer is slow or stalled, repack the column. Carefully load the reaction mixture from Part A onto the column. Allow the mixture to enter the column resin. Rinse the reaction vial with ~100 µl of elution buffer and apply to the column. Allow this solution to enter the column.
5. Slowly add elution buffer, taking care not to disturb the column bed. Continue adding elution buffer until the labeled protein has been eluted (about 50 min).
6. As the column runs, periodically illuminate the column with a handheld UV lamp. You should observe two colored bands, which represent the separation of labeled protein from unincorporated dye. Collect the first band, which contains the labeled protein, into one of the provided collection tubes. Add elution buffer to the column as necessary. Do not collect the slower moving band, which consists of unincorporated dye.
7. Store the labeled protein – which will be in PBS, pH 7.2, containing ~2mM sodium azide- at 2-6°C, protected from light. If the final concentration of purified protein conjugate is less than 1mg/ml, add BSA or other stabilizing protein to 1-10mg/ml. The conjugate should be stable at 4°C for several months. For long-term storage, divide the solution into small aliquots and freeze at ≤-20°C.

It is good practice to centrifuge solutions of conjugates in a microcentrifuge before use; only the supernatant should then be used in the experiment. This step will remove any aggregates that may have formed during storage.

BIOTINYLATION OF EAV RECOMBINANT VIRUSES

Materials

1. Amersham ECL Protein Biotinylation Module (RPN2203)
2. Orbital shaker
3. PBS, pH 7.5
4. PBS containing 1% BSA
5. Distilled water

Methods

1. Determine the concentration of protein to be biotinylated (see BCA method using nanodrop)
2. Prepare a 40 mM working concentration of bicarbonate buffer (BB) by diluting 1:20 in distilled water. (prepare always fresh)
3. Place the biotinylation reagent at RT and ensure the vial has equilibrated to RT prior to opening.
4. Dilute the protein to 1mg/ml in the diluted bicarbonate buffer. The maximum volume suitable for loading on to the column is 2.5 ml (the minimum volume is 2.0 ml). Add 40ul of biotinylation reagent for each mg of protein.
5. Incubate at RT for 1 h with constant agitation.

6. Discard the buffer at the top of the Sephadex G25 column, and cut 1-2 mm off the tip seal. Equilibrate the column with 5 ml of PBS-1% BSA (pH 7.5) followed by 20 ml of PBS. Discard the column washings. **Do not allow the column to run dry.**
7. Allow the buffer level in the top of the column to fall to the level of the plastic sinter at the top of the gel bed.
8. Apply the protein sample (in 2.0-2.5 ml) to the column. Allow the sample volume to enter the column before eluting with PBS and collecting fractions.
9. Elute the sample in 5 ml of PBS (use 2-3 mls of PBS to wash the tubes containing virus). **Collect 1 ml fractions (total 5 fractions)**. Measure protein concentration of 1-5 fractions to determine the eluted protein containing fractions.
10. Measure either protein concentration or UV absorbance at 280nm to verify the fraction number containing the eluted protein.
11. Aliquot in 0.5ml/tube. Make one tube with 110 µl of biotinylated EAV for titration. Store at -80C

VIRUS BINDING ASSAY

Keep everything at 4°C during the whole experiment

1. See EEC in 6 well plates and wait to grow 100% confluent.
2. Place cells at 4°C for 30 min to cool down.
3. Wash cells with cold PBS-2%FBS (PBS-F) 3 times before adding biotinylated VBS into each well.
4. Incubate the virus and cell mixtures at 4°C on a shaker for 60 min.
5. Remove the inocula and wash the unbound cells extensively (3X) with cold PBS-F
6. Add the non-enzymatic cell dissociation solution (Sigma, #C-5914, 1X, 1 ml/25cm^2 flask), 400ul/well and mix on a shaker.
7. Incubate at 4°C until cells are dissociated form the plates.
8. Add 1ml PBS-F to each well to the cells and pipet repeatedly to dissociate clumps. Transfer the cell suspension in 1.5ml eppendorf tube. Spin at 1000xg for 5 min (in real time PCR room, cool centrifuge at 4C prior to the experiment) and wash with 1ml PBS-F once to remove non-enzymatic buffer.
9. Incubate the washed cell pellets with 200ul 1:100 diluted streptavidin-FITC conjugated (Amersham, #RPN 1232) in PBS F for 60 min at 4C on a shaker
10. Wash cells once with ice cold PBS, and resuspend in 500 ul PBS F for immediate flow cytometric analysis.

Modified protocol for PBMC (EEC for control)

1. Prepare PBMC as for conventional flow cytometry staining. Process AD and NAD cells separately. Incubate on ice to keep it at 4C. Also resuspend EEC cells to use as control. Count the cells and place 10^6 cells into each well or tube.
2. Wash cells twice with ice cold PBS-2% FBS (PBS-F) at 4C
3. Incubate cells with anti-equine CD3 MAb (100ul) and biot-EAV (10ug protein, m.o.i. of 100? I am not sure how much difference is between these or which one will work better yet) in facs buffer (1% NGS; prepare newly and keep it sterile) for 45 min on ice.
4. Wash once with PBS-F
5. Incubate and anti-mouse IgG PE and streptavidin-FITC (total volume 100ul) for 45 min on ice
6. Wash twice with ice cold PBS-F followed by one wash with ice-cold PBS
7. Resuspend in 300ul of 2% paraformaldehyde.

INDIRECT IMMUNOFLUORESCENT ASSAY

Materials:

1. Chamber slides (Lab-Tek® [Chamber Slide™]; Nunc, Inc.) or coverslips for 24-well plate
2. Cover slips (large).
3. Confluent monolayer of cells (BHK21, RK13 etc.)
4. Cell medium (10% BCS-EMEM)

5. Fixative: **4% paraformaldehyde**
6. Wash buffer: **10mM glycine in PBS**
7. Permeabilization buffer: **PBS w/ 0.2% Triton-X 100**
8. Primary antibody dilution: **PBS w/ 5% FBS**
9. Secondary antibody dilution buffer: **PBS w/ 5% FBS or 0.02% evans blue in PBS**
10. FITC-conjugated goat anti-mouse IgG F(ab')2 (Caltag)
11. Mounting medium (Vector, Vectashield H-1000)

Method:

1. Trypsinize cells (T-75 flask) and resuspend into 60 mls of growth media. Plate 0.3 ml per well on to 8-well chamber slides (in this case, usually cells in chamber slides will be ready for infection in 24 hours). Incubate at 37°C. **OR** T-25 flask of cells were resuspended into 12 ml of growth medium. Plate 300µl cells per well on to eight chamber slides. Incubate at 37°C
2. Twenty four hours later or when cells are subconfluent aspirate media and infect with EAV at a m.o.i. of 5 (100 µl of diluted VBS53 EAV). Adsorb for 1 hour at 37°C. Add 0.3 ml of fresh medium and incubate for 24 hours.
3. Aspirate cell media.
4. Wash one time with **cold** PBS (0.6 ml per well).
5. Fix with 4% paraformaldehyde in PBS for at least 30 min at room temperature.
6. Rinse 3X in PBS/10mM glycine. 0.5-0.6ml/well. Leave the cells in your last PBS-glycine wash and store them at 4°C until labeling
7. Permeablize with PBS containing 0.2% Triton-X 100, leave at RT 5-10min.
8. Wash 3X with PBS/10mM glycine with slides on a shaker.
9. Dilute mouse MAb 12A4 against EAV nsp1
   Make 1:250 dilutions for unconjugated 12A4 (3.5µg/ml)
   Make 1:100 dilutions for AF488 conjugated 12A4 (1mg/ml)
10. Place 100µl drops of diluted Ab to each well. Incubate at RT for 1 hour. Leave slides on a shaker.
11. Wash 3X with PBS/10mM glycine 3 times with slides on a shaker.
12. Dilute secondary Ab [FITC-conjugated goat anti-mouse IgG F(ab')2 (Cat # 31543, Pierce Biotechnology) and FITC-conjugated goat anti-rabbit IgG(H+L) F(ab')2 (Cat # 31573, Pierce Biotechnology)]
    Make 1:100 dilutions
13. Incubate in dark for 1h at RT with slides on a shaker.
14. Wash 3X with PBS/10mM glycine with slides on a shaker.
15. Remove gaskets. Peel off the plastic stickers. Add a drop of mounting medium with DAPI (Vector, Vectashield H-1500) on each well of the chamber slides. Then place a coverslip over the stained slide. Store at 4°C in dark.

FLOW PROTOCOL FOR SURFACE AND INTRACELLULAR LABELING of AD and NAD PBMCs

Materials

1. 4% paraformaldehyde fixation
2. FACS buffer (DPBS with 0.1% (w/v) sodium azide. Filter 0.2 µm pore membrane. Store at 4°C. Add 1% NGS when needed)
3. Permeabilization buffer: DPBS, 1% heat-inactivated NGS, 0.1% (w/v) sodium azide, 0.1% saponin (w/v) and sterile filter (0.2 µm pore membrane)
4. Antibodies with appropriate dilution (All intracellular antibody dilutions will be performed in permeabilization buffer/ surface marker Abs are diluted in FACS buffer)
5. Secondary antibodies
6. Blocking solution (Flow buffer with 10% FBS)

Methods

Virus infection

1. Plate cells in each 150 mm culture dish and infect with virus at m.o.i. of 5. Dilute the virus in minimum volume of plain media (7 ml of plain RPMI is enough to cover 150 mm dish) Note: Include control cells (e.g. equine endothelial cells T-75 has approx. 1.5×10^7 cells)
2. Adsorb virus for 1 h and add 18 ml of 10% cRPMI media into each dish. Incubate for 12, 18, 36 h.
3. Cell collection.
4. Non-adherent cells: collect TCF. Wash twice with PBS (10 ml each time) and pull them together with TCF.
   Adherent cells: discard TCF and wash with PBS (10 ml each time) and discard the washed fluid. After washing, collect adherent cells using a scrapper and wash the dish with PBS and collect the PBS wash.
5. Pellet cells and count them.

Surface staining

1. Dilute the surface markers in facs buffer. Dilute cell pellet in facs buffer and equally aliquot ~1.0×10^6 cells into each of V-bottomed 96 well plate.
2. Label cells with 100ul of cell surface marker. Mix by pipetting and incubate for 30 minutes at 4°C (ice-bucket).
3. Wash once with 200ul facs buffer, centrifuge at 500 *g* for 5 minutes.
4. Label cells with 100ul of 2° Ab (goat anti-mouse IgG-PE conjugated diluted 1:200 in facs buffer). Incubate for 30 minutes at 4°C covered with aluminum foil
5. Wash once with 200ul facs buffer, centrifuge at 500 *g* for 5 min. Flick off excess

E. INTRACELLULAR EAV STAINING

6. Fix the cells with 200µl 4% paraformaldehyde for 30 minutes at RT in dark. Centrifuge at 500 *g* for 5 minutes.
7. Wash once with 200ul facs buffer.
8. Permeabilize membrane with permeabilization buffer (200 µl /tube) for 5 minutes.
9. Centrifuge at 500 *g* for 5 minutes.
10. Block Fc receptors with 10% FBS in FACS buffer for 30 minutes at RT in dark.
11. Dilute the intracellular labeling antibody in permeabilization buffer.
12. Label with fluorochrome- conjugated intracellular antibody for 30 minutes at RT in dark.
13. Wash 1X with 200 ul FACS buffer.
14. Resuspend in 200 ul of 0.5% paraformaldehyde/PBS and store at 4°C for next day acquisition.

SDS-PAGE and WESTERN BLOTTING

A. SDS-PAGE

Materials

1. BIO-RAD minigel apparatus
2. Glass plates with 1.5 mm spacers (Bio-Rad Cat #1653312)
3. Glass plates (short plates; Bio-Rad Cat#1653308)
4. 1.5 mm combs, 10 lanes (Bio-Rad Cat #1653365) or 15 lanes (Bio-Rad Cat#1653366)
5. Gaskets (Bio-Rad Cat #1653305)
6. Casting frames (Bio-Rad Cat#1653304)
7. 1.5 M Tris HCl pH 8.8, ml (Bio-Rad #161-0798)
8. 0.5 M Tris HCl pH 6.8, ml (Bio-Rad #161-0799)
9. Acrylamide/Bis, 30%/0.8% (Bio-Rad Cat #161-0158)
10. 10% SDS, µl (Bio-Rad Cat #161-0416)

11. TEMED, µl (Bio-Rad Cat #161-0801)
12. 10% Ammonium persulfate (APS; Bio-Rad Cat #161-0700)
13. Dissolve 1g of APS in 10ml of DW
14. Prepare 1 ml aliquots and store at -20°C
15. Laemmli sample buffer (Bio-Rad Cat #161-0737)
16. No-Weigh™ Dithiothreitol (DTT; Pierce Cat # 20291)
17. BenchMark Pre-stained protein ladder (Invitrogen, Cat #10748-010)
18. MagicMark XP (Invitrogen, Cat #LC5602)
19. Molecular grade water

<Gel Recipes: to make 2 mini-gels of 1.5mm thickness>

	Resolving (lower) gel		Stacking (upper) gel
	10%	12%	4%
30% AA	4.9	6 ml	0.675 ml
1.5 M Tris HCl pH 8.8	3.75	3.75 ml	-
0.5 M Tris HCl pH 6.8	-	-	1.25 ml
dH2O	6	4.95 ml	3 ml
10% SDS	150 µl	150 ul	50 µl
10% AP	75 µl	75 µl	30 µl
TEMED	15 µl	15 µl	5.5 µl

Buffers (See below for buffer recipe)

1. 1X TGS Running Buffer

Methods

1. Assemble the minigel apparatus: Wash glass plates and spacers with distilled water and detergent. Air-dry in a rack. The glass plates must be absolutely clean. Just before assembly wipe the glass plates with 70% ethanol.
2. Preparation of gel solutions using following table: Make up 12% resolving gels for viral proteins. Make up 10% resolving gel if looking for heavy (50,000 kDa) and light (25,000 kDa) of purified immunoglobulins. This will give best separation and resolution of heavy and light chains. Make up 5% stacking gel at the same time.
3. Prepare both gel solutions according to the recipe. Do not add TEMED until just before pouring the gel into the apparatus.
4. Pour the gel solution between the glass plates. Leave enough space for the stacking gel (comb depth + 1 cm approx). Overlay the gel with dH_2O.
5. Let the gel to polymerize (approx. 30 min), pour off the overlay and wash the top of gel several times with dH_2O. Remove any remaining H_2O with the edge of a paper towel.
6. Add TEMED to the prepared stacking gel solution, mix and immediately pour over top of resolving gel. Add close to the top. Place combs (before placing the combs should be washed with warm water and dried) in to the stacking gel (stop 3-5 mm above the inter phase of stacking and resolving gels). Avoid air bubbles. Allow 15 minutes for polymerization (during this time get the samples ready). Remove combs. Air bubbles should run in to replace combs.
7. Make up one liter of 1X SDS-PAGE running buffer (4X = 232 g glycine, 48 g Tris base, 16 g SDS made up to 4 liters) and pour 500 ml into the buffer tank.
8. Remove the gels (molds with the plexiglass holders) from the casting stand and lock into the central unit with thumbs pushing from the bottom. Small glass plate goes against the rubber gasket. Bottom clicks into place on base pate of the central unit.
9. Drop assemble unit into the buffer tank. Add running buffer to center compartment until gels get submerged. Do not allow inside buffer and buffer in the tank to communicate (not imperative). Flush out each well with pipette before loading the samples.
10. Preparation of Samples and Running the Gel: Denature protein in sample buffer (with the appropriate concentrations of DTT Pierce #20291) for 1-3 minutes. Can store the samples at -20^{0}C or -70^{0}C. Mix

1 tube of DTT (500mM) with 250ul of sample buffer. Mix with sample 1:1 dilution (e.g. 15ul of DTT in sample buffer + 15ul of sample)

11. Load 30-35 μl (10 lane combs) or 15 μl (15 lane combs) per lane. Use long slender pipette tips. Slip into space between two glass plates gently eject the sample into the well made by the comb. Load 1X sample buffer into lane 1 and 10 (or 15; do not load samples into these lanes and this will avoid the smiling effect). Load appropriate molecular weight markers to the second lane.
12. Add running buffer to the buffer tank until the level of the top of the gels.
13. Cover minigel unit (fits only one way) and fix red to red (positive), black to black (negative). Proteins are negatively charged and they migrate to the anode at the bottom. Run at 200 V, 30~40 min.
14. Stop when the dye front reaches the bottom. Turn off the power, pull off top and remove central gel unit and mark the left side of the glass plates with a "Sharpie" pen (this will indicate the lane one). Take apart the plates and cut the corner of the gel with a blade for identification (e.g. top left corner for gel).
15. Gels are ready for transfer (for western immunoblotting), autoradiography (for immunoprecipitation), or staining with Coomassie or silver stains. Proceed to appropriate protocol.

B. <u>Gel transfer to PVDF membrane</u>

Materials

1. Immun-Blot® PVDF membrane (7×8.4 cm; Bio-Rad Cat #162-0174)
2. Extra thick blot paper (cut to same size as blot membranes; Bio-Rad Cat#1703969)
3. Methanol (Fisher Cat#A412-4)
4. Clean forceps

Buffers (See below for buffer recipe)

1. Transfer buffer
2. TBS-T

Methods

1. Soak 2 filter papers for each gel in transfer buffer.
2. Pre-wet PVDF membrane in 100% methanol for 1-2 min and equilibrate the membrane in DW for 2 min and let it in transfer buffer.
3. Equilibrate the gel for 10 min in transfer buffer
4. For transfer, place one filter paper, PVDF membrane, SDS-PAGE and on top the second filter paper.
5. Assemble the transfer unit. Run at 15V for 1hr.
6. Rinse the transferred membrane in TBS-T buffer and proceed to western blotting step.

C. <u>Western Blotting</u>

Materials

1. Skim milk (Bio-Rad Cat#170-6404)
2. Antibody saver trays (Scienceware, small size)
3. Primary antibody (e.g. anti-EAV nsp1 [12A4] purified IgG)
4. Biotinylated goat anti-mouse IgG (Zymed Cat #81-6540) or biotinylated goat anti-rabbit IgG (Zymed Cat #81-6140)
5. Streptavidin-HRP (Zymed Cat #43-8323)
6. ECL™ Western blotting analysis system (GE Healthcare Cat #RPN2109)
7. Rad Tape (Midsci Cat #RAD-10)

Buffers (See below for buffer recipe)

1. TBS-T
2. Antibody dilution buffer (ADB)
3. 5% nonfat dry milk/PBS blocking buffer

Methods

1. Block the membrane in blocking buffer at 4°C O/N on a shaker or 1-2 hr at RT.
2. Wash the membrane with TBS-T once.
3. Incubate with primary antibody (most of MAb work at 1µg/ml) 1 hr at RT.
4. Wash 3 times with TBS-T (10 min/each)
5. Incubate with 1:5,000 diluted secondary antibody (Biotin-conjugated anti-Ms or anti-Rb) in ADB 1hr at RT.
6. Wash 3 times with TBS-T (10 min/each)
7. Incubate with 1:2,000 diluted Stv-HRP in Stv-HRP dilution buffer 1hr at RT.
8. Wash 3 times with TBS-T (10 min/each)
9. Mix 1:1 components of ECL to develop the membrane.

COOMASSIE BLUE R PROTEIN STAINING FOR DETECTION OF PROTEIN IN SDS-PAGE GELS

1. Place the gels on a glass dish and add 100 ml of Coomassie blue stain and leave on the rocker for 4 hours or more (can stain over night) to allow staining.
2. Remove the Coomassie blue stain (save can reuse) and add 200-250 ml of gel destaining buffer (40% methanol, 10% acetic acid in distilled water). Leave on the rocker for 8 hours. Keep a sponge or kimwipes in the glass dish to absorb stain.
3. Dry the gels on cellophane/perspex frames. Get two 12'' x 10'' cellophane sheets and wet with distilled water (wet one at a time). Lay one wet cellophane sheet on the bottom frame (with center in place to support cellophane) and place the gels over that. Overlay with second wet cellophane, avoid air bubbles, make good contact between gels and the cellophane sheets. Place the top frame (no center needed). Clamp edges together with bulldog clips while pulling cellophane tight. Make small hole for drainage in bottom corner and leave upright. Allow to dry 8-12 hours and remove the frames and store the gels.

NORTHERN BLOT

Materials

Before starting Northern Blot, check availability of following reagents

Gel Running

1. 10X Denaturing Gel buffer (Ambion #8676; 4°C)
2. 1X MOPS Gel Running Buffer (Ambion #8671; 4°C)
3. Formaldehyde Load Dye (Ambion #8551; -20°C)
4. Water bath or heat block 65°C

Transfer RNA to the membrane and hybridization steps (made in the lab)

1. Depurination solution:
   0.25M HCl
2. Denaturation solution:
   1.5M NaCl (43.8g for 500 ml or 87.6g for 1L)
   0.5 M NaOH (10g for 500 ml or 20g for 1L)

Add molecular biology grade distilled water to a final volume of 500 ml or 1 L and filter through a 0.45 um membrane.

3. Neutralization solution (pH 7.5):
   1.0M Tris Base (60.55g for 500 ml or 121.1g for 1L)
   1.5M NaCl (43.5g for 500 ml or 87g for 1L)
   Add molecular biology grade distilled water to a volume 400 ml or 800 ml.

Adjust to pH 7.5 with HCl. Make up to a final volume of 500 ml or 1L with distilled water and filter through a 0.45um membrane.

4. Transfer solution 20X SSC [(pH 7.0-7.2)]

NaCl	175g
Trisodium citrate (Na3C6H5O7.H20)	88.2g

Add distilled molecular biology grade distilled water to a final volume 1L.
If necessary, adjust to pH 7.0-7.2 with concentrated citric acid. Filter through a 0.45um membrane.
or
20X SSC ready packs form Ambion (Cat # 9762)
Dissolve in 1 liter of molecular biology grade water and make it alkaline by adding NaOH to a 10 mM concentration (0.4 gram per liter). This works well for transfer.

5. DIG Easy Hyb (Roche Biochemicals # 1 603 558)
6. Water bath 68°C
7. Hybridization oven 68°C
8. Boiling water or heat block >95°C

After hybridization
Low Stringency Buffer (2X SSC containing 0.1% SDS)
High Stringency Buffer (0.1X SSC containing 0.1% SDS) preheat to 68°C

GENERATION RECOMBINANT VIRUS FROM *IN VITRO* TRANSCRIBED RNA

A. PURIFICATION OF LINEARIZED PLASMID

1. Linearization of plasmid EAV infectious cDNA clone. Digestion of each plasmid DNA with *Xho I* to linearize the plasmid DNA.

Plasmid DNA	35.0 µl
Xho I (40U/µl, Roche)	1.0 µl
Buffer H (10x) (Roche)	4.0 µl
Total:	40.0 µl

Prepare 1 digestion reaction for each plasmid DNA. Incubate at 37°C for 2 hours.

2. Run 1 µl digested plasmid DNA on 1% agarose gel to make sure that the plasmid DNA is linearized.

Digested plasmid DNA	1.0 µl
6x loading buffer	2.0 µl
nuclease free water	9.0 µl
Total:	12.0 µl---------loading amount per well

Run 12 µl 1 kb DNA ladder (Invitrogen)

3. Add 2 µl of 20 mg/ml Proteinase K (Ambion) and bring the volume to 200 µl with nuclease free water and incubate at 37°C for 30 min.

4. 2× phenol chloroform extract and precipitate the DNA with 100% ethanol.
   - add 200 µl of phenol : chloroform : isoamyl alcohol (25:24:1) (Cat # P3803, Sigma) and mix until an emulsion is formed
   - centrifuge at 13,000 rpm for 4 min at room temperature
   - remove 180 µl of the upper aqueous phase into a new tube
   - add 180 µl of phenol : chloroform : isoamyl alcohol (25:24:1) and repeat the extraction
   - remove 160 µl of the upper aqueous phase into a new tube
   - add 500 µl of 100% ethanol and 16 µl of 3M sodium acetate to the DNA sample
   - mix and centrifuge at 13,000 rpm for 10 min

5. Wash with 140 µl of 70% ethanol. Spin at 13,000 rpm for 4 min. Aspirate the 70% ethanol and dry on the bench for 4-5 min.

6. Resuspend the pellet in 32 µl of nuclease free water and run 1 µl on gel.

Phenol chloroform extracted linearized plasmid DNA	1.0 µl
6x loading buffer	2.0 µl
nuclease free water	9.0 µl
Total	12.0 µl---------loading amount per well

B. *IN VITRO* TRANSCRIPTION

1. Prepare *in vitro* transcription reactions as follows. For linear DNA, rNTPs, BSA, DTT, 5 x transcription buffers, and cap analog, thaw them out at room temperature. Mix well before use. Always leave RNA guard RNase inhibitor and T7 RNA polymerase on ice. Use XhoI-linearized and phenol-chloroform purified plasmid DNA

***Master mix for in vitro* transcription**

Linear DNA	15.0 µl
rNTPs mix (10mM each)	5.0 µl
BSA (1mg/ml)	5.0 µl
100 mM DTT	2.5 µl
5X T7 Transcription buffer	10.0 µl
Cap analog (10mM)	5.0 µl
RNA guard RNase Inhibitor	2.5 µl
T7 RNA polymerase	2.5 µl
Nuclease free water	2.5 µl
	50.0 µl

Incubate at 37ºC for 2 hours.

2. Wash electrophoresis unit (electrophoresis tank, gel cast and running trays, comb) thoroughly with detergent. Then rinse thoroughly with dH_2O. Spray electrophoresis unit with RNaseZap, then rinse thoroughly with dH_2O. Let it air dry.
3. Prepare 1x TAE buffer. Cast 0.8% agarose gel.
4. After 1 h of *in vitro* transcription at 37ºC, run 2 µl of *in vitro* transcribed RNA on a 0.8% agarose gel.

TE Buffer (pH=7.2)	8.0 µl
10%SDS	1.0 µl
0.5M EDTA (pH=8.0)	0.25 µl
RNA	2.0 µl

- place mix at 70ºC for 2 minutes and then place on ice for 2 minutes
- add 2.25 µl of 6X gel loading buffer
- load 13.5 µl mixtures to each well of the gel. Run the gel at 90V.

5. Check the gel under UV light.
6. Measure RNA concentration with spectrophotometry.
7. Dilute 2 µl *in vitro* transcribed RNA into 198 µl nuclease-free water and measure A260. Use nuclease-free water as blank control.

C. TRANSFECTION OF BHK21 CELLS WITH ELECTROPORATION

Preparation of cells

1. Make sure to use cells that are not confluent. Typically a flask of BHK21 cells were split 1:4 two days before planning to do the electroporation. One T-150 cm^2 flask of BHK21 cells will be used for 2 electroporations.

2. Aspirate the medium from T-150 flasks of subconfluent BHK21 (P67) cells. Wash cells twice with PBS. Add 4 ml ATV to each T-150 flask. Shake for 30 sec. Let it sit at room temperature for 1 min. Then remove the ATV and put the flasks at 37ºC for a few minutes.
3. After cells slough off, add 10 ml EMEM to each T-150 flask.
4. Use a pipet with a wide bore to transfer cells to 50 ml conical centrifuge tube. **Place immediately on ice.**
5. Spin cells at 4ºC, 600 rpm for 5min. Place cells back on ice.
6. Remove medium and add 25 ml sterile ice cold PBS. Resuspend cell pellet by gentle shaking of tube. If you need to use a pipet to resuspend cells, use a wide bore pipet and pipet gently.
7. Spin cells at 4ºC, 600 rpm for 5min. Place cells back on ice.
8. Remove media and wash cells by the addition of 25 ml sterile ice cold PBS. At this time take a small sample of cells for counting with a hemocytometer.
9. Spin cells at 4ºC, 600 rpm for 5min. Place cells back on ice.
10. Remove PBS with a pipet and resuspend cell pellet in ice cold PBS to a final concentration of 1 x 10^7 cells/ml.

Electroporation of cells

1. Place 25 µl of freshly thawed *in vitro* transcribed into each microcentrifuge tube. Set up one tube without RNA as negative control.
2. Add 500 µl of BHK21 cells (5× 10^6 cells) into microcentrifuge tube containing *in vitro* transcribed RNA and mix gently.
3. Transfer RNA-cells mixture into each electroporation cuvette (0.4 cm electrode gap). Place the cuvette into the cuvette holder and pulse cells twice. The following settings are used: 850 volts, capacitance set at 25 µF, and the pulse controller set at infinite ohms. When doing pulses, push the two buttons together until you hear the beep, then immediately push them again until you hear the second beep.
4. After electroporation is complete, set cells aside (room temperature) for a 10 min 'recovery period'.
5. Do the next sample.
6. After the recovery period is complete, transfer the cells from the cuvette into 15 ml of room temperature growth medium (EMEM) in a T-75 flask. Aliquot 0.15 ml of cells to each well of 8-well chamber slides for immunofluorescence assay (2 wells-mock transfected and 2 wells transfected).
7. Place cells at 37ºC CO_2 incubator. Check the development of CPE. When CPE is complete (usually 72-96 h post transfection), tissue culture fluids were harvested and centrifuged at 1900 rpm for 10 min at 4ºC. The tissue culture fluids were titrated in RK13 cells.

<u>ELECTROPORATION USING BTXPRESS ELECTROPORATOR AND ELECTROPORATION SOLUTION</u>

Method

A. PREPARE THE CELLS

Divide the cells 18-24 hours prior to electroporation as needed and culture overnight.

B. PREPARE FOR ELECTROPORATION

1. Warm all solutions to RT before use.
2. Harvest cells for electroporation, and count cells to determine cells/ml.

3. Determine the total volume needed for all the electroporations. Multiply the number of electroporations needed by 0.1 ml (for 0.2 cm cuvettes) OR by 0.25 ml (for 0.4 cm cuvettes) and add 10% more for pipetting errors. Total volume needed= _____ ml.
4. Determine the volume of cells required for each electroporation according to the formula:

5. Volume needed (ml) = (#cells needed/ml [5 x 10^6 cells/ml]/# counted cells/ml) × Total volume of BTXpress Solution from step C

6. Enter the calculated volume needed = _____ml
7. Pipette the volume of cells determined in step d into a new tube and centrifuge at 1000 ×g for 5 minutes. Aspirate the supernatant.
8. Prepare a culture vessel with pre-warmed complete medium.
9. Immediately transfer to 60mm petri dish (21 cm^2 surface area) containing growth medium. (Each well of 6 well-plate is 10 cm^2)→ I decide to put everything in 6 well plate with 4 ml growth medium. Then take 500 ul into chamber slides for IFA.
10. Resuspend the centrifuged cells from step e in ____ ml BTXpress Solution according to the volume determined in step c.

C. Add _____ µl IVT RNA (use 20 µg/ml of cells= 5 µg) to the cells. Mix gently.
   i) pEAV-GFP IVT RNA (total 49 µl RNA)
   ii) mock infection

   b) Aliquot 100 µl (0.25 cm cuvette) or 250 ul (0.4 cm cuvette) DNA/cell mix to each cuvette.
   c) Eletroporate at RT. Using a square wave system set the voltage and pulse length given for your cells as described in Table1. If using an exponential decay set the capacitance to 950 µF and resistance to "None". Use the voltage given for your cells from Table 1&2 for complete protocol. Voltage=____260 V____

D. Electroporation settings:

Choose Mode:	**T**	500 V/Capacitance & Resistance (LV)
Capacitance:	**C**	950□F
Set Resistance:	**R**	R1 (13ohm)
Chamber Gap: BTX Disposable Cuvette P/N 640 (4mm gap)		
Set Charging Voltage:	**S**	260V
Desired Field Strength:	**E**	650 V/cm
Desired Pulse Length:	**t**	Approximately 9 msec (Reality: 10 msec)

   a) Immediately mix the cells gently and transfer to the dish prepared in step B-f.
   b) Incubate in complete medium for 12-72 hours or as required.
   c) Harvest cells and perform assay as required.

MAMMALIAN CELL TRANSFECTION USING LIPID-BASED TRANSFECTION REAGENT

Materials

1. Lipofectamine™ 2000 (Invitrogen, Cat# 11668-027)
2. Fugene HD (Roche, Cat# E2311)

Method

1. Place sterile glass cover slips onto wells to be used for IFA staining.
2. Trypsinize T-75 flask of Vero 76 (ATCC #CRL-1587) cells and count the cells (One confluent T-75 contains approx. 1 × 10^7 Vero cells).

3. One day before transfection, plate 2×10^5 cells/well in 500 µl of growth medium so that cells will be 90-95% confluent at the time of transfection.
4. For each transfection sample, prepare complexes as follows:
   a. Dilute 0.8 µg of plasmid DNA in 50 µl of Opti-MEM I. Mix gently.
   b. Mix Lipofectamine™ 2000 gently before use, then dilute 2.0 µl of Lipofectamine in 50 µl of Opti-MEM I medium. Incubate for 5 min at RT.
   c. After the 5 min incubation, combine the diluted DNA with diluted Lipofectamine™ 2000 (total volume = 100 µl). Mix gently and incubate for 20 min at RT.
5. Add the 100 µl of transfection mix to each well containing cells and medium. Mix gently by rocking the plate back and forth.
6. Incubate cells at 37°C in a CO2 incubator for 4 hr.

   After incubation for 4 hr with the transfection mix, replace the mix with 500 µl of growth media (containing FBS). Incubate at 37°C for 18-48 hours prior to testing for transgene expression.

DETECTION OF EAV SUBGENOMIC RNA IN INFECTED CELLS

Method

A. TOTAL RNA EXTRACTION FROM EAV INFECTED CELLS

1. Prepare 2 T-25 for infected cells and 2-T25 for uninfected cells. Final number of tubes for each group will be 4 (total 8 tubes)
2. Infect confluent monolayer of EECs in a T-25 flask at an m.o.i of 2 (diluted in 1ml of plain MEM) and incubate for 1 h. Add 9 ml of growth media and incubate for 18 h.
3. Decant the excess media and wash with ice-cold PBS (Gibco) 3 times. Scrape the cells and pellet down in a microcentrifuge tube at 3000g for 15 minutes.
4. Aspirate the medium and wash 1X in PBS.
5. Extract RNA using MagMAX™-96 Total RNA Isolation Kit (Ambion, AM1830). According to the protocol, it lyses up to 2×10^6 cells in 140µl of Lysis/Binding Solution. So a pellet from 1 T-25 flask can be divided into two and extract RNA simultaneously as two different samples. Elute RNA in 50 µl of elution buffer. Store RNA at -80°C.

B. REVERSE TRANSCRIPTION

Material

1. SuperScript III First-Strand synthesis System for RT-PCR (Invitrogen; Cat# 18080-051)

Method

3. Prepare the following mixture:

RNA	2.0 µl
Reverse primer (20 µM)	1.0 µl
dNTP mix (10 mM each)	1.0 µl
RNase-free water	6.0 µl

2. Mix and briefly centrifuge each component before use.
3. Prepare RNA/primer mixtures in sterile 0.2 ml tubes as above.
4. Incubate each sample at 65C for 5 min, then place on ice for at least 1 min.
5. Prepare the following cDNA Synthesis Mix, adding each component in the indicated order:

10X RT buffer	2 µl
25mM MgCl2	4 µl
0.1M DTT	2 µl
Rnase OUT Rnase Inhibitor	1µl
Superscript III RT	1µl

6. Add 10ul of cDNA Synthesis Mix to each RNA/primer mixture, mix gently, and collect by brief centrifugation.
7. Incubate at 50C for 60 min.
8. Terminate the reactions at 85C for 5 min. Chill on ice.
9. Collect the reactions by brief centrifugation. Add 1 ul of Rnase H (2 units/ul) to each tube and incubate for 20 min at 37C.
10. The final volume of the product is 21ul. cDNA synthesis reaction can be stored at -20C or used for PCR immediately.
11. For long-term storage, place the reactions at -20C.

C. PCR USING PFU TURBO DNA POLYMERASE (STRATAGENE)

cDNA template	2.0 µl
Forward primer (20 µM)	0.5 µl
Reverse primer (20 µM)	0.5 µl
dNTP mix (25 mM each)	0.2 µl
10X Pfu Turbo PCR buffer	2.5 µl
Pfu Turbo DNA polymerase	0.5 µl
RNase-free water	18.8 µl

D. PCR CONDITION

Cycles	Temp	Duration
1	95C	2 min
35	95C	45 sec
	48C	45 sec
	72C	3 min
1	72C	10 min

D. PRODUCT SIZE

Product	Size (bp)
gmRNA	12704
sgmRNA2	3200
sgmRNA3	2684
sgmRNA4	2251
sgmRNA5	1883
sgmRNA6	1041
sgmRNA7	659

REFERENCES

1. Eigen M (1993) The origin of genetic information: viruses as models. Gene 135: 37-47.
2. Jeffares DC, Poole AM, Penny D (1998) Relics from the RNA world. Journal of molecular evolution 46: 18-36.
3. Lai MM, Cavanagh D (1997) The molecular biology of coronaviruses. Adv Virus Res 48: 1-100.
4. Lai MMC, Holmes KV (2001) Coronaviruses. In: Knipe DM, Howley PM, editors. Fields Virology. Philadelphia, PA: Lippindcott, Williams & Wilkins. pp. 1163-1185.
5. Siddell SG, Ziebuhr J, Snijder EJ (2005) Coronaviruses, toroviruses and arteriviruses. In: Mahy BWJ, ter Meulen V, editors. Topley & Wilson's Microbiology and Microbial Infections: Virology. pp. 823-856.
6. Ziebuhr J (2004) Molecular biology of severe acute respiratory syndrome coronavirus. Current opinion in microbiology 7: 412-419.
7. Cavanagh D (1997) Nidovirales: a new order comprising Coronaviridae and Arteriviridae. Arch Virol 142: 629-633.
8. Gorbalenya AE, Enjuanes L, Ziebuhr J, Snijder EJ (2006) Nidovirales: evolving the largest RNA virus genome. Virus Res 117: 17-37.
9. Gonzalez JM, Gomez-Puertas P, Cavanagh D, Gorbalenya AE, Enjuanes L (2003) A comparative sequence analysis to revise the current taxonomy of the family Coronaviridae. Arch Virol 148: 2207-2235.
10. den Boon JA, Snijder EJ, Chirnside ED, de Vries AA, Horzinek MC, et al. (1991) Equine arteritis virus is not a togavirus but belongs to the coronaviruslike superfamily. J Virol 65: 2910-2920.
11. Gorbalenya AE, Koonin EV, Donchenko AP, Blinov VM (1989) Coronavirus genome: prediction of putative functional domains in the non-structural polyprotein by comparative amino acid sequence analysis. Nucleic Acids Res 17: 4847-4861.
12. Snijder EJ, den Boon JA, Bredenbeek PJ, Horzinek MC, Rijnbrand R, et al. (1990) The carboxyl-terminal part of the putative Berne virus polymerase is expressed by ribosomal frameshifting and contains sequence motifs which indicate that toro- and coronaviruses are evolutionarily related. Nucleic Acids Res 18: 4535-4542.
13. Cowley JA, Dimmock CM, Spann KM, Walker PJ (2000) Gill-associated virus of Penaeus monodon prawns: an invertebrate virus with ORF1a and ORF1b genes related to arteri- and coronaviruses. J Gen Virol 81: 1473-1484.
14. Snijder EJ, SIddell SG, Gorbalenya AE (2005) The order Nidovirales. In: Mahy BWJ, ter Meulen V, editors. Topley & Wilson's Microbiology and Microbial Infections. London, United Kingdom: VIrology.
15. MacLachlan NJ, Balasuriya, U.B., Murtaugh, M.P., Barthold, S.W., and Lowenstine, L.J (2008) Arterivirus pathogenesis and immune response. In: Perlman S. GT, Snijder E.J., editor. Nidoviruses. Washingon, D.C.: ASM Press.
16. Drosten C, Preiser W, Gunther S, Schmitz H, Doerr HW (2003) Severe acute respiratory syndrome: identification of the etiological agent. Trends in molecular medicine 9: 325-327.

17. Kuiken T, Fouchier RA, Schutten M, Rimmelzwaan GF, van Amerongen G, et al. (2003) Newly discovered coronavirus as the primary cause of severe acute respiratory syndrome. Lancet 362: 263-270.
18. Rota PA, Oberste MS, Monroe SS, Nix WA, Campagnoli R, et al. (2003) Characterization of a novel coronavirus associated with severe acute respiratory syndrome. Science 300: 1394-1399.
19. Drosten C, Gunther S, Preiser W, van der Werf S, Brodt HR, et al. (2003) Identification of a novel coronavirus in patients with severe acute respiratory syndrome. The New England journal of medicine 348: 1967-1976.
20. Wang LF, Shi Z, Zhang S, Field H, Daszak P, et al. (2006) Review of bats and SARS. Emerging infectious diseases 12: 1834-1840.
21. Mihindukulasuriya KA, Wu G, St Leger J, Nordhausen RW, Wang D (2008) Identification of a novel coronavirus from a beluga whale by using a panviral microarray. Journal of virology 82: 5084-5088.
22. Flegel TW (1997) Major viral diseases of the black tiger prawn (Penaeus monodon) in Thailand. World J Microbiol Biotechnol 13: 433-442.
23. Zirkel F, Kurth A, Quan PL, Briese T, Ellerbrok H, et al. (2011) An insect nidovirus emerging from a primary tropical rainforest. mBio 2: e00077-00011.
24. Enjuanes L, Gorbalenya AE, de Groot RJ, Cowley JA, Ziebuhr J, et al. (2008) Nidovirales. In: Mahy BWJ, an Regenmortel MHV, editors. Encyclopedia of Virology. Oxford: Elsevier. pp. 419-430.
25. Brierley I, Digard P, Inglis SC (1989) Characterization of an efficient coronavirus ribosomal frameshifting signal: requirement for an RNA pseudoknot. Cell 57: 537-547.
26. Van Hemert MJ, Snijder EJ (2008) The Arterivirus Replicase. In: Perlman S, Gallagher T, Snijder EJ, editors. Nidoviruses. Washington, DC: American Society for Microbiology. pp. 83-101.
27. Baric RS, Stohlman SA, Lai MM (1983) Characterization of replicative intermediate RNA of mouse hepatitis virus: presence of leader RNA sequences on nascent chains. J Virol 48: 633-640.
28. de Vries AA, Chirnside ED, Bredenbeek PJ, Gravestein LA, Horzinek MC, et al. (1990) All subgenomic mRNAs of equine arteritis virus contain a common leader sequence. Nucleic Acids Res 18: 3241-3247.
29. Lai MM, Baric RS, Brayton PR, Stohlman SA (1984) Characterization of leader RNA sequences on the virion and mRNAs of mouse hepatitis virus, a cytoplasmic RNA virus. Proc Natl Acad Sci U S A 81: 3626-3630.
30. Spaan W, Delius H, Skinner M, Armstrong J, Rottier P, et al. (1983) Coronavirus mRNA synthesis involves fusion of non-contiguous sequences. Embo J 2: 1839-1844.
31. Porterfield JS, Casals J, Chumakov MP, Gaidamovich SY, Hannoun C, et al. (1978) Togaviridae. Intervirology 9: 129-148.
32. Westaway EG, Brinton MA, Gaidamovich S, Horzinek MC, Igarashi A, et al. (1985) Togaviridae. Intervirology 24: 125-139.
33. Snijder EJ, Horzinek MC, Spaan WJ (1993) The coronaviruslike superfamily. Adv Exp Med Biol 342: 235-244.

34. Snijder EJ, Meulenberg JJ (1998) The molecular biology of arteriviruses. J Gen Virol 79: 961-979.
35. Hyllseth B (1970) Buoyant density studies on equine arteritis virus. Arch Gesamte Virusforsch 30: 97-104.
36. Hyllseth B (1973) Structural proteins of equine arteritis virus. Arch Gesamte Virusforsch 40: 177-188.
37. Maess J (1971) [Complement dependent neutralization of equine arteritis virus. Brief report]. Arch Gesamte Virusforsch 33: 194-196.
38. van der Zeijst BA, Horzinek MC (1975) The genome of equine arteritis virus. Virology 68: 418-425.
39. Keffaber KK (1989) Reproductive failure of unknown etiology. American Association of Swine Practitioners 1: 1-9.
40. Benfield DA, Nelson E, Collins JE, Harris L, Goyal SM, et al. (1992) Characterization of swine infertility and respiratory syndrome (SIRS) virus (isolate ATCC VR-2332). Journal of veterinary diagnostic investigation : official publication of the American Association of Veterinary Laboratory Diagnosticians, Inc 4: 127-133.
41. Allende R, Lewis TL, Lu Z, Rock DL, Kutish GF, et al. (1999) North American and European porcine reproductive and respiratory syndrome viruses differ in non-structural protein coding regions. J Gen Virol 80 (Pt 2): 307-315.
42. Suarez P, Zardoya R, Martin MJ, Prieto C, Dopazo J, et al. (1996) Phylogenetic relationships of european strains of porcine reproductive and respiratory syndrome virus (PRRSV) inferred from DNA sequences of putative ORF-5 and ORF-7 genes. Virus Res 42: 159-165.
43. Fang Y, Schneider P, Zhang WP, Faaberg KS, Nelson EA, et al. (2007) Diversity and evolution of a newly emerged North American Type 1 porcine arterivirus: analysis of isolates collected between 1999 and 2004. Arch Virol 152: 1009-1017.
44. Ropp SL, Wees CE, Fang Y, Nelson EA, Rossow KD, et al. (2004) Characterization of emerging European-like porcine reproductive and respiratory syndrome virus isolates in the United States. Journal of virology 78: 3684-3703.
45. Tian K, Yu X, Zhao T, Feng Y, Cao Z, et al. (2007) Emergence of fatal PRRSV variants: unparalleled outbreaks of atypical PRRS in China and molecular dissection of the unique hallmark. PLoS One 2: e526.
46. Tong GZ, Zhou YJ, Hao XF, Tian ZJ, An TQ, et al. (2007) Highly pathogenic porcine reproductive and respiratory syndrome, China. Emerging infectious diseases 13: 1434-1436.
47. Zhou YJ, Hao XF, Tian ZJ, Tong GZ, Yoo D, et al. (2008) Highly virulent porcine reproductive and respiratory syndrome virus emerged in China. Transboundary and emerging diseases 55: 152-164.
48. Feng Y, Zhao T, Nguyen T, Inui K, Ma Y, et al. (2008) Porcine respiratory and reproductive syndrome virus variants, Vietnam and China, 2007. Emerging infectious diseases 14: 1774-1776.
49. Normile D (2007) Virology. China, Vietnam grapple with 'rapidly evolving' pig virus. Science 317: 1017.

50. Li K, Schuler T, Chen Z, Glass GE, Childs JE, et al. (2000) Isolation of lactate dehydrogenase-elevating viruses from wild house mice and their biological and molecular characterization. Virus Res 67: 153-162.
51. Plagemann PG, Moennig V (1992) Lactate dehydrogenase-elevating virus, equine arteritis virus, and simian hemorrhagic fever virus: a new group of positive-strand RNA viruses. Adv Virus Res 41: 99-192.
52. Sillevis Smitt PA, de Jong JM (1989) Animal models of amyotrophic lateral sclerosis and the spinal muscular atrophies. Journal of the neurological sciences 91: 231-258.
53. Espana C (1974) Viral epizootics in captive nonhuman primates. Laboratory animal science 24: 167-176.
54. Myers MG, Vincent MM, Hensen SA, Tauraso NM (1972) Problems in the laboratory isolation of simian hemorrhagic fever viruses and isolatse metaboli enterobacteriaceae classificat enterobacteriaceae enzymology hydrogen peroxide metaboli enterobacteriaceae metaboliion of the agent responsible for the Sussex-69 epizootic. Applied microbiology 24: 62-69.
55. Gravell M, London WT, Leon ME, Palmer AE, Hamilton RS (1986) Differences among isolates of simian hemorrhagic fever (SHF) virus. Proceedings of the Society for Experimental Biology and Medicine Society for Experimental Biology and Medicine 181: 112-119.
56. Snijder EJ (2001) Arteriviruses. In: Knipe DM, Howley, P. M., editor. Fields Virology. Philadelphia, PA: Lippincott Williams and Wilkins. pp. 1205-1220.
57. de Vries AA, Chirnside ED, Horzinek MC, Rottier PJ (1992) Structural proteins of equine arteritis virus. J Virol 66: 6294-6303.
58. Snijder EJ, van Tol H, Pedersen KW, Raamsman MJ, de Vries AA (1999) Identification of a novel structural protein of arteriviruses. J Virol 73: 6335-6345.
59. Wieringa R, de Vries AA, van der Meulen J, Godeke GJ, Onderwater JJ, et al. (2004) Structural protein requirements in equine arteritis virus assembly. J Virol 78: 13019-13027.
60. Konishi S, Akashi H, Sentsui H, Ogata M (1975) Studies on equine viral arteritis. I. Characterization of the virus and trial survey on antibody with vero cell cultures. Nippon Juigaku Zasshi 37: 259-267.
61. McCollum WH, Doll ER, Wilson JC, Johnson CB (1961) Propagation of equine arteritis virus in monolayer cultures of equine kidney. Am J Vet Res 22: 731-735.
62. Harry TO, McCollum WH (1981) Stability of viability and immunizing potency of lyophilized, modified equine arteritis live-virus vaccine. Am J Vet Res 42: 1501-1505.
63. Zhang J, Timoney PJ, Shuck KM, Seoul G, Go YY, et al. Molecular epidemiology and genetic characterization of equine arteritis virus isolates associated with the 2006-2007 multi-state disease occurrence in the USA. J Gen Virol 91: 2286-2301.
64. van Dinten LC, den Boon JA, Wassenaar AL, Spaan WJ, Snijder EJ (1997) An infectious arterivirus cDNA clone: identification of a replicase point mutation that abolishes discontinuous mRNA transcription. Proc Natl Acad Sci U S A 94: 991-996.

65. van Dinten LC, Rensen S, Gorbalenya AE, Snijder EJ (1999) Proteolytic processing of the open reading frame 1b-encoded part of arterivirus replicase is mediated by nsp4 serine protease and Is essential for virus replication. J Virol 73: 2027-2037.
66. Ziebuhr J, Snijder EJ, Gorbalenya AE (2000) Virus-encoded proteinases and proteolytic processing in the Nidovirales. J Gen Virol 81: 853-879.
67. de Vries AA, Post SM, Raamsman MJ, Horzinek MC, Rottier PJ (1995) The two major envelope proteins of equine arteritis virus associate into disulfide-linked heterodimers. J Virol 69: 4668-4674.
68. Snijder EJ, Dobbe JC, Spaan WJ (2003) Heterodimerization of the two major envelope proteins is essential for arterivirus infectivity. J Virol 77: 97-104.
69. Balasuriya UB, Dobbe JC, Heidner HW, Smalley VL, Navarrette A, et al. (2004) Characterization of the neutralization determinants of equine arteritis virus using recombinant chimeric viruses and site-specific mutagenesis of an infectious cDNA clone. Virology 321: 235-246.
70. Chirnside ED, de Vries AA, Mumford JA, Rottier PJ (1995) Equine arteritis virus-neutralizing antibody in the horse is induced by a determinant on the large envelope glycoprotein GL. J Gen Virol 76: 1989-1998.
71. Deregt D, de Vries AA, Raamsman MJ, Elmgren LD, Rottier PJ (1994) Monoclonal antibodies to equine arteritis virus proteins identify the GL protein as a target for virus neutralization. J Gen Virol 75: 2439-2444.
72. Glaser AL, de Vries AA, Dubovi EJ (1995) Comparison of equine arteritis virus isolates using neutralizing monoclonal antibodies and identification of sequence changes in GL associated with neutralization resistance. J Gen Virol 76: 2223-2233.
73. Balasuriya UB, Heidner HW, Hedges JF, Williams JC, Davis NL, et al. (2000) Expression of the two major envelope proteins of equine arteritis virus as a heterodimer is necessary for induction of neutralizing antibodies in mice immunized with recombinant Venezuelan equine encephalitis virus replicon particles. J Virol 74: 10623-10630.
74. Balasuriya UB, Patton JF, Rossitto PV, Timoney PJ, McCollum WH, et al. (1997) Neutralization determinants of laboratory strains and field isolates of equine arteritis virus: identification of four neutralization sites in the amino-terminal ectodomain of the G(L) envelope glycoprotein. Virology 232: 114-128.
75. Balasuriya UB, Rossitto PV, DeMaula CD, MacLachlan NJ (1993) A 29K envelope glycoprotein of equine arteritis virus expresses neutralization determinants recognized by murine monoclonal antibodies. J Gen Virol 74: 2525-2529.
76. Balasuriya UB, MacLachlan NJ (2004) The immune response to equine arteritis virus: potential lessons for other arteriviruses. Vet Immunol Immunopathol 102: 107-129.
77. Timoney PJ, McCollum WH (1993) Equine viral arteritis. Vet Clin North Am Equine Pract 9: 295-309.
78. Balasuriya UB, Evermann JF, Hedges JF, McKeirnan AJ, Mitten JQ, et al. (1998) Serologic and molecular characterization of an abortigenic strain of equine arteritis virus isolated from infective frozen semen and an aborted equine fetus. J Am Vet Med Assoc 213: 1586-1589, 1570.

79. Balasuriya UB, Hedges JF, Nadler SA, McCollum WH, Timoney PJ, et al. (1999) Genetic stability of equine arteritis virus during horizontal and vertical transmission in an outbreak of equine viral arteritis. J Gen Virol 80 (Pt 8): 1949-1958.
80. Hedges JF, Balasuriya UB, Timoney PJ, McCollum WH, MacLachlan NJ (1999) Genetic divergence with emergence of novel phenotypic variants of equine arteritis virus during persistent infection of stallions. J Virol 73: 3672-3681.
81. Firth AE, Zevenhoven-Dobbe JC, Wills NM, Go YY, Balasuriya UB, et al. Discovery of a small arterivirus gene that overlaps the GP5 coding sequence and is important for virus production. J Gen Virol 92: 1097-1106.
82. Nitschke M, Korte T, Tielesch C, Ter-Avetisyan G, Tunnemann G, et al. (2008) Equine arteritis virus is delivered to an acidic compartment of host cells via clathrin-dependent endocytosis. Virology 377: 248-254.
83. Fang Y, Snijder EJ (2010) The PRRSV replicase: exploring the multifunctionality of an intriguing set of nonstructural proteins. Virus Res 154: 61-76.
84. Pedersen KW, van der Meer Y, Roos N, Snijder EJ (1999) Open reading frame 1a-encoded subunits of the arterivirus replicase induce endoplasmic reticulum-derived double-membrane vesicles which carry the viral replication complex. J Virol 73: 2016-2026.
85. Snijder EJ, van Tol H, Roos N, Pedersen KW (2001) Non-structural proteins 2 and 3 interact to modify host cell membranes during the formation of the arterivirus replication complex. J Gen Virol 82: 985-994.
86. van der Meer Y, van Tol H, Locker JK, Snijder EJ (1998) ORF1a-encoded replicase subunits are involved in the membrane association of the arterivirus replication complex. J Virol 72: 6689-6698.
87. van Dinten LC, Wassenaar AL, Gorbalenya AE, Spaan WJ, Snijder EJ (1996) Processing of the equine arteritis virus replicase ORF1b protein: identification of cleavage products containing the putative viral polymerase and helicase domains. J Virol 70: 6625-6633.
88. Gallie DR (1998) A tale of two termini: a functional interaction between the termini of an mRNA is a prerequisite for efficient translation initiation. Gene 216: 1-11.
89. Pasternak AO, Spaan WJ, Snijder EJ (2006) Nidovirus transcription: how to make sense...? J Gen Virol 87: 1403-1421.
90. Sawicki SG, Sawicki DL (1995) Coronaviruses use discontinuous extension for synthesis of subgenome-length negative strands. Adv Exp Med Biol 380: 499-506.
91. Sawicki SG, Sawicki DL, Siddell SG (2007) A contemporary view of coronavirus transcription. J Virol 81: 20-29.
92. van Marle G, Dobbe JC, Gultyaev AP, Luytjes W, Spaan WJ, et al. (1999) Arterivirus discontinuous mRNA transcription is guided by base pairing between sense and antisense transcription-regulating sequences. Proc Natl Acad Sci U S A 96: 12056-12061.
93. Snijder EJ, Spaan WJ (2006) Arteriviruses. In: Knipe DM, Howley, P.M., editor. Fields Virology. 5th ed. Philadelphia: Lippincott Williams & Wilkins. pp. 1337-1355.

94. Siddell SG, Ziebuhr J, Snijder EJ (2005) Coronaviruses, toroviruses and arteriviruses. In: Mahy BWJ, ter Meulen V, editors. Topley & Wilson's Microbiology and Microbial Infections, Virology: Hodder Arnold. pp. 823-856.
95. Sawicki D, Wang T, Sawicki S (2001) The RNA structures engaged in replication and transcription of the A59 strain of mouse hepatitis virus. J Gen Virol 82: 385-396.
96. Pasternak AO, van den Born E, Spaan WJ, Snijder EJ (2001) Sequence requirements for RNA strand transfer during nidovirus discontinuous subgenomic RNA synthesis. Embo J 20: 7220-7228.
97. Pasternak AO, van den Born E, Spaan WJ, Snijder EJ (2003) The stability of the duplex between sense and antisense transcription-regulating sequences is a crucial factor in arterivirus subgenomic mRNA synthesis. J Virol 77: 1175-1183.
98. van den Born E, Posthuma CC, Gultyaev AP, Snijder EJ (2005) Discontinuous subgenomic RNA synthesis in arteriviruses is guided by an RNA hairpin structure located in the genomic leader region. J Virol 79: 6312-6324.
99. den Boon JA, Kleijnen MF, Spaan WJ, Snijder EJ (1996) Equine arteritis virus subgenomic mRNA synthesis: analysis of leader-body junctions and replicative-form RNAs. J Virol 70: 4291-4298.
100. de Vries AAF, Horzinek, M.C., Rottier, P.J.M., de Groot, R.J. (1997) The genome organization of the *Nidovirales*: similarities and differences between arteri-, toro-, and coronaviruses. Semin Virol 8: 33-47.
101. Stueckemann JA, Holth M, Swart WJ, Kowalchyk K, Smith MS, et al. (1982) Replication of lactate dehydrogenase-elevating virus in macrophages. 2. Mechanism of persistent infection in mice and cell culture. J Gen Virol 59: 263-272.
102. Wood O, Tauraso N, Liebhaber H (1970) Electron microscopic study of tissue cultures infected with simian haemorrhagic fever virus. J Gen Virol 7: 129-136.
103. Breese SS, Jr., McCollum WH. Electron microscopic characterization of equine arteritis virus. In: Bryans JT, Gerber HS, editors; 1970; Basel, Switzerland. Karger.
104. Pol JM, Wagenaar F (1992) Morphogenesis of Lelystad virus in porcine lung alveolar macrophages. American Association of Swine Practitioners Newsletter. pp. 29.
105. Pol JM, Wagenaar F, Reus JEG (1997) Comparative morphogenesis of three PRRS virus strains. Veterinary Microbiology 55: 203-208.
106. Snijder EJ, van der Meer Y, Zevenhoven-Dobbe J, Onderwater JJ, van der Meulen J, et al. (2006) Ultrastructure and origin of membrane vesicles associated with the severe acute respiratory syndrome coronavirus replication complex. J Virol 80: 5927-5940.
107. van der Meer Y, Snijder EJ, Dobbe JC, Schleich S, Denison MR, et al. (1999) Localization of mouse hepatitis virus nonstructural proteins and RNA synthesis indicates a role for late endosomes in viral replication. J Virol 73: 7641-7657.
108. Stertz S, Reichelt M, Spiegel M, Kuri T, Martinez-Sobrido L, et al. (2007) The intracellular sites of early replication and budding of SARS-coronavirus. Virology 361: 304-315.

109. Gosert R, Kanjanahaluethai A, Egger D, Bienz K, Baker SC (2002) RNA replication of mouse hepatitis virus takes place at double-membrane vesicles. J Virol 76: 3697-3708.
110. Snijder EJ, Wassenaar AL, Spaan WJ (1994) Proteolytic processing of the replicase ORF1a protein of equine arteritis virus. J Virol 68: 5755-5764.
111. Wassenaar AL, Spaan WJ, Gorbalenya AE, Snijder EJ (1997) Alternative proteolytic processing of the arterivirus replicase ORF1a polyprotein: evidence that NSP2 acts as a cofactor for the NSP4 serine protease. J Virol 71: 9313-9322.
112. van Hemert MJ, de Wilde AH, Gorbalenya AE, Snijder EJ (2008) The in vitro RNA synthesizing activity of the isolated arterivirus replication/transcription complex is dependent on a host factor. J Biol Chem 283: 16525-16536.
113. van Aken D, Zevenhoven-Dobbe J, Gorbalenya AE, Snijder EJ (2006) Proteolytic maturation of replicase polyprotein pp1a by the nsp4 main proteinase is essential for equine arteritis virus replication and includes internal cleavage of nsp7. J Gen Virol 87: 3473-3482.
114. Snijder EJ, Wassenaar AL, van Dinten LC, Spaan WJ, Gorbalenya AE (1996) The arterivirus nsp4 protease is the prototype of a novel group of chymotrypsin-like enzymes, the 3C-like serine proteases. J Biol Chem 271: 4864-4871.
115. Laity JH, Lee BM, Wright PE (2001) Zinc finger proteins: new insights into structural and functional diversity. Current opinion in structural biology 11: 39-46.
116. Snijder EJ, Wassenaar AL, Spaan WJ (1992) The 5' end of the equine arteritis virus replicase gene encodes a papainlike cysteine protease. J Virol 66: 7040-7048.
117. Tijms MA, Nedialkova DD, Zevenhoven-Dobbe JC, Gorbalenya AE, Snijder EJ (2007) Arterivirus subgenomic mRNA synthesis and virion biogenesis depend on the multifunctional nsp1 autoprotease. J Virol 81: 10496-10505.
118. den Boon JA, Faaberg KS, Meulenberg JJ, Wassenaar AL, Plagemann PG, et al. (1995) Processing and evolution of the N-terminal region of the arterivirus replicase ORF1a protein: identification of two papainlike cysteine proteases. J Virol 69: 4500-4505.
119. Tijms MA, van Dinten LC, Gorbalenya AE, Snijder EJ (2001) A zinc finger-containing papain-like protease couples subgenomic mRNA synthesis to genome translation in a positive-stranded RNA virus. Proc Natl Acad Sci U S A 98: 1889-1894.
120. Tijms MA, van der Meer Y, Snijder EJ (2002) Nuclear localization of non-structural protein 1 and nucleocapsid protein of equine arteritis virus. J Gen Virol 83: 795-800.
121. Snijder EJ, Wassenaar AL, Spaan WJ, Gorbalenya AE (1995) The arterivirus Nsp2 protease. An unusual cysteine protease with primary structure similarities to both papain-like and chymotrypsin-like proteases. J Biol Chem 270: 16671-16676.
122. Posthuma CC, Pedersen KW, Lu Z, Joosten RG, Roos N, et al. (2008) Formation of the arterivirus replication/transcription complex: a key role for nonstructural protein 3 in the remodeling of intracellular membranes. J Virol 82: 4480-4491.
123. Gorbalenya AE, Koonin EV, Lai MM (1991) Putative papain-related thiol proteases of positive-strand RNA viruses. Identification of rubi- and aphthovirus proteases and delineation of a novel conserved domain associated with proteases of rubi-, alpha- and coronaviruses. FEBS Lett 288: 201-205.

124. Manolaridis I, Gaudin C, Posthuma CC, Zevenhoven-Dobbe JC, Imbert I, et al. Structure and genetic analysis of the arterivirus nonstructural protein 7{alpha}. J Virol.
125. te Velthuis AJ, van den Worm SH, Sims AC, Baric RS, Snijder EJ, et al. Zn(2+) inhibits coronavirus and arterivirus RNA polymerase activity in vitro and zinc ionophores block the replication of these viruses in cell culture. PLoS Pathog 6: e1001176.
126. van Dinten LC, van Tol H, Gorbalenya AE, Snijder EJ (2000) The predicted metal-binding region of the arterivirus helicase protein is involved in subgenomic mRNA synthesis, genome replication, and virion biogenesis. J Virol 74: 5213-5223.
127. Gorbalenya AE, Koonin EV (1989) Viral proteins containing the purine NTP-binding sequence pattern. Nucleic Acids Res 17: 8413-8440.
128. Gorbalenya AE, Blinov VM, Donchenko AP, Koonin EV (1989) An NTP-binding motif is the most conserved sequence in a highly diverged monophyletic group of proteins involved in positive strand RNA viral replication. J Mol Evol 28: 256-268.
129. Gorbalenya AE, Koonin EV, Donchenko AP, Blinov VM (1988) A novel superfamily of nucleoside triphosphate-binding motif containing proteins which are probably involved in duplex unwinding in DNA and RNA replication and recombination. FEBS Lett 235: 16-24.
130. Seybert A, van Dinten LC, Snijder EJ, Ziebuhr J (2000) Biochemical characterization of the equine arteritis virus helicase suggests a close functional relationship between arterivirus and coronavirus helicases. J Virol 74: 9586-9593.
131. Seybert A, Posthuma CC, van Dinten LC, Snijder EJ, Gorbalenya AE, et al. (2005) A complex zinc finger controls the enzymatic activities of nidovirus helicases. J Virol 79: 696-704.
132. Posthuma CC, Nedialkova DD, Zevenhoven-Dobbe JC, Blokhuis JH, Gorbalenya AE, et al. (2006) Site-directed mutagenesis of the Nidovirus replicative endoribonuclease NendoU exerts pleiotropic effects on the arterivirus life cycle. J Virol 80: 1653-1661.
133. Ivanov KA, Hertzig T, Rozanov M, Bayer S, Thiel V, et al. (2004) Major genetic marker of nidoviruses encodes a replicative endoribonuclease. Proc Natl Acad Sci U S A 101: 12694-12699.
134. Nedialkova DD, Ulferts R, van den Born E, Lauber C, Gorbalenya AE, et al. (2009) Biochemical characterization of arterivirus nonstructural protein 11 reveals the nidovirus-wide conservation of a replicative endoribonuclease. J Virol 83: 5671-5682.
135. Horzinek M, Maess J, Laufs R (1971) Studies on the substructure of togaviruses. II. Analysis of equine arteritis, rubella, bovine viral diarrhea, and hog cholera viruses. Arch Gesamte Virusforsch 33: 306-318.
136. Magnusson P, Hyllseth B, Marusyk H (1970) Morphological studies on equine arteritis virus. Arch Gesamte Virusforsch 30: 105-112.
137. Wieringa R, de Vries AA, Raamsman MJ, Rottier PJ (2002) Characterization of two new structural glycoproteins, GP(3) and GP(4), of equine arteritis virus. J Virol 76: 10829-10840.

138. Thaa B, Kabatek A, Zevenhoven-Dobbe JC, Snijder EJ, Herrmann A, et al. (2009) Myristoylation of the arterivirus E protein: the fatty acid modification is not essential for membrane association but contributes significantly to virus infectivity. J Gen Virol 90: 2704-2712.
139. de Vries AA, Raamsman MJ, van Dijk HA, Horzinek MC, Rottier PJ (1995) The small envelope glycoprotein (GS) of equine arteritis virus folds into three distinct monomers and a disulfide-linked dimer. J Virol 69: 3441-3448.
140. Wieringa R, De Vries AA, Post SM, Rottier PJ (2003) Intra- and intermolecular disulfide bonds of the GP2b glycoprotein of equine arteritis virus: relevance for virus assembly and infectivity. J Virol 77: 12996-13004.
141. Molenkamp R, van Tol H, Rozier BC, van der Meer Y, Spaan WJ, et al. (2000) The arterivirus replicase is the only viral protein required for genome replication and subgenomic mRNA transcription. J Gen Virol 81: 2491-2496.
142. Hedges JF, Balasuriya UB, Timoney PJ, McCollum WH, MacLachlan NJ (1996) Genetic variation in open reading frame 2 of field isolates and laboratory strains of equine arteritis virus. Virus Res 42: 41-52.
143. Hedges JF, Balasuriya UB, MacLachlan NJ (1999) The open reading frame 3 of equine arteritis virus encodes an immunogenic glycosylated, integral membrane protein. Virology 264: 92-98.
144. Wieringa R, de Vries AA, Rottier PJ (2003) Formation of disulfide-linked complexes between the three minor envelope glycoproteins (GP2b, GP3, and GP4) of equine arteritis virus. J Virol 77: 6216-6226.
145. Glaser AL, de Vries AA, Dubovi EJ (1995) Comparison of equine arteritis virus isolates using neutralizing monoclonal antibodies and identification of sequence changes in GL associated with neutralization resistance. J Gen Virol 76 (Pt 9): 2223-2233.
146. Stadejek T, Bjorklund H, Bascunana CR, Ciabatti IM, Scicluna MT, et al. (1999) Genetic diversity of equine arteritis virus. J Gen Virol 80 (Pt 3): 691-699.
147. Dobbe JC, van der Meer Y, Spaan WJ, Snijder EJ (2001) Construction of chimeric arteriviruses reveals that the ectodomain of the major glycoprotein is not the main determinant of equine arteritis virus tropism in cell culture. Virology 288: 283-294.
148. Chirnside ED, de Vries AA, Mumford JA, Rottier PJ (1995) Equine arteritis virus-neutralizing antibody in the horse is induced by a determinant on the large envelope glycoprotein GL. J Gen Virol 76 (Pt 8): 1989-1998.
149. Deregt D, de Vries AA, Raamsman MJ, Elmgren LD, Rottier PJ (1994) Monoclonal antibodies to equine arteritis virus proteins identify the GL protein as a target for virus neutralization. J Gen Virol 75 (Pt 9): 2439-2444.
150. Nugent J, Sinclair R, deVries AA, Eberhardt RY, Castillo-Olivares J, et al. (2000) Development and evaluation of ELISA procedures to detect antibodies against the major envelope protein (G(L)) of equine arteritis virus. J Virol Methods 90: 167-183.
151. Balasuriya UB, Maclachlan NJ, De Vries AA, Rossitto PV, Rottier PJ (1995) Identification of a neutralization site in the major envelope glycoprotein (GL) of equine arteritis virus. Virology 207: 518-527.

152. Balasuriya UB, Rossitto PV, DeMaula CD, MacLachlan NJ (1993) A 29K envelope glycoprotein of equine arteritis virus expresses neutralization determinants recognized by murine monoclonal antibodies. J Gen Virol 74 (Pt 11): 2525-2529.
153. Verheije MH, Welting TJ, Jansen HT, Rottier PJ, Meulenberg JJ (2002) Chimeric arteriviruses generated by swapping of the M protein ectodomain rule out a role of this domain in viral targeting. Virology 303: 364-373.
154. Balasuriya UB, Heidner HW, Davis NL, Wagner HM, Hullinger PJ, et al. (2002) Alphavirus replicon particles expressing the two major envelope proteins of equine arteritis virus induce high level protection against challenge with virulent virus in vaccinated horses. Vaccine 20: 1609-1617.
155. Castillo-Olivares J, de Vries AA, Raamsman MJ, Rottier PJ, Lakhani K, et al. (2001) Evaluation of a prototype sub-unit vaccine against equine arteritis virus comprising the entire ectodomain of the virus large envelope glycoprotein (G(L)): induction of virus-neutralizing antibody and assessment of protection in ponies. J Gen Virol 82: 2425-2435.
156. Deshpande A, Wang S, Walsh MA, Dokland T (2007) Structure of the equine arteritis virus nucleocapsid protein reveals a dimer-dimer arrangement. Acta Crystallogr D Biol Crystallogr 63: 581-586.
157. Fukunaga Y, McCollum WH (1977) Complement-fixation reactions in equine viral arteritis. Am J Vet Res 38: 2043-2046.
158. Balasuriya UB, Timoney PJ, McCollum WH, MacLachlan NJ (1995) Phylogenetic analysis of open reading frame 5 of field isolates of equine arteritis virus and identification of conserved and nonconserved regions in the GL envelope glycoprotein. Virology 214: 690-697.
159. Chirnside ED, Wearing CM, Binns MM, Mumford JA (1994) Comparison of M and N gene sequences distinguishes variation amongst equine arteritis virus isolates. J Gen Virol 75 (Pt 6): 1491-1497.
160. Murphy TW, McCollum WH, Timoney PJ, Klingeborn BW, Hyllseth B, et al. (1992) Genomic variability among globally distributed isolates of equine arteritis virus. Vet Microbiol 32: 101-115.
161. Sugita S, Kondo T, Sekiguchi K, Yamaguchi S, Kamada M, et al. Molecular characterization of the M gene of equine arteritis virus. In: Nakajima H, Plowright W, editors; 1994; Tokyo, Japan. R&W Pulications, Newmarket, England. pp. 39-43.
162. Murphy TW, Timoney PJ, McCollum WH. Analysis of genetic variation among strains of equine arteritis virus. In: Powell DG, editor; 1987; Lexington, KY. University Press Kentucky, Lexington, KY. pp. 3-12.
163. Archambault D, Laganiere G, Carman S, St-Laurent G (1997) Comparison of nucleic and amino acid sequences and phylogenetic analysis of open reading frames 3 and 4 of various equine arteritis virus isolates. Vet Res 28: 505-516.
164. Balasuriya UB, Hedges JF, Smalley VL, Navarrette A, McCollum WH, et al. (2004) Genetic characterization of equine arteritis virus during persistent infection of stallions. J Gen Virol 85: 379-390.
165. Hedges JF, Balasuriya UB, Topol JB, Lee DW, MacLachlan NJ (2001) Genetic variation of ORFs 3 and 4 of equine arteritis virus. Adv Exp Med Biol 494: 69-72.

166. Larsen LE, Storgaard T, Holm E (2001) Phylogenetic characterisation of the G(L) sequences of equine arteritis virus isolated from semen of asymptomatic stallions and fatal cases of equine viral arteritis in Denmark. Vet Microbiol 80: 339-346.
167. Lepage N, St-Laurent G, Carman S, Archambault D (1996) Comparison of nucleic and amino acid sequences and phylogenetic analysis of the Gs protein of various equine arteritis virus isolates. Virus Genes 13: 87-91.
168. St-Laurent G, Lepage N, Carman S, Archambault D (1997) Genetic and amino acid analysis of the GL protein of Canadian, American and European equine arteritis virus isolates. Can J Vet Res 61: 72-76.
169. Hornyak A, Bakonyi T, Tekes G, Szeredi L, Rusvai M (2005) A novel subgroup among genotypes of equine arteritis virus: genetic comparison of 40 strains. J Vet Med B Infect Dis Vet Public Health 52: 112-118.
170. Stadejek T, Mittelholzer C, Oleksiewicz MB, Paweska J, Belak S (2006) Highly diverse type of equine arteritis virus (EAV) from the semen of a South African donkey: short communication. Acta Vet Hung 54: 263-270.
171. de Boer GF, Osterhaus AD, van Oirschot JT, Wemmenhove R (1979) Prevalence of antibodies to equine viruses in the Netherlands. Tijdschr Diergeneeskd 104: suppl 65-74.
172. Herbst W, Danner K (1985) [Serologic studies on the occurrence of the arteritis virus in the horse in West Germany]. Dtsch Tierarztl Wochenschr 92: 461-463.
173. Huntington PJ, Forman AJ, Ellis PM (1990) The occurrence of equine arteritis virus in Australia. Aust Vet J 67: 432-435.
174. Lang G, Mitchell WR (1984) A serosurvey by ELISA for antibodies to EAV in Ontario racehorses. J Equine Vet Sci 4: 153-157.
175. McCollum WH, Bryans JT. Serological identification of infection by equine arteritis virus in horses of several countries. In: Gerber JTBaH, editor; 1973; Paris. S. Karger, Basel. pp. 256-263.
176. Moraillon A, Moraillon R (1978) Results of an epidemiological investigation on viral arteritis in France and some other European and African countries. Ann Rech Vet 9: 43-54.
177. Timoney PJ, McCollum, W.H (1987) Equine viral arteritis. Can Vet J 28: 693-695.
178. Paweska JT (1994) Equine viral arteritis in donkeys in South Africa. J S Afr Vet Assoc 65: 40.
179. Paweska JT, Aitchison H, Chirnside ED, Barnard BJ (1996) Transmission of the South African asinine strain of equine arteritis virus (EAV) among horses and between donkeys and horses. Onderstepoort J Vet Res 63: 189-196.
180. Paweska JT, Barnard BJ (1993) Serological evidence of equine arteritis virus in donkeys in South Africa. Onderstepoort J Vet Res 60: 155-158.
181. Barnard BJ, Paweska JT (1993) Prevalence of antibodies against some equine viruses in zebra (Zebra burchelli) in the Kruger National Park, 1991-1992. Onderstepoort J Vet Res 60: 175-179.
182. Paweska JT, Binns MM, Woods PS, Chirnside ED (1997) A survey for antibodies to equine arteritis virus in donkeys, mules and zebra using virus neutralisation (VN) and enzyme linked immunosorbent assay (ELISA). Equine Vet J 29: 40-43.

183. Borchers K, Wiik H, Frolich K, Ludwig H, East ML (2005) Antibodies against equine herpesviruses and equine arteritis virus in Burchell's zebras (Equus burchelli) from the Serengeti ecosystem. J Wildl Dis 41: 80-86.
184. Weber H, Beckmann K, Haas L (2006) [Case report: equine arteritis virus (EAV) as the cause of abortion in alpacas?]. DTW Deutsche tierarztliche Wochenschrift 113: 162-163.
185. Bryans JT, Doll ER, Knappenberger RE (1957) An outbreak of abortion caused by the equine arteritis virus. Cornell Vet 47: 69-75.
186. Cole JR, R.F. Hall, H.S. Gosser, J.B. Hendricks, A.R. Pursell, D.A. Senne, J.E. Pearson, and C.A. Gipson (1986) Transmissibility and abortogenic effect of equine viral arteritis in mares. J Am Vet Med Assoc 189: 769-771.
187. McCollum WH, Prickett ME, Bryans JT (1971) Temporal distribution of equine arteritis virus in respiratory mucosa, tissues and body fluids of horses infected by inhalation. Res Vet Sci 12: 459-464.
188. Timoney PJ, McCollum WH, Murphy TW, Roberts AW, Willard JG, et al. (1987) The carrier state in equine arteritis virus infection in the stallion with specific emphasis on the venereal mode of virus transmission. J Reprod Fertil Suppl 35: 95-102.
189. Timoney PJ, McCollum WH, Roberts AW, Murphy TW (1986) Demonstration of the carrier state in naturally acquired equine arteritis virus infection in the stallion. Res Vet Sci 41: 279-280.
190. Neu SM, P.J. Timoney, and W.H. McCollum. Persistent infection of the reproductive tract in stallions experimentally infected with equine arteritis virus. In: Powell DG, editor; 1987; Lexington, Kentucky. The University Press of Kentucky, Lexington, KY. pp. 149-154.
191. Broaddus CC, Balasuriya UB, Timoney PJ, White JL, Makloski C, et al. (2011) Infection of embryos following insemination of donor mares with equine arteritis virus infective semen. Theriogenology 76: 47-60.
192. Collins JK, S.Kari, S.L. Ralston, D.G.Bennet, J.L. Traub Dargatz, and A.O. McKinnon (1987) Equine viral arteritis in a veterinary teaching hospital. Prev Vet Med 4: 389-397.
193. Timoney PJ, McCollum WH (1988) Equine viral arteritis: epidemiology and control. Journal of Equine Veterinary Science 8: 54-59.
194. Vaala WE, Hamir AN, Dubovi EJ, Timoney PJ, Ruiz B (1992) Fatal, congenitally acquired infection with equine arteritis virus in a neonatal thoroughbred. Equine Vet J 24: 155-158.
195. Doll ER, Bryans JT, McCollum WH, Crowe ME (1957) Isolation of a filterable agent causing arteritis of horses and abortion by mares; its differentiation from the equine abortion (influenza) virus. Cornell Vet 47: 3-41.
196. Bryans JT, Crowe ME, Doll ER, McCollum WH (1957) Isolation of a filterable agent causing arteritis of horses and abortion by mares; its differentiation from the equine abortion (influenza) virus. Cornell Vet 47: 3-41.
197. Clark I (1892) Transmission of pink-eye from apparently healthy stallions to mares. J Comp Pathol 5: 261.
198. Pottie A (1888) The propagation of influenza from stallions to mares. J Comp Pathol 1: 37-38.

199. Timoney PJ (2000) Factors influencing the international spread of equine diseases. Veterinary clinics of North America, The Equine practice 16: 537-551.
200. Bell SA, Pusterla, N., Balasuriya, U. B. R., Mapes, S. M., Nyberg, N. L., and MacLachlan, N. J. (2007) Isolation of a gammaherpesvirus similar to asinine herpesvirus-2 (AHV-2) from a mule and a survey of mules and donkeys for AHV-2 infection by real-time PCR.
201. Glaser AL, Chirnside ED, Horzinek MC, de Vries AA (1997) Equine arteritis virus. Theriogenology 47: 1275-1295.
202. Glaser AL, de Vries AA, Rottier PJ, Horzinek MC, Colenbrander B (1996) Equine arteritis virus: a review of clinical features and management aspects. Vet Q 18: 95-99.
203. Johnson B, Baldwin C, Timoney P, Ely R (1991) Arteritis in equine fetuses aborted due to equine viral arteritis. Vet Pathol 28: 248-250.
204. Timoney PJ, McCollum WH (1987) Equine Viral Arteritis. Can Vet J 28: 693-695.
205. Jaksch W, Sibalin M, Taussig E, Pichler L, Burki F (1973) [Natural cases and experimental transmissions of equine viral arteritis in Austria]. Dtsch Tierarztl Wochenschr 80: 317-320 contd.
206. Jones TC (1969) Clinical and pathologic features of equine viral arteritis. J Am Vet Med Assoc 155: 315-317.
207. Carman S, Rae C, Dubovi E (1988) Ontario. Equine arteritis virus isolated from a Standardbred foal with pneumonia. Can Vet J 29: 937.
208. Golnik W, Michalska Z, Michalak T (1981) Natural equine viral arteritis in foals. Schweiz Arch Tierheilkd 123: 523-533.
209. Bryans JT, Crowe ME, Doll ER, McCollum WH (1957) The blood picture and thermal reaction in experimental viral arteritis of horses. Cornell Vet 47: 42-52.
210. Doll ER, Knappenberger RE, Bryans JT (1957) An outbreak of abortion caused by the equine arteritis virus. Cornell Vet 47: 69-75.
211. Cole JR, Hall RF, Gosser HS, Hendricks JB, Pursell AR, et al. (1986) Transmissibility and abortogenic effect of equine viral arteritis in mares. J Am Vet Med Assoc 189: 769-771.
212. Broaddus CC, Balasuriya UB, White JL, Timoney PJ, Funk RA, et al. (2011) Evaluation of the safety of vaccinating mares against equine viral arteritis during mid or late gestation or during the immediate postpartum period. J Am Vet Med Assoc 238: 741-750.
213. MacLachlan NJ, Balasuriya UB, Rossitto PV, Hullinger PA, Patton JF, et al. (1996) Fatal experimental equine arteritis virus infection of a pregnant mare: immunohistochemical staining of viral antigens. J Vet Diagn Invest 8: 367-374.
214. Timoney PJ, McCollum, W. H. Equine viral arteritis: Current clinical and economic significance; 1990. pp. 403.
215. Timoney PJ, McCollum WH, Murphy TW. A longitudinal study of equine arteritis virus infection in Standardbred stallions with special reference to occurrence of the carrier state; 1992; Cambridge. pp. 231-237.
216. McCollum WH, Timoney PJ, Lee Jr. JW, Habacker PL, Balasuriya UBR, et al. (1999) Features of an outbreak of equine viral arteritis on a breeding farm associated with abortion and fatal interstitial pneumonia in neonatal foals.;

Wernery U, Wade, J.F., Mumford, J.A., Kaaden, O.R., editor. Newmarket, UK: R&W Publications (Newmarket) Limited. pp. 559-560 p.
217. Little TV, Holyoak, G.R., McCollum, W.H., Timoney, P.J. Output of equine arteritis virus from persistently infected stallions is testosterone dependent. In: Plowright W, Rossdale, P.D., Wade, J.F., editor; 1992; Newmarket, England. R&W Publications. pp. 225-229.
218. McCollum WH, Little TV, Timoney PJ, Swerczek TW (1994) Resistance of castrated male horses to attempted establishment of the carrier state with equine arteritis virus. J Comp Pathol 111: 383-388.
219. McDonald LE, Pineda NH (1989) Veterinary endocrinology and reproduction; Febiger L, editor. Philadelphia, PA.
220. Shivaji S, Scheit KH, Bhargava PM (1990) Immunosuppressive factors in seminal plasma; Sons JW, editor. New York, NY.
221. Hedges JF, Balasuriya UB, Ahmad S, Timoney PJ, McCollum WH, et al. (1998) Detection of antibodies to equine arteritis virus by enzyme linked immunosorbant assays utilizing G(L), M and N proteins expressed from recombinant baculoviruses. J Virol Methods 76: 127-137.
222. Holyoak GR, Giles RC, McCollum WH, Little TV, Timoney PJ (1993) Pathological changes associated with equine arteritis virus infection of the reproductive tract in prepubertal and peripubertal colts. J Comp Pathol 109: 281-293.
223. Holyoak GR, Little TV, McCollam WH, Timoney PJ (1993) Relationship between onset of puberty and establishment of persistent infection with equine arteritis virus in the experimentally infected colt. J Comp Pathol 109: 29-46.
224. Patton JF, Balasuriya UB, Hedges JF, Schweidler TM, Hullinger PJ, et al. (1999) Phylogenetic characterization of a highly attenuated strain of equine arteritis virus from the semen of a persistently infected standardbred stallion. Arch Virol 144: 817-827.
225. Lavi E, Suzumura A, Hirayama M, Highkin MK, Dambach DM, et al. (1987) Coronavirus mouse hepatitis virus (MHV)-A59 causes a persistent, productive infection in primary glial cell cultures. Microb Pathog 3: 79-86.
226. Arbour N, Cote G, Lachance C, Tardieu M, Cashman NR, et al. (1999) Acute and persistent infection of human neural cell lines by human coronavirus OC43. J Virol 73: 3338-3350.
227. Arbour N, Ekande S, Cote G, Lachance C, Chagnon F, et al. (1999) Persistent infection of human oligodendrocytic and neuroglial cell lines by human coronavirus 229E. J Virol 73: 3326-3337.
228. Chan PK, To KF, Lo AW, Cheung JL, Chu I, et al. (2004) Persistent infection of SARS coronavirus in colonic cells in vitro. J Med Virol 74: 1-7.
229. Mizutani T, Fukushi S, Ishii K, Sasaki Y, Kenri T, et al. (2006) Mechanisms of establishment of persistent SARS-CoV-infected cells. Biochem Biophys Res Commun 347: 261-265.
230. Palacios G, Jabado O, Renwick N, Briese T, Lipkin WI (2005) Severe acute respiratory syndrome coronavirus persistence in Vero cells. Chin Med J (Engl) 118: 451-459.

231. Yamate M, Yamashita M, Goto T, Tsuji S, Li YG, et al. (2005) Establishment of Vero E6 cell clones persistently infected with severe acute respiratory syndrome coronavirus. Microbes Infect 7: 1530-1540.
232. Baybutt HN, Wege H, Carter MJ, ter Meulen V (1984) Adaptation of coronavirus JHM to persistent infection of murine sac(-) cells. J Gen Virol 65 (Pt 5): 915-924.
233. Sawicki SG, Lu JH, Holmes KV (1995) Persistent infection of cultured cells with mouse hepatitis virus (MHV) results from the epigenetic expression of the MHV receptor. J Virol 69: 5535-5543.
234. Hofmann MA, Senanayake SD, Brian DA (1993) A translation-attenuating intraleader open reading frame is selected on coronavirus mRNAs during persistent infection. Proc Natl Acad Sci U S A 90: 11733-11737.
235. Hofmann MA, Senanayake SD, Brian DA (1993) An intraleader open reading frame is selected from a hypervariable 5' terminus during persistent infection by the bovine coronavirus. Adv Exp Med Biol 342: 105-109.
236. Zhang J, Timoney PJ, MacLachlan NJ, McCollum WH, Balasuriya UB (2008) Persistent equine arteritis virus infection in HeLa cells. J Virol 82: 8456-8464.
237. Crawford TB, Henson JB (1972) Viral arteritis of horses. Adv Exp Med Biol 22: 175-183.
238. Estes PC, Cheville NF (1970) The ultrastructure of vascular lesions in equine viral arteritis. Am J Pathol 58: 235-253.
239. Prickett ME, McCollum WH, Bryans JT (1972) The gross and microscopic pathology observed in horses exerimentally infected with the equine arteritis virus. 3rd International Conference on Equine Infectious Diseases: 265-272.
240. Fukunaga Y, H. Imagawa, E. Tabuchi, and Y. Akiyama (1981) Clinical and virological findings on experimental equine viral arteritis in horses. Bull Equine Res Inst 18: 110-118.
241. Neu SM, P.J. Timoney, and S.R. Lowry (1992) Changes in semen quality following experimental equine arteritis virus infection in the stallion. Theriogenology 37: 407-431.
242. Del Piero F (2000) Equine viral arteritis. Vet Pathol 37: 287-296.
243. Coignoul FL, Cheville NF (1984) Pathology of maternal genital tract, placenta, and fetus in equine viral arteritis. Vet Pathol 21: 333-340.
244. McCollum WH, Timoney PJ (1984) The pathogenic qualities of the 1984 strain of equine arteritis virus. Grayson Foundation International Conference of Thoroughbred Breeders Organizations: 34-84.
245. Jones TC, Doll ER, Bryans JT (1957) The lesions of equine viral arteritis. Cornell Vet 47: 52-68.
246. Balasuriya UB, Hedges JF, MacLachlan NJ (2001) Molecular epidemiology and evolution of equine arteritis virus. Adv Exp Med Biol 494: 19-24.
247. Horohov DW (2000) Equine T-cell cytokines. Protection and pathology. Vet Clin North Am Equine Pract 16.
248. Albina E, Carrat C, Charley B (1998) Interferon-alpha response to swine arterivirus (PoAV), the porcine reproductive and respiratory syndrome virus. Journal of interferon and cytokine research the official journal of the International Society for Interferon and Cytokine Research 18: 485-490.

249. Buddaert W, Van-Reeth K, Pensaert M (1998) In vivo and in vitro interferon (IFN) studies with the porcine reproductive and respiratory syndrome virus (PRRSV). Advances in experimental medicine and biology: 461-467.
250. Murtaugh MP, Xiao Z, Zuckermann F (2002) Immunological responses of swine to porcine reproductive and respiratory syndrome virus infection. Viral immunology 15: 533-547.
251. Royaee AR, Husmann RJ, Dawson HD, Calzada-Nova G, Schnitzlein WM, et al. (2004) Deciphering the involvement of innate immune factors in the development of the host response to PRRSV vaccination. Vet Immunol Immunopathol 102: 199-216.
252. Batista L, Pijoan C, Dee S, Olin M, Molitor T, et al. (2004) Virological and immunological responses to porcine reproductive and respiratory syndrome virus in a large population of gilts. Canadian journal of veterinary research; Revue canadienne de recherche veterinaire 68: 267-273.
253. Xiao Z, Batista L, Dee S, Halbur P, Murtaugh MP (2004) The level of virus-specific T-cell and macrophage recruitment in porcine reproductive and respiratory syndrome virus infection in pigs is independent of virus load. Journal of virology 78: 5923-5933.
254. Cho HJ, Entz SC, Deregt D, Jordan LT, Timoney PJ, et al. (2000) Detection of antibodies to equine arteritis virus by a monoclonal antibody-based blocking ELISA. Can J Vet Res 64: 38-43.
255. Lopez-Fuertes L, Campos E, Domenech N, Ezquerra A, Castro JM, et al. (2000) Porcine reproductive and respiratory syndrome (PRRS) virus down-modulates TNF-alpha production in infected macrophages. Virus research 69: 41-46.
256. Lee SM, Schommer SK, Kleiboeker SB (2004) Porcine reproductive and respiratory syndrome virus field isolates differ in in vitro interferon phenotypes. Veterinary Immunol Immunopathol 102: 217-231.
257. Moore BD, Balasuriya UB, Watson JL, Bosio CM, MacKay RJ, et al. (2003) Virulent and avirulent strains of equine arteritis virus induce different quantities of TNF-alpha and other proinflammatory cytokines in alveolar and blood-derived equine macrophages. Virology 314: 662-670.
258. McCollum WH. Vaccination for equine viral arteritis. In: Bryans JT, Gerber, H., editor; 1969; Paris. S. Karger, Basel. pp. 143-151.
259. Radwan AI, Burger D, Davis WC (1973) The fate of sensitized equine arteritis virus following neutralization by complement of anti-IgG serum. Virology 53: 372-378.
260. Radwan AI, Burger D (1973) The role of sensitizing antibody in the neutralization of equine arteritis virus by complement or anti-IgG serum. Virology 53: 366-371.
261. Radwan AI, Burger D (1973) The complement-requiring neutralization of equine arteritis virus by late antisera. Virology 51: 71-77.
262. Radwan AI, Crawford TB (1974) The mechanisms of neutralization of sensitized equine arteritis virus by complement components. J Gen Virol 25: 229-237.
263. Fukunaga Y, Imagawa H, Kanemaru T, Kamada M (1993) Complement-dependent serum neutralization with virulent and avirulent Bucyrus strains of equine arteritis virus. Vet Microbiol 36: 379-383.

264. Doll ER, Bryans JT, Wilson JC, McCollum WH (1968) Immunization against equine viral arteritis using modified live virus propagated in cell cultures of rabbit kidney. Cornell Vet 48: 497-524.
265. McCollum WH (1970) Vaccination for equine viral arteritis. Proceedings of the Second International Conference (Equine Infectious Diseases): 143-151.
266. McCollum WH (1986) Responses of horses vaccinated with avirulent modified-live equine arteritis virus propagated in the E. Derm (NBL-6) cell line to nasal inoculation with virulent virus. Am J Vet Res 47: 1931-1934.
267. McCollum WH (1969) Development of a modified virus strain and vaccine for equine viral arteritis. J Am Vet Med Assoc 155: 318-322.
268. MacLachlan NJ, Balasuriya UB, Hedges JF, Schweidler TM, McCollum WH, et al. (1998) Serologic response of horses to the structural proteins of equine arteritis virus. J Vet Diagn Invest 10: 229-236.
269. Fukunaga Y, Wada R, Matsumura T, Sugiura T, Imagawa H (1990) Induction of immune response and protection from equine viral arteritis (EVA) by formalin inactivated-virus vaccine for EVA in horses. Zentralbl Veterinarmed B 37: 135-141.
270. Fukunaga Y, Wada R, Matsumura T, Sugiura T, Imagawa H. An attempt to protect against persistent infection of equine viral arteritis in the reproductive tract of stallions using formalin inactivated-virus vaccine. In: Plowright W, Rossdale PD, Wade JF, editors; 1991; Cambridge. R&W Publication. pp. 239-244.
271. McCollum WH (1976) Studies of passive immunity in foals to equine viral arteritis. Veterinary Microbiology 1: 45-54.
272. Hullinger PJ, Wilson WD, Rossitto PV, Patton JF, Thurmond MC, et al. (1998) Passive transfer, rate of decay, and protein specificity of antibodies against equine arteritis virus in horses from a Standardbred herd with high seroprevalence. J Am Vet Med Assoc 213: 839-842.
273. Chirnside ED, Cook RF, Lock MW, Mumford JA. Monoclonal antibodies to equine arteritis virus In: Powell DG, editor; 1988; Lexington, KY. University of Kentucky. pp. 262-267.
274. Chirnside ED, Francis PM, de Vries AA, Sinclair R, Mumford JA (1995) Development and evaluation of an ELISA using recombinant fusion protein to detect the presence of host antibody to equine arteritis virus. J Virol Methods 54: 1-13.
275. Chirnside ED, Francis PM, Mumford JA (1995) Expression cloning and antigenic analysis of the nucleocapsid protein of equine arteritis virus. Virus Res 39: 277-288.
276. Kheyar A, Martin S, St-Laurent G, Timoney PJ, McCollum WH, et al. (1997) Expression cloning and humoral immune response to the nucleocapsid and membrane proteins of equine arteritis virus. Clin Diagn Lab Immunol 4: 648-652.
277. Kondo T, Sugita, S., Fukunaga, Y., Imagawa, H. (1998) Identification of the major epitope in the G_L protein of equine arteritis virus (EAV) recognized by antibody in EAV-infected horses using synthetic peptides. J Equine Science 9: 19-23.
278. Westcott D, Lucas, M., Paton, D. Equine arteritis virus: antigenic analysis of strain variation. In: Schwyzer M, Ackermann, M, editor; 1995; 17 rue Bourgelat, Lyon, France. pp. 479-483.

279. Weiland E, Bolz S, Weiland F, Herbst W, Raamsman MJ, et al. (2000) Monoclonal antibodies directed against conserved epitopes on the nucleocapsid protein and the major envelope glycoprotein of equine arteritis virus. J Clin Microbiol 38: 2065-2075.
280. Jeronimo C, Archambault D (2002) Importance of M-protein C terminus as substrate antigen for serodetection of equine arteritis virus infection. Clin Diagn Lab Immunol 9: 698-703.
281. Abbas AK, and Lichtman, A.H. (2000) Cellular and Molecular Immunology: Saunders, USA.
282. Castillo Olivares J, Tearle JP, Montesso F, Westcott D, Kydd JH, et al. (2003) Detection of equine arteritis virus (EAV)-specific cytotoxic CD8+ T lymphocyte precursors from EAV-infected ponies. J Gen Virol 84: 2745-2753.
283. Bautista EM, Molitor TW (1997) Cell-mediated immunity to porcine reproductive and respiratory syndrome virus in swine. Viral Immunology 10: 83-94.
284. Bautista EM, Suarez P, Molitor TW (1999) T cell responses to the structural polypeptides of porcine reproductive and respiratory syndrome virus. Arch Virol 144: 117-134.
285. Even C, Rowland RR, Plagemann PG (1995) Cytotoxic T cells are elicited during acute infection of mice with lactate dehydrogenase-elevating virus but disappear during the chronic phase of infection. J Virol 69: 5666-5676.
286. de Vries AF, Chirnside ED, Horzinek MC, Rottier PJ (1993) Equine arteritis virus contains a unique set of four structural proteins. Adv Exp Med Biol 342: 245-253.
287. Hyllseth B (1969) A plaque assay of equine arteritis virus in BHK-21 cells. Arch Gesamte Virusforsch 28: 26-33.
288. Maess J, Reczko E, Bohm HO (1970) [Equine arteritis virus: multiplication in BHK 21-cells buoyant density and electron microscopical demonstration]. Arch Gesamte Virusforsch 30: 47-58.
289. Shinagawa M, Yanagawa R, Inoue T, Akiyama Y (1976) Growth of equine arteritis virus in cells derived from infectious canine hepatitis virus-induced hamster tumor and transformed cells. Nippon Juigaku Zasshi 38: 25-32.
290. Burki F (1965) [Properties of the equine arteritis virus]. Pathol Microbiol (Basel) 28: 939-949.
291. McCollum WH, Doll, E.R., Wilson, J.C., Cheatham, J. (1962) Isolation and propagation of equine arteritis virus in monolayer cell cultures of rabbit kidney. Cornell Vet 52: 452-458.
292. OIE Manual of Diagnostic Tests and Vaccines for Terrestrial Animals (2004) OIE Manual of Diagnostic Tests and Vaccines for Terrestrial Animals. Paris, France: Office International des Epizooties.
293. Chirnside ED, Spaan WJ (1990) Reverse transcription and cDNA amplification by the polymerase chain reaction of equine arteritis virus (EAV). J Virol Methods 30: 133-140.
294. Gilbert SA, Timoney PJ, McCollum WH, Deregt D (1997) Detection of equine arteritis virus in the semen of carrier stallions by using a sensitive nested PCR assay. J Clin Microbiol 35: 2181-2183.

295. Ramina A, Dalla Valle L, De Mas S, Tisato E, Zuin A, et al. (1999) Detection of equine arteritis virus in semen by reverse transcriptase polymerase chain reaction-ELISA. Comp Immunol Microbiol Infect Dis 22: 187-197.
296. Sekiguchi K, Sugita S, Fukunaga Y, Kondo T, Wada R, et al. (1995) Detection of equine arteritis virus (EAV) by polymerase chain reaction (PCR) and differentiation of EAV strains by restriction enzyme analysis of PCR products. Arch Virol 140: 1483-1491.
297. Starick E (1998) Rapid and sensitive detection of equine arteritis virus in semen and tissue samples by reverse transcription-polymerase chain reaction, dot blot hybridisation and nested polymerase chain reaction. Acta Virol 42: 333-339.
298. St-Laurent G, Morin G, Archambault D (1994) Detection of equine arteritis virus following amplification of structural and nonstructural viral genes by reverse transcription-PCR. J Clin Microbiol 32: 658-665.
299. Balasuriya UB, Leutenegger CM, Topol JB, McCollum WH, Timoney PJ, et al. (2002) Detection of equine arteritis virus by real-time TaqMan reverse transcription-PCR assay. J Virol Methods 101: 21-28.
300. Westcott DG, King DP, Drew TW, Nowotny N, Kindermann J, et al. (2003) Use of an internal standard in a closed one-tube RT-PCR for the detection of equine arteritis virus RNA with fluorescent probes. Vet Res 34: 165-176.
301. Mankoc S, Hostnik P, Grom J, Toplak I, Klobucar I, et al. (2007) Comparison of different molecular methods for assessment of equine arteritis virus (EAV) infection: a novel one-step MGB real-time RT-PCR assay, PCR-ELISA and classical RT-PCR for detection of highly diverse sequences of Slovenian EAV variants. J Virol Methods 146: 341-354.
302. Lu Z, Branscum A, Shuck KM, Zhang J, Dubovi E, et al. (2008) Comparison of two real-time reverse transcription polymerase chain reaction assays for the detection of equine arteritis virus nucleic acid in equine semen and tissue culture fluid. J Vet Diagn Invest 20: (in press).
303. Miszczak F, Shuck KM, Lu Z, Go YY, Zhang J, et al. (2011) Evaluation of Two Magnetic Bead-Based Viral Nucleic Acid Purification Kits and Three Real-Time RT-PCR Reagent Systems in Two TaqMan(R) Assays for Equine Arteritis Virus Detection in Semen. J Clin Microbiol.
304. Kondo T, Fukunaga Y, Sekiguchi K, Sugiura T, Imagawa H (1998) Enzyme-linked immunosorbent assay for serological survey of equine arteritis virus in racehorses. J Vet Med Sci 60: 1043-1045.
305. Starik E, Ginter A, Coppe P (2001) ELISA and direct immunofluorescence test to detect equine arteritis virus (EAV) using a monoclonal antibody directed to the EAV-N protein. J Vet Med B Infect Dis Vet Public Health 48: 1-9.
306. Wagner HM, Balasuriya UB, James MacLachlan N (2003) The serologic response of horses to equine arteritis virus as determined by competitive enzyme-linked immunosorbent assays (c-ELISAs) to structural and non-structural viral proteins. Comp Immunol Microbiol Infect Dis 26: 251-260.
307. Duthie S, Mills H, Burr P (2008) The efficacy of a commercial ELISA as an alternative to virus neutralisation test for the detection of antibodies to EAV. Equine Vet J 40: 182-183.

308. McCollum WH (1981) Pathologic features of horses given avirulent equine arteritis virus intramuscularly. Am J Vet Res 42: 1218-1220.
309. Timoney PJ, Umphenour NW, McCollum WH (1988) Safety evaluation of commercial modified live equine arteritis virus vaccine for use in stallions. Proceedings of the Fifth International Conference on Equine Infectious Diseases: 19-27.
310. McKinnon AO, Colbern GT, Collins JK, Bowen RA, Voss JL, et al. (1986) Vaccination of stallions with modified live equine viral arteritis virus. Journal of Equine Veterinary Science 6: 66-69.
311. Fukunaga Y, Wada R, Hirasawa K, Kamada M, Kumanomido T, et al. (1982) Effect of the modified Bucyrus strain of equine arteritis virus experimentally inoculated into horses. Bulletin of Equine Research Institute 19: 97-101.
312. Fukunaga Y, Wada R, Kanemaru T, Imagawa H, Kamada M, et al. Protection against abortion in pregnant mares vaccinated with killed vaccine after exposure to equine arteritis virus. In: Nakajima HP, W., editor; 1994; Newmarket. R&W Publications. pp. 340.
313. Fukunaga Y, Wada R, Kanemaru T, Imagawa H, Kamada M, et al. (1996) Immune potency of lyophilized, killed vaccine for equine viral arteritis and its protection against abortion in pregnant mares. Journal of Equine Veterinary Science 16: 217-221.
314. Tobiasch E, Kehm R, Bahr U, Tidona CA, Jakob NJ, et al. (2001) Large envelope glycoprotein and nucleocapsid protein of equine arteritis virus (EAV) induce an immune response in Balb/c mice by DNA vaccination; strategy for developing a DNA-vaccine against EAV-infection. Virus Genes 22: 187-199.
315. Giese M, Bahr U, Jakob NJ, Kehm R, Handermann M, et al. (2002) Stable and long-lasting immune response in horses after DNA vaccination against equine arteritis virus. Virus Genes 25: 159-167.
316. Zhang J, Stein DA, Timoney PJ, Balasuriya UB Curing of HeLa cells persistently infected with equine arteritis virus by a peptide-conjugated morpholino oligomer. Virus Res 150: 138-142.
317. van den Born E, Stein DA, Iversen PL, Snijder EJ (2005) Antiviral activity of morpholino oligomers designed to block various aspects of Equine arteritis virus amplification in cell culture. J Gen Virol 86: 3081-3090.
318. Summerton J, Weller D (1997) Morpholino antisense oligomers: design, preparation, and properties. Antisense Nucleic Acid Drug Dev 7: 187-195.
319. Summerton J (1999) Morpholino antisense oligomers: the case for an RNase H-independent structural type. Biochim Biophys Acta 1489: 141-158.
320. Stein D, Foster E, Huang SB, Weller D, Summerton J (1997) A specificity comparison of four antisense types: morpholino, 2'-O-methyl RNA, DNA, and phosphorothioate DNA. Antisense Nucleic Acid Drug Dev 7: 151-157.
321. Abes S, Moulton HM, Clair P, Prevot P, Youngblood DS, et al. (2006) Vectorization of morpholino oligomers by the (R-Ahx-R)4 peptide allows efficient splicing correction in the absence of endosomolytic agents. J Control Release 116: 304-313.

322. van der Meer FJ, de Haan CA, Schuurman NM, Haijema BJ, Peumans WJ, et al. (2007) Antiviral activity of carbohydrate-binding agents against Nidovirales in cell culture. Antiviral Res 76: 21-29.
323. Sentsui H, Wu D, Murakami K, Kondo T, Matsumura T Antiviral effect of recombinant equine interferon-gamma on several equine viruses. Vet Immunol Immunopathol 135: 93-99.
324. Heinrich A, Riethmuller D, Gloger M, Schusser GF, Giese M, et al. (2009) RNA interference protects horse cells in vitro from infection with Equine Arteritis Virus. Antiviral Res 81: 209-216.
325. de Vries AA, Glaser AL, Raamsman MJ, de Haan CA, Sarnataro S, et al. (2000) Genetic manipulation of equine arteritis virus using full-length cDNA clones: separation of overlapping genes and expression of a foreign epitope. Virology 270: 84-97.
326. Glaser AL, de Vries AA, Raamsman MJ, Horzinek MC, Rottier PJM (1998) An infectious cDNA clone of equine arteritis virus: a tool for future fundamental studies and vaccine development. In: Wernery U, Wade JF, Mumford JA, Kaaden OR, editors. The Eight International Conference on Equine Infectious Diseases. Newmarket, UK: R & W Publications. pp. 166-176.
327. Balasuriya UB, Snijder EJ, van Dinten LC, Heidner HW, Wilson WD, et al. (1999) Equine arteritis virus derived from an infectious cDNA clone is attenuated and genetically stable in infected stallions. Virology 260: 201-208.
328. Balasuriya UB, Snijder EJ, Heidner HW, Zhang J, Zevenhoven-Dobbe JC, et al. (2007) Development and characterization of an infectious cDNA clone of the virulent Bucyrus strain of Equine arteritis virus. J Gen Virol 88: 918-924.
329. Zhang J, Go YY, Meade BJ, Lu Z, Timoney PJ, et al. (2009) Recombinant equine arteritis virus derived from a infectious cDNA clone of the modified live virus vaccine strain mimics biological properties of its parental virus *in vitro* and *in vivo*. Manuscript in preparation.
330. Go YY, Zhang J, Timoney PJ, Cook RF, Horohov DW, et al. (2010) Complex interactions between the major and minor envelope proteins of equine arteritis virus determine its tropism for equine CD3+ T lymphocytes and CD14+ monocytes. J Virol 84: 4898-4911.
331. Zhang J, Go YY, MacLachlan NJ, Meade BJ, Timoney PJ, et al. (2008) Amino acid substitutions in the structural or nonstructural proteins of a vaccine strain of equine arteritis virus are associated with its attenuation. Virology 378: 355-362.
332. van den Born E, Posthuma CC, Knoops K, Snijder EJ (2007) An infectious recombinant equine arteritis virus expressing green fluorescent protein from its replicase gene. J Gen Virol 88: 1196-1205.
333. Moore KW, de Waal Malefyt R, Coffman RL, O'Garra A (2001) Interleukin-10 and the interleukin-10 receptor. Annu Rev Immunol 19: 683-765.
334. McCollum WH, Timoney PJ (1999) Experimental observation on the virulence of isolates of equine arteritis virus; Wernery U, Wade, J.F., Mumford, J.A., Kaaden, O.R., editor. Newmarket, UK: R&W Publications (Newmarket) Limited. pp. 558-559 p.

335. Del Piero F, Wilkins PA, Lopez JW, Glaser AL, Dubovi EJ, et al. (1997) Equine viral arteritis in newborn foals: clinical, pathological, serological, microbiological and immunohistochemical observations. Equine Vet J 29: 178-185.
336. McCollum WH, Doll ER, Wilson JC (1961) The recovery of virus from horses with experimental cases of equine arteritis using monolayer cell cultures of rabbit kidney. Am J Vet Res 23: 465-469.
337. Senne DA, Pearson, J.E., Carbrey, E.A. (1985) Equine viral arteritis: a standard procedure for the virus neutralization test and comparison of results of a proficiency test performed at five laboratories. Proceedings of the 89th Annual Meeting of the United States Animal Health Association: 29-34.
338. Blanchard-Channell M, Moore PF, Stott JL (1994) Characterization of monoclonal antibodies specific for equine homologues of CD3 and CD5. Immunology 82: 548-554.
339. Lunn DP, Holmes MA, Antczak DF, Agerwal N, Baker J, et al. (1998) Report of the Second Equine Leucocyte Antigen Workshop, Squaw valley, California, July 1995. Vet Immunol Immunopathol 62: 101-143.
340. Lunn DP, Holmes MA, Duffus WP (1991) Three monoclonal antibodies identifying antigens on all equine T lymphocytes, and two mutually exclusive T-lymphocyte subsets. Immunology 74: 251-257.
341. Ibrahim S, Steinbach F (2007) Non-HLDA8 animal homologue section anti-leukocyte mAbs tested for reactivity with equine leukocytes. Vet Immunol Immunopathol 119: 81-91.
342. Mayall S, Siedek E, Hamblin AS (2001) The anti-human CD21 antibody, BU33, identifies equine B cells. J Comp Pathol 124: 83-87.
343. Hedges JF, Demaula CD, Moore BD, McLaughlin BE, Simon SI, et al. (2001) Characterization of equine E-selectin. Immunology 103: 498-504.
344. Moore BD, Balasuriya UB, Hedges JF, MacLachlan NJ (2002) Growth characteristics of a highly virulent, a moderately virulent, and an avirulent strain of equine arteritis virus in primary equine endothelial cells are predictive of their virulence to horses. Virology 298: 39-44.
345. Jones DT (2007) Improving the accuracy of transmembrane protein topology prediction using evolutionary information. Bioinformatics 23: 538-544.
346. Jones DT, Taylor WR, Thornton JM (1994) A model recognition approach to the prediction of all-helical membrane protein structure and topology. Biochemistry 33: 3038-3049.
347. Krogh A, Larsson B, von Heijne G, Sonnhammer EL (2001) Predicting transmembrane protein topology with a hidden Markov model: application to complete genomes. J Mol Biol 305: 567-580.
348. Claros MG, von Heijne G (1994) TopPred II: an improved software for membrane protein structure predictions. Comput Appl Biosci 10: 685-686.
349. Reed LJ, and H.A. Muench (1938) A simple method of estimating fifty percent endpoints. Am J Hyg 27: 493-497.
350. Brinton MA (2001) Host factors involved in West Nile virus replication. Ann N Y Acad Sci 951: 207-219.
351. Brinton MA, Perelygin AA (2003) Genetic resistance to flaviviruses. Adv Virus Res 60: 43-85.

352. Das PB, Dinh PX, Ansari IH, de Lima M, Osorio FA, et al. (2009) The Minor Envelope Glycoproteins GP2a and GP4 of Porcine Reproductive and Respiratory Syndrome Virus Interact with the Receptor CD163. J Virol.
353. Holyoak GR, Balasuriya UB, Broaddus CC, Timoney PJ (2008) Equine viral arteritis: current status and prevention. Theriogenology 70: 403-414.
354. Balasuriya UB, MacLachlan NJ (2007) Equine viral arteritis. In: Sellon DC, Long MT, editors. Equine Infectious Diseases. St. Louis, MO: Elsevier. pp. 153-164.
355. Balasuriya UB, MacLachlan, N. J (2007) Equine Viral Arteritis. In: Sellon DC, Long MT, editors. Equine infectious diseases. St. Louis, Mo.: Saunders/Elsevier. pp. 153-164.
356. Hullinger PJ, Gardner IA, Hietala SK, Ferraro GL, MacLachlan NJ (2001) Seroprevalence of antibodies against equine arteritis virus in horses residing in the United States and imported horses. J Am Vet Med Assoc 219: 946-949.
357. Newton JR, Wood JL, Castillo-Olivares FJ, Mumford JA (1999) Serological surveillance of equine viral arteritis in the United Kingdom since the outbreak in 1993. Vet Rec 145: 511-516.
358. Wade CM, Giulotto E, Sigurdsson S, Zoli M, Gnerre S, et al. (2009) Genome sequence, comparative analysis, and population genetics of the domestic horse. Science 326: 865-867.
359. Broome D (2005) Encyclopedia of the horse. In: Peplow E, editor: Barnes & Nobles.
360. Pluddemann A, Neyen C, Gordon S (2007) Macrophage scavenger receptors and host-derived ligands. Methods 43: 207-217.
361. Perry SJ, Lefkowitz RJ (2002) Arresting developments in heptahelical receptor signaling and regulation. Trends Cell Biol 12: 130-138.
362. Chen W, Kirkbride KC, How T, Nelson CD, Mo J, et al. (2003) Beta-arrestin 2 mediates endocytosis of type III TGF-beta receptor and down-regulation of its signaling. Science 301: 1394-1397.
363. Chen W, ten Berge D, Brown J, Ahn S, Hu LA, et al. (2003) Dishevelled 2 recruits beta-arrestin 2 to mediate Wnt5A-stimulated endocytosis of Frizzled 4. Science 301: 1391-1394.
364. Valsdottir R, Hashimoto H, Ashman K, Koda T, Storrie B, et al. (2001) Identification of rabaptin-5, rabex-5, and GM130 as putative effectors of rab33b, a regulator of retrograde traffic between the Golgi apparatus and ER. FEBS Lett 508: 201-209.
365. Bitko V, Oldenburg A, Garmon NE, Barik S (2003) Profilin is required for viral morphogenesis, syncytium formation, and cell-specific stress fiber induction by respiratory syncytial virus. BMC Microbiol 3: 9.
366. Lilley BN, Ploegh HL (2005) Multiprotein complexes that link dislocation, ubiquitination, and extraction of misfolded proteins from the endoplasmic reticulum membrane. Proc Natl Acad Sci U S A 102: 14296-14301.
367. Ye Y, Shibata Y, Kikkert M, van Voorden S, Wiertz E, et al. (2005) Recruitment of the p97 ATPase and ubiquitin ligases to the site of retrotranslocation at the endoplasmic reticulum membrane. Proc Natl Acad Sci U S A 102: 14132-14138.
368. Oda Y, Okada T, Yoshida H, Kaufman RJ, Nagata K, et al. (2006) Derlin-2 and Derlin-3 are regulated by the mammalian unfolded protein response and are required for ER-associated degradation. J Cell Biol 172: 383-393.

369. Lilley BN, Ploegh HL (2004) A membrane protein required for dislocation of misfolded proteins from the ER. Nature 429: 834-840.
370. Ye Y, Shibata Y, Yun C, Ron D, Rapoport TA (2004) A membrane protein complex mediates retro-translocation from the ER lumen into the cytosol. Nature 429: 841-847.
371. Dorner C, Ullrich A, Haring HU, Lammers R (1999) The kinesin-like motor protein KIF1C occurs in intact cells as a dimer and associates with proteins of the 14-3-3 family. J Biol Chem 274: 33654-33660.
372. Lefkowitz RJ, Shenoy SK (2005) Transduction of receptor signals by beta-arrestins. Science 308: 512-517.
373. Sun Y, Cheng Z, Ma L, Pei G (2002) Beta-arrestin2 is critically involved in CXCR4-mediated chemotaxis, and this is mediated by its enhancement of p38 MAPK activation. J Biol Chem 277: 49212-49219.
374. Revankar CM, Vines CM, Cimino DF, Prossnitz ER (2004) Arrestins block G protein-coupled receptor-mediated apoptosis. J Biol Chem 279: 24578-24584.
375. Fong AM, Premont RT, Richardson RM, Yu YR, Lefkowitz RJ, et al. (2002) Defective lymphocyte chemotaxis in beta-arrestin2- and GRK6-deficient mice. Proc Natl Acad Sci U S A 99: 7478-7483.
376. DeFea KA, Vaughn ZD, O'Bryan EM, Nishijima D, Dery O, et al. (2000) The proliferative and antiapoptotic effects of substance P are facilitated by formation of a beta -arrestin-dependent scaffolding complex. Proc Natl Acad Sci U S A 97: 11086-11091.
377. DeFea KA, Zalevsky J, Thoma MS, Dery O, Mullins RD, et al. (2000) beta-arrestin-dependent endocytosis of proteinase-activated receptor 2 is required for intracellular targeting of activated ERK1/2. J Cell Biol 148: 1267-1281.
378. Luttrell LM, Roudabush FL, Choy EW, Miller WE, Field ME, et al. (2001) Activation and targeting of extracellular signal-regulated kinases by beta-arrestin scaffolds. Proc Natl Acad Sci U S A 98: 2449-2454.
379. Luttrell LM, Daaka Y, Lefkowitz RJ (1999) Regulation of tyrosine kinase cascades by G-protein-coupled receptors. Curr Opin Cell Biol 11: 177-183.
380. Luttrell LM, Ferguson SS, Daaka Y, Miller WE, Maudsley S, et al. (1999) Beta-arrestin-dependent formation of beta2 adrenergic receptor-Src protein kinase complexes. Science 283: 655-661.
381. Gao H, Sun Y, Wu Y, Luan B, Wang Y, et al. (2004) Identification of beta-arrestin2 as a G protein-coupled receptor-stimulated regulator of NF-kappaB pathways. Mol Cell 14: 303-317.
382. Witherow DS, Garrison TR, Miller WE, Lefkowitz RJ (2004) beta-Arrestin inhibits NF-kappaB activity by means of its interaction with the NF-kappaB inhibitor IkappaBalpha. Proc Natl Acad Sci U S A 101: 8603-8607.
383. McDonald PH, Chow CW, Miller WE, Laporte SA, Field ME, et al. (2000) Beta-arrestin 2: a receptor-regulated MAPK scaffold for the activation of JNK3. Science 290: 1574-1577.
384. Fan H, Luttrell LM, Tempel GE, Senn JJ, Halushka PV, et al. (2007) Beta-arrestins 1 and 2 differentially regulate LPS-induced signaling and pro-inflammatory gene expression. Mol Immunol 44: 3092-3099.

385. Wang Y, Tang Y, Teng L, Wu Y, Zhao X, et al. (2006) Association of beta-arrestin and TRAF6 negatively regulates Toll-like receptor-interleukin 1 receptor signaling. Nat Immunol 7: 139-147.
386. Gomez-Cambronero J, Di Fulvio M, Knapek K (2007) Understanding phospholipase D (PLD) using leukocytes: PLD involvement in cell adhesion and chemotaxis. Journal of leukocyte biology 82: 272-281.
387. Abel S, Hundhausen C, Mentlein R, Schulte A, Berkhout TA, et al. (2004) The transmembrane CXC-chemokine ligand 16 is induced by IFN-gamma and TNF-alpha and shed by the activity of the disintegrin-like metalloproteinase ADAM10. J Immunol 172: 6362-6372.
388. Landro L, Damas JK, Halvorsen B, Fevang B, Ueland T, et al. (2009) CXCL16 in HIV infection - a link between inflammation and viral replication. Eur J Clin Invest 39: 1017-1024.
389. Matloubian M, David A, Engel S, Ryan JE, Cyster JG (2000) A transmembrane CXC chemokine is a ligand for HIV-coreceptor Bonzo. Nat Immunol 1: 298-304.
390. Ludwig A, Weber C (2007) Transmembrane chemokines: versatile 'special agents' in vascular inflammation. Thromb Haemost 97: 694-703.
391. Martinon F, Mayor A, Tschopp J (2009) The inflammasomes: guardians of the body. Annu Rev Immunol 27: 229-265.
392. Fahrenkrog B, Aebi U (2003) The nuclear pore complex: nucleocytoplasmic transport and beyond. Nat Rev Mol Cell Biol 4: 757-766.
393. Xylourgidis N, Roth P, Sabri N, Tsarouhas V, Samakovlis C (2006) The nucleoporin Nup214 sequesters CRM1 at the nuclear rim and modulates NFkappaB activation in Drosophila. J Cell Sci 119: 4409-4419.
394. Wiermer M, Germain H, Cheng YT, Garcia AV, Parker JE, et al. Nucleoporin MOS7/Nup88 contributes to plant immunity and nuclear accumulation of defense regulators. Nucleus 1: 332-336.
395. Balasuriya UB, MacLachlan NJ (2007) Infectious Diseases of the Horse; Sellon DC, Long MT, editors: Elsevier.
396. Chambers TM, Quinlivan M, Sturgill T, Cullinane A, Horohov DW, et al. (2009) Influenza A viruses with truncated NS1 as modified live virus vaccines: pilot studies of safety and efficacy in horses. Equine Vet J 41: 87-92.
397. Adams AA, Sturgill TL, Breathnach CC, Chambers TM, Siger L, et al. (2011) Humoral and cell-mediated immune responses of old horses following recombinant canarypox virus vaccination and subsequent challenge infection. Vet Immunol Immunopathol 139: 128-140.
398. Breathnach CC, Sturgill-Wright T, Stiltner JL, Adams AA, Lunn DP, et al. (2006) Foals are interferon gamma-deficient at birth. Vet Immunol Immunopathol 112: 199-209.
399. Murphy BA, Vick MM, Sessions DR, Cook RF, Fitzgerald BP (2007) Acute systemic inflammation transiently synchronizes clock gene expression in equine peripheral blood. Brain Behav Immun 21: 467-476.
400. Quinlivan M, Nelly M, Prendergast M, Breathnach C, Horohov D, et al. (2007) Pro-inflammatory and antiviral cytokine expression in vaccinated and unvaccinated horses exposed to equine influenza virus. Vaccine 25: 7056-7064.

401. Saulez MN, Godfroid J, Bosman A, Stiltner JL, Breathnach CC, et al. (2010) Cytokine mRNA expressions after racing at a high altitude and at sea level in horses with exercise-induced pulmonary hemorrhage. Am J Vet Res 71: 447-453.
402. Vick MM, Adams AA, Murphy BA, Sessions DR, Horohov DW, et al. (2007) Relationships among inflammatory cytokines, obesity, and insulin sensitivity in the horse. J Anim Sci 85: 1144-1155.
403. Ramakers C, Ruijter JM, Deprez RH, Moorman AF (2003) Assumption-free analysis of quantitative real-time polymerase chain reaction (PCR) data. Neurosci Lett 339: 62-66.
404. Livak KJ, Schmittgen TD (2001) Analysis of relative gene expression data using real-time quantitative PCR and the 2(-Delta Delta C(T)) Method. Methods 25: 402-408.
405. Fiorentino DF, Bond MW, Mosmann TR (1989) Two types of mouse T helper cell. IV. Th2 clones secrete a factor that inhibits cytokine production by Th1 clones. J Exp Med 170: 2081-2095.
406. Mosser DM, Zhang X (2008) Interleukin-10: new perspectives on an old cytokine. Immunological reviews 226: 205-218.
407. Maloy KJ, Powrie F (2001) Regulatory T cells in the control of immune pathology. Nature immunology 2: 816-822.
408. Timoney PJ (2000) The increasing significance of international trade in equids and its influence on the spread of infectious diseases. Ann N Y Acad Sci 916: 55-60.
409. Takeuchi O, Akira S (2008) MDA5/RIG-I and virus recognition. Current opinion in immunology 20: 17-22.
410. Randall RE, Goodbourn S (2008) Interferons and viruses: an interplay between induction, signalling, antiviral responses and virus countermeasures. J Gen Virol 89: 1-47.
411. Thanos D, Maniatis T (1995) Virus induction of human IFN beta gene expression requires the assembly of an enhanceosome. Cell 83: 1091-1100.
412. Miller LC, Laegreid WW, Bono JL, Chitko-McKown CG, Fox JM (2004) Interferon type I response in porcine reproductive and respiratory syndrome virus-infected MARC-145 cells. Archives of virology 149: 2453-2463.
413. Luo R, Xiao S, Jiang Y, Jin H, Wang D, et al. (2008) Porcine reproductive and respiratory syndrome virus (PRRSV) suppresses interferon-beta production by interfering with the RIG-I signaling pathway. Molecular immunology 45: 2839-2846.
414. Beura LK, Sarkar SN, Kwon B, Subramaniam S, Jones C, et al. (2009) Porcine reproductive and respiratory syndrome virus non structural protein 1{beta} modulates host innate immune response by antagonizing IRF3 activation. J Virol.
415. Chen Z, Lawson S, Sun Z, Zhou X, Guan X, et al. (2010) Identification of two auto-cleavage products of nonstructural protein 1 (nsp1) in porcine reproductive and respiratory syndrome virus infected cells: nsp1 function as interferon antagonist. Virology 398: 87-97.
416. Kim O, Sun Y, Lai FW, Song C, Yoo D (2010) Modulation of type I interferon induction by porcine reproductive and respiratory syndrome virus and degradation of CREB-binding protein by non-structural protein 1 in MARC-145 and HeLa cells. Virology 402: 315-326.

417. Sun Z, Chen Z, Lawson SR, Fang Y (2010) The cysteine protease domain of porcine reproductive and respiratory syndrome virus nonstructural protein 2 possesses deubiquitinating and interferon antagonism functions. Journal of virology 84: 7832-7846.
418. Sever JL (1962) Application of a microtechnique to viral serological investigations. Journal of immunology 88: 320-329.
419. Dalton KP, Rose JK (2001) Vesicular stomatitis virus glycoprotein containing the entire green fluorescent protein on its cytoplasmic domain is incorporated efficiently into virus particles. Virology 279: 414-421.
420. Go YY, Snijder EJ, Timoney PJ, Balasuriya UB Characterization of equine humoral antibody response to the nonstructural proteins of equine arteritis virus. Clin Vaccine Immunol 18: 268-279.
421. Niwa H, Yamamura K, Miyazaki J (1991) Efficient selection for high-expression transfectants with a novel eukaryotic vector. Gene 108: 193-199.
422. Yoneyama M, Suhara W, Fukuhara Y, Sato M, Ozato K, et al. (1996) Autocrine amplification of type I interferon gene expression mediated by interferon stimulated gene factor 3 (ISGF3). Journal of biochemistry 120: 160-169.
423. Komatsu T, Takeuchi K, Gotoh B (2007) Bovine parainfluenza virus type 3 accessory proteins that suppress beta interferon production. Microbes Infect 9: 954-962.
424. Yoo D, Song C, Sun Y, Du Y, Kim O, et al. (2010) Modulation of host cell responses and evasion strategies for porcine reproductive and respiratory syndrome virus. Virus Res 154: 48-60.
425. Haller O, Weber F (2007) Pathogenic viruses: smart manipulators of the interferon system. Current topics in microbiology and immunology 316: 315-334.
426. Samuel CE (2001) Antiviral actions of interferons. Clinical microbiology reviews 14: 778-809, table of contents.
427. Cardenas WB, Loo YM, Gale M, Jr., Hartman AL, Kimberlin CR, et al. (2006) Ebola virus VP35 protein binds double-stranded RNA and inhibits alpha/beta interferon production induced by RIG-I signaling. Journal of virology 80: 5168-5178.
428. Meylan E, Curran J, Hofmann K, Moradpour D, Binder M, et al. (2005) Cardif is an adaptor protein in the RIG-I antiviral pathway and is targeted by hepatitis C virus. Nature 437: 1167-1172.
429. Seth RB, Sun L, Ea CK, Chen ZJ (2005) Identification and characterization of MAVS, a mitochondrial antiviral signaling protein that activates NF-kappaB and IRF 3. Cell 122: 669-682.
430. Xu LG, Wang YY, Han KJ, Li LY, Zhai Z, et al. (2005) VISA is an adapter protein required for virus-triggered IFN-beta signaling. Molecular cell 19: 727-740.
431. Kawai T, Takahashi K, Sato S, Coban C, Kumar H, et al. (2005) IPS-1, an adaptor triggering RIG-I- and Mda5-mediated type I interferon induction. Nature immunology 6: 981-988.
432. Powell PP, Dixon LK, Parkhouse RM (1996) An IkappaB homolog encoded by African swine fever virus provides a novel mechanism for downregulation of proinflammatory cytokine responses in host macrophages. Journal of virology 70: 8527-8533.

433. Wang X, Li M, Zheng H, Muster T, Palese P, et al. (2000) Influenza A virus NS1 protein prevents activation of NF-kappaB and induction of alpha/beta interferon. Journal of virology 74: 11566-11573.
434. Connolly JL, Rodgers SE, Clarke P, Ballard DW, Kerr LD, et al. (2000) Reovirus-induced apoptosis requires activation of transcription factor NF-kappaB. Journal of virology 74: 2981-2989.
435. Goodkin ML, Ting AT, Blaho JA (2003) NF-kappaB is required for apoptosis prevention during herpes simplex virus type 1 infection. Journal of virology 77: 7261-7280.
436. Waris G, Livolsi A, Imbert V, Peyron JF, Siddiqui A (2003) Hepatitis C virus NS5A and subgenomic replicon activate NF-kappaB via tyrosine phosphorylation of IkappaBalpha and its degradation by calpain protease. J Biol Chem 278: 40778-40787.
437. Landt O, Grunert, H. -P., Hahn, U. (1990) A general method for rapid site-directed mutagenesis using the polymerase chain reaction. Gene 96: 125-128.
438. Han W, Wu JJ, Deng XY, Cao Z, Yu XL, et al. (2009) Molecular mutations associated with the in vitro passage of virulent porcine reproductive and respiratory syndrome virus. Virus Genes 38: 276-284.
439. de Vries AA, Glaser AL, Raamsman MJ, Rottier PJ (2001) Recombinant equine arteritis virus as an expression vector. Virology 284: 259-276.
440. Johnson CR, Griggs TF, Gnanandarajah J, Murtaugh MP (2011) Novel structural protein in porcine reproductive and respiratory syndrome virus encoded by an alternative ORF5 present in all arteriviruses. J Gen Virol 92: 1107-1116.
441. McCollum WH (1969) Development of a modified virus strain and vaccine for equine viral arteritis. Journal of the American Veterinary Medical Association 155: 318-322.
442. Cullinane AA (2004) Testing for equine arteritis virus. Vet Rec 155: 647-648.
443. Lenihan P (2004) Presented at the International Workshop on the Diagnosis of Equine Arteritis Virus Infection. Lexington, Kentucky.
444. Shuck KM, P. J. Timoney, J. Zhang and W. H. McCollum (2004) Presented at the International Workshop on the Diagnosis of Equine Arteritis VIrus Infection. Lexington, Kentucky.
445. Vickers ML. 2004; Lexington, Kentucky.
446. Nugent J, Sinclair R, deVries AA, Eberhardt RY, Castillo Olivares J, et al. (2000) Development and evaluation of ELISA procedures to detect antibodies against the major envelope protein (G(L)) of equine arteritis virus. J Virol Methods 90: 167-183.
447. Wong SJ, Demarest VL, Boyle RH, Wang T, Ledizet M, et al. (2004) Detection of human anti-flavivirus antibodies with a west nile virus recombinant antigen microsphere immunoassay. J Clin Microbiol 42: 65-72.
448. Dias D, Van Doren J, Schlottmann S, Kelly S, Puchalski D, et al. (2005) Optimization and validation of a multiplexed luminex assay to quantify antibodies to neutralizing epitopes on human papillomaviruses 6, 11, 16, and 18. Clin Diagn Lab Immunol 12: 959-969.
449. Wong SJ, Boyle RH, Demarest VL, Woodmansee AN, Kramer LD, et al. (2003) Immunoassay targeting nonstructural protein 5 to differentiate West Nile virus

infection from dengue and St. Louis encephalitis virus infections and from flavivirus vaccination. J Clin Microbiol 41: 4217-4223.
450. Balasuriya UB, Shi PY, Wong SJ, Demarest VL, Gardner IA, et al. (2006) Detection of antibodies to West Nile virus in equine sera using microsphere immunoassay. J Vet Diagn Invest 18: 392-395.
451. Johnson AJ, Cheshier RC, Cosentino G, Masri HP, Mock V, et al. (2007) Validation of a microsphere-based immunoassay for detection of anti-west nile virus and anti-st. Louis encephalitis virus immunoglobulin m antibodies. Clinical and vaccine immunology CVI 14: 1084-1093.
452. McCollum WH, K. Shuck, J. Zhang and P. J. Timoney. Factors important to the isolation of Equine Arteritis Virus in cell culture; 2004; Lexington , KY. OIE.
453. Balasuriya UB, Snijder EJ, Heidner HW, Zhang J, Zevenhoven-Dobbe JC, et al. (2007) Development and characterization of an infectious cDNA clone of the virulent Bucyrus strain of Equine arteritis virus. Journal of general virology 88: 918-924.
454. Pepe MS (2003) The Statistical Evaluation of Medical Tests for Classification and Prediction. New York: Oxford Statistical Science Series: Oxford University Press.
455. Choi YK, Johnson, W.O., Collins, M.T., and Gardner, I.A. (2006) Bayesian estimation of ROC curves in the absence of a gold standard. Journal of Agricultural, Biological, and Environmental Statistics 11: 210-229.
456. Spiegelhalter D, A. Thomas and N. Best. (2004) User manual, WinBUGS: Bayesian inference using Gibbs sampling, version 1.4. MRC Biostatistics Unit. Cambridge.
457. Barajas-Rojas JA, Riemann, H.P., Franti, C.E (1993) Notes about determining the cut-off value in enzyme-linked immunosorbent assay (ELISA). Prev Vet Med 15: 231-233.
458. Denac H, Moser C, Tratschin JD, Hofmann MA (1997) An indirect ELISA for the detection of antibodies against porcine reproductive and respiratory syndrome virus using recombinant nucleocapsid protein as antigen. Journal of virological methods 65: 169-181.
459. Greiner M (1996) Two-graph receiver operating characteristic (TG-ROC): update version supports optimisation of cut-off values that minimise overall misclassification costs. Journal of immunological methods 191: 93-94.
460. Greiner M, Sohr D, Gobel P (1995) A modified ROC analysis for the selection of cut-off values and the definition of intermediate results of serodiagnostic tests. Journal of immunological methods 185: 123-132.
461. Jacobson RH (1998) Validation of serological assays for diagnosis of infectious diseases. Revue scientifique et technique International Office of Epizootics 17: 469-526.
462. Cook RF, Gann SJ, Mumford JA (1989) The effects of vaccination with tissue culture-derived viral vaccines on detection of antibodies to equine arteritis virus by enzyme-linked immunosorbent assay (ELISA). Vet Microbiol 20: 181-189.
463. Geraghty RJ, Newton JR, Castillo Olivares J, Cardwell JM, Mumford JA (2003) Testing for equine arteritis virus. Vet Rec 152: 478-479.
464. Go YY, Wong SJ, Branscum AJ, Demarest VL, Shuck KM, et al. (2008) Development of a fluorescent-microsphere immunoassay for detection of

antibodies specific to equine arteritis virus and comparison with the virus neutralization test. Clin Vaccine Immunol 15: 76-87.
465. van Aken D, Benckhuijsen WE, Drijfhout JW, Wassenaar AL, Gorbalenya AE, et al. (2006) Expression, purification, and in vitro activity of an arterivirus main proteinase. Virus Res 120: 97-106.
466. Allen PM, Strydom DJ, Unanue ER (1984) Processing of lysozyme by macrophages: identification of the determinant recognized by two T-cell hybridomas. Proc Natl Acad Sci U S A 81: 2489-2493.
467. Allen PM, Unanue ER (1984) Differential requirements for antigen processing by macrophages for lysozyme-specific T cell hybridomas. J Immunol 132: 1077-1079.
468. Oleksiewicz MB, Botner A, Normann P (2001) Semen from boars infected with porcine reproductive and respiratory syndrome virus (PRRSV) contains antibodies against structural as well as nonstructural viral proteins. Vet Microbiol 81: 109-125.
469. Oleksiewicz MB, Botner A, Toft P, Normann P, Storgaard T (2001) Epitope mapping porcine reproductive and respiratory syndrome virus by phage display: the nsp2 fragment of the replicase polyprotein contains a cluster of B-cell epitopes. J Virol 75: 3277-3290.
470. Brown E, Lawson S, Welbon C, Gnanandarajah J, Li J, et al. (2009) Antibody response to porcine reproductive and respiratory syndrome virus (PRRSV) nonstructural proteins and implications for diagnostic detection and differentiation of PRRSV types I and II. Clin Vaccine Immunol 16: 628-635.
471. de Lima M, Pattnaik AK, Flores EF, Osorio FA (2006) Serologic marker candidates identified among B-cell linear epitopes of Nsp2 and structural proteins of a North American strain of porcine reproductive and respiratory syndrome virus. Virology 353: 410-421.
472. Yan Y, Guo X, Ge X, Chen Y, Cha Z, et al. (2007) Monoclonal antibody and porcine antisera recognized B-cell epitopes of Nsp2 protein of a Chinese strain of porcine reproductive and respiratory syndrome virus. Virus Res 126: 207-215.

VITA
Yun Young Go

PERSONAL INFORMATION:
Date of Birth: June 17, 1977 (Seoul, South Korea)

ACADEMIC DEGREES:

M.S., 2002 College of Veterinary Medicine Graduate Program of Immunology, Konkuk University, Seoul, Korea (Special emphasis on Veterinary Immunology)

D.V.M., 2000 College of Veterinary Medicine, Konkuk University, Seoul, Korea

PROFESSIONAL EXPERIENCE:

2005 - 2011 Graduate Research Assistant, Department of Veterinary Science, Maxwell H. Gluck Equine Research Center, University of Kentucky

2004 - 2005 Research Fellow, College of Veterinary Medicine, KonKuk University, Seoul, Korea

2001 - 2004 Equine Veterinary Clinician, Equine Veterinary Hospital, Korea Racing Authority (KRA), Korea

2000 - 2002 M.S. College of Veterinary Medicine Graduate Program of Immunology, Konkuk University, Seoul, Korea (Special emphasis on Veterinary Immunology). **Thesis Title: *Bifidobacterium longum* BL730 confers protective potential against salmonella infection to mice.**

BOARD CERTIFICATION

2011 Diplomate American College of Veterinary Microbiologists (Virology)

HONORS/AWARDS AND FELLOWSHIPS:

1. Student Travel Award, the American Society for Virology, 2011, Minneapolis, MN, USA
2. Student Travel Award, XIIth Internationals Nidovirus Symposium, 2011, Traverse City, Michigan, USA.
3. The Don Kahn Award of the American College of Veterinary Microbiologists (ACVM) for outstanding overall presentation at "The 90th Annual Meeting of Conference for Research Workers in Animal Diseases (CRWAD)", December 6th-8th, 2009, Chicago, IL
4. Student Travel Award, the American Society for Virology, 2009, Vancouver, British Columbia, Canada
5. Conference/Research Student Support Funding, the Graduate School, University of Kentucky (2008, 2009, 2010)
6. Geoffrey C. Hughes Foundation Fellowship, University of Kentucky (2005-Present)

7. Merit Scholarships, Department of Veterinary Medicine, KonKuk University (1997-1999)

ORGANIZATIONAL AFFILIATIONS:

1. Associate Member, American Society for Virology (2006 - Present)

PEER-REVIEWED PUBLICATIONS:

1. **Go Y.Y.,** Cho, I.H., Kim, J.E., Kim, J.W., Lee, J.I., Kim, H.S., Lee, J.B., Kim, T.J., Song, C.S., Park, S.Y. 2003. *Bifidobacterium longum* BL730 confers protective potential against salmonella infection to mice. Food Sci. Biotechnol. 12:625-630

2. **Go Y.Y.,** Lee J.K., Ye J.Y., Lee J.B., Park S.Y., Song C.S., Kim S.K., Choi I.S. 2005. Experimental reproduction of proliferative enteropathy and the role of IFN-gamma in protective immunity against *Lawsonia intracellularis* in mice. J Vet Sci. Dec;6(4):357-9

3. **Go Y.Y.,** Wong, S.J., Branscum, J.A., Demarest, V.L., Shuck, K.M., Vickers, M.L., Zhang, J., McCollum, W.H., Timoney, P.J., and Balasuriya, U.B.R. 2008. Development of a fluorescent microsphere immunoassay for detection of antibodies specific to equine arteritis virus and comparison with the virus neutralization test. Clin Vaccine Immunol. 15(1):76-87

4. Zhang J., **Go Y.Y.,** MacLachlan N.J., Meade B.J., Timoney P.J., and Balasuriya U.B.R. 2008. Amino acid substitutions in the structural or nonstructural proteins of a vaccine strain of equine arteritis virus are associated with its attenuation. Virology 378(2): 355-362

5. **Go Y.Y.,** Zhang J., Timoney P.J., Cook R.F., Horohov D.W., and Balasuriya U.B.R. 2010. Complex Interactions between the Major and Minor Envelope Proteins of Equine Arteritis Virus Determine its Tropism for Equine $CD3^+$ T Lymphocytes and $CD14^+$ Monocytes. J Virol. 84(10):4898-911

6. Zhang, J., Timoney, P.J., Shuck, K.M., Seoul, G., **Go Y.Y.,** Lu, Z., Powell, D.G., Meade, B.J., and Balasuriya, U.B.R. 2010. Molecular characterization of equine arteritis virus isolates associated with the 2006/2007 multi-state disease occurrence in the USA. J. Gen. Virol. Sep;91:2286-301

7. Lu, Z., Crawford, P.C., Dubovi, E.J., Sells, S., **Go Y.Y.,** Loynachan, A.T., Branscum, A.J., Chambers, T.M., Timoney, P.J. and Balasuriya, U.B.R. 2010. Diagnostic application of H3N8 specific equine influenza real-time RT-PCR assays for the detection of canine influenza virus in clinical specimens. J Vet Diagn Invest. Nov;22(6): 942-5

8. Summers-Lawyer K.A., **Go Y.Y.,** Lu Z., Timoney P., McCue P.M., Zhang J., Shuck K.M., Bruemmer. 2011. Response of Stallions to Primary Immunization with a Modified Live Equine Viral Arteritis Vaccine. J. Equine Vet. Sci. 31: 129-138

9. **Go Y.Y.,** Snijder E.J., Timoney P.J., and Balasuriya U.B.R. 2011. Characterization of Equine Humoral Antibody Response to the Nonstructural Proteins of Equine Arteritis Virus. Clin Vaccine Immunol. 18(2):268-279

10. Firth A.E., Zevenhoven-Dobbe J.C., Wills N.M., **Go Y.Y.,** Balasuriya U.B.R., Atkins J.F., Snijder E.J., Posthuma C.C. 2011. Discovery of a small arterivirus gene that overlaps the GP5 coding sequence and is important for virus production. J. Gen. Virol. 92(5):1097-1106

11. Miszczak F., Shuck K.M., Lu Z., **Go Y.Y.,** Zhang J., Sells S., Vabret A., Pronost S., Fortier G., Timoney P.J., Balasuriya U.B.R. 2011. Evaluation of two magnetic bead-based viral nucleic acid purification kits and three real-time RT-PCR reagent systems in two TaqMan assays for equine arteritis virus detection. J. Clin. Microbiol. Oct; 49(10):3694-6

12. **Go, Y.Y.**, Bailey, E., Cook, D., Coleman, S., Timoney, P.J., Chen, K., Balasuriya, U.B.R. Genome-wide association study identifies a common haplotype in horses associated with $CD3^+$ T cell susceptibility to equine arteritis virus infection. J. Virol. 2011 Dec; 85(24):13174-84. Epub 2011 Oct 12.

13. **Go, Y.Y.,** Cook, R.F., Fulgencio, J.Q., Campos, J.R., Henney, P., Timoney, P.J., Balasuriya U.B.R. Assessment of correlation between *in vitro* CD3+ T cell susceptibility to EAV infection and clinical outcome following experimental infection. Vet Microbiol (accepted)

NON-REFEREED PUBLICATIONS:

1. **Go, Y.Y.**, Balasuriya, U.B.R., and Bailey, E. 2011. Genome wide association study for susceptibility of horses for *in vitro* infection with equine arteritis virus. J. Eq. Vet. Sci. 31(5):244-245

PUBLICATIONS IN PREPARATION:

1. Zhang J., **Go Y.Y.**, Meade B.J., Lu Z., Zevenhoven-Dobbe J.C., Snijder E.J., Huang C., Timoney P.J., Balasuriya U.B.R. 2011. Development and characterization of an infectious cDNA clone of the modified live virus vaccine strain of equine arteritis virus and its potential as a vaccine vector. Vaccine (in final preparation)

2. ***Go Y.Y.,** Li Y., Yoo D., Timoney P.J., Fang Y., Balasuriya U.B.R. Equine arteritis virus does not induce type I interferon α/β production in equine endothelial cells. (in preparation)

3. **<u>*Go. Y. Y.,</u>** Bailey, E., Shuck, K.M., Timoney, P.J., Balasuriya, U.B.R. *In vitro* susceptibility of $CD3^+$ T lymphocytes to EAV infection reflects genetic trait of stallions at risk to become carriers. (in preparation)

**Publications from PhD dissertation research project*

GRANTS SUBMITTED AND NOT FUNDED:

1. Principal investigator of: "Genome-wide Scan to Identify Genetic Factors Responsible for Establishment of Equine Arteritis Virus Carrier State in Stallions". American Quarter Horse Foundation. 2010 Young Investigator Application. 2010-2011, $29,940

2. Principal investigator of: "Improved Microsphere Immunoassay for Diagnosis of EVA". Storm Cat Award, Grayson Jockey Club Research Foundation Inc. 2011-2012, $15,000

3. Co-principal investigator and co-author of: "Improved Microsphere Immunoassay for Serologic Diagnosis and Seroepidemiological Survey of Equine Arteritis Virus Infection in American Quarter Horses". American Quarter Horse Foundation. 2011-2012, 49,999

ABSTRACTS/PRESENTATIONS:

1. **<u>Go, Y.Y.</u>**, Wong, S.J., Branscum, A.J., Demarest, V.L., Shuck, K.M., Vickers, M.L., Zhang, J., McCollum, W.H., Timoney, P.J., and Balasuriya, U.B.R. 2007. Development and comparison of a fluorescent microsphere immunoassay with the virus neutralization test for the detection of antibodies to equine arteritis virus. *American Association Veterinary Laboratory Diagnosticians, October 18th-24th, 2007, Reno, NV*

2. **<u>Go, Y.Y.</u>**, Wong, S.J., Branscum, A.J., Demarest, V.L., Shuck, K.M., Vickers, M.L., Zhang, J., McCollum, W.H., Timoney, P.J., and Balasuriya, U.B.R. 2008. Development of a fluorescent microsphere immunoassay for detection of antibodies specific to equine arteritis virus and comparison with the virus neutralization test. *XIth Nidovirus Symposium, June 22nd-27th, 2008, University of Oxford, Oxford, United Kingdom*

3. **<u>Go, Y.Y.,</u>** Timoney, P.J., Horohov, D.W., and Balasuriya, U.B.R. 2008. Flow cytometric analysis of *in vitro* equine arteritis virus infected equine peripheral blood mononuclear cells. *XIth Nidovirus Symposium, June 22nd-27th, 2008, University of Oxford, Oxford, United Kingdom*

4. **<u>Go, Y.Y.</u>**, Wong, S.J., Branscum, A.J., Demarest, V.L., Shuck, K.M., Vickers, M.L.,

Zhang, J., McCollum, W.H., Timoney, P.J., and Balasuriya, U.B.R. 2008. Development of a fluorescent microsphere immunoassay for detection of antibodies specific to equine arteritis virus and comparison with the virus neutralization test. *Second International Workshop on Equine Viral Arteritis, October 13th-15th, 2008, Lexington, Kentucky*

5. Zhang, J., Shuck, K.M., Seoul, G., **Go, Y.Y.**, Lu, Z., Meade, B.J., Powell, D.G., Timoney P.J., and Balasuriya, U.B.R. 2008. Molecular characterization of equine arteritis virus isolates associated with the 2006/2007 multi-state disease occurrence in the USA. *Second International Workshop on Equine Viral Arteritis, October 13th-15th, 2008, Lexington, KY*

6. Zhang, J., Shuck, K.M., Seoul, G., **Go, Y.Y.**, Lu, Z., Meade, B.J., Powell, D.G., Timoney, P.J., and Balasuriya, U.B.R. 2009. Molecular characterization of equine arteritis virus isolates associated with the 2006/2007 multi-state disease occurrence in the USA. *American Society for Virology, July 11th-15th, 2009, Vancouver, British Columbia, Canada*

7. **Go, Y.Y.**, Zhang, J., Timoney, P.J., Horohov, D.W., Cook R.F., and Balasuriya, U.B.R. 2009. *In vitro* analysis of virulent and avirulent strains of equine arteritis virus infection in equine peripheral blood mononuclear cells. *American Society for Virology, July 11th-15th, 2009, Vancouver, British Columbia, Canada*

8. **Go, Y.Y.**, Zhang, J., Timoney, P.J., Horohov, D.W., Cook R.F., and Balasuriya, U.B.R. 2009. *In Vitro* characterization of equine arteritis virus chimeras derived from infectious cDNA clones. *American Society for Virology, July 11th-15th, 2009, Vancouver, British Columbia, Canada*

9. **Go, Y.Y.**, Zhang, J., Timoney, P.J., Cook, R.F., Horohov, D.W., and Balasuriya, U.B.R. 2009. Major and minor envelope proteins of equine arteritis virus determine tropism for peripheral blood mononuclear cells. *Conference of Research Workers in Animal Disease, December 6th-8th, 2009, Chicago, Illinois*

10. **Go, Y.Y.**, Bailey, E., Cook, D., Timoney, P.J., Cook, R.F., Balasuriya, U.B.R. 2010. Genome-wide scan to identify genetic factors responsible for the susceptibility of horses to equine arteritis virus infection. *The Ninth International Symposium on Positive-Strand RNA Viruses, May 17th-21st, 2010, Atlanta, Georgia*

11. Zhang J., Go, Y.Y., Lu Z., Meade B.J., Timoney P.J., Balasuriya U.B.R. 2010. Development and characterization of an infectious cDNA clone of the modified live virus vaccine strain of equine arteritis virus and its potential as a vaccine vector. *The Ninth International Symposium on Positive-Strand RNA Viruses, May 17th-21st, 2010, Atlanta, Georgia*

12. Miszczak, F., Lu, Z, Shuck, K.M., Timoney, P.J., Go, Y.Y., Zhang, J., Sells, S.F., Branscum, A.J., Legrand, L., Vabret, A., Pronost, S., Balasuriya, U.B.R. 2010.

Comparison of commercial nucleic acid purification and real-time RT-PCR amplification kits for the detection of equine arteritis virus in equine semen using two previously described one-step real-time RT-PCR assays. *1st Biennial Congress of European Association of Veterinary Laboratory Diagnosticians, 2010,* ***15th- 17th September, Lelystad, The Netherlands***

13. Miszczak, F., Lu, Z, Shuck, K.M., Timoney, P.J., Go, Y.Y., Zhang, J., Sells, S.F., Branscum, A.J., Legrand, L., Vabret, A., Pronost, S., Balasuriya, U.B.R. 2010. Comparison and optimization of two previously described real-time RT-PCR assays for the detection of equine arteritis virus in equine semen samples. *53rd Annual AAVLD/USAHAMeeting, Minneapolis, MN, November 11th-17th, 2010*

14. Go, Y.Y., Timoney P.J., Snijder E., Balasuriya U.B.R. 2010. Characterization of equine humoral antibody response to the nonstructural proteins of equine arteritis virus. *Conference of Research Workers in Animal Disease, December 5th-7th, 2010, Chicago, Illinois*

15. **Go, Y.Y.**, Fulgencio J.Q., Campos, J.R., Heney P.J., Cook R. F., Timoney P. J., Balasuriya, U.B.R. 2011. *In vitro* susceptibility or resistance of equine $CD3^+$ T lymphocytes to equine arteritis virus: is there a correlation with clinical outcome to infection in horses? *XIIth Internationals Nidovirus Symposium, June 4th-9th, 2011, Traverse City, Michigan, USA.*

16. **Go, Y.Y.**, Timoney, P.J., Snijder E.J., and Balasuriya, U.B.R. 2011. Humoral antibody response to the nonstructural proteins of equine arteritis virus. *XIIth Internationals Nidovirus Symposium, June 4th-9th, 2011, Traverse City, Michigan, USA.*

17. **Go, Y.Y.**, Li Y., Chen, Z., Yoo, D., Timoney, P.J., Snijder, E.J., Fang Y., and Balasuriya, U.B.R. 2011. Equine arteritis virus does not induce type I interferon α/β production in equine endothelial cells: Identification of nonstructural protein 1 as a main interferon antagonist. *XIIth Internationals Nidovirus Symposium, June 4th-9th, 2011, Traverse City, Michigan, USA.*

18. **Go, Y.Y.**, Cook, D., Timoney, P.J., Bailey, E., and Balasuriya, U.B.R. 2011. Genome wide association study to identify the genetic determinants of susceptibility of horses to equine arteritis virus infection. *XIIth Internationals Nidovirus Symposium, June 4th-9th, 2011, Traverse City, Michigan, USA.*

19. Shuck, K.M., Miszczak, F., Lu, Z., **Go, Y.Y.**, Zhang, J., Stephen, S., Vabret, A., Pronost, S., Fortier, G., Timoney, P.J., and Balasuriya, U.B.R. 2011. Evaluation of two magnetic bead-based viral nucleic acid purification kits and three real-time RT-PCR reagent systems in two TaqMan assays compared to virus isolation for equine arteritis virus detection in semen. *XIIth Internationals Nidovirus Symposium, June 4th-9th, 2011, Traverse City, Michigan, USA.*

20. **Go, Y.Y.**, Balasuriya, U.B.R., and Bailey, E. 2011. Genome wide association study for susceptibility of horses for *in vitro* infection with equine arteritis virus. *Equine Science Society Meeting, June 1-3, 2011; Munfreesboro, TN.*

21. Balasuriya U.B.R., Firth A.E., Zevenhoven-Dobbe J. C., Wills N.M., **Go Y.Y.**, Atkins J.F., Snijder E.J., Posthuma C. C. 2011. Discovery of a novel small arterivirus gene that overlaps the GP5 coding sequence and is important for virus production. *American Society for Virology, July 16th-20th, 2011, Minneapolis, Minnesota.*

22. **Go Y.Y.**, Li Y., Yoo D., Timoney P.J., Fang Y., Balasuriya U.B.R. 2011. Equine arteritis virus does not induce type I interferon α/β production in equine endothelial cells. *American Society for Virology, July 16th-20th, 2011, Minneapolis, Minnesota.*

23. Fulgêncio J.Q., **Go Y.Y.**, Balasuriya U.B., Gonçalves de Oliveira F., Guerra de Moura R. E., Pimenta dos Reis J.K., Leite R.C. 2011. Serological evidence of equine arteritis virus infection in *equidae* of Minas Gerais, Brazil. *XXII National Meeting of the Virology Brazilian Society, October 23rd-26th, 2011, Atibai, São Paulo, Brazil*